Catalysis and Molecular Recognition:

Harnessing Hydrogen Bonds and the Power of Charged Substituents

A DISSERTATION

SUBMITTED TO THE FACULTY OF THE GRADUATE SCHOOL

OF THE UNIVERSITY OF MINNESOTA

BY

Masoud Samet

IN PARTIAL FULFILLMENT OF THE REQUIREMENTS

FOR THE DEGREE OF

DOCTOR OF PHILOSOPHY

Steven R. Kass, Advisor

July 2015

Acknowledgements

I would like to express my sincere appreciation and thanks to my advisor Prof. Steven Kass for the continuous support of my PhD study, for his patience, motivation, enthusiasm, and immense knowledge. I would like to thank him for allowing me to grow as a scientist. His advice on both research as well as on my career have been priceless.

A special thanks to my lovely wife, Fateme, for her endless love, kindness and support she has shown during the past years it has taken me to finalize my advanced studies. I would like to thank my family and wife's family. Words cannot express how grateful I am to them for all of their love and support during my studies. Their prayer for me was what sustained me thus far. I would also like to thank all of my friends who supported me in writing, and incented me to strive towards my goal.

To my wife,

FATEME

Abstract

Enzymes employ a variety of approaches to stabilize transition states and facilitate chemical reactions, but none of them are more important than hydrogen bond networks (HBNs) and electrostatic interactions. Herein, hydrogen bonds are studied and exploited. Their strengths are measured in compounds with rigid structures to better understand enzymatic reactions and design stronger organocatalysts. Anion recognition abilities of a series of rigid OH based receptors are also studied to probe the role of hydrogen bonds in anion channels. At the same time, novel strong Brønsted acids are developed and their catalytic reactivities in different organic reactions are explored. Hydrogen bonding interactions and charged substituents provide a remarkable means for developing novel Brønsted acid catalysts and new anion receptors.

Table of Contents

List of Tables

Appendix for Chapter 3

Appendix for Chapter 4

Appendix for Chapter 5

Appendix for Chapter 6

List of Figures

Chapter 3

Chapter 4

Chapter 5

Chapter 6

Appendix for Chapter 3

Appendix for Chapter 4

Appendix for Chapter 6

List of Schemes

Chapter 1

Chapter 4

List of Abbreviations

ACN	acetonitrile
ADE	adiabatic detachment energy
Asp	aspartic acid
ATR	attenuated total reflectance
BAr^F_4	tetrakis(3,5-bis(trifluoromethyl)phenyl)borate
BnBr	benzyl bromide
°C	degrees Celsius
Calcd	calculated
Cat	catalyst
Conv	conversion
δ	chemical shift in part per million
DDQ	2,3-dichloro-5,6-dicayano-1,4-benzoquinone
DFT	density functional theory
DMF	dimethylformamide
DMP	Dess-Martin preiodinane
DMSO	dimethyl sulfoxide
ε	dielectric constant
ESI	electrospray ionization
eV	electron volts
exptl	experimental
Fig	figure
FT-IR	Fourier transform infrared
g	gram
Glu	glutamic acid
HB	hydrogen bond
HBN	hydrogen bond network
HRMS	high resolution mass spectrometry
hrs(h)	hour(s)

K	Kelvin
kcal/mol	kilocalorie per mole
LBHB	low barrier hydrogen bond
M06-2X	Minnesota 06 functional with double the amount of nonlocal exchange
MBH	Morta-Baylis-Hillman
MHz	megahertz
mM	millimolar
mmol	millimole
min	minute(s)
mL	milliliter
µL	microliter
MPLC	medium pressure liquid chromatography
m/z	mass to charge ratio
NMR	nuclear magnetic resonance
PEG	polyethylene glycol
Ph	phenyl
PMBCl	p-methoxybenzyl chloride
ppm	parts per million
SWHB	single well hydrogen bond
TBACl	tetrabutylammonium chloride
TBAF	tetrabutylammonium fluoride
TBS	*tert*-butyldimethylsilyl
TEA	triethylamine
THF	tetrahydrofuran
TLC	thin layer chromatography
TMS	trimethylsilane
$TMSCF_3$	trimethyl(trifluoromethyl)silane
TOF	time of flight
UV	ultraviolet
VDE	vertical detachment energy
zpe	zero point energy

tc	thermal corrections

Chapter 1: Background and Introduction*

1.1. Hydrogen Bonds

Hydrogen bonds (HBs) are defined as an attractive interaction between an electron deficient hydrogen in A-H and an electron rich atom B in A-H···B where A and B are usually highly electronegative N, O, and/or F atoms.[1,2] These interactions are prevalent in nature and play a vital role in biological processes.[3] For instance, DNA double helix strands are held together by hydrogen bond networks (HBNs).[2] They are also responsible for the high catalytic efficiency of enzymes, molecular recognition, and ion transport. One example is serine proteases (Scheme 1, left)

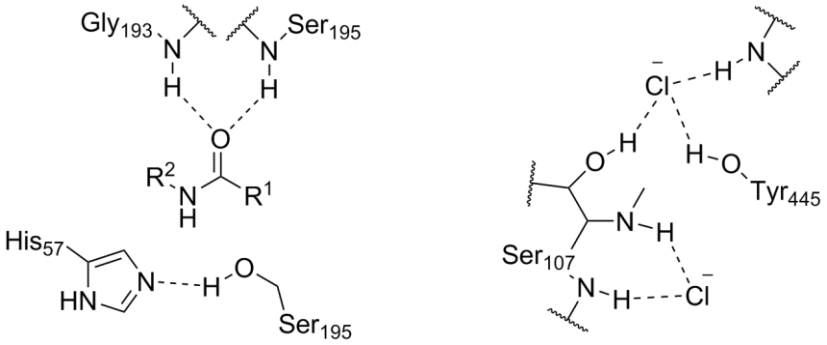

Scheme 1. HB interactions (dotted lines) in the active site of serine proteases (left) and the ClC chloride ion channel (right).

which use two amine HBs to activate a carbonyl group and facilitate the cleavage of a peptide bond.[4] Another instance is a Cl^- ion channel (Scheme 1, right), which employs

* This chapter has been taken from my 2010 written preliminary examination at the University of Minnesota and this dossier was used as the template for the subsequent sections.

multiple amine and hydroxyl groups to facilitate chloride transport across non-polar cellular membrane phospholipid bilayers.[5]

There are three categories of HBs between atoms (i.e. A-H···B):[2,6] (1) normal HBs where the hydrogen atom is attached more tightly to one of the heteroatoms, (2) low-barrier hydrogen bonds (LBHBs) in which the hydrogen can move freely between A and B, and (3) single well hydrogen bonds (SWHBs) where the hydrogen is centered between the donor A and acceptor B. The last two are typically stronger (LBHBs = 12-24 kcal/mol and SWHBs > 24 kcal/mol) than a normal HB which is considered to be worth 2.4-12 kcal/mol.[7]

1.2. Factors Affecting the Strength of a HB

1.2.1. Distances between Hydrogen Donors and Acceptors, and Hydrogen Bond Angles

The energy diagrams for the 3 different types of HBs between atoms A and B are depicted in Fig. 1.[7] Formation of strong HBs are possible when the distance (R_{A--B}) between the two heteroatoms is less than the sum of their van der Waals radii. In the case of [O-H-O] and [O-H-N] HBs, R_{A--B} needs to be smaller than 2.55 Å and 2.65 Å, respectively.[6,7] When this condition is met and the heteroatoms are close together (b, Fig. 1), the barrier for hydrogen transfer is at or below the zero-point energy level (i.e., the dotted lines in Fig. 1).[7]

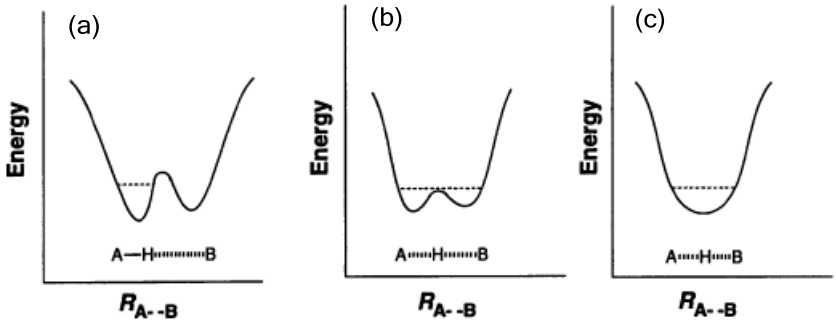

Figure 1. Potential energy diagrams for different types of HBs where $R_{A—B}$ is the distance between the two heteroatoms A and B; Normal HB (a), LBHB (b) and SWHB (c).

In hydroxyl containing compounds, the difference between free OH and hydrogen bonded OH stretching frequencies (Δυ) in their IR spectra are related to the HB strengths (i.e., Δ*H*).[8] In other words, a stronger HB results in a bigger Δυ. However, IR studies on acyclic monomethyl diols indicate that this correlation does not apply for intramolecular HBs (Table 1).[9] The thermodynamic data show that enthalpy (Δ*H*) and entropy (Δ*S*) are changing in going from 2-methoxyethanol to 4-methoxybutanol, but Δ*S* has a greater influence than Δ*H* on the equilibrium constants (i.e., K_{eq}).

Table 1. Liquid-phase IR spectra and thermodynamic data for monomethyl ethers of diols (CCl_4, T = 20 ℃).

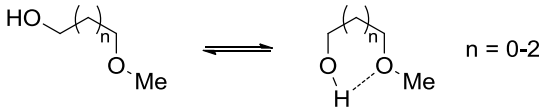

Cmpd	υ_o (cm^{-1})[a]	υ_b (cm^{-1})[b]	Δυ	Δ*H* (kcal/mol)	Δ*S* (cal/mol.K)	Δ*G* (kcal/mol)	K_{eq}
2-methoxyethanol	3645	3615	30	-2.2	-2.9	-1.4	11.1
3-methoxypropanol	3644	3558	86	-2.1	-6.4	-0.22	1.5
4-methoxybutanol	3645	3465	180	-2.7	-10.0	0.24	0.66

[a]"Free" OH

[b]Hydrogen bonded OH: Intramolecular OH···O HB

As a result, 1,2 and 1,3 relationships between the hydroxyl groups in acyclic diols lead to stronger (based upon ΔG) intramolecular HBs.

Directionality is one of the key properties of HBs. In A-H···B interactions, bond angles spanning from 120°–140° have substantially reduced strengths and smaller angles generally lead to insignificant interactions.[10] For example, computations on methanol – pyridine complexes revealed that the HB strength diminishes by 85% as the bond angle decreases from 180° to 120° (i.e., from 6.7 to 1.0 kcal/mol).

1.2.2. Substituent Effects

The strength of a HB depends not only on its geometry, but also the pK_a values for HA and HB.[2,6,11] For instance, the free energy of formation of a HB between *para*-substituted phenols (4-X-C_6H_4OH) and different bases in CCl_4 (ΔG^o_{HB}) correlates with the difference in the gas-phase acidities (ΔG_A) and basicities (ΔG_B) of the HB donors and acceptors (Table 2).[12] As a result, *N*,*N*-dimethylacetamide forms stronger HBs than acetone because it is more basic, and electron-withdrawing groups on the phenol increase its acidity leading to the formation of stronger HBs.

Table 2. Formation energies of HBs between phenol derivatives and two carbonyl containing compounds.

4-X-C_6H_4OH (HA)	Base (B)	$-\Delta G^o_{HB}$ (kcal/mol)	ΔG_A-ΔG_B
X = H	CH_3COCH_3	1.40	154.6
H	$(CH_3)_2NCOCH_3$	2.98	134.1
CH_3O	$(CH_3)_2NCOCH_3$	2.70	135.3
Cl	$(CH_3)_2NCOCH_3$	3.48	128.2
NO_2	$(CH_3)_2NCOCH_3$	4.70	113.2

1.2.3. Solvent Effects

HBs are stronger in aprotic solvents than in protic ones.[2] For instance, ΔG for HB formation between 4-nitrophenol and 4-nitrophenolate is 7-8 kcal/mol more favorable in acetonitrile and tetrahydrofuran than in water, and an intramolecular HB in o-hydroxybenzoic acid is 4.1 pK_a units stronger in DMSO than in water (i.e., $\Delta\Delta pK_a = 5.6$ kcal/mol, Scheme 2).[13] These energetic differences are predominantly determined by solvent abilities to solvate separated HB donor and acceptor groups.[14]

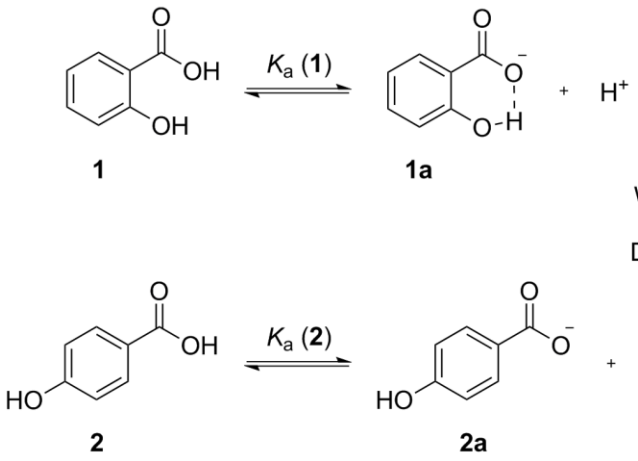

	pK_a (**1**)	pK_a (**2**)	ΔpK_a
Water	2.9	4.6	1.7
DMSO	6.6	12.4	5.8

Scheme 2. Aqueous and DMSO ionization equilibrium constants for o- and p-hydroxybenzoic acids.

A solvent's dielectric constant (ε) also affects HB strengths.[15] In fact, the strength of a HB increases as the solvent's ε decreases. For example, intramolecular HBs in the monoanions of α- and β-hydroxycarboxylic acids and dicarboxylic acids are stronger in ACN than DMSO (Scheme 3).

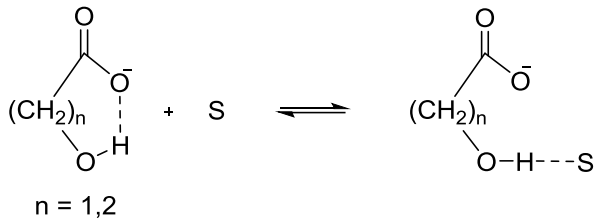

Scheme 3. The equilibrium between an intra- and intermolecular HB in an aprotic solvent.

This is due not only to the smaller dielectric constant of ACN (ε = 35.87 at 25 ℃)[16] compared to DMSO (ε = 47.13 at 25 ℃),[17] but also to DMSO's stronger ability to form an intermolecular HB with the OH group in the monoanions of the corresponding alcohols and carboxylic acids.[18] In other words, the equilibrium between an intra- and intermolecular HB is greater in DMSO than in ACN because the former solvent is a better HB acceptor. These results indicate that in order to maximize HB strength, poorly solvating nonpolar aprotic solvents should be employed.

1.3. Exploiting Hydrogen Bond Interactions

1.3.1. Effects on Acidities

Intramolecular HBs affect acidities of carboxylic acids and alcohols.[19] For instance, the contribution of multiple HBs on the acidities of benzoic acid derivatives in DMSO were measured by Herschlag and Shan (Table 3).[19d] The results indicate that the pK_a values decrease with the number of HBs. Moreover, the ΔpK_a values show large and nearly additive effects for each HB.

Table 3. Measured pK_a's for benzoic acids in DMSO at 25 ℃.

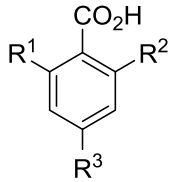

R^1	R^2	R^3	pK_a	ΔpK_a (pK_a ($PhCO_2H$) – pK_a ($ArCO_2H$))
H	H	H	11.08 ± 0.06	0.00
H	OH	H	6.60 ± 0.05	4.48
OH	OH	H	3.08 ± 0.10	8.00

Crowder and his co-workers found the gas-phase acidities of diols are greater than those of the corresponding alcohols (Table 4).[19c] More specifically, propane-1,3-diol and butane-1,4-diol are more acidic than 1-propanol and 1-butanol due to the intramolecular HBs that form in their conjugate bases.

Table 4. Gas-phase acidities of diols, their corresponding mono alcohols and HBr at 25 ℃.[a]

Cmpd	ΔH_{acid} (kcal/mol)	ΔS_{acid} (cal/mol.K)	ΔG_{acid} (kcal/mol)
CH_3CH_2OH	378.3	22.1	371.7
$HO(CH_2)_2OH$	365.1	14.1	360.9
$CH_3(CH_2)_2OH$	375.7	22.1	369.1
$HO(CH_2)_3OH$	358.0	7.4	355.8
$CH_3(CH_2)_3OH$	375.3	22.1	368.7
$HO(CH_2)_4OH$	356.1	5.0	354.6
$CH_3(CH_2)_4OH$	374.1	22.1	367.5
$HO(CH_2)_5OH$	356.1	2.0	355.5
$(CH_3)_2CHOH$	375.1	22.1	368.5
$(HO(CH_2)_2)_2CHOH$ (**1**)	344.3	6.4	342.4
$(CH_3)_3COH$	374.7	22.1	368.1
$(HO(CH_2)_2)_3COH$ (**2**)	333.0	-4.7	334.4
$(HO(CH_2)_2CH(OH)(CH_2)_2)_3COH$ (**4**)	319.8	21.1	313.5
HBr	323.5	17.4	318.3

[a]All acidities come from ref. 19c, 19e, 19f, and 20.

More recently, Kass et al. reported that successive incorporation of hydroxyl groups into an alcohol produces acidic polyols, and that heptaol **4** is stronger than hydrobromic acid by 4.8 kcal/mol, because its alkoxide anion (**4a**) is stabilized by 3 direct (primary) and 3 indirect (secondary) HBs (Figure 2).[19e,19f] Comparison of deprotonation enthalpies of $(CH_3)_3COH$, **2**, and **4** indicates that the 3 primary interactions provide 41.7 kcal/mol (13.9 kcal/mol per bond) of stabilization while the secondary ones are worth 13.2 kcal/mol or 4.4 kcal/mol per bond.

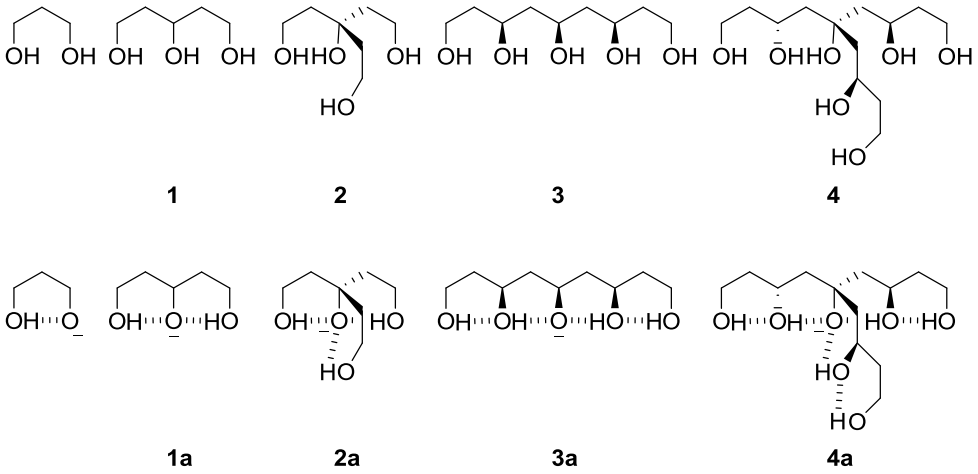

Figure 2. Propane-1,3-diol, polyols **1 – 4**, and their stabilized corresponding conjugate bases **1a – 4a** through the formation of intramolecular HBs (dotted line).

Alkoxide stabilization energies by HBNs in the conjugate bases of alcohols **1** – **4** were also studied in the gas phase by negative ion photoelectron spectroscopy.[19g,21] This technique measures the electron binding energy (adiabatic detachment energy, ADE) of anions. The ADE provides a measure of the stability of an anion, and the larger the value the more stable the ion is with respect to its corresponding radical. For instance, the predicted ADE of deprotonated propane-1,3-diol is 0.84 ev (19.4 kcal/mol) larger than the

experimental value for 1-propoxide due to the presence of an intramolecular HB in the former case (Table 5).

Table 5. Experimental and computed ADEs of a series of deprotonated alcohols.

Cmpd	Exptl (ev)	M06-2X/maug-cc-pVT(+d)Z (ev)
$CH_3CH_2CH_2O^-$	1.79	1.63
$HOCH_2CH_2CH_2O^-$		2.47
1a	3.30	3.18
2a	3.85	3.66
3a	4.05	3.82
4a	4.60	4.45

Compound **3a** has 2 additional secondary HBs relative to **1a** which provide 17.3 kcal/mol of stabilization energy. Its ADE is also larger than that for **2a** by 4.6 kcal/mol despite the fact that the latter ion has 3 primary HBs. This indicates that the combination of 2 weak secondary HBs can provide more stabilization energy than a strong primary one.

Liquid-phase DMSO acidities of propane-1,3-diol and 1-propanol (Table 6) indicate that the former compound is more acidic than the latter one by 4.6 pK_a units.[19f]

Table 6. Experimental DMSO acidities of polyols in DMSO.

Cmpd	pK_a	ΔpK_a (PrOH – ROH)
$CH_3CH_2CH_2OH$	30.0	0.0
$HO(CH_2)_3OH$	25.4	4.6
$(HO(CH_2)_2)_2CHOH$ (**1**)	19.7	10.3
$(HO(CH_2)_2)_3COH$ (**2**)	16.1	13.9
$(HO(CH_2)_2CH(OH)(CH_2)_2)_3COH$ (**4**)	11.4	18.6

Successive addition of hydroxyl groups leads to heptaol **4** which is ~19 and ~1 pK_a units more acidic than 1-propanol and acetic acid (pK_a = 12.3), respectively. This is because of the stabilization of the oxyanion in the conjugate base of polyol **4** by 3 primary and 3 secondary HBs.

1.3.2. Hydrogen Bond Catalysis

Lewis and Brønsted acids are ubiquitous in the synthesis of organic compounds and materials.[22] However, environmental considerations and their sensitivity to water have limited their applications.[23] Moreover, some Lewis acid-promoted reactions need a large amount of the catalyst because of the presence of basic sites in the products.[24] Thus, product inhibition is another problem associated with Lewis acids.[25] To address these issues chemists have developed a variety of HB catalysts by mimicking enzyme catalysis in nature. For example, a great deal of research has focused on alcohols, phenols, and thioureas capable of utilizing multiple HBs to accelerate a variety of chemical transformations.[3,26]

1.3.2.1. OH Based Catalysts

Compounds containing two hydroxyl groups such as 1,8-biphenylenediols (**5**),[27] TADDOLs (**6**),[28] and binols (**7**)[29] (Fig. 3)

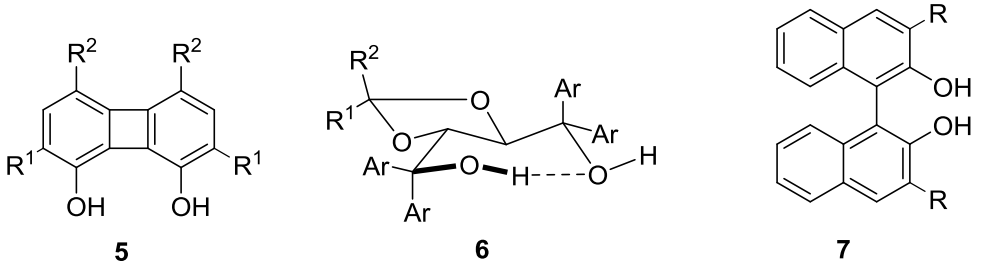

Figure 3. 1,8-Biphenylenediols (**5**), TADDOLs (**6**), and binols (**7**).

have been employed as catalysts in numerous organic reactions.

Biphenols **5** developed by Hine and Kelly are one of the first examples of 2 HB donor catalysts. They were shown to accelerate epoxide ring openings and Diels-Alder reactions.[27] The catalytic properties of TADDOLs (**6**) have been reported, and their ability to catalyze reactions has been attributed to their increased acidities due to the formation of an intramolecular HB. [28,30] Binols (**7**) also have been employed as 2 HBs donor catalysts. For example, Yamad and Ikegami found that a Morta-Baylis–Hillman (MBH) reaction between 2-cyclopenten-1-one and 3-phenyl-1-propanal proceeds much faster in the presence of binol.[29]

Kass and his group have recently used HBNs along with electron-withdrawing trifluoromethyl (CF_3) groups to develop strongly acidic aliphatic alcohols (i.e., **8** – **10**).[26c] These compounds are capable of catalyzing organic transformations such as the Friedel-Crafts reaction between β-nitrostyrene and *N*-methylindole (Scheme 4).

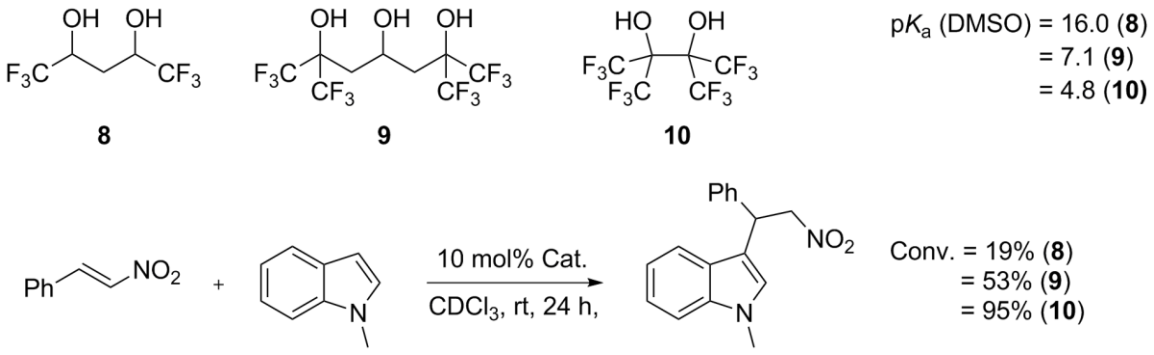

Scheme 4. A Friedel-Crafts reaction between β-nitrostyrene and *N*-methylindole catalyzed by fluorinated alcohols **8** – **10**. Product conversions were determined after 24 hrs and are a reflection of the reaction rates.

It was found that their catalytic activity follows their DMSO acidities and that the strongest acid (i.e., **10**) is the most active catalyst.

1.3.2.2. NH Based Catalysts

Thioureas (RNHCSNHR') are one of the most commonly used organocatalysts that employ 2 HBs to facilitate chemical reactions.[24e] Their utility as accelerating agents was first demonstrated in a Strecker reaction (Scheme 5),[31] but subsequently thioureas were found to have broad applicability and have been used to catalyze many types of transformations.[32] Two distinctly different modes of action have been suggested for these species. One involves electrophilic activation via the formation of a doubly hydrogen bonded complex while the other proceeds by anion abstraction and ion pair formation (Fig. 4).[32a,33]

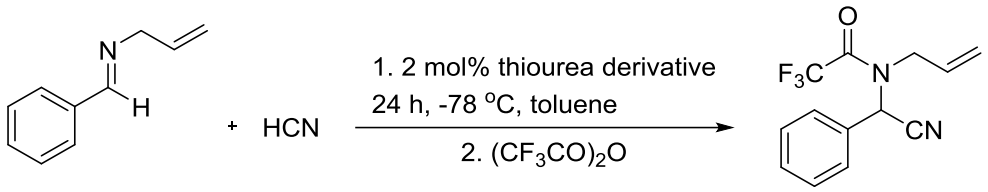

Scheme 5. Thiourea-catalyzed Strecker reaction.

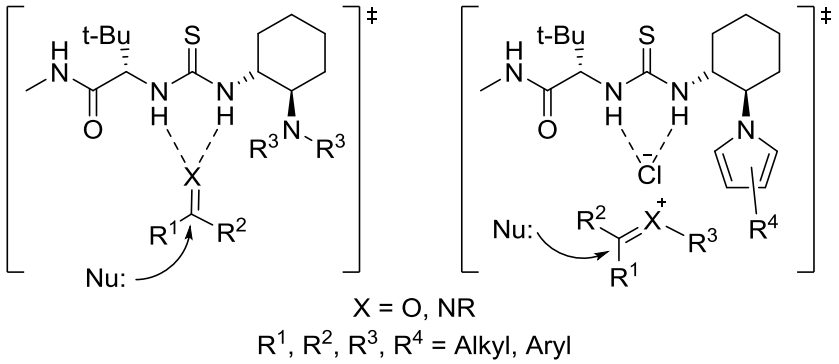

Figure 4. Two distinct mechanisms for thiourea catalysis; double HB activation (left) versus counter-ion catalysis (right).

Incorporation of electron-withdrawing groups like CF_3 into the *meta* or *para* positions of thioureas containing phenyl groups (**12** – **14**; Scheme 6) increases their acidities, and as a result enhances their catalytic activities.[34]

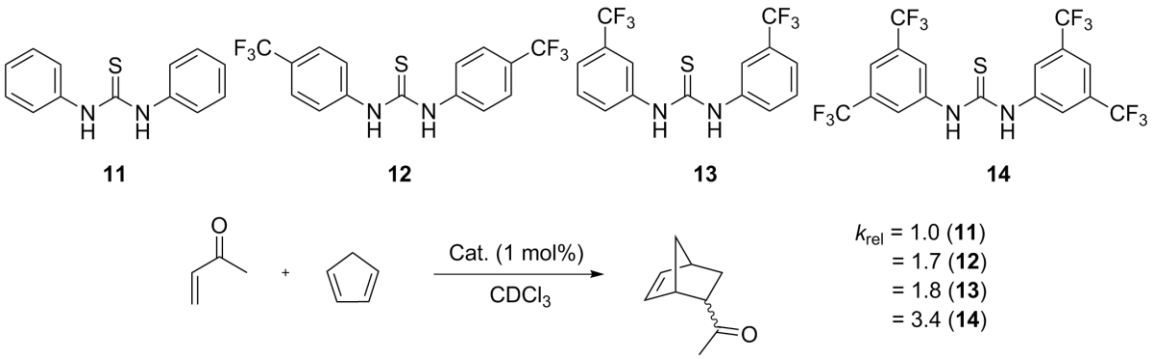

Scheme 6. Thiourea-catalyzed Diels-Alder reaction of methyl vinyl ketone with cyclopentadiene and relative rate data.

More elaborate thioureas in which additional HBs are used to organize the complex between it and the substrate have been reported recently to increase the stereoselectivity. For example, **15** has several internal HBs involving the urea moiety that improve its catalytic abilities. If this group is omitted, the yield of the Mukaiyama-Mannich reaction (Scheme 7) is reduced (72% vs 97%) as is the stereoselectivity (95% vs 99%).[35]

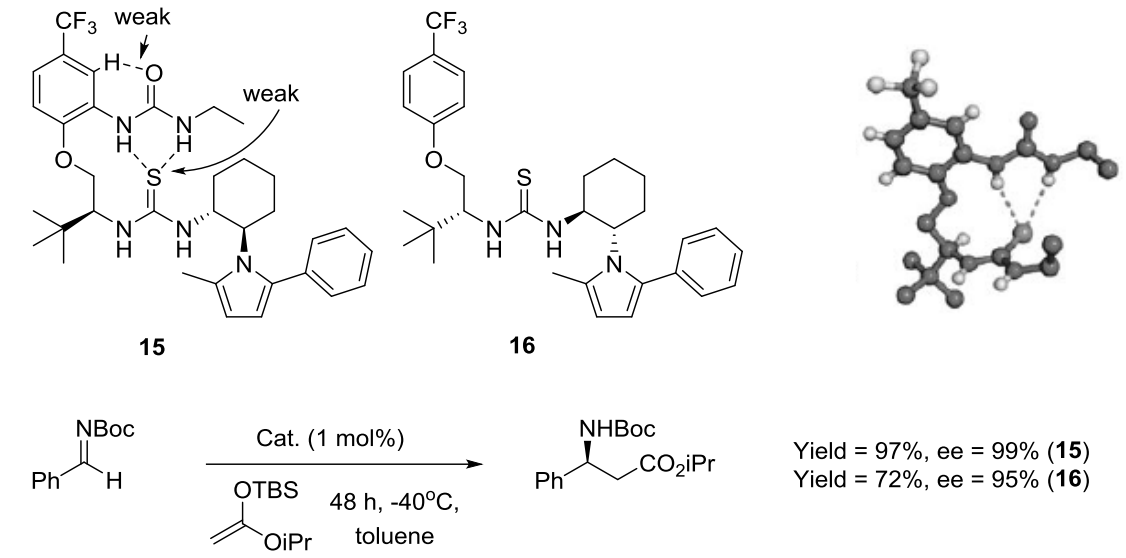

Scheme 7. Asymmetric Mukaiyama-Mannich reaction and an X-ray structure of catalyst **15**.

Protonated thioureas such as **17** (Scheme 8) has been recently reported by Seidel.[36]

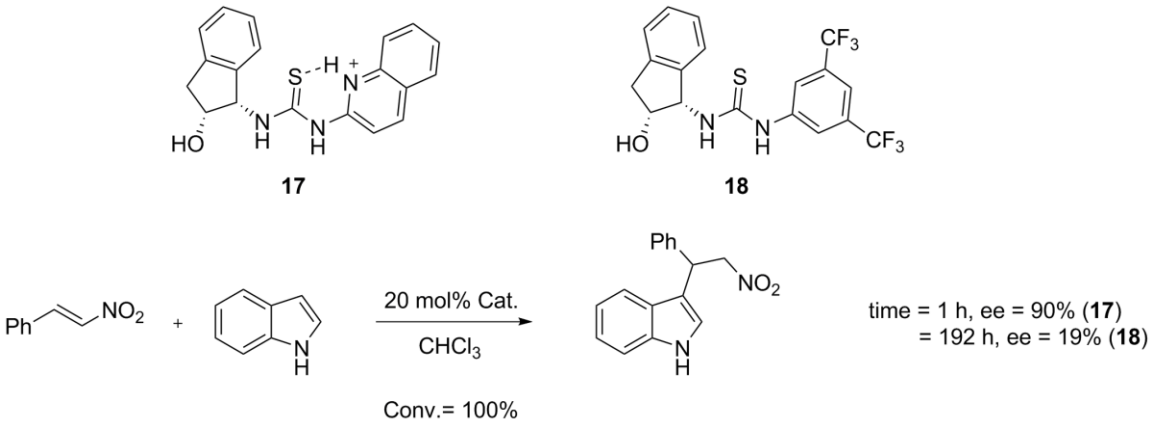

Scheme 8. Friedel-Crafts addition of indole to β-nitrostyrene using protonated and neutral thioureas **17** and **18**.

Because of the positively charged pyridinium substituent, **17** is significantly more active than its analogue with 2 electron-withdrawing CF_3 groups.

Squaramides (**19**) are another family of dual HB catalysts that have been successfully employed in several organic transformations (Scheme 9).[37]

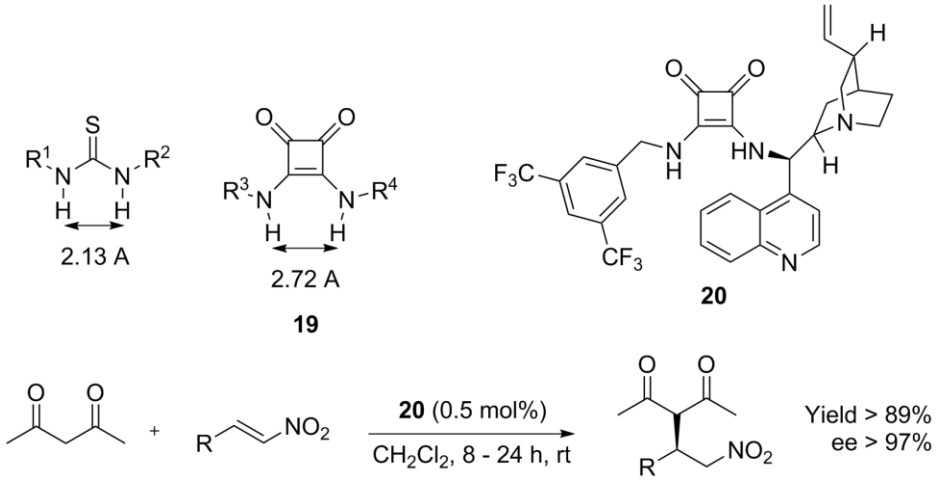

Scheme 9. The conjugate addition of pentane-2,4-one to β-nitrostyrene catalyzed with squaramide **20**.

Their cavity size is 0.6 Å larger than for thioureas and they have rigid structures that give them entropic advantages. Squaramide **20** is an example of bifunctional catalyst that can accelerate the conjugate addition of pentane-2,4-one to β-nitrostyrene with high yields and stereoselectivities.[37a]

1.3.3. Molecular Anion Recognition

HBNs are exploited in nature to enable anion recognition and transport across non-polar cellular membrane phospholipid bilayers. Misregulation of anion channels in humans can lead to life-threatening diseases. For instance, faulty chloride channels play a key role in the pathology of cystic fibrosis.[38] The discovery and study of these processes over the last few decades has led to the development of artificial HB receptors for pharmaceutical and environmental applications.[39] Neutral proteins possessing multiple HB donors regulate

anion transport in nature, and as a result much effort has been devoted to the design and synthesis of uncharged anion receptors having multiple hydrogen-bonding sites.[40] Many studies focus on anion receptors bearing the NH groups of amides, ureas, thioureas, and pyrroles.[41] Anion receptors containing OH substituents acting as HB donors are little studied, even though they are inherently more acidic than NH groups. Furthermore, interactions involving hydroxyl substituents play a critical role in a broad range of recognition processes.[42] For instance, in the active site of ribokinase from *E. coli*, the carboxylate of two Asp and one Glu groups serve as HB acceptors in order to recognize D-ribose (i.e., the substrate, Fig. 5).[43]

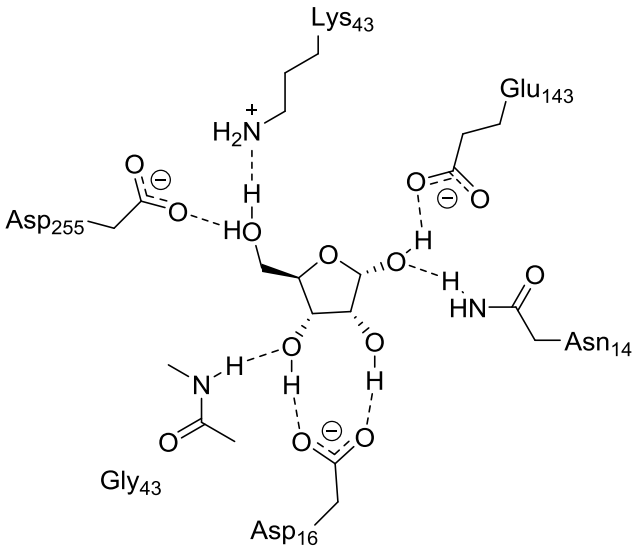

Figure 5. Schematic drawing of the active site of ribokinase with D-ribose from *E. coli* generated from PDB data.

Cholic acid derivatives developed by Davis and his co-workers are one of the earliest examples of hydroxyl-based anion receptors (Figure 6).[44] These compounds make use of three hydroxyl groups to bind anions, and their relatively rigid structure prevents them from

forming intramolecular HBs. They bind tridentate oxoanions such as p-toluenesulfonate in benzene, but do not associate with chloride.

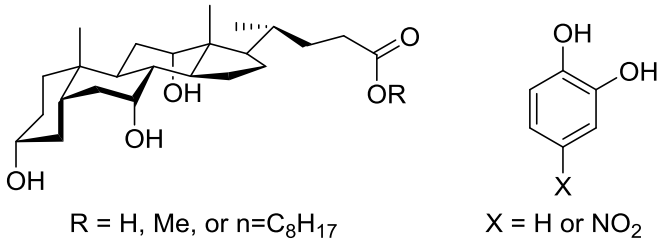

Figure 6. Structure of cholic acid and catechol derivatives.

Inspired by the critical role of phenolic receptors in the ClC chloride channel, Smith and co-workers studied the anion binding abilities of resorcinol and catechol derivatives by ^{1}H NMR spectroscopy.[45] They found catechol can bind chloride ~21 times more strongly than phenol in a polar environment such as ACN (K_a (Cl^-) = 1015 and 48 M^{-1}, respectively). Incorporation of an electron withdrawing nitro group increases the acidity of the resulting nitrocatechol and its chloride ion affinity to K_a (Cl^-) = 3800 M^{-1}. Hydroxyl-based receptors capable of forming 3 HBs to Cl^- were recently developed by the Kass research group (Figure 7). Polyphenol **21** has two rotamors that can associate with anions. *Syn*-isomer (**21s**) binds chloride ion ~ 500 times more strongly than its anti derivative (**21a**) (K_a = 1.27 × 10^5 vs 240 M^{-1} in ACN), because the former employs an additional primary HB to interact with Cl^-.

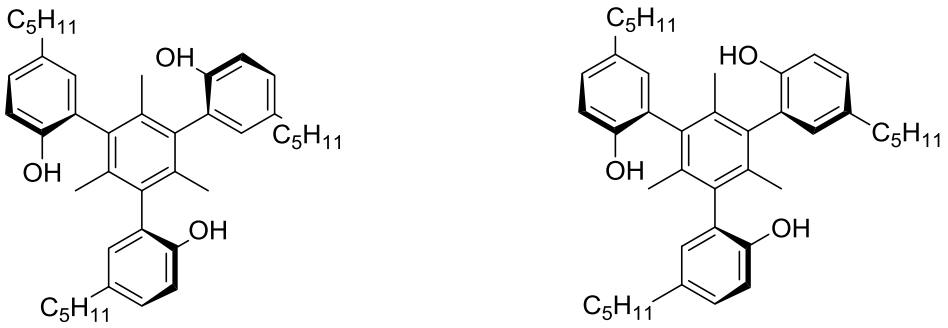

Figure 7. *Syn*- and *anti*-isomers of triphenol **21**.

1.4. Focus of This Work

In this dissertation, a combination of experimental and theoretical approaches are employed to characterize HB energetics, novel molecular anion receptors, and hydrogen bond / Brønsted acid catalysts. Following this introduction, chapter 2 explains the synthesis of rigid tricyclic locked in all axial cyclohexane-1,3,5-triol derivatives with 0-3 trifluoromethyl groups. It also provides HB energetics in a preorganized HBN and explores the stabilization of the conjugate bases via negative ion photoelectron spectroscopy. Chapter 3 concerns anion recognition with neutral hydroxyl-based rigid triols and the energetic effects of a remote hydroxyl group on anion affinities. Infrared (IR) spectroscopy is used in this work to characterize the solution structures of bound anion receptors for the first time. Chapter 4 explores the impact of stereoelectronic effects on anion recognition in a series of neutral anion receptors. IR spectroscopy is also used to probe the structures of the bound complexes. Chapter 5 describes a simple analytical methodology for measuring relative acidities of a series of structurally related compounds in nonpolar media using IR spectroscopy and introduces a new class of Brønsted acids, charge-enhanced acidity acids.

Finally, chapter 6 explores the acidities of small rigid triols in DMSO followed by an evaluation of their catalytic abilities in several organic transformations.

Chapter 2: A Preorganized Hydrogen Bond Network and Its Effect on Anion Stability*

2.1. Introduction

Enzymes employ a variety of approaches to stabilize transition states and facilitate chemical reactions, but none of them are more important than hydrogen bond networks (HBNs) and electrostatic interactions.[1-4] In some cases such as for triosphosphate and ketosteroid isomerases they also take advantage of rigid active sites to achieve greater specificity and reaction rates.[5,6] Drawing inspiration from nature, considerable effort has been expended to develop metal-free hydrogen bond catalysts.[7] Simple model compounds recently were investigated to probe the consequences of HBNs. For example, *syn*-triol **1s** (Fig. 1) was reported to be ~160 times more active than its anti isomer **1a** in a Friedel-Crafts reaction.[8]

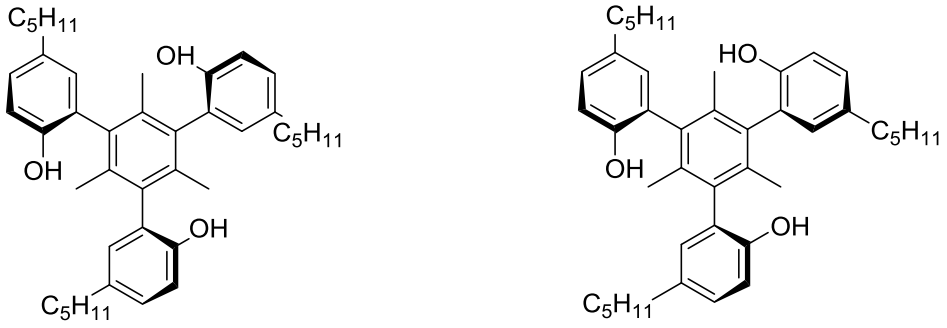

Figure 1. *Syn*- and *anti*-isomers of triphenol **1**.

* Samet, M.; Wang, X. –B.; Kass, S. R., A Preorganized Hydrogen Bond Network and Its Effect on Anion Stability. *J. Phys. Chem. A*, **2014**, *118*, 5989-5993. Copyright ACS. Reproduced with permission.

These results indicate that three hydrogen bond donors can be significantly more effective catalysts than their analogous two hydrogen bond analogs, even though the latter type of species have been the focus of the field.

Energetic information on the consequences of HBNs were also recently reported.[9-14] For example, deprotonation of a pentaol and heptaol with 5 and 7 hydroxyl (OH) groups (i.e., $(HOCH_2CH_2CH(OH)CH_2)_2CHOH$ and $(HOCH_2CH_2CH(OH)CH_2)_3COH$) were found to afford stabilized oxyanion conjugate bases.[12,14] Negative ion photoelectron spectroscopy revealed that in the gas phase this stabilization corresponds to 52.1 and 64.8 kcal mol^{-1}, respectively.[11,14] Electron withdrawing groups in combination with hydrogen bonds were found to lead to even larger enhancements of the adiabatic detachment energies (ADEs) (e.g., the ADE of $(CF_3)_2C(OH)C(O^-)(CF_3)_2$ is 75.8 kcal mol^{-1} bigger than that for $CH_3CH_2O^-$).[13] All of these studies have focused on conformationally flexible compounds even though rigid triol **1s** is a promising type of HBN catalyst and preorganized dipoles in the active site of an enzyme are thought to play a critical role in their catalytic abilities.[15] In this paper, the energetic consequences of small model compounds derived from *myo*-inositol (**2(0) – 2(3)**, Fig. 2), a naturally occurring and renewable compound derived from corn and beans, were characterized by negative ion photoelectron spectroscopy. Their conjugate bases and chloride-bound clusters are reported along with companion computations.

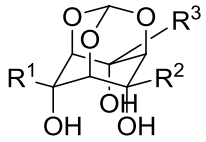

2(0): R^1, R^2, R^3 = H
2(1): R^1 = CF_3, R^2, R^3 = H
2(2): R^1, R^2 = CF_3, R^3 = H
2(3): R^1, R^2, R^3 = CF_3

Figure 2. Rigid tricyclic locked in all axial 1,3,5-cyclohexanetriol derivatives **2(0) – 2(3)**.

2.2. Experimental Section

Synthetic details and NMR spectra for **2(1)** – **2(3)** are provided in the supporting information and appendix for chapter 2, respectively, whereas **2(0)** was produced as described in the literature.[16-18]

2.2.1. Computational Methods

B3LYP[19,20] and M06-2X[21-23] geometry optimizations and subsequent vibrational frequency calculations were carried out with the 6-31+G(d,p) and aug-cc-pVDZ[24] basis sets, respectively using Gaussian 09[25] at the Minnesota Supercomputer Institute for Advanced Computational Research. M06-2X/maug-cc-pVT(+d)Z[26] single point energies were also obtained to provide adiabatic and vertical detachment energies (i.e., ADEs and VDEs) as well as cluster energies. The former two quantities are given as enthalpies at 0 K whereas the latter values were corrected to 298 K. Zero point energy (ZPE) corrected energies for the optimized structures of the anions and radicals were used to obtain the ADEs whereas non-relaxed structures for the radicals were utilized to compute the VDEs. That is, the electronic energy of the radical with the optimized geometry of the anion minus the electronic energy of the anion without any ZPE or thermal corrections afford the VDEs. Additional details (xyz coordinates, electronic energies, ZPEs and thermal corrections to 298 K) for the most stable conformers of each structure and a few higher energy species are provided in the appendix for chapter 2.

2.2.2. Photoelectron Spectroscopy

Electrospray ionization of ~10^{-3} M aqueous methanolic solutions of **2(0)** – **2(3)** afforded their $(M - 1)^-$ anions and the addition of a small amount of sodium chloride resulted in

their $(M + Cl)^-$ ions being formed. Photoelectron spectra were recorded at 20 K with an instrument that has been reported previously using ArF and F_2 excimer lasers at 193 nm (6.424 eV) and 157 nm (7.867 eV), respectively.[27] Both lasers were operated at 20 Hz to enable shot-to-shot background subtraction of each acquired spectrum. A 5.2 m flight tube was used to collect and analyze the photoelectrons which were calibrated using known spectra of I^- and $Cu(CN)_2^-$. The resulting spectra have a resolution of ~50 meV for electrons with kinetic energies of ~2.5 eV.

2.3. Results

The conjugate bases of a series of *scyllo*-inositol monoorthoformate derivatives (**2(0)** – **2(3)**) were generated by electrospray ionization and their low temperature photoelectron spectra were recorded at 157 and 193 nm. Since both sets of data are equally informative only the former results are provided in Fig. 3. These spectra display a series of broad bands that correspond to formation of the radical in its ground and excited states. Vertical detachment energies (VDEs) were obtained from the peak maxima of the lowest energy bands whereas a linear extrapolation of their rapidly growing onset region (obtained by drawing a straight line along the rising edge and adding the instrumental resolution to the crossing point with the binding energy axis) provided the ADEs. The resulting values are given in Table 1 but due to the broadness of the first bands we adopt a conservative experimental uncertainty of 0.1 eV for both the ADEs and VDEs.

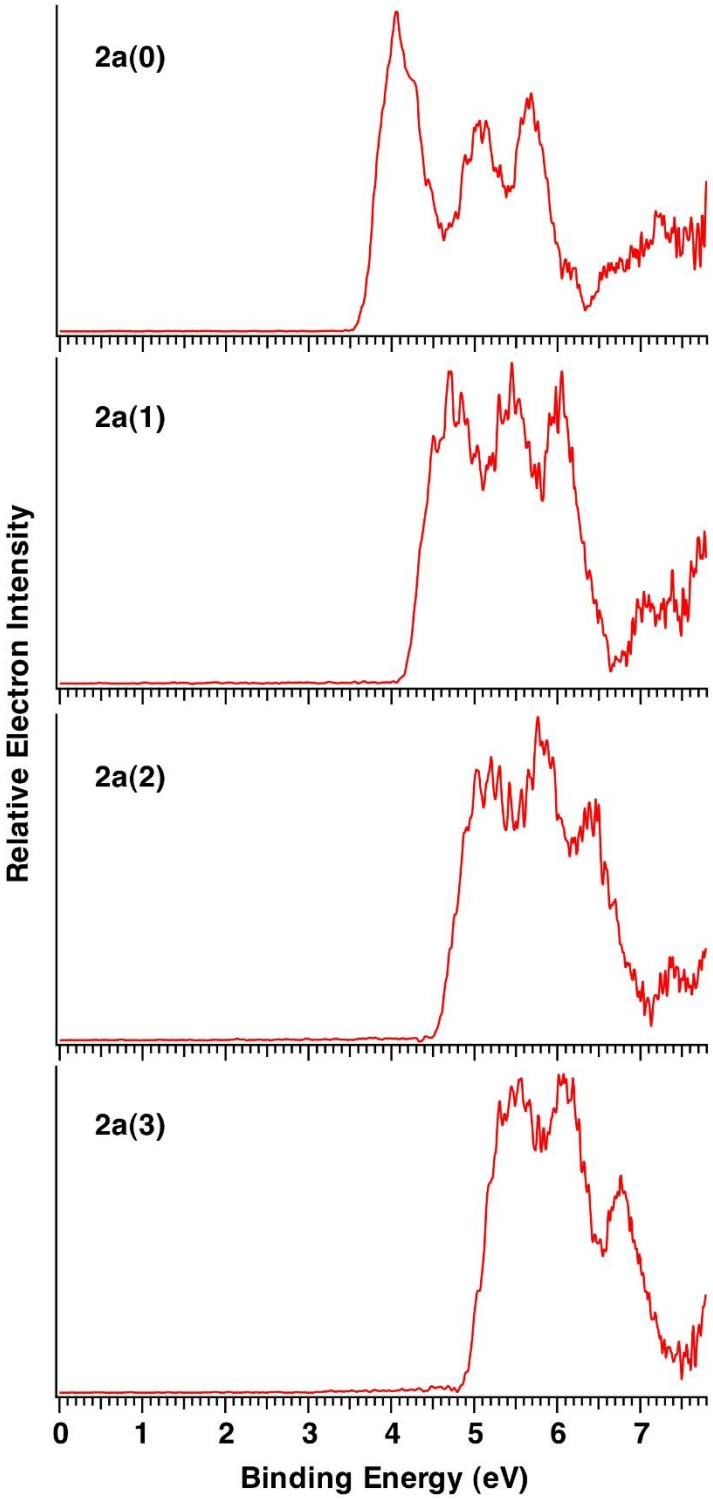

Figure 3. Low temperature (20 K) photoelectron spectra of the conjugate bases of **2(0) – 2(3)** (i.e., **2a(0) – 2a(3)**) at 157 nm (7.867 eV).

Table 1. Experimental and calculated ADEs and VDEs in eV for the conjugate bases of **2(0)** – **2(3)** and their chloride anion clusters.

Cmpd	expt[a]		B3LYP (M06-2X)[b]	
	ADE	VDE	ADE	VDE
2a(0)	3.75 ± 0.10	4.07 ± 0.10	3.39 (3.56)	3.78
2a(1)	4.28 ± 0.10	4.70 ± 0.10	3.95 (4.17)	4.32
2a(2)	4.65 ± 0.10	5.10 ± 0.10	4.34 (4.55)	4.76
2a(3)	5.00 ± 0.10	5.50 ± 0.10	4.71 (4.83)	5.10
2(0) • Cl^-	5.36 ± 0.10	5.60 ± 0.10	4.84 (5.01)	5.20
2(1) • Cl^-	5.60 ± 0.10	5.82 ± 0.10	5.12 (5.13)	5.51
2(2) • Cl^-	5.80 ± 0.10	6.05 ± 0.10	5.31 (5.43)	5.77
2(3) • Cl^-	6.00 ± 0.10	6.23 ± 0.10	5.50 (5.60)	5.99

[a]At 20 K. [b]B3LYP/6-31+G(d,p) and M06-2X/maug-cc-pVT(+d)Z//M06-2X/aug-cc-pVDZ (in parentheses) energies.

Addition of sodium chloride to an aqueous methanolic solution of triols **2(0)** – **2(3)** afforded their chloride anion clusters (**2(0)** • Cl^- – **2(3)** • Cl^-) upon electrospray ionization. The photoelectron spectra of these species were also recorded at 20 K with a F_2 excimer laser that provides 157 nm photons (Fig. 4). A single broad band is observed in these spectra and the resulting thermodynamic data are given in Table 1.

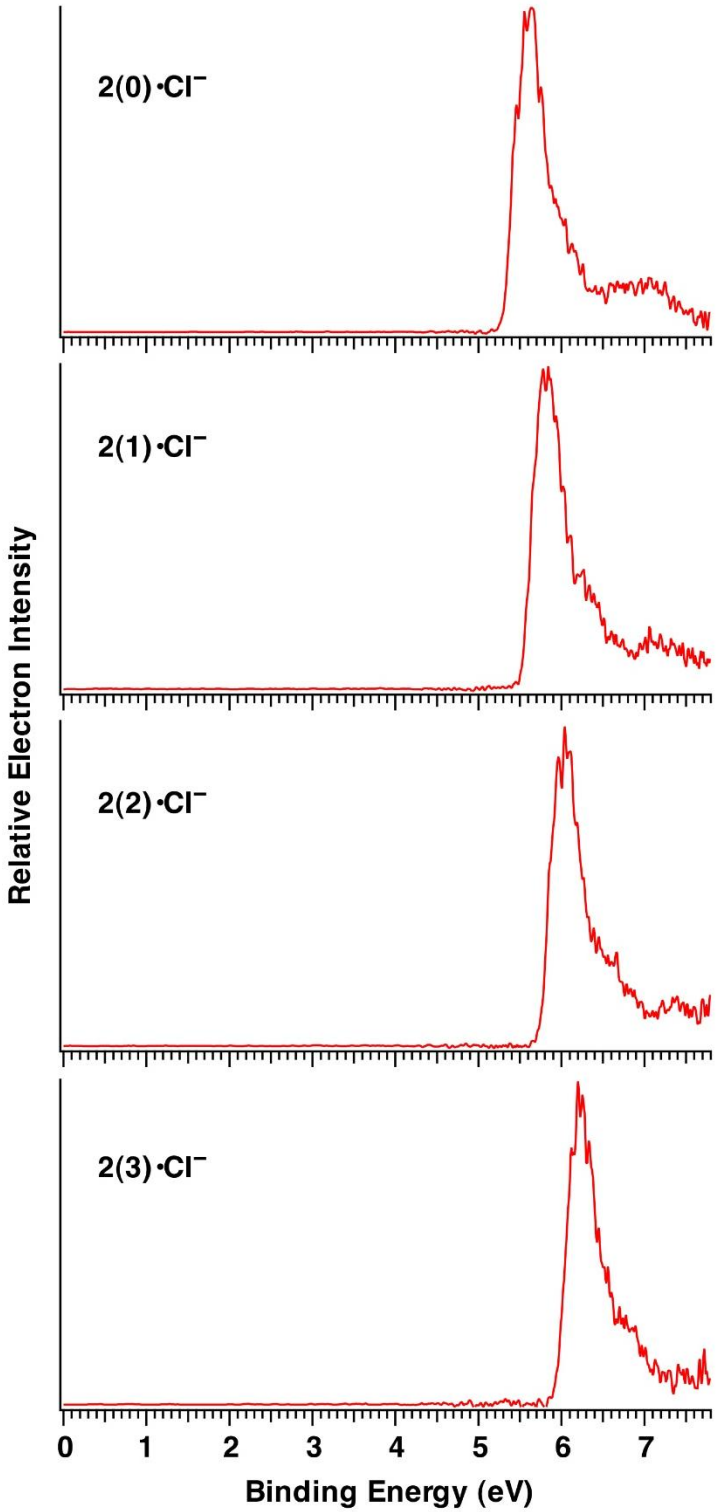

Figure 4. Low temperature (20 K) photoelectron spectra of **2(0)** • Cl^- – **2(3)** • Cl^- at 157 nm (7.867 eV).

B3LYP and M06-2X geometry optimizations were carried out with the 6-31+G(d,p) and aug-cc-pVDZ basis sets, respectively on the triols, their conjugate bases and corresponding radicals, and their chloride anion and chlorine atom clusters. The most favorable M06-2X structures for **2a(0)** – **2a(3)** and **2(0)** • Cl^- – **2(3)** • Cl^- are illustrated in Figs. 5 and 6, and the xyz Cartesian coordinates are given in the appendix for chapter 2. Single point energies with the larger maug-cc-pVT(+d)Z basis set were also computed to obtain the ADEs with the M06-2X functional since it is known to be sensitive and improve with the flexibility of the basis set.[21-23] A series of related compounds (**2'(0)** – **2'(3)**, **2''(0)**, **2''(2)**, **3**, **4(0)**, and **4(3)** in Fig. 7) were examined as well to systematically probe the energetic contributions of hydrogen bonds and inductive effects on the ADEs (Table 2).

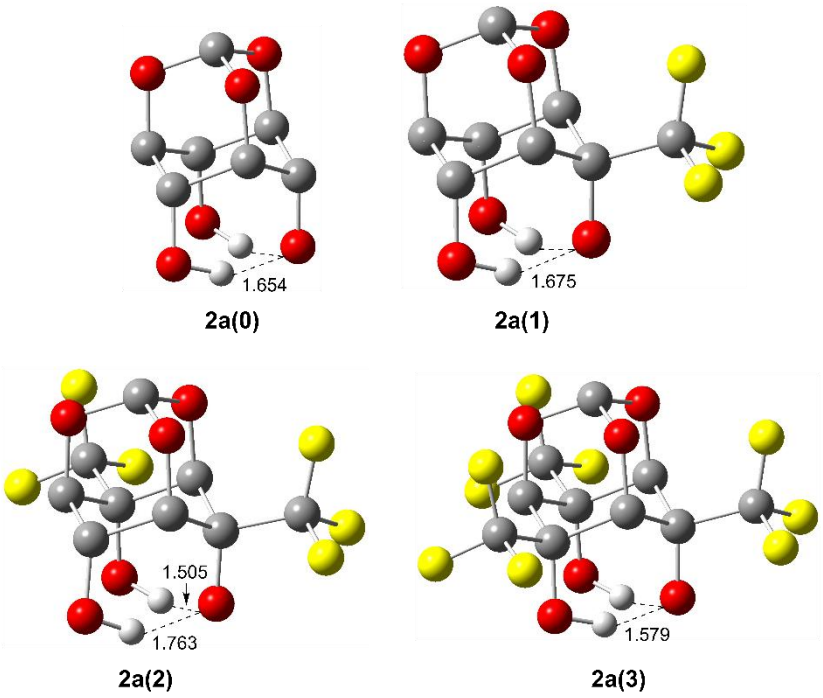

Figure 5. Lowest energy M06-2X/aug-cc-pVDZ conformers for the conjugate bases of triols **2(0) – 2(3)**. All of the structures except **2a(2)** have C_S symmetry.

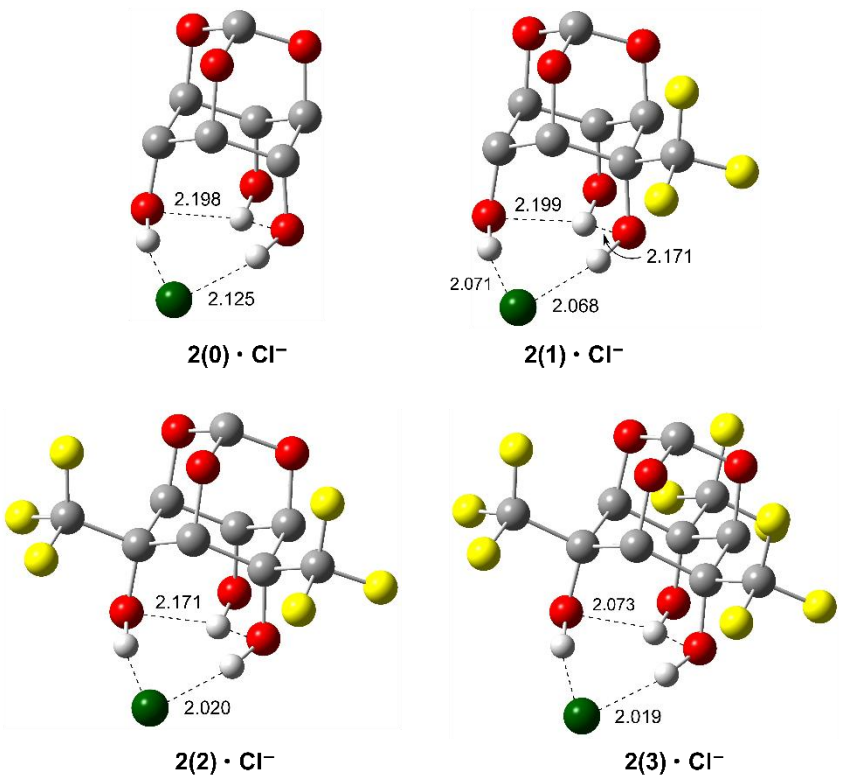

Figure 6. Most favorable M06-2X/aug-ccpVDZ geometries located for **2(0)** • Cl^- – **2(3)** • Cl^-. All of the structures except **2(1)** • Cl^- have C_S symmetry.

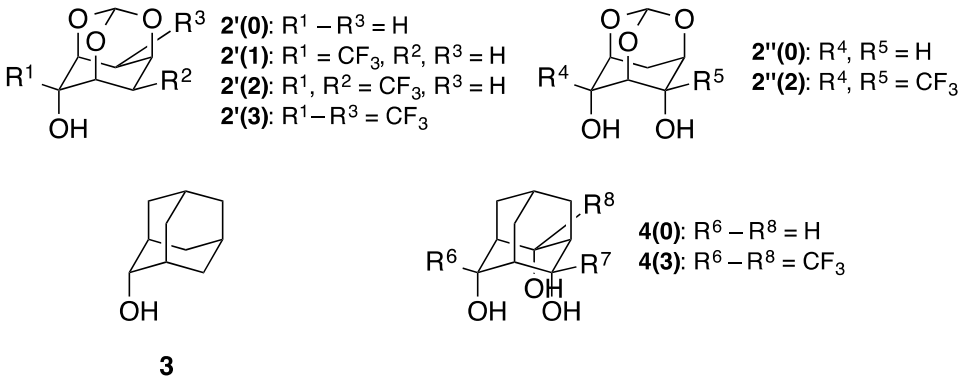

Figure 7. Polycyclic alcohols used to examine the consequences of hydrogen bonds and electron withdrawing groups on ADEs.

Table 2. M06-2X/maug-cc-pVT(+d)Z//M06-2X/aug-cc-pVDZ ADEs in eV for the conjugate bases and chloride anion clusters of a series of polycyclic alcohols.

cmpd (ROH)	ADE (eV)	
	RO^-	$ROH \bullet Cl^-$
2'(0)	2.43	4.56
2'(1)	3.16	
2'(2)	3.57	
2'(3)	3.95	
2''(0)	3.14	4.68
2''(2)	4.26	
3	1.95	4.00
4(0)	3.03	
4(3)	4.41	

2.4. Discussion

The ADEs of **2a(0)** – **2a(3)** span from 3.75 to 5.00 eV and these values are all much larger than for the conjugate bases of isopropanol (ADE($(CH_3)_2CHO^-$) = 1.847 ± 0.004 eV)[28] and trifluoroethanol (ADE($CF_3CH_2O^-$) = 2.5541 ± 0.0043 eV).[29] They generally are also bigger than the conjugates bases of strong acids such as CH_3CO_2H,[30] HNO_3,[31] $HClO_3$[32] and H_3PO_4[33] (i.e., 3.25 ± 0.01, 3.937 ± 0.014, 4.25 ± 0.10, and 4.570 ± 0.010 eV, respectively). These results indicate that the oxyanions of **2a(0)** – **2a(3)** are extensively stabilized due to the hydrogen bond networks in these ions and the electron withdrawing groups that are present. That is, the oxygen atoms in the ring skeleton and the trifluoromethyl substituents.

To assess the effect of the CF_3 groups, their sequential impact on the ADEs was found to be 0.53, 0.37, and 0.35 eV (Table 1). These energy differences are well reproduced by both B3LYP/6-31+G(d,p) and M06-2X/maug-cc-pVT(+d)Z//M06-2X/aug-cc-pVDZ computations (i.e., 0.56, 0.39, and 0.37 eV (B3LYP) and 0.61, 0.38, and 0.28 eV (M06-

2X)) and indicate that the first CF_3 substituent only has a slightly larger effect than the second and third ones. This might appear to be surprising in that the inductive effect is distance dependent and the latter two CF_3 groups are further away from the ionization site, but they enhance the acidity of the hydroxyl groups and their effect can be transmitted through the hydrogen bond network. This is analogous to resonance stabilization which takes place through conjugated π-electron systems, but represents a new long-range stabilizing mechanism.

The effect of the oxygen atoms in the ring skeleton was also considered by carrying out computations on the conjugate bases of **3**, **4(0)**, and **4(3)**. Their predicted ADEs are smaller than those for deprotonated **2'(0)**, **2(0)**, and **2(3)** by 0.48, 0.53, and 0.42 eV, respectively. Stabilization of the *scyllo*-inositol derivative **2a(0)** relative to its adamantane analog, consequently, is about the same as incorporating 1 CF_3 group into the former species (i.e., ADE(**2a(1)** – **2a(0)**) = 0.53 eV).

To evaluate the importance of the hydroxyl groups and the hydrogen bond network in **2a(0)**, its computed ADE was compared to those for **2'a(0)** and **2"a(0)**. These results reveal that incorporation of a second hydroxyl group into **2'a(0)** increases the electron binding energy by 0.71 eV (i.e., ADE(**2"a(0)** – **2'a(0)**) and the third OH substituent adds another 0.42 eV to the ADE. This leads to a total stabilization resulting from the hydrogen bond network in this rigid system of 1.13 eV. Sequential addition of trifluoromethyl groups to **2a(0)** increases the ADEs further, but due to the leveling effect the total impact of the hydroxyl groups diminishes by ~0.1 eV per CF_3 substituent (i.e., 1.01 (**2a(1)**), 0.98 (**2a(2)**), and 0.88 eV (**2a(3)**)). A total stabilization of 2.88 eV is found in going from **3a** to **2a(3)**

due to the hydrogen bonds and inductive effect in the latter species. These findings suggest that **2(3)** is a strong Brønsted acid in aprotic solvents and may be an active organic catalyst.

Triols **2(0)** – **2(3)** readily form chloride anion complexes via electrospray ionization. Their ADEs are larger than that for Cl^- (3.613577 ± 0.000044 eV)[34] by 1.75 – 2.39 eV and range from 5.36 to 6.00 eV. These large values are due to the strong clustering energies of **2(0)** – **2(3)** which are predicted to range from 1.7 to 2.3 eV (39 – 54 kcal mol^{-1}) at the M06-2X/maug-cc-pVT(+d)Z//M06-2X/aug-cc-pVDZ level. The most stable structures all have three hydrogen bonds, but contrary to expectation only two are formed to the chloride anion; the third is a bifurcated secondary hydrogen bond between the remote hydroxyl group and the two OH substituents directly interacting with the chloride anion. Structures with one and three hydrogen bonds to Cl^- were also located for **2(0)** • Cl^- but they are 1.9 and 4.9 kcal mol^{-1} less stable, respectively at the B3LYP/6-31+G(d,p) level. Direct hydrogen bonds to an anionic center typically are favored, but in this case the resulting structure with three hydrogen bonds suffers from electron - electron repulsion due to the overlap of the lone pairs of electrons on the oxygen atoms. This is the result of the rigidity and cavity size of the ring system.

Each CF_3 group increases the ADE of the cluster ion by ~ 0.2 eV and the three oxygen atoms in the ring skeleton are predicted to have a net stabilization of 0.56 eV when the substrate has just one OH substituent (i.e., ADE(**2'(0)** • Cl^-) = 4.56 eV vs ADE(**3** • Cl^-) = 4.00 eV). As for the hydrogen bond network, we estimate that the first OH group increases the ADE of chloride ion by 0.39 eV (i.e., ADE((**3** • Cl^-) – ADE(Cl^-)) whereas the second and third hydroxy substituents lead to sequential stabilizations of 0.12 and 0.33 eV. The smaller of these latter two values is due to the rigidity of the ring system and arises from

the lone pair–lone pair electron repulsion between the two oxygen atoms in **2"(0)** • Cl^- due to the formation of the two Cl^-•••HO hydrogen bonds. This destabilizing effect is alleviated by the presence of the third hydroxyl group in **2(0)**. As a result, the third OH group is energetically almost as important as the first and substantially more favorable than the second hydroxyl substituent. These results suggest that **2(3)** might function as an anion receptor and a hydrogen bond catalyst in condensed media.

2.5. Conclusions

The photoelectron spectra of a series of rigid triol $(M - 1)^-$ and $(M + Cl)^-$ anions were recorded and the structures and energetics of these species were modeled via density functional computations. Intramolecular hydrogen bonds and inductive stabilization resulting from three additional oxygen atoms and up to three trifluoromethyl groups lead to enhanced ADEs of 1.61 – 2.88 eV for the conjugate bases and 1.01 – 1.60 eV for the chloride anion clusters. These results suggest that these rigid triols may prove to be effective Brønsted hydrogen bond catalysts as well as anion molecular recognition reagents. A new long range stabilization mechanism is also suggested whereby the inductive effect is transmitted over distance via hydrogen bonds.

2.6. Supporting Information

2.6.1. General

Dess-Martin periodinane (DMP) was prepared according to previously reported procedures.[35,36] Anhydrous dichloromethane (CH_2Cl_2) and dimethylformamide (DMF) were bought from EMD Chemicals Inc. Trimethyl(trifluoromethyl)silane ($TMSCF_3$) and 2,3-dichloro-5,6-dicyano-1,4-benzoquinone (DDQ) were purchased from Matrix Scientific

and Combi-Blocks, respectively. All other reactants, reagents and solvents came from Sigma-Aldrich. Tetrahydrofuran (THF) was dried over sodium metal at reflux under an argon atmosphere using benzophenone as an indicator and was subsequently distilled. Glassware (e.g., vials, NMR tubes and flasks) was dried in ovens and allowed to cool under a stream of argon or nitrogen. Hydrogenation reactions were carried out in a 600 mL Parr stainless steel reactor. TLC analyses were performed on precoated (250 mm) silica gel 60 F-254 plates (Merck) and were visualized by staining with $KMnO_4$ or a hand-held UV lamp. Medium pressure liquid chromatography (MPLC) was carried out with a Biotage Isolera 1 in which the samples were dissolved in a minimal amount of CH_2Cl_2 and syringed on to a silica gel (Premium R_f Silica Gel, 60A, 40-75µm) column. Melting points (m.p.) were measured with a Uni-Melt apparatus (Thomas Hoover) and are uncorrected. Proton, ^{13}C, and ^{19}F NMR spectra were obtained with Varian VXR 300, VI 300 and 500 MHz, and Bruker AV 500 MHz spectrometers and are reported in ppm. In all cases, the signals were referenced to the residual solvent as follows: $CHCl_3$ = 7.27 δ (^1H), 77.0 δ (^{13}C); CHD_2CN = 1.94 δ (^1H), 1.39 δ (^{13}C) and CF_3CO_2H = -78.5 δ (^{19}F). IR spectra of neat samples were recorded on a Nicolet iS5 FT-IR spectrometer with an ATR source while mass spectra were obtained with a Bruker ESI-BioTOF. In the latter case, methanolic solutions were used and high resolution data were obtained using PEG as an internal standard.

2.6.2. Synthetic Procedures for Compounds 2(0) – 2(3)

*1-Trifluoromethyl-3,5-dibenzyloxy scyllo-inositol monoorthoformate (**6**)*: In a dry 200 mL round bottomed flask, 1.00 g (2.70 mmol) of dibenzyl alcohol **5**[16,17] was dissolved in 30 mL of dry CH_2Cl_2 under argon. Dess-Martin periodinane (DMP, 1.72 g, 4.05 mmol) was transferred to the flask all at once, and the mixture was magnetically stirred overnight

(~ 16 h). Diethyl ether (60 mL) and 50 mL of an aqueous solution consisting of 25 mL of 10% $Na_2S_2O_3$ and 25 mL of 5% $NaHCO_3$ were subsequently added and the resulting mixture was vigorously stirred with a magnetic stir bar for 15 min. Both layers were clear at this point, so they were separated and the aqueous solution was extracted with 30 mL of diethyl ether. The combined organic material was washed with 20 mL of brine, dried over Na_2SO_4 and concentrated under reduced pressure to afford 0.95 g (95%) of a white solid. Its IR spectrum had a band at 1759 cm^{-1} for the ketone and an OH stretch at 3463 cm^{-1}, but it was used without further purification in the next step.

In a 100 mL round bottomed flask containing 0.880 g (2.39 mmol) of the resulting ketone in 20 mL of THF, 0.710 mL (0.680 g, 4.78 mmol) of $TMSCF_3$ was added under argon at room temperature. This solution was then cooled to 0 ˚C and 35.0 μL (35.0 μmol) of 1.00 M TBAF solution in THF was added in one portion. The stirred reaction mixture was slowly allowed to warm to room temperature overnight and then more TBAF (7.20 mL, 7.20 mmol) was added. After stirring the reaction mixture for an additional 45 min, it was concentrated under reduced pressure. The resulting material was dissolved in 20 mL of diethyl ether and passed through a small plug of silica gel. More ether (50 mL) was used to wash the silica gel, and the combined organic material was concentrated under reduced pressure. A light brown solid was obtained and it was purified by MPLC (5/95 EtOAc/hexanes to 40/60 EtOAc/hexanes) to afford 0.60 g (51% overall) of a white solid (R_f = 0.42 in 20/80 EtOAc/hexanes, m.p. 124 – 126 ˚C). ^{1}H NMR (500 MHz, $CDCl_3$) δ 7.35 – 7.28 (m, 6H), 7.26 – 7.22 (m, 4H), 5.54 (s, 1H), 5.41 (s, 1H), 4.69 (d, *J* = 10.8 Hz, 2H), 4.65 (d, *J* = 11.2 Hz, 2H), 4.61 (m, 3H), 4.52 (dd, *J* = 3.4, 3.5 Hz, 2H). ^{13}C (75 MHz, $CDCl_3$) δ 136.1, 128.6, 128.3, 128.1, 124.0 (q, *J* = 284 Hz), 102.1, 73.6, 72.0, 69.4 (q, *J* =

28.4 Hz), 67.5, 67.2. ^{19}F (282 MHz, $CDCl_3$) δ -82.0. IR (ATR source) 3416, 3035, 2917 cm^{-1}. HRMS-ESI: calc for $C_{22}H_{21}F_3NaO_6^+$ $(M + Na)^+$ 461.1199, found 461.1182.

*1-Trifluoromethyl scyllo-inositol monoorthoformate (**2**)*: Dibenzyl alcohol **6** (0.60 g, 1.40 mmol) was dissolved in 10 mL of THF in a 50 mL round bottomed flask and 0.20 g of 20% $Pd(OH)_2$ on carbon was added. This flask was placed in a hydrogenation reactor and evacuated and then charged with hydrogen to a pressure of 100 psi three times in succession. The resulting reaction mixture was stirred with a magnetic stir bar at room temperature overnight and then was vented. Diethyl ether (30 mL) was added and the solution was filtered through a small plug of silica gel. After rinsing the silica gel twice with 20 mL portions of diethyl ether, the combined ethereal solution was concentrated under reduced pressure to obtain a white solid. It was washed with a minimal amount of chloroform to afford 0.24 g (69%) of **2** (m.p. 115 – 117 ˚C). ^{1}H NMR (500 MHz, CD_3CN) δ 5.49 (s, 1H), 5.27 (br s, 1H), 4.54 (m , 2H), 4.40 (dd, *J* = 1.5, 4.4 Hz , 2H), 4.30 (m, 1H), 4.14 (br s, 2H). ^{13}C (75 MHz, CD_3CN) δ 125.6 (q, *J* = 284 Hz), 102.5, 71.8, 70.8 (q, *J* = 27.5 Hz), 69.8, 68.4. ^{19}F (282 MHz, CD_3CN) δ -82.6. IR (ATR source) 3471, 3432, 3305, 3058, 2983, 2939, 2924 cm^{-1}. HRMS-ESI: calc for $C_8H_8F_3O_6^-$ $(M – H)^-$ 257.0278, found 257.0258.

*3-tert-Butyldimethylsilyloxy-5-p-methoxybenzyloxy myo-inositol monoorthoformate (**8**)*: Diol **7**[18] (18.0 g, 59.1 mmol) was dissolved in 200 mL of anhydrous DMF in a 500 mL round bottomed flask under argon. This solution was cooled to 0 ˚C and 2.60 g (65.0 mmol) of NaH (60% dispersion in oil) was added in several portions. After 30 min of stirring 8.87 mL (10.2 g, 65.0 mmol) of *p*-methoxybenzyl chloride (PMBCl) was added over the course of 3 min. The resulting reaction mixture was allowed to warm to room temperature

overnight and then was quenched by slowly adding 10 mL of saturated aqueous NH_4Cl. Concentration of this solution under vacuum at 60 ˚C resulted in a residue that was rinsed and filtered 3 times with 200 mL portions of diethyl ether. The combined organic material was successively washed with 50 mL of water and 50 mL of brine, and then was dried over Na_2SO_4. Rotary evaporation of the solvent resulted in an oil which was purified by MPLC (5/95 EtOAc/hexanes to 50/50 EtOAc/hexanes) to afford 19.0 g (76%) of an oily, viscous and colorless compound which upon standing overnight formed white crystals (R_f = 0.48 in 25/75 EtOAc/hexanes, m.p. 68 – 70 ˚C). ^{1}H NMR (500 MHz, $CDCl_3$) δ 7.24 (m, 2H), 6.91 (m, 2H), 5.49 (d, *J* = 1.5 Hz, 1H), 4.60 (s, 2H), 4.45 – 4.40 (m, 1H), 4.37 (m, 1H), 4.23 – 4.19 (m, 2H), 4.14 – 4.10 (m, 2H), 3.83 (s, 3H), 3.70 (d, *J* = 10 Hz, 1H), 0.953 (s, 9H), 0.157 (s, 3H), 0.153 (s, 3H). ^{13}C NMR (125 MHz, $CDCl_3$) δ 160.0, 129.8, 128.0, 114.2, 102.5, 74.9, 74.4, 72.8, 72.6, 68.3, 67.5, 60.9, 55.3, 25.9, 18.4, -4.6, -4.7. IR (ATR source) 3472, 3009, 2956, 2932, 2855 cm^{-1}. HRMS-ESI: calc for $C_{21}H_{32}NaO_7Si^+$ $(M + Na)^+$ 447.1831, found 447.1815.

*3-tert-Butyldimethylsilyloxy-2-benzyloxy-5-p-methoxybenzyloxy scyllo-inositol mono-orthoformate (**9**)*: Silyl ether **8** (18.7 g, 44.0 mmol) was dissolved in 120 mL of dry THF in a 500 mL round bottomed flask under argon. Sodium hydride (3.50 g of a 60% dispersion in oil, 88.0 mmol) was slowly added to the flask at 0 ˚C with stirring. Benzyl bromide (BnBr, 10.3 mL, 15.1 g, 88.0 mmol) was slowly syringed into the flask 30 min later and the resulting solution was stirred overnight and allowed to warm to room temperature. Water (10 mL) was used to quench the reaction and then it was concentrated under reduced pressure. The flask and the residue were rinsed twice with 100 mL portions of diethyl ether and the combined organic material was extracted with 50 mL of water, 50 mL of brine, and

then dried with Na_2SO_4. Concentration under reduced pressure afforded an oily residue that was purified by MPLC (5/95 EtOAc/hexanes to 25/75 EtOAc/hexanes) to afford 19.0 g (83%) of **9** as a viscous and colorless oil (R_f = 0.63 in 25/75 EtOAc/hexanes). ^{1}H NMR (500 MHz, $CDCl_3$) δ 7.33 – 7.25 (m, 5H), 7.19 (m, 2H), 6.81 (m, 2H), 5.53 (d, *J* = 1.5 Hz, 1H), 4.66 (d, *J* = 12.0 Hz, 1H), 4.59 (d, *J* = 7.0 Hz, 1H), 4.57 (d, *J* = 7.0 Hz, 1H), 4.51 (d, *J* = 11.5, 1H), 4.39 (m, 2H), 4.32 (m, 2H), 4.15 (m, 1H), 4.12 (m, 1H), 3.81 (s, 3H), 0.935 (s, 9H), 0.134 (s, 6H). ^{13}C NMR (125 MHz, $CDCl_3$) δ 159.2, 137.7, 129.7, 129.1, 128.4, 127.7, 127.4, 113.7, 103.1, 74.2, 73.9, 73.3, 73.2, 71.4, 71.3, 68.0, 61.7, 55.2, 26.0, 18.4, -4.6. IR (ATR source) 3064, 3030, 3006, 2955, 2928, 2855 cm^{-1}. HRMS-ESI: calc for $C_{28}H_{38}NaO_7Si^+$ $(M+Na)^+$ 537.2284, found 537.2305.

*1-Trifluoromethyl-1-trimethylsilyloxy-3-benzyloxy-5-p-methoxybenzyloxy scyllo-inositol monoorthoformate (**10**)*: In a 500 mL round bottomed flask, 100 mL of a 1.0 M TBAF solution in THF was added in one portion with stirring to 18.5 g (35.9 mmol) of **9** in 50 mL of anhydrous THF under argon. After 45 min, the THF was removed under reduced pressure and the residue was dissolved in 200 mL of diethyl ether. This solution was filtered through a plug of silica gel which was then rinsed with 200 mL of diethyl ether. Concentration of the combined solutions under reduced pressure afforded 14.0 g (97%) of the TBS deprotected alcohol as white crystals (R_f = 0.13 in 25/75 EtOAc/hexanes). Their IR spectrum had a band at 3461 cm^{-1} and they were used in the next step without further purification.

In a 500 mL round bottomed flask, 100 mL of CH_2Cl_2 and 1.95 mL (2.92 g, 23.0 mmol) of oxalyl chloride were mixed at room temperature under an inert atmosphere. After cooling to -78 ^{o}C, 3.25 mL (3.59 g, 46.0 mmol) of anhydrous DMSO was syringed into

the flask in one portion and 5 min later 4.60 g (11.5 mmol) of the TBS deprotected alcohol in 200 mL of CH_2Cl_2 was added through a cannula over the course of 30 min. Triethylamine (16.0 mL, 11.6 g, 115 mmol) was slowly added an hour later and after an additional 45 min the reaction mixture was allowed to warm to room temperature. Removal of the solvent under reduced pressure led to a solid residue that was partially dissolved with 150 mL of diethyl ether, and this solution was filtered through a small plug of silica gel. An additional 200 mL of ether was used to rinse the silica gel and the combined organic material was concentrated under reduced pressure. The resulting oil was purified by MPLC (15/85 EtOAc/hexanes to neat EtOAc) to afford 4.00 g (87%) of a colorless and viscous oil that turned to a solid upon standing overnight. Its IR spectrum had a carbonyl stretch at 1755 cm^{-1} and this compound was used in the next step without further purification.

In a 200 mL round bottomed flask, 3.50 g (8.79 mmol) of the intermediate ketone was dissolved in 40 mL of anhydrous THF under an argon atmosphere. Trimethyl(trifluoromethyl)silane ($TMSCF_3$, 2.60 mL, 2.50 g, 17.6 mmol) was added to the room temperature solution and then was cooled with an ice-water bath. Tetrabutylammonium fluoride in THF (1.0 M, 0.26 mL) was syringed into the flask in one portion and then the reaction mixture was allowed to warm up to room temperature overnight. Removal of the solvent under reduced pressure afforded an oily residue that was dissolved in 50 mL of diethyl ether and filtered through a small plug of silica gel. The latter material was washed with 100 mL of diethyl ether and the combined ethereal solution was concentrated under reduced pressure. Purification of the residue by MPLC (5/95 EtOAc/hexanes to 30/70 EtOAc/hexanes) gave 3.50 g (74%) of **10** as a white crystalline compound (R_f = 0.52 in 14/86 EtOAc/hexanes, m.p. 90 – 92 ˚C). ^1H NMR (500 MHz,

$CDCl_3$) δ 7.38 – 7.31 (m, 5H), 7.28 (m, 2H), 6.88 (m, 2H), 5.44 (s, 1H), 4.66 (d, *J* = 11.9 Hz, 1H), 4.59 (d, *J* = 11.1 Hz, 2H), 4.54 (d, *J* = 11.6 Hz, 1H), 4.48 – 4.44 (m, 2H), 4.37 – 4.33 (m, 3H), 3.83 (s, 3H), 0.030 (s, 9H). ^{13}C NMR (125 MHz, $CDCl_3$) δ 159.4, 137.4, 129.9, 129.4, 128.4, 128.2, 127.9, 125.0 (q, *J* = 289 Hz), 113.7, 102.4, 73.6, 73.2, 71.7, 71.4, 70.4 (q, *J* = 27.1 Hz), 68.9, 68.7, 68.0, 55.3, 1.62 (q, *J* = 1.8 Hz). ^{19}F (471 MHz, $CDCl_3$) δ -78.5. IR (ATR source) 3094, 3070, 3020, 2957, 2937, 2903, 2865, 2842 cm^{-1}. HRMS-ESI: calc for $C_{26}H_{31}F_3NaO_7Si^+$ $(M + Na)^+$ 563.1689, found 563.1704.

*5-Trifluoromethyl-5-trimethylsilyloxy-3-benzyloxy scyllo-inositol monoorthoformate (**11**)*: In a 250 mL round bottomed flask, 2.80 g (5.18 mmol) of **10**, 50 mL of CH_2Cl_2, 2.35 g (10.7 mmol) of DDQ, and 2.5 mL of water were sequentially added at room temperature under argon. After 3 h, the dark orange solution was decanted and the precipitate in the flask was rinsed with 100 mL of diethyl ether. The combined organic material was washed with 50 mL of saturated $NaHCO_3$ followed by 50 mL of water. It was then vigorously stirred with a 100 mL of saturated $NaHSO_3$ in a 500 mL round bottomed flask using a stir bar until the solution turned very light yellow (~ 30 min). The organic layer was separated and the water phase was extracted with 50 mL of diethyl ether. The combined non-aqueous solution was dried over Na_2SO_4, concentrated under reduced pressure, and the resulting oily residue was purified by MPLC (5/95 EtOAc/hexanes to 30/70 EtOAc/hexanes) to afford 1.90 g (87%) of **11** as a white solid (R_f = 0.43 in 14/86 EtOAc/hexanes, m.p. 103 – 105 ˚C). ^{1}H NMR (500 MHz, $CDCl_3$) δ 7.40 – 7.34 (m, 5H), 5.47 (s, 1H), 4.70 (d, *J* = 11.8 Hz, 1H), 4.65 (d, *J* = 11.3 Hz, 1H), 4.54 (m, 1H), 4.50 – 4.43 (m, 4H), 3.80 (d, *J* = 12.3 Hz, 1H), 0.080 (s, 9H). ^{13}C NMR (75 MHz, $CDCl_3$) δ 135.9, 129.0, 128.7, 124.0 (q, *J* = 289 Hz), 110.3, 101.9, 73.8, 72.7, 71.5 (q, *J* = 27.4 Hz), 69.3, 68.7, 68.2, 67.7, 1.24. ^{19}F

NMR (282 MHz, $CDCl_3$) δ -78.2. IR (ATR source) 3512, 3494, 3060, 3031, 2973, 2960, 2942, 2905, 2885 cm^{-1}. HRMS-ESI: calc for $C_{18}H_{23}F_3NaO_6Si^+$ $(M + Na)^+$ 443.1114, found 443.1126.

*1,3-Trifluoromethyl-5-benzyloxy scyllo-inositol (**12**)*: Alcohol **11** (1.00 g, 2.40 mmol) was dissolved in 20 mL of dry CH_2Cl_2 in a 100 mL round bottomed flask under argon. Sodium bicarbonate (2.00 g, 24.0 mmol) and 1.52 g (3.60 mmol) of DMP were rapidly added in succession and the reaction mixture was stirred at room temperature for 16 hrs. Diethyl ether (50 mL), 10% aqueous $Na_2S_2O_3$ (15 mL) and 5% aqueous $NaHCO_3$ (15 mL) were then added and after 20 min of stirring the cloudy organic layer became clear. It was separated from the aqueous phase and the later was extracted with 25 mL of diethyl ether. The combined organic material was washed with 20 mL of brine, dried over Na_2SO_4 and concentrated under reduced pressure to afford an oily residue. Purification by MPLC (5/95 EtOAc/hexanes to 40/60 EtOAc/hexanes) gave 0.82 g (82%) of the intermediate ketone as a white solid. Its IR spectrum had a carbonyl absorption at 1764 cm^{-1} and a residual OH stretch at 3406 cm^{-1}, but it was used in the next step without further purification.

The intermediate ketone (0.820 g, 2.00 mmol) was dissolved in 4.0 mL of dry THF in a 25 mL round bottomed flask under an inert argon atmosphere. Trimethyl-(trifluoromethyl)silane (0.580 mL, 0.557 g, 3.92 mmol) was added at room temperature in one portion and then the flask was cooled to 0 ˚C. A solution of 1.0 M TBAF in THF (0.040 mL) was syringed into the flask all at once and the reaction mixture was allowed to warm up to room temperature overnight. To remove both TMS protecting groups, an additional 5.90 mL of the 1.00 M TBAF solution was added to the reaction flask. After 30 min, the solvent was removed under reduced pressure and 20 mL of diethyl ether was added. This

solution was passed through a plug of silica gel which was then rinsed with 100 mL of diethyl ether. The combined organic material was concentrated under reduced pressure and the resulting oily residue was purified by MPLC (5/95 EtOAc/hexanes to 30/70 EtOAc/hexanes) to afford 0.640 g (57% overall) of **12** as a white solid. A small sample was recrystallized with hexanes for characterization purposes (R_f = 0.58 in 25/75 EtOAc/hexanes, m.p. 120 – 122 ˚C). ^{1}H NMR (500 MHz, $CDCl_3$) δ 7.44 – 7.37 (m, 3H), 7.36 – 7.32 (m, 2H), 5.56 (s, 1H), 4.74 (s, 2H), 4.64 (t, *J* = 1.8 Hz, 1H), 4.59 – 4.55 (m, 3H), 4.38 (s, 1H). ^{13}C NMR (125 MHz, $CDCl_3$) δ 135.2, 129.03, 128.97, 123.0 (q, *J* = 285 Hz), 128.4, 101.4, 73.6, 72.8, 70.3 (q, *J* = 28.9 Hz), 67.0, 66.8. ^{19}F NMR (471 MHz, $CDCl_3$) δ -81.1 ppm. IR (ATR source) 3344, 3059, 3034, 2978, 2960, 2926, 2877 cm^{-1}. HRMS-ESI: calc for $C_{16}H_{13}F_6O_6^-$ $(M - H)^-$ 415.0622, found 415.0610.

*1,3-Trifluoromethyl scyllo-inositol monoorthoformate (**3**)*: In a 25 mL round bottomed flask, 0.600 g (1.44 mmol) of diol **12**, 6.0 mL of THF, and 0.200 g of 20% $Pd(OH)_2$ on carbon were added and the flask was placed in a hydrogenation apparatus. The reactor was evacuated and charged with hydrogen to a pressure of 500 psi three times in succession and then was magnetically stirred overnight. After releasing the pressure, the reaction mixture was diluted with 10 mL of diethyl ether and passed through a small plug of silica gel. An additional 30 mL of diethyl ether was used to wash the silica gel and the combined material was concentrated under reduced pressure. The resulting oily residue was purified by MPLC (neat CH_2Cl_2 to 20/80 MeOH/CH_2Cl_2) to afford 0.400 g (85%) of triol **3** as a white solid (R_f = 0.57 in 10/90 MeOH/ CH_2Cl_2) = 0.57, m.p. 158 – 160 ˚C). ^{1}H NMR (500 MHz, CD_3CN) δ 5.57 (s, 1H), 5.31 (s, 2H), 4.68 (dt, *J* = 3.9, 4.4 Hz, 1H), 4.60 (t, *J* = 2.0 Hz, 1H), 4.48 (dd, *J* = 2.0, 3.4 Hz, 2H), 4.43 (br d, *J* = 5.4 Hz, 1H). ^{13}C NMR (75 MHz,

CD_3CN) δ 125.0 (q, *J* = 285 Hz), 102.0, 71.3 (q, *J* = 27.9 Hz), 69.5, 68.0, 67.7. ^{19}F NMR (282 MHz, CD_3CN) δ -80.2 IR (ATR source) 3438, 3367, 2981, 2954, 2929 cm^{-1}. HRMS-ESI: calc for $C_9H_7F_6O_6^-$ $(M - H)^-$ 325.0152, found 325.0144.

*1-Trifluoromethyl-3-tert-butyldimethylsilyloxy-5-p-methoxybenzyloxy myo-inositol mo-noorthoformate (**13**)*: Anhydrous dichloromethane (240 mL) and 2.49 mL (3.68 g, 29.0 mmol) of oxalyl chloride were mixed in a 1.0 L round bottomed flask under a flow of argon. After cooling to -78 ˚C, 4.12 mL (4.53 g, 58.0 mmol) of anhydrous DMSO was syringed into the flask all at once and the resulting solution stirred for 5 min. Alcohol **8** (6.00 g, 14.0 mmol) was dissolved in 400 mL of anhydrous CH_2Cl_2 under argon and slowly transferred to the 1.0 L round bottomed flask through a cannula with a positive pressure of argon over the course of 45 min. The reaction mixture was stirred at -78 ˚C for 1 h and then 19.5 mL (14.2 g, 140 mmol) of TEA was slowly added via syringe over 5 min while the reaction mixture was allowed to warm up to room temperature over ~ 45 min. The solvent was removed under reduced pressure at room temperature to obtain a yellow solid residue which was rinsed twice with 100 mL portions of diethyl ether and filtered through a plug of silica gel. The silica was washed with an additional 200 mL of diethyl ether and the combined ethereal solution was concentrated under reduced pressure. An oily residue resulted which was purified by MPLC (5/95: EtOAc/hexanes to 50/50: EtOAc/hexanes) to afford 5.50 g (92%) of the corresponding ketone as a light yellow oil. Its IR spectrum had a band at 1766 cm^{-1} for the ketone and an OH stretch at 3452 cm^{-1}, but it was used in the next step without further purification.

The ketone intermediate (5.50 g, 13.0 mmol) was dissolved in 55 mL of dry THF in a 200 mL round bottomed flask under argon. Trimethyl(trifluoromethyl)silane ($TMSCF_3$,

4.80 mL, 4.69 g, 33.0 mmol) was added and then the reaction mixture was cooled to 0 ˚C. Tetrabutylammonium fluoride in THF (1.00 M, 0.150 mL) was syringed into the flask all at once and the reaction mixture was stirred while it was allowed to warm up to room temperature overnight. To selectively remove the TMS protecting group, the THF was removed under reduced pressure and 100 mL of anhydrous methanol and 12.0 g (84.0 mmol) of K_2CO_3 were then added to the flask. The resulting suspension was stirred for 5 h and then the methanol was removed under reduced pressure at room temperature. The solid residue was rinsed with 150 mL of diethyl ether and the ethereal solution was successively washed with 50 mL of water and 50 mL of brine. The aqueous layer was extracted with 100 mL of diethyl ether and the combined ethereal solution was dried over Na_2SO_4. It was concentrated under reduced pressure, and the residue was purified by MPLC (5/95: EtOAc/hexanes to 25/75: EtOAc/hexanes) to afford 4.40 g (64% overall) of alcohol **13** as a colorless viscous oil (R_f = 0.49 in 20/80: EtOAc/hexanes). ^{1}H NMR (500 MHz, $CDCl_3$) δ 7.25 (m, 2H), 6.92 (m, 2H), 5.50 (d, *J* = 1.2 Hz, 1H), 5.06 (s, 1H), 4.65 (s, 2H), 4.43 (dd, *J* = 4.0, 4.0 Hz, 1H), 4.28 (ddd, *J* = 1.5, 3.7, 3.7 Hz, 1H), 4.25 (dd, *J* = 1.8, 3.1 Hz, 1H), 4.20 (dd, *J* = 1.9, 4.0 Hz, 1H), 4.07 (m, 1H), 3.84 (s, 3H), 0.951 (s, 9H), 0.159 (s, 3H), 0.149 (s, 3H). ^{13}C NMR (125 MHz, $CDCl_3$) δ 160.2, 130.0, 127.2, 124.0 (q, *J* = 283 Hz), 114.4, 102.2, 73.8, 73.5, 72.6, 72.0, 70.3 (q, *J* = 28.0 Hz), 65.8, 61.4, 55.3, 25.8, 18.3, -4.7, -4.8. ^{19}F NMR (471 MHz, $CDCl_3$) δ -81.0. IR (ATR source) 3391, 2953, 2929, 2885, 2856 cm^{-1}. HRMS-ESI: calc for $C_{22}H_{31}F_3NaO_7Si^+$ $(M + Na)^+$ 515.1689, found 515.1691.

*1-Trifluoromethyl-1-benzyloxy-3-tert-butyldimethylsilyloxy-5-p-methoxybenzyl myo-inositol monoorthoformate (**14**)*: In a 200 mL round bottomed flask, 4.40 g (8.90 mmol) of **13** was dissolved in 60 mL of anhydrous DMF under argon. After cooling to 0 ˚C, 0.704 g

(17.6 mmol) of NaH (60% dispersion in mineral oil) was added portion wise and the resulting solution was stirred for 30 min. Benzyl bromide (BnBr, 2.08 mL, 3.01 g, 17.6 mmol) was added over the course of 1 min and then the reaction mixture was allowed to warm up to room temperature. After 2 h of stirring, 10 mL of saturated NH_4Cl was slowly added and the resulting solution was concentrated under vacuum at 60 ˚C. The gummy residue was rinsed with 200 mL of diethyl ether and the latter was successively washed with 50 mL of water and twice with 30 mL portions of brine. The aqueous phase was extracted with 50 mL of diethyl ether and the combined organic material was dried over Na_2SO_4 and concentrated under reduced pressure. The oily residue was purified by MPLC (hexanes to 20/80: EtOAc/hexanes) to afford 4.30 g (83%) of **14** as a colorless viscous oil (R_f = 0.26 in 10/90: EtOAc/hexanes). ^{1}H NMR (500 MHz, $CDCl_3$) δ 7.26 – 7.23 (m, 3H), 7.22 – 7.19 (m, 2H), 7.10 (m, 2H), 6.82 (m, 2H), 5.58 (d, *J* = 1.2 Hz, 1H), 4.82 (d, *J* = 10.4 Hz, 1H), 4.74 (ddd, *J* = 1.9, 3.7, 3.7 Hz, 1H), 4.62 (d, *J* = 10.1 Hz, 1H), 4.50 (m, 1H), 4.51 (d, *J* = 11.3 Hz, 1H), 4.46 (d, *J* = 11.6 Hz, 1H), 4.41 (dd, *J* = 3.7, 3.7 Hz, 1H), 4.24 (dd, *J* = 1.9, 4 Hz, 1H), 4.09 (m, 1H), 3.81 (s, 3H), 0.938 (s, 9H), 0.134 (s, 3H), 0.116 (s, 3H). ^{13}C NMR (125 MHz, $CDCl_3$) δ 159.6, 137.1, 129.7, 128.8, 128.0, 127.4, 127.0, 124.5 (q, *J* = 291), 114.0, 102.9, 74.1, 79.3 (q, *J* = 25.3), 72.6, 72.4, 72.1, 67.5, 66.9, 62.0, 55.2, 25.9, 18.4, -4.7, -4.8. ^{19}F NMR (471 MHz, $CDCl_3$) δ -75.3. IR (ATR source) 3067, 3033, 2955, 2931, 2897, 2858 cm^{-1}. HRMS-ESI: calc for $C_{29}H_{37}F_3NaO_7Si^+$ $(M + Na)^+$ 605.2158, found 605.2154.

*3-Trifluoromethyl-3-benzyloxy-5-tert-butyldimethylsilyloxy myo-inositol monoortho-formate (**15**)*: In a 200 mL round bottomed flask, 4.00 g (6.90 mmol) of silyl ether **14** was dissolved in 100 mL of CH_2Cl_2 and then 3.29 g (14.9 mmol) of DDQ and 5 mL of water

were added under argon. After 17 h of stirring, the reaction mixture was decanted and the orange precipitate was rinsed twice with 50 mL portions of CH_2Cl_2. The combined organic material was washed with 100 mL of saturated $NaHCO_3$ and then vigorously stirred with 150 mL of saturated $NaHSO_3$ in a 500 mL round bottomed flask until the organic solution turned very light yellow (~ 30 min). The aqueous solution was separated and extracted with 50 mL of CH_2Cl_2. The combined organic material was dried over Na_2SO_4 and concentrated under reduced pressure and the gummy residue was dissolved in 100 mL of THF/MeOH (1/1). After cooling to 0 ˚C, 2.60 g (69.0 mmol) of $NaBH_4$ was slowly added and the reaction mixture was stirred for 30 min at room temperature. The organic material was concentrated under reduced pressure and the yellow oily residue was rinsed three times with 60 mL portions of diethyl ether. The ethereal solution was washed with 50 mL of water and 50 mL of brine, dried over Na_2SO_4, and concentrated under reduced pressure. Purification of the oily residue by MPLC (5/95: EtOAc/hexanes to 25/75: EtOAc/hexanes) resulted in 2.30 g (72%) of alcohol **15** as a white solid (R_f = 0.39 in 20/80: EtOAc/hexanes, m.p. 96 – 98 ˚C) . ^{1}H NMR (500 MHz, $CDCl_3$) δ 7.43 – 7.37 (m, 3H), 7.32 - 7.29 (m, 2H), 5.57 (d, *J* = 1.2 Hz, 1H), 4.82 (d, *J* = 9.8 Hz, 1H), 4.60 (dd, *J* = 1.9, 4.0 Hz, 1H), 4.56 (d, *J* = 10.1 Hz, 1H), 4.49 (m, 1H), 4.46 (ddd, *J* = 1.9, 3.7, 3.7 Hz, 1H), 4.23 (dd, *J* = 1.8, 3.4 Hz, 1H), 4.11 (m, 1H), 3.38 (d, *J* = 9.8 Hz, 1H), 0.980 (s, 9H), 0.194 (s, 3H), 0.181 (s, 3H). ^{13}C NMR (125 MHz, $CDCl_3$) δ 134.8, 129.1, 127.9, 124.0 (q, *J* = 288.9), 102.4, 75.6 (q, *J* = 26.2 Hz), 74.3, 70.6, 68.2, 67.7, 67.6, 61.2, 25.7, 18.2, -4.45, -4.50. ^{19}F NMR (471 MHz, $CDCl_3$) δ -73.1. IR (ATR source) 3381, 2956, 2932, 2888, 2860 cm^{-1}. HRMS-ESI: calc for $C_{21}H_{29}F_3NaO_6Si^+$ $(M + Na)^+$ 485.1583, found 485.1577.

*1,3-Bis(trifluoromethyl)-3-benzyloxy-5-tert-butyldimethylsilyloxy myo-inositol mono-orthoformate (**16**)*: In a 200 mL round bottomed flask, 2.20 g (4.80 mmol) of **15** was dissolved in 80 mL of CH_2Cl_2 under argon. Dess-Martin periodinane (2.50 g, 5.80 mmol) was added and the resulting cloudy solution was stirred at room temperature overnight (~ 16 hrs). To work up the reaction, 60 mL of CH_2Cl_2 was removed under reduced pressure and 100 mL of diethyl ether and 60 mL of an aqueous solution consisting of 30 mL of 10% $Na_2S_2O_3$ and 30 mL of 5% $NaHCO_3$ were added. This mixture was vigorously stirred until the organic layer became clear (~ 15 min). The aqueous layer was extracted with 100 mL of diethyl ether and the combined organic material was washed with 30 mL of brine and dried over Na_2SO_4. Concentration of the solution under reduced pressure and purification of the resulting residue by MPLC (5/95 EtOAc/hexanes to 25/75 EtOAc/hexanes) afforded 1.90 g (86%) of the TBS-protected ketone as a white solid. Its IR spectrum showed a band at 1771 cm^{-1} for the ketone and an OH stretch at 3481 cm^{-1}, but it was used without further purification in the next step.

The ketone intermediate (1.90 g, 4.13 mmol) was dissolved in 20 mL of dry THF in a 100 mL round bottomed flask under argon. Trimethyl(trifluoromethyl)silane ($TMSCF_3$, 1.22 mL, 1.17 g, 8.26 mmol) was added all at once and the solution was cooled to 0 ˚C. Tetrabutylammonium fluoride in THF (1.00 M, 0.040 mL) was syringed into the flask in one portion and the reaction mixture was stirred over night while it was allowed to warm up to room temperature. To remove the TMS protecting group, the THF was removed under reduced pressure and then 30 mL of anhydrous methanol and 3.70 g (27.0 mmol) of K_2CO_3 were added to the flask. After 5 hrs of vigorous stirring at room temperature under argon, the methanolic suspension was concentrated under reduced pressure and the solid

residue was rinsed twice with 75 mL portions of diethyl ether. The ethereal solution was washed with 30 mL portions of water and brine, dried over Na_2SO_4, and concentrated under reduced pressure. Purification of the residue by MPLC (hexanes to 20/80: EtOAc/hexanes) resulted in 1.70 g (68% overall) of alcohol **16** as a colorless viscous oil (R_f = 0.34 in 10/90: EtOAc/hexanes). ^{1}H NMR (500 MHz, $CDCl_3$) δ 7.42 (m, 3H), 7.30 (m, 2H), 5.62 (d, *J* = 1.2 Hz, 1H), 4.86 (dd, *J* = 1.3, 9.8 Hz, 1H), 4.83 (d, *J* = 0.6 Hz, 1H), 4.68 (dd, *J* = 2.2, 4.0 Hz, 1H), 4.57 (d, *J* = 9.8 Hz, 1H), 4.55 (dd, *J* = 2.1, 2.2 Hz, 1H), 4.32 (dd, *J* = 2.2, 3.4 Hz, 1H), 4.21 (dd, *J* = 1.8, 3.7 Hz, 1H), 0.999 (s, 9H), 0.224 (s, 3H), 0.211 (s, 3H). ^{13}C NMR (125 MHz, $CDCl_3$) δ 133.8, 129.7, 129.3, 123.7 (q, *J* = 284 Hz), 123.6 (q, *J* = 290 Hz), 102.1, 75.4 (q, *J* = 26.2 Hz), 72.2, 70.2 (q, *J* = 28.0 Hz), 70.1, 68.5, 66.0, 61.4, 25.6, 18.1, -4.44, -4.49. ^{19}F NMR (282 MHz, $CDCl_3$) δ -72.4, -79.9. IR (ATR source) 3449, 3094, 3069, 3035, 2955, 2932, 2898, 2860 cm^{-1}. HRMS-ESI: calc for $C_{22}H_{28}F_6NaO_6Si^+$ $(M + Na)^+$ 553.1457, found 553.1473.

*3,5-Bis(trifluoromethyl)-3,5-dibenzyloxy myo-inositol monoorthoformate (**17**)*: Alcohol **16** (1.60 g, 3.00 mmol) was dissolved in 20 mL of dry DMF in a 100 mL round bottomed flask under argon. After cooling to 0 ˚C, 0.240 g (6.00 mmol) of NaH (60% dispersion in oil) was slowly added and stirred for 30 min. Benzyl bromide (BnBr, 0.710 mL, 1.03 g, 6.00 mmol) was syringed into the flask over the course of 1 min and the resulting solution was allowed to warm up to room temperature for 2.5 h. To quench the reaction, 60 mL of wet diethyl ether was slowly added and the resulting mixture was washed with 20 mL of water and 20 mL of brine. The aqueous solution was extracted twice with 40 mL portions of diethyl ether/hexanes (1/1) and the combined ethereal solution was dried over Na_2SO_4, concentrated under reduced pressure and purified by MPLC (hexanes to 10/90

EtOAc/hexanes). The resulting white solid (R_f = 0.35 in 5/95 EtOAc/hexanes) had a small residual amount of BnBr as indicated by ^{1}H NMR, but it was used in the next step without further purification.

The dibenzyloxy *myo*-inositol monoorthoformate intermediate was dissolved in 30 mL of THF in a 100 mL round bottomed flask under an inert argon atmosphere. Tetrabutylammonium fluoride in THF (1.00 M, 9.00 mL) was added and this solution was stirred for 45 min at room temperature. Removal of the THF under reduced pressure afforded a residue that was dissolved in 50 mL of diethyl ether and filtered through a small plug of silica gel. The silica was subsequently washed with 100 mL of diethyl ether and the combined ethereal solution was concentrated under reduced pressure. Purification of the residue by MPLC (5/95: EtOAc/hexanes to 40/60: EtOAc/hexanes) afforded 1.00 g (66% overall) of dibenzyl alcohol **17** as a white solid. A small sample was recrystallized in hot MeOH with a minimal amount of water for characterization purposes (R_f = 0.26 in 20/80: EtOAc/hexanes, m.p. = 148 – 151 ˚C). ^{1}H NMR (500 MHz, $CDCl_3$) δ 7.24 – 7.19 (m, 2H), 7.18 – 7.11 (m, 4H), 6.97 – 6.91 (m, 4H), 5.65 (d, *J* = 1.2 Hz, 1H), 4.92 (dd, *J* = 1.9, 2.1 Hz, 1H), 4.68 (d, *J* = 10.4 Hz, 2H), 4.55 (dd, *J* = 1.8, 2.2 Hz, 2H), 4.51 (d, *J* = 10.1 Hz, 2H), 4.41 – 4.35 (m, 1H), 3.38 (d, *J* = 12.8 Hz, 1H). ^{13}C NMR (125 MHz, $CDCl_3$) δ 135.8, 128.3, 127.9, 127.5, 124.5 (q, *J* = 292 Hz), 102.70, 74.4 (q, *J* = 25.3 Hz), 70.9, 67.4, 66.8, 62.1. ^{19}F NMR (471 MHz, $CDCl_3$) δ -71.7. IR (ATR source) 3348, 3092, 3067, 3037, 2950, 2923, 2907, 2886 cm^{-1}. HRMS-ESI: calc for $C_{23}H_{20}F_6NaO_6^+$ $(M + Na)^+$ 529.1062, found 529.1060.

*1,3,5-Tris(trifluoromethyl)-3,5-dibenzyloxy scyllo-inositol monoorthoformate (**18**)*: Alcohol **17** (1.00 g, 2.00 mmol) was dissolved in 30 mL of dry CH_2Cl_2 in a 250 mL round

bottomed flask under argon. Dess-Martin periodinane (1.00 g, 2.40 mmol) was added to the flask all at once and the resulting cloudy solution was stirred for 20 h at room temperature. It was then diluted with 100 mL of diethyl ether followed by the addition of 50 mL of an aqueous solution consisting of 25 mL of 10% $Na_2S_2O_3$ and 25 mL of 5% $NaHCO_3$. Vigorous stirring was carried out for ~ 15 min until the organic layer became clear and then the aqueous solution was saturated with NaCl and extracted with 50 mL of diethyl ether. The combined ethereal solution was dried over Na_2SO_4, concentrated under reduced pressure, and the residue was purified by MPLC (5/95: EtOAc/hexanes to 25/75: EtOAc/hexanes) to afford 0.84 g (84%) of the dibenzyloxy ketone as a white solid (R_f = 0.58 in 20/80: EtOAc/hexanes). Its IR spectrum showed a carbonyl band at 1780 cm^{-1} and this material was used in the next step without further purification.

The ketone intermediate (0.300 g, 0.600 mmol) was dissolved in 3 mL of dry THF in a 10 mL round bottomed flask under an inert argon atmosphere. Trimethyl(trifluoromethyl)silane ($TMSCF_3$, 96.0 µL, 93.8 mg, 0.660 mmol) was added to the flask in one portion at room temperature and after cooling to 0 ˚C, 6.00 µL of a 1.0 M TBAF solution in THF was syringed into the flask in one portion. The resulting solution was stirred while it was allowed to warm up to room temperature and then it was concentrated by removing the THF under reduced pressure. Dilution of the oily residue with 2.0 mL of dry THF was followed by the addition of 1.20 mL of a 1.0 M TBAF solution. After 1 h of stirring, the reaction mixture was concentrated under reduced pressure and the residue was purified by MPLC (hexanes to 10/90: EtOAc/hexanes) to afford 0.120 g (35%) of alcohol **18** as a white solid. A small sample was recrystallized in hot MeOH with a minimal amount of water for characterization purposes (R_f = 0.42 in 4/96:

EtOAc/hexanes, m.p. = 112 – 115 ˚C). ^{1}H NMR (500 MHz, $CDCl_3$) δ 7.25 (m, 2H), 7.21 – 7.16 (m, 4H), 6.89 (m, 4H), 5.69 (s, 1H), 5.61 (q, *J* = 1.2 Hz, 1H), 5.01 (t, *J* = 2.2 Hz, 1H), 4.86 (d, *J* = 2.2 Hz, 2H), 4.73 (d, *J* = 9.5 Hz, 2H), 4.68 (d, *J* = 9.5 Hz, 2H). ^{13}C NMR (125 MHz, $CDCl_3$) δ 134.5, 128.7, 128.6, 128.5, 123.9 (q, *J* = 293 Hz), 123.6 (q, *J* = 289 Hz), 101.6, 75.4 (q, *J* = 25.3 Hz), 70.3 (q, *J* = 28.0 Hz), 69.0 (q, *J* = 2.7 Hz), 67.0, 66.3. ^{19}F NMR (282 MHz, $CDCl_3$) δ -70.3, -80.1. IR (ATR source) 3435, 3097, 3071, 3042, 2977, 2913 cm^{-1}. HRMS-ESI: calc for $C_{240}H_{18}F_9O_6^-$ $(M - H)^-$ 573.0965, found 573.0952.

*1,3,5-Tris(trifluoromethyl) scyllo-inositol monoorthoformate (**4**)*: Alcohol **18** (0.110 g, 0.192 mmol) was dissolved in 2.0 mL of THF in a 10 mL round bottomed flask. Palladium hydroxide on carbon (20% w/w, 0.037 g) was then added and the flask was placed in a hydrogenation reactor, which was evacuated and charged 3 times in succession with hydrogen to a pressure of 200 psi. After 15 h of stirring with a magnetic stir bar at room temperature, the reaction mixture was vented, diluted with 5 mL of diethyl ether and filtered through a small plug of silica gel. Diethyl ether (30 mL) was used to rinse the silica gel and the resulting organic solution was concentrated to afford 0.070 g (93%) of triol **4** as a white solid (m.p. 179 – 181 ˚C) which turned light brown at 170 ˚C. ^{1}H NMR (500 MHz, $CDCl_3$) δ 5.67 (s, 1H), 5.51 (br s, 3H), 4.73 (s, 3H). ^{13}C NMR (125 MHz, $CDCl_3$) δ 126.0 (q, *J* = 286 Hz), 102.0, 71.7 (q, *J* = 28.0 Hz), 67.9. ^{19}F NMR (471 MHz, $CDCl_3$) δ -73.9. IR (ATR source) 3365, 3026, 2976 cm^{-1}. HRMS-ESI: calc for $C_{10}H_6F_9O_6^-$ $(M - H)^-$ 393.0026, found 393.0024.

Chapter 3: Power of a Remote Hydrogen Bond Donor: Anion Recognition and Structural Consequences Revealed by IR Spectroscopy*

3.1. Introduction

Hydrogen bond networks (HBN) are routinely exploited in nature to enable anion transport across non-polar cellular membrane phospholipid bilayers.[1-6] One example is the ClC chloride ion channel which uses a series of NH and OH hydrogen bond donors to bind Cl^-.[4] HBN are also employed in synthetic anion receptors containing multiple amides, (thio)ureas, and aryl and aliphatic hydroxyl substituents.[7-13] For example, a flexible polyol with seven hydroxyl substituents (i.e., $(HOCH_2CH_2CH(OH)CH_2)_3COH$), was found to bind chloride in acetonitrile with a binding constant of 362 M^{-1}.[9] The structures of host-guest complexes and bound catalysts of small systems are most commonly determined by X-ray crystallography and gas phase computations whereas NMR studies have been used and play a large role in biological studies.[14] Both of the former approaches, however, may give different representations of the structures in solution. In this report, IR spectroscopy is used to determine the geometries of anion-receptor complexes for the first time. The binding constants of a series of rigid triols (**1(0) - 1(3)**, Fig. 1) and several monoprotected ethers with tetrabutylammonium salts are also reported. The tris(trifluoromethyl) derivative **1(3)** is found to be the strongest hydroxyl-based chloride receptor to date, and has high selectivity for Cl^- over interfering anions such as, Br^-, NO_3^- and NCS^-.[15] A "noninteracting" hydroxyl group is also found to influence the structure of the bound

* Samet, M.; Danesh-Yazdi, M.; Fattahi, A.; Kass, S. R., Power of a Remote Hydrogen Bond Donor: Anion Recognition and Structural Consequences Revealed by IR Spectroscopy. *J. Org. Chem.*, **2015**, *80*, 1130–1135. Copyright ACS. Reproduced with permission.

substrate and has as large or a larger influence on the association constants than two OH substituents that form hydrogen bonds to the anionic guest.

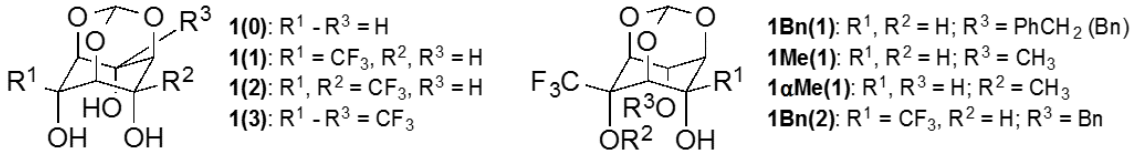

Figure 1. Rigid tricyclic locked in all axial 1,3,5-cyclohexanetriol derivatives **1(0)** – **1(3)** and a series of monoprotected ethers.

3.2. Results and Discussion

scyllo-Inositol monoorthoformate **1(0)** was found to bind chloride ion in acetonitrile with an association constant (*K*) of 540 M^{-1}. To increase this value, one of the equatorial hydrogens in **1(0)** was replaced by an electron withdrawing CF_3 group. The resulting triol **1(1)** has a binding constant of 2800 M^{-1}, which is 5 times larger than for **1(0)**. It is also ~2 and 20 times bigger than for catechol (1,2-$C_6H_4(OH)_2$) and resorcinol (1,3-$C_6H_4(OH)_2$), respectively.[16] Sequential incorporation of a second and third trifluoromethyl group into **1(0)** leads to further enhancements of more than three orders of magnitude relative to the unsubstituted triol (Table 1).[17] The association constant for **1(3)** is also 10 and 130 times bigger than for **2** and **3** (Fig. 2), respectively.[10,11] It is also the largest value reported to date for a non-charged alcohol even though it is an aliphatic alcohol rather than a phenol; the latter species are inherently more acidic and typically have high anion affinities.

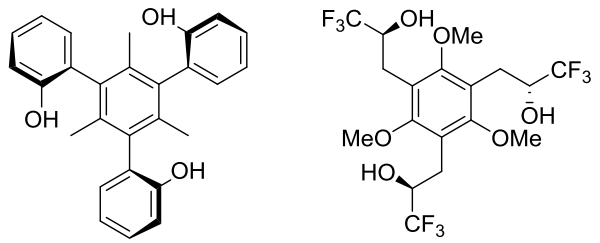

2 **3**

Figure 2. Triarylbenzene **2** and the tripodal hydroxyl-based anion receptor **3**.

Table 1. Measured binding constants and selectivities for **1(0) - 1(3)**.

ion[a,b]	*K* (M^{-1})[c]			
	1(0)	**1(1)**	**1(2)**	**1(3)**
Cl^-	540	2800	1.2×10^4	1.1×10^6
Br^-	94	190	860	3300
I^-			27	110
NO_3^-		68	120	970
NCS^-				270
Cl^-/Br^-	5.8	15	14	340
Cl^-/I^-			430	1.0×10^4
Cl^-/NO_3^-		42	98	1100
Cl^-/NCS^-				4200

[a]Tetrabutylammonium salts were used in all cases. [b]For HSO_4^- *K* was too small to measure with **1(3)**. [c]Estimated errors are ~20% except for **1(3)** with Cl^- which is less certain since NMR determinations are less reliable when $K \geq 10^5$ M^{-1} (ref. 17).

Anion recognition and selective binding plays a critical role in the development of synthetic ion transporters and sensors.[15,18] Triol **1(3)** is a preorganized receptor and was found to selectively bind Cl^- over common interfering anions such as Br^-, NO_3^- and NCS^-. Interestingly, the selectivity order follows the gas–phase acidities of the conjugate acids and not the Hofmeister series (i.e., $Cl^- > NO_3^- > Br^- > I^- > SCN^-$).[19] That is, ΔG°_{acid} HCl (328.1 ± 0.1) < HBr (318.3 ± 0.2) < HNO_3 (317.8 ± 0.2) < HNCS (≤ 317.6 ± 1.4) < HI (309.3 ± 0.1) < H_2SO_4 (302.3 ± 5.5 kcal mol^{-1}) where HCl is the least acidic of these acids

and H_2SO_4 is the strongest one.[20] Sterics, electrostatics and the size of the binding cavity must play a role too in the observed selectivities and the magnitudes of the binding constants.

One would expect the chloride anion complexes of triols **1(0) - 1(3)** to adopt structures with three direct (i.e., primary) OH•••Cl^- interactions because hydrogen bonds to anionic centers are known to be very stabilizing,[21] and this is the reported bonding motif for **2** and **3**.[10,11] Gas phase B3LYP/6-31+G(d,p) computations were carried out on all four triols and their bound cluster anions, and structures with 1-3 OH•••Cl^- interactions were located in all four cases (Fig. 3 and appendix for chapter 3). Surprisingly, the most stable conformers were found to have two primary hydrogen bonds and one bifurcated secondary interaction (***a*** and ***b***). The less stable structures (***c*** and ***d***) suffer from electron - electron repulsion due to the overlap of the lone pairs of electrons on the oxygen and fluorine atoms whereas this effect is mitigated by the secondary hydrogen bond in ***a*** and ***b***. The least stable species (***d***) also has distorted C–O–H bond angles to accommodate the three OH•••Cl^- interactions. As for the small differences in the stability between ***a*** and ***b***, this may appear to be surprising since one would expect the OH on the carbon bearing the CF_3 group to be the most acidic site and the better hydrogen bond donor. In ***a*** this substituent also serves as a hydrogen bond acceptor but the CF_3 group diminishes its capability in this regard.

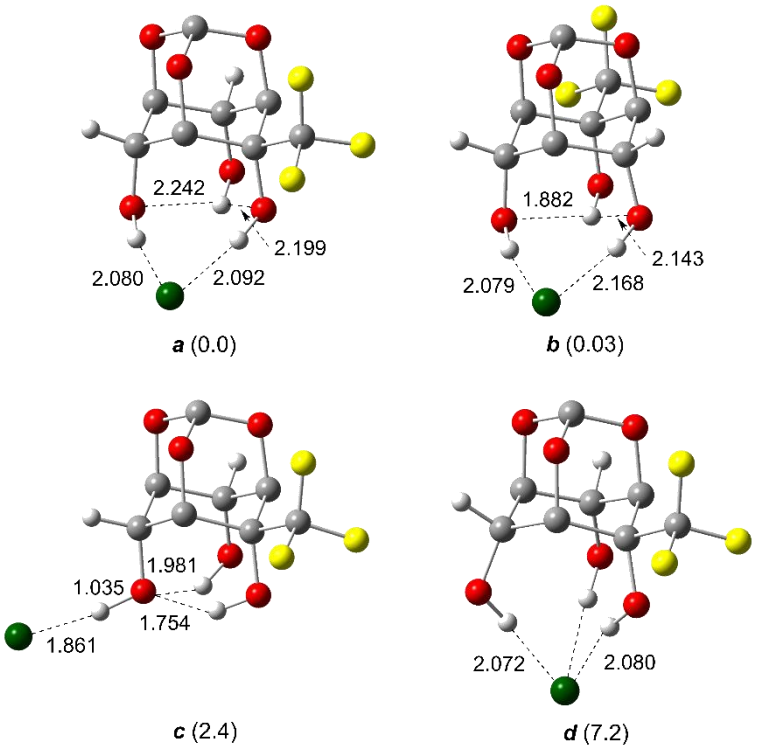

Figure 3. DFT geometries of **1(1)** • Cl^- where the bridgehead and apical hydrogens are removed for clarity; parenthetical values are relative energies in kcal mol^{-1}, O–H distances are < 1.00 Å unless specified and *d* has C_S symmetry.

In ***b*** this OH substituent does not directly interact with the chloride anion but it only functions as a hydrogen bond donor. As a result, there is little preference as to which two OH groups are used to hydrogen bond to Cl^-.

To experimentally probe the structures of the anion - receptor complexes, 10 mM solutions of **1(1)**, **1(3)** and their tetra-*n*-butylammonium chloride (TBACl) complexes were studied in 10 : 90 CD_3CN/CCl_4 mixtures by IR spectroscopy.[22,23] The spectra for both compounds are similar, so only the results for triol **1(1)** are discussed and the data for **1(3)** is given in the supporting information (Figure S5 and Table S5). A strong broad OH band at 3436 cm^{-1} and four weak C–H

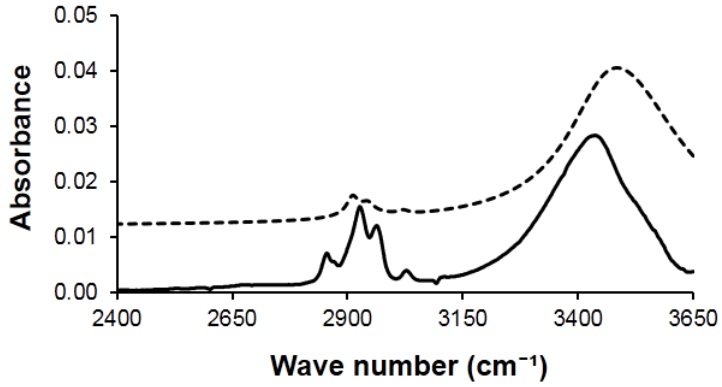

Figure 4. Experimental (solid line) and B3LYP/6-31+G(d,p) calculated (dashed line) IR spectra of **1(1)**. Computed frequencies are scaled by 0.945 and the simulated spectrum was obtained using Lorentzian functions with peak widths at half height ranging from 10-100 cm^{-1}.

absorptions at 3029, 2970, 2930 and 2856 cm^{-1} are observed for **1(1)** (Fig. 4). The former feature is ~178 cm^{-1} lower than the free OH stretch of *cis*-cyclohexane-1,3-diol in CCl_4[24] due, at least in large part, to the hydrogen bond accepting ability of the acetonitrile co-solvent.[25] Gas phase B3LYP/6-31+G(d,p) computations reproduce the experimental spectrum nevertheless, and the predicted bands at 3492, 3024, 2945, and 2915 cm^{-1} are within 5 to 59 cm^{-1} of the observed frequencies.

Upon the addition of 1 equivalent of TBACl to **1(1)** two new OH stretching bands appeared at 3513 and 3217 cm^{-1} (Fig. 5). The former feature is due to a relatively free hydroxyl group with a weak hydrogen bond whereas the large 219 cm^{-1} red shift for the latter band is the result of strong OH•••Cl^- interactions. A new weak C–H stretch is also observed below 2900 cm^{-1} at 2882 cm^{-1} in addition to four little changed bands at 3028, 2973, 2934 and 2853 cm^{-1}. These results suggest that the major structure of **1(1)** • Cl^- has two OH•••Cl^- hydrogen bonds and a weak OH•••X one, where X = OH or $NCCD_3$. The alternative structures with 1 and 3 primary

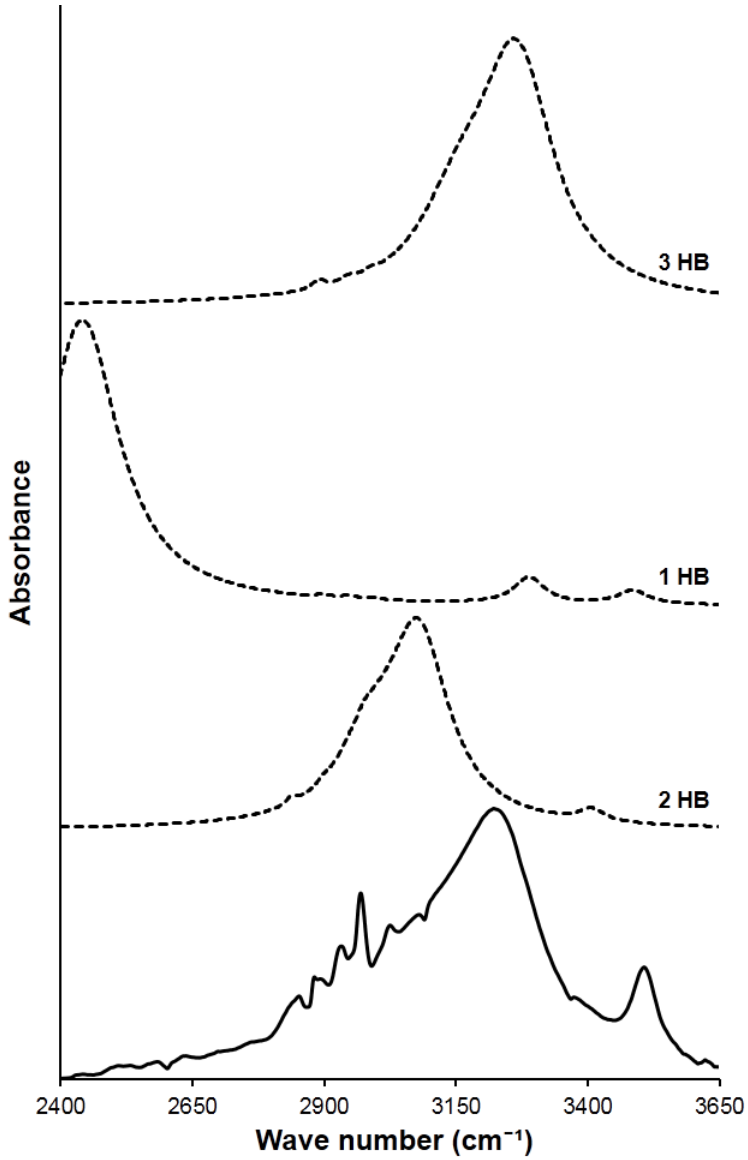

Figure 5. Experimental (solid line) and B3LYP/6-31+G(d,p) computed (dashed lines) IR spectra of **1(1)** • Cl^-. Computed spectra are for conformers with 1-3 primary hydrogen bonds (HB) to Cl^- as indicated.

interactions are inconsistent with the experimental data. That is, the red shift for the O–H stretch of the former species should be much larger (e.g., it is 672 cm^{-1} for $(CF_3)_3COH$ • Cl^-) and the latter conformer has no weakly bound OH groups. Proton transfer also can be

ruled out since Cl^- is a weak base, the H–Cl stretch appears at 2833 cm^{-1} in CCl_4[26] and its hydrogen bonded complex should be located at even lower frequency.

Computed B3LYP/6-31+G(d,p) IR spectra for the different conformers of **1(1)** • Cl^- are distinct and the one with two primary hydrogen bonds is in good accord with experiment as expected (Fig. 5).[27] The red shift for the structure with 1 HB is too large and the species with 3 HB does not have a free OH band. An expansion of the low frequency C–H stretching region due to the equatorial methine hydrogens is also diagnostic when the spectrum is recorded in 30% CD_3CN/70% CCl_4 with Ph_4PCl, and is in accord with the two OH•••Cl^- structure (Figs. S7-S8). Energetically this species is predicted to be the most stable as well in that the enthalpies at 298 K for the 1-3 hydrogen bond structures are 2.4, 0.0, and 7.2 kcal mol^{-1}, respectively.

These results suggest that the third hydroxyl group in **1(0) - 1(3)** maybe relatively unimportant with respect to anion binding and the resulting structure of the bound complex. To address this issue, several monoprotected ethers were prepared and examined. The association constants for the two methyl ethers of **1(1)** (i.e., **1Me(1)** and **1αMe(1)**) in CD_3CN upon adding TBACl were both found to be 210 M^{-1}. These values correspond to an ~15 fold reduction in the binding constants relative to **1(1)** which indicates that the third hydroxyl group is worth at least as much as one of the other two even though it does not directly interact with the chloride anion. An even larger reduction of 130 fold was found for the benzyl ether of **1(2)** (i.e., **1Bn(2)**) in that K = 90 M^{-1}. Sterics may play a minor role in the diminishment of this association constant, but are unlikely to be of major significance since there is essentially no difference in K for **1Me(1)** and **1Bn(1)** which are 210 and 170 M^{-1}, respectively. This indicates that the remote hydroxyl substituent in **1(2)** has a bigger

effect on the binding constant than the two OH substituents that hydrogen bond directly to the chloride anion in the bound complex. This finding is in keeping with a similar observation based upon gas phase photoelectron spectra and computations,[28] and has obvious implications in biological processes such as binding, catalysis, protein folding, etc.

IR spectra of **1Bn(1)**, **1Bn(2)** and their TBACl complexes in carbon tetrachloride were recorded to investigate the structures of the bound monoprotected triols (Fig. 6 and S9). Due to the enhanced solubility of these compounds in CCl_4, CD_3CN was not needed or used as a cosolvent.

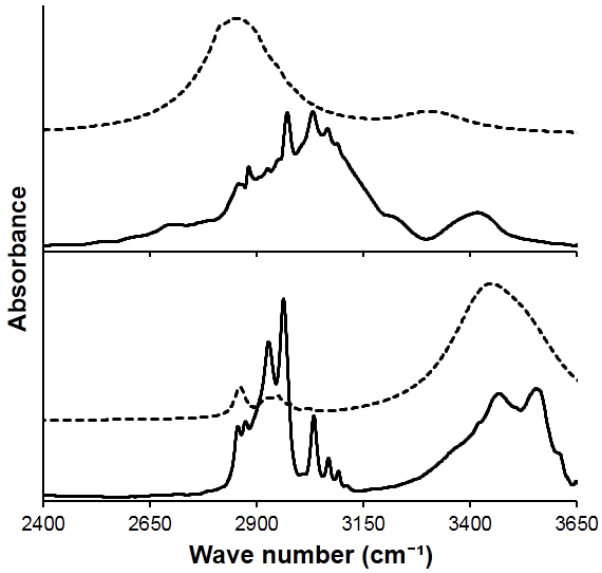

Figure 6. Experimental (solid lines) IR spectra of **1Bn(1)** (bottom) and **1Bn(1)** • Cl^- (top) and B3LYP/6-31+G(d,p) predictions of the corresponding methyl ethers (dashed lines).

A strong red shifted OH absorption at ≤ 3000 $cm^{-1}$and a weak OH stretch at ~3430 cm^{-1} were observed in both of the bound complexes. The latter features are due to relatively free hydroxyl groups that are slightly red shifted (i.e., < 100 cm^{-1}) due to intramolecular O–H•••O interactions, and they indicate that the bound receptors adopt structures with only

one hydrogen bond to the chloride anion (Fig. 7). This structural change in the two diols relative to their unprotected triols is in accord with computations. That is, B3LYP/6-31+G(d,p) energies of the corresponding methyl ethers favor the structures with one rather than two hydrogen bonds to Cl^- by 5.2 (**1Me(1)**) and 1.5 (**1Me(2)**) kcal mol^{-1}.[29]

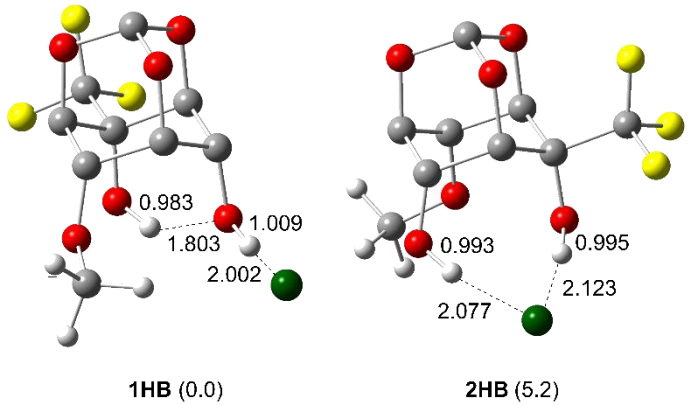

Figure 7. B3LYP/6-31+G(d,p) geometries of **1Me(1)** • Cl^- as models for the benzyl ether; bridgehead and apical hydrogens are removed for clarity and parenthetical values are relative energies in kcal mol^{-1}.

The predicted IR spectra of these species are also in line with this finding, and so the absence of a hydroxyl group that does not directly interact with Cl^- in the bound complexes can nevertheless alter the structures of the bound receptors.

3.3. Conclusions

IR spectroscopy was used to determine the structures of small chloride anion–receptor complexes and their geometries were found to employ one less hydrogen bond to the ion than was available in the triol (i.e., two rather than three). Protection as an ether of one of the three hydroxyl groups was found, nevertheless, to have as large an effect as one or both of the remaining OH substituents on the chloride anion association constants. It also altered

the structures of the bound complexes by eliminating one of the OH•••Cl^- hydrogen bonds. These results are accounted for by the presence (or absence) of secondary OH•••OH hydrogen bond interactions which enable a remote hydroxyl group to play a large structural and energetic role in binding. This has readily apparent implications in numerous biological processes as well as site-directed mutagenesis studies. It is worth noting too that triol **1(3)** is found to be a strong and selective binder of Cl^- in a polar environment.

3.4. Experimental Section

3.4.1. General

Triols **1(0)** – **1(3)** were synthesized as previously reported.[28] Acetonitrile-d_3 was stored over activated 3 Å molecular sieves for several days, tetrabutylammonium chloride and tetraphenylphosphonium chloride (Ph_4PCl) were stored in a desiccator containing phosphorous pentoxide and Dess-Martin periodinane (DMP) was prepared according to previously reported procedures.[30] Glassware, vials, NMR tubes and microsyringes were dried in ovens and allowed to cool under a stream of dry nitrogen or argon. THF was dried by refluxing it over sodium metal under an argon atmosphere using benzophenone as an indicator and subsequently was distilled. Hydrogenation reactions were carried out in a 600 mL stainless steel reactor. TLC analyses were performed on precoated (250 mm) silica gel 60 Å pore size F-254 plates and were visualized by staining with $KMnO_4$ or a hand-held UV lamp. Medium pressure liquid chromatography (MPLC) was carried out with a commercial instrument in which the samples were dissolved in a minimal amount of CH_2Cl_2 and syringed on to a silica gel (Premium R_f Silica Gel, 60A, 40-75μm) column. Reported melting points (m.p.) are uncorrected. Proton, ^{13}C, and ^{19}F NMR spectra were

obtained with 300 and 500 MHz spectrometers, and the chemical shifts are reported in ppm and were referenced to the residual solvent as follows: $CHCl_3$ = 7.27 δ (^{1}H), 77.0 δ (^{13}C); CHD_2CN = 1.94 δ (^{1}H), 1.39 δ (^{13}C). For the ^{19}F spectra, CF_3CO_2H was used as an external calibrant and assigned a value of -78.5 δ. IR spectra of neat samples were recorded with an ATR source while the solution studies are described below. ESI-TOF mass spectra were obtained using methanolic solutions and PEG was employed as an internal standard for acquiring high resolution data.

3.4.2. Synthetic Procedures for Compounds 1αMe(1), 1Bn(1), and 1Me(1)

1-Trifluoromethyl-1-methoxy scyllo-inositol monoorthoformate (**1αMe(1)**). 1-Trifluoro-methyl-3,5-dibenzyloxy *scyllo*-inositol monoorthoformate[28] (0.850 g, 1.90 mmol) was dissolved in 20 mL of dry THF in a 100 mL round bottomed flask under argon. This solution was stirred and cooled down to 0 ˚C, and 0.150 g (3.80 mmol) of a 60% dispersion of NaH in mineral oil was added in several portions. After 30 min, CH_3I (1.06 mL, 2.42 g, 17.1 mmol) was slowly syringed into the flask and the reaction mixture was allowed to warm up to room temperature overnight. It was quenched by careful addition of 10 mL of a saturated aqueous solution of NH_4Cl and the organic layer was separated. Two 20 mL portions of diethyl ether were used to extract the aqueous phase and the combined organic material was washed with 10 mL of brine. The resulting solution was dried over Na_2SO_4 and concentrated under reduced pressure to afford an oily residue that was purified by MPLC (2/98 to 35/65 EtOAc/hexanes) to give 0.300 g (35%) of 1-trifluoromethyl-1-methoxy-3,5-dibenzyloxy *scyllo*-inositol monoorthoformate as a white gummy compound (R_f = 0.45 in 14/86 EtOAc/hexanes). Its ^{19}F NMR showed a new signal at -74.1 ppm and a small residual absorption at -82.0 for the starting material, but an OH stretch was not

observed in its IR spectrum. This intermediate compound was consequently taken on without further purification.

1-Trifluoromethyl-1-methoxy-3,5-dibenzyloxy *scyllo*-inositol monoorthoformate (0.200 g, 0.442 mmol) was dissolved in 6.0 mL of dry THF in a 25 mL round bottomed flask. Pearlman's catalyst (20% $Pd(OH)_2/C$, 0.0667 g) was added and the flask was placed in a hydrogenation apparatus where it was magnetically stirred. The reactor was evacuated and then filled with hydrogen to a pressure of 250 psi three times in succession followed by a 24 h reaction period. Diethyl ether (10 mL) was added to the reaction flask after venting the system and the resulting solution was filtered through a small plug of silica gel which was subsequently rinsed with 20 mL of diethyl ether. The combined organic material was concentrated under reduced pressure to afford an oily residue and purification by MPLC (10/90 EtOAc/hexanes to neat EtOAc) gave 0.115 g (96 %) of **1αMe(1)** as a white solid (R_f = 0.19 in 1/1 EtOAc/hexanes, m.p. = 167 – 170 ˚C) that turned light brown at 165 ˚C. ^{1}H NMR (500 MHz, CD_3CN) δ 5.50 (s, 1H), 4.62 (m, 2H), 4.49 – 4.41 (m, 2H), 4.21 (m, 1H), 4.00 (d, *J* = 8.8 Hz, 2H), 3.46 (q, *J* = 2.0 Hz, 3H). ^{13}C NMR (125 MHz, CD_3CN) δ 125.8 (q, *J* = 291 Hz), 102.7, 74.5 (q, *J* = 25.3 Hz), 71.9, 69.3, 68.4, 54.7 (q, *J* = 1.8 Hz). ^{19}F (282 MHz, CD_3CN) δ -73.5. IR (ATR source) 3494, 3370, 3029, 3011, 2993, 2961, 2920, 2855 cm^{-1}. HRMS-ESI: calc for $C_9H_{10}F_3O_6^-$ $(M - H)^-$ 271.0435, found 271.0426.

1-Trifluoromethyl-3-benzyloxy scyllo-inositol monoorthoformate (**1Bn(1)**). 5-Trifluoromethyl-5-trimethylsilyloxy-3-benzyloxy *scyllo*-inositol monoorthoformate[28] (1.00 g, 2.38 mmol) was dissolved in 10 mL of dry THF and stirred in a round bottomed flask under argon. A 1.0 M TBAF solution in THF (7.2 mL) was added in one portion and after 45 min the resulting light brown mixture was concentrated under reduced pressure.

The resulting material was diluted with 50 mL of diethyl ether and passed through a plug of silica gel which was subsequently rinsed with 100 mL of diethyl ether. Concentration of the combined solutions under reduced pressure and purification by MPLC (1/9 EtOAc/hexanes to neat EtOAc) afforded 0.790 g (96%) of **1Bn(1)** as a white solid (R_f = 0.38 in 1/1 EtOAc/hexanes, m.p. = 115 – 117 ˚C). ^{1}H NMR (500 MHz, $CDCl_3$) δ 7.42 – 7.31 (m, 5H), 5.52 (s, 1H), 4.76 (d, *J* = 11.3 Hz, 1H), 4.69 (d, *J* = 11.3 Hz, 1H), 4.63 (m, 1H), 4.56 (s, 1H), 4.51 (m, 4H), 3.27 (d, *J* = 8.3 Hz, 1H). ^{13}C NMR (125 MHz, $CDCl_3$) δ 135.8, 128.9, 128.8, 128.2, 123.9 (q, *J* = 284.4 Hz), 101.8, 73.7, 72.6, 69.6 (q, *J* = 28.9 Hz), 68.9, 68.5, 67.9, 67.0. ^{19}F NMR (471 MHz, $CDCl_3$) δ -82.2. IR (ATR source) 3434, 3329, 3096, 3068, 3029, 2975, 2943, 2880 cm^{-1}. HRMS-ESI: calc for $C_{15}H_{14}F_3O_6^-$ $(M - H)^-$ 347.0748, found 347.0774.

1-Trifluoromethyl-5-methoxy scyllo-inositol monoorthoformate (**1Me(1)**). 3-Benzyloxy-5-methoxy *myo*-inositol monoorthoformate[31] (0.89 g, 3.02 mmol) was dissolved in 25 mL of dry CH_2Cl_2 in a 100 mL round bottomed flask under argon. Dess-Martin periodinane (1.54 g, 3.60 mmol) was added and the reaction mixture was stirred overnight. Removal of the solvent afforded a residue that was diluted with 30 mL of diethyl ether and an equal volume of an aqueous solution consisting of 10% $Na_2S_2O_3$ (15 mL) and 5% $NaHCO_3$ (15 mL). The resulting slurry was vigorously stirred for 15 min and then the organic layer was separated, dried over Na_2SO_4, and concentrated under vacuum to afford 0.84 g (95%) of a viscous yellow oil. This oxidation product showed carbonyl and OH bands in its IR spectrum at 1763 cm^{-1} and 3464 cm^{-1}, respectively and was carried on without further purification.

A 25 mL round bottomed flask was filled with 0.84 g (2.87 mmol) of the crude ketone, 2.55 mL (2.45 g, 17.2 mmol) of $TMSCF_3$ and 10 mL of anhydrous THF under an argon atmosphere at 0 ˚C. A 1.0 M tetrabutylammonium fluoride solution in THF (0.10 mL) was slowly added with stirring and the resulting mixture was allowed to warm up to room temperature overnight. Concentration of this material under reduced pressure afforded an oily residue that was diluted with 10 mL of dry THF. More TBAF (2.90 mL) was added and the resulting solution was stirred for 1 h. Evaporation of the volatile materials under reduced pressure afforded a residue that was purified by MPLC (1/19 to 1/1 EtOAc/hexanes) to give 0.10 g (10%) of the desired trifluoromethyl–substituted alcohol as a light yellow oil (R_f = 0.35 in 1/3 EtOAc/hexanes). ^{1}H NMR (500 MHz, $CDCl_3$) δ 7.35 (m, 5H), 5.53 (s, 1H), 5.31 (s, 1H), 4.71 (d, *J* = 11.3 Hz, 1H), 4.68 (d, *J* = 11.3 Hz, 1H), 4.59 (m, 2H), 4.55 (m, 1H), 4.47 (m, 1H), 4.31 (m, 1H), 3.51 (s, 3H). ^{19}F NMR (282 MHz, $CDCl_3$) δ -81.9. IR (ATR) 3435 cm^{-1} (broad OH band).

The alcohol intermediate (0.10 g, 0.28 mmol) was dissolved in 2 mL of THF in a 10 mL round bottomed flask. Pearlman's catalyst (33 mg) was added to the reaction mixture and the flask was placed in a Parr hydrogenation apparatus where it was evacuated and filled with hydrogen to a pressure of 500 psi three times in succession. After 24 h the system was vented, 5 mL of diethyl ether was added, and the resulting solution was filtered through a small plug of silica gel which was subsequently rinsed with 10 mL of diethyl ether. Concentration of the combined organic material under reduced pressure gave a light yellow solid which was partially dissolved in hot $CHCl_3$ and allowed to cool down to give 60 mg (79%) of **1Me(1)** as a white solid (m.p. = 88 – 91 ˚C). ^{1}H NMR (500 MHz, CD_3CN) δ 5.51 (s, 1H), 5.26 (s, 1H), 4.55 (m, 2H), 4.47 (m, 1H), 4.38 (m, 1H), 4.26 (m, 1H), 4.16 (d, *J* =

6.1 Hz, 1H), 3.46 (s, 3H). ^{13}C NMR (125 MHz, CD_3CN) δ 125.6 (q, J = 284 Hz), 102.7, 76.74, 76.73, 70.6 (q, J = 27.1 Hz), 69.7, 68.2, 68.1, 58.2. ^{19}F (471 MHz, CD_3CN) δ -81.2. IR (ATR source) 3288, 3062, 3000, 2967, 2947, 2914, 2849 cm^{-1}. HRMS-ESI: calc for $C_9H_{10}F_3O_6^-$ $(M - H)^-$ 271.0435, found 271.0444.

3.4.3. Binding Measurements

Anion affinities were measured in acetonitrile-d_3 at constant and non-aggregating concentrations of **1(1)** – **1(3)** (i.e., < 0.60 mM). These host solutions were titrated with a mixture of the TBAX salt and the alcohol of interest in oven dried NMR tubes, and changes in the equatorial methine hydrogens chemical shifts were followed except for **1(3)** where the bridgehead hydrogen was monitored. Non-linear 1:1 fits of the data with the Solver add-on for Excel were carried out to obtain the binding constants (K (M^{-1})).[32] Representative tetrabutylammonium chloride titration results and binding isotherms for **1(0)** – **1(3)** are provided in Tables S1–S4 and Figures S1–S4.

3.4.4. IR Studies

Background corrected IR spectra of receptor solutions and their 1:1 TBACl complexes were recorded in NaCl cells with 0.10 and 1.0 mm fixed path lengths. Compounds **1Bn(1)** (4.8 mM) and **1Bn(2)** (6.0 mM) were examined in CCl_4, whereas 10 mM 10% CD_3CN/90% CCl_4 solutions were used for **1(1)** and **1(3)**. Computed B3LYP/6-31+G(d,p) frequencies were fit with Lorentzian functions and the resulting intensities at each wavelength n in the spectral window are given by $I(n) = aI_o/(1 + \{(n - bn_o)^2/2S^2\})$, where a, b, n_o, I_o and S are the intensity correction parameter, frequency scaling factor, computed frequency and intensity, and peak width at half height, respectively. To minimize the average least squares

error for the summation of the fitted curves to the experimental spectrum, a wide range of feasible values for the peak widths spanning from 10 – 100 cm^{-1} were examined by a Monte Carlo approach to find the optimum value using MATLAB. Different scaling factors were also examined, and a value of 0.945 was adopted in this work.

3.4.5. Computations

Full geometry optimizations and subsequent vibrational frequency determinations were carried out at the Minnesota Supercomputer Institute for Advanced Computational Research with Gaussian 09.[33] The Becke three-parameter hybrid exchange and Lee−Yang−Parr correlation density functional (B3LYP) was used in conjunction with the 6-31+G(d,p) basis set.[34,35] Zero-point energies (zpe) and thermal corrections to the 298 K enthalpies (tc) were obtained from unscaled vibrational frequencies. The resulting geometries and energies are given in ref. 16 or are provided in Table S6.

Chapter 4: Stereoelectronic Effects: A Simple yet Powerful Tool to Manipulate Anion Affinity*

4.1. Introduction

Anion recognition is critical in a number of biological processes such as enzyme catalysis[1,2] and anion transport through cellular phospholipid bilayers.[3-7] Drawing inspiration from these pathways, chemists have mimicked nature to develop anion transporters,[8-11] metal-free catalysts,[12-15] and sensors.[16,17] A variety of strategies have been employed in designing ion receptors that make use of hydrogen bond networks,[15,18-20] electrostatic effects[21] and inductive stabilization.[22-26] Stereoelectronic effects are largely unexplored,[20,27,28] however, even though they play an important role in many enzymatic transformations (e.g., serine proteases, lysozyme, and [NiFe]-hydrogenases).[29-32]

The orientation of substituents that directly interact with an anion can have a large impact on the binding constant of a host compound.[20,27,33] For instance, *syn*-triphenol **1s** (Fig. 1) uses all three hydroxyl groups to interact with chloride anion and the resulting association constant with tetrabutylammonium chloride (TBACl) in acetonitrile-d_3 is 1.3 x 10^5 M^{-1}. In contrast, the *anti*-rotamer **1a** can only make use of two hydrogen bonds in the 1:1 complex with TBACl, and its binding constant of 240 M^{-1} corresponds to a reduction of a little more than 500 fold.[20] The effect of the spatial arrangement of a non-interacting group is little studied but Kondo, Kobayashi, and Unno reported on the two anomers of a

* Samet, M.; Fattahi, A.; Kass, S. R., Stereoelectronic Eeffects: A Simple yet Powerful Tool to Manipulate Anion Affinity. *Org. Biomol. Chem.*, **2015**, *13*, 2170-2176. Copyright RSC. Reproduced with permission.

D-ribose derivative (**2**).[28] As one might expect, small $K_{2\beta}/K_{2\alpha}$ ratios were observed for a variety of anion salts in polar (CD_3CN) and nonpolar ($CDCl_3$) solvents. These values varied from 5 – 34, but a larger difference of 130 was obtained in the latter noncompetitive solvent with tetrabutylammonium dihydrogen phosphate.

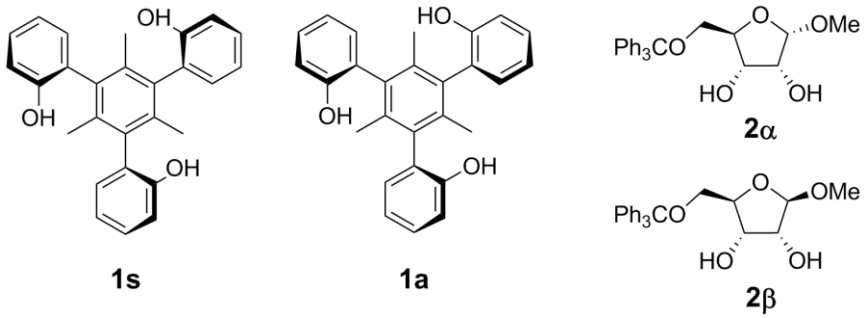

Figure 1. *Syn*- and *anti*-isomers of triphenol **1** and anomers of a D-ribose derivative.

scyllo-Inositol derivatives (**3**, Fig. 2) can serve as Brønsted and hydrogen bond catalysts and anion recognition reagents.[34,35] These triols bind TBACl with good affinity and selectivity even though only two of the three hydroxyl groups interact directly with the chloride ion.

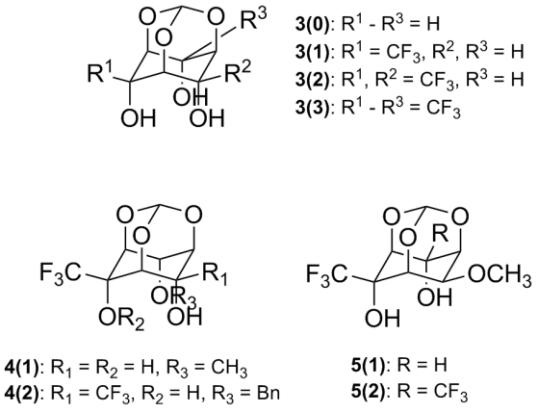

Figure 2. *scyllo*- and *myo*-Inositol structures used previously (**3** and **4**) and in this work (**5**).

The remaining OH substituent also serves as a hydrogen bond donor but it forms a bifurcated hydrogen bond with the oxygen atoms of the other two hydroxyl groups. This remote hydrogen bond plays a significant role in the molecular recognition properties of these compounds. For example, the 1:1 binding equilibrium constant of **3(2)** and TBACl in CD_3CN is 12,000 M^{-1} but drops to 90 M^{-1} in **4(2)** due to the conversion of the remote hydroxyl group to a benzyl ether. Steric effects seem to play a small role indicating that the hydrogen bond due to the distal OH substituent is energetically as important as the two OH•••Cl^- hydrogen bonds. To assess this further and examine the stereoelectronic consequences of the remote substituent, diols **5(1)** and **5(2)** with equatorial ether groups were synthesized, their TBACl association constants are reported, and the structures of the bound complexes in solution are characterized by IR spectroscopy and accompanied by DFT computations.

4.2. Results and Discussion

Diols **5(1)** and **5(2)** with an equatorial methoxy substituent and one or two trifluoromethyl groups were synthesized from previously prepared starting materials as illustrated in Schemes 1 and 2. Their binding isotherms with TBACl were obtained by monitoring the C3 and C5 axial and equatorial hydrogen signals for **5(1)** and the C2 and C5 axial and equatorial resonances for **5(2)** in their ^1H NMR spectra (Fig. S1). Non-linear 1:1 fits of the data afforded $K_{5(1)}$ = 890 M^{-1} and $K_{5(2)}$ = 29,000 M^{-1}. The former value is ~4 times larger than the axial ether **4(1)** and ~3 times smaller than the corresponding triol **3(1)**.[34]

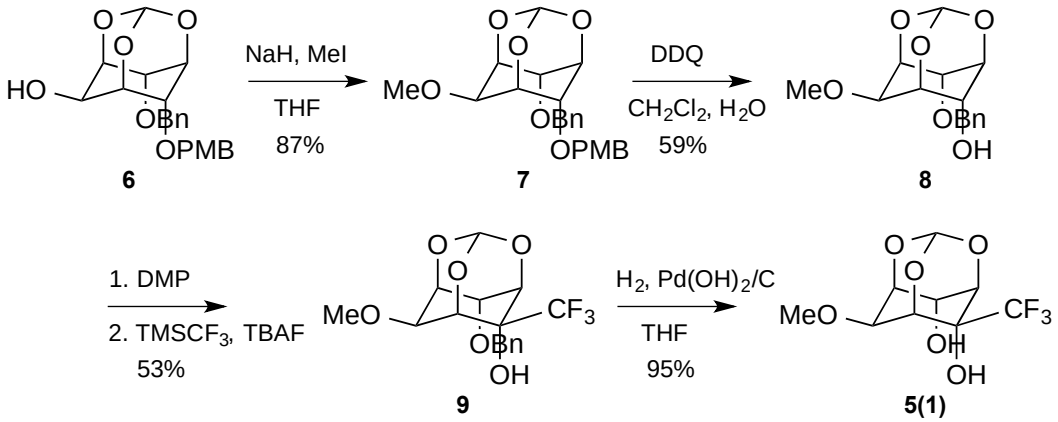

Scheme 1. Synthetic route for the preparation of **5(1)**.

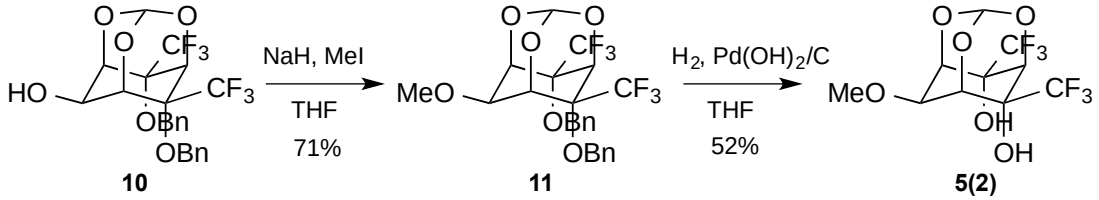

Scheme 2. Synthetic route for the preparation of **5(2)**.

On the other hand, the association constant for alcohol **5(2)** is between two and three orders of magnitude larger than for **4(2)** and is even bigger than that for triol **3(2)** even though the latter compound has an additional hydrogen bond donating substituent. To probe these results further, the structures of the TBACl complexes of **5(1)** and **5(2)** were characterized by IR spectroscopy and DFT computations.

Dilute 1:9 CD_3CN/CCl_4 solutions of diols **5(1)** and **5(2)** were prepared and the background corrected IR spectrum of **5(1)** is illustrated in Fig. 3 (top); acetontrile-d_3 was used for solubility purposes. A strong and broad OH absorption at 3370 cm^{-1} along with a shoulder at 3510 cm^{-1} are observed in addition to four weak CH bands at 3032, 2976, 2934

and 2825 cm^{-1}. The former red-shifted OH stretch is ~250 cm^{-1} smaller than that for the free OH band in *cis*-cyclohexane-1,3-diol[36] mostly due to the interaction with CD_3CN whereas an ~100 cm^{-1} reduction is observed for the weaker intramolecular OH•••OH hydrogen bond.[37,38] Gas phase B3LYP/6-31+G(d,p) computations reproduce the experimental spectrum except for the position of hydroxyl group at 3370 cm^{-1} undoubtedly because of the OH•••$NCCD_3$ interaction which is not accounted for in the calculation.

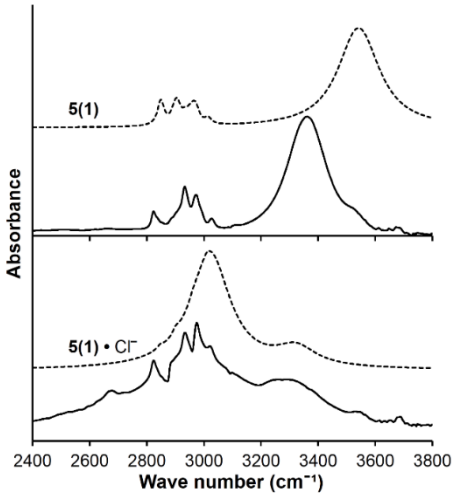

Figure 3. Experimental (solid line) and calculated B3LYP/6-31+G(d,p) (dotted line) IR spectra of **5(1)** (top) and **5(1)** • Cl^- (bottom).

Upon addition of 1 equivalent of TBACl to **5(1)**, two new broad OH bands at 3285 and 2960 cm^{-1} appear in the IR spectrum (Fig. 3, bottom). The former frequency is due to a weak hydrogen bond (i.e., a OH•••X interaction, where X = OH or $NCCD_3$) whereas the latter absorption into the CH region of the spectrum arises from a stronger OH•••Cl^- hydrogen bond. These features indicate that the major structure adopted by **5(1)** • Cl^- only uses one hydroxyl group to interact with the chloride anion and that alternative species with two OH•••Cl^- hydrogen bonds are inconsistent with the experimental data.

Computations are in accord with this assignment in that the most stable structure of the bound complex has both OH•••Cl^- and OH•••OH hydrogen bonds (Fig. 4). Its predicted IR spectrum is also in excellent accord with the observed one (Fig. 3, bottom).[39] A slightly higher energy conformer (1.0 kcal mol^{-1}) with two OH•••Cl^- interactions was located, but it only has one OH band at 3255 cm^{-1} (Fig. S2) and gives a poor fit to the experimental data.[40]

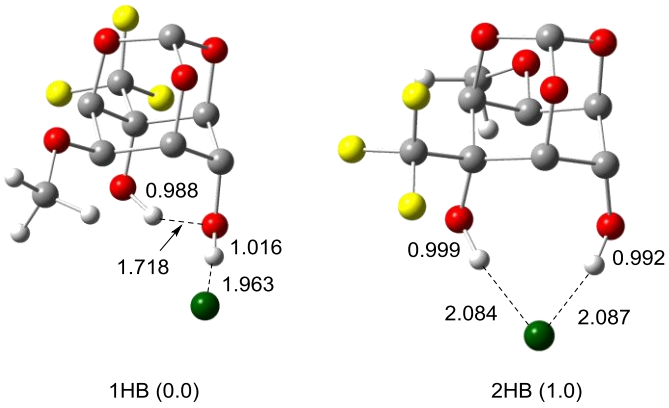

Figure 4. Computed B3LYP/6-31+G(d,p) structures for **5(1)** • Cl^- and their relative enthalpies in parentheses at 298 K in kcal mol^{-1}.

A similar IR spectrum was obtained for **5(2)**, but its two hydroxyl groups at 3427 and 3226 cm^{-1} are better resolved and appear at lower frequencies than in **5(1)** because of the presence of two trifluoromethyl groups which undoubtedly enhance its acidity (Fig. 5, top). Four resolved C–H bands are observed at 3039, 2983, 2935, and 2833 cm^{-1} which are on average 6 cm^{-1} higher in frequency than in **5(1)**.

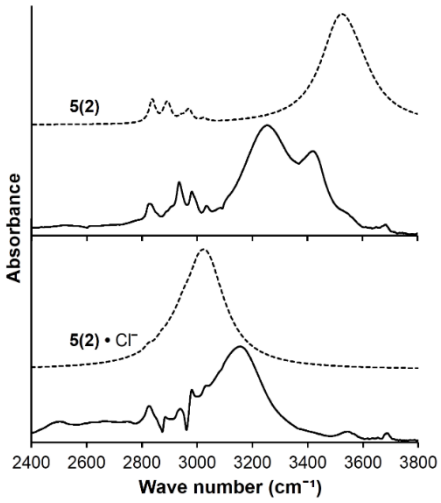

Figure 5. Experimental (solid line) and computed B3LYP/6-31+G(d,p) (dotted line) IR spectra of **5(2)** (top) and **5(2)** • Cl^- (bottom).

This spectrum is well modeled by B3LYP/6-31+G(d,p) calculations except for the O–H stretch at 3370 cm^{-1} which is red-shifted due to its interaction with acetonitrile just as was the case for **5(1)**.

Addition of 1 equivalent of TBACl to **5(2)** affords a single broad OH absorption at 3160 cm^{-1} (Fig. 5, bottom). A second feature corresponding to a weakly hydrogen bonded hydroxyl group is not observed which indicates that both hydroxyl groups directly interact with chloride anion at least in the main structure. Computations on the structure with two OH•••Cl^- hydrogen bonds reproduce the experimental spectrum but this conformer is predicted to be 0.4 kcal mol^{-1} less stable than when there is one such interaction (Fig. 6). The computed spectrum for the latter structure, however, is a poor match of the observed one (Fig. S3). It is also predicted to be destabilized in acetonitrile, and B3LYP/6-31+G(d,p) calculations with the conductor-like polarized continuum model (CPCM) indicate that

there is an energetic reversal leading to a 0.5 kcal mol^{-1} preference for the structure with two OH•••Cl^- hydrogen bonds.

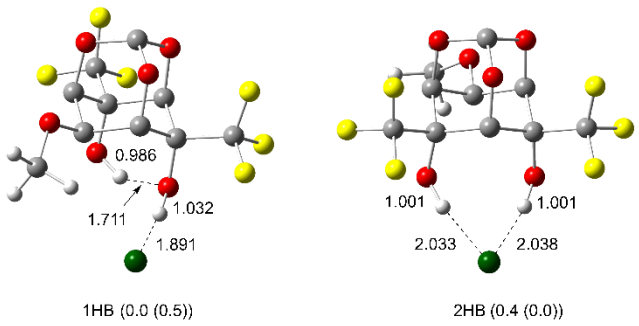

Figure 6. Computed B3LYP/6-31+G(d,p) structures for **5(2)** • Cl^- and their relative gas- and liquid-phase (CH_3CN) enthalpies at 298 K in kcal mol^{-1}; the latter value is given in parentheses.

Both the experimental and computational results above indicate that structures with one and two OH•••Cl^- hydrogen bonds can be adopted, and that there is little energetic difference between them. A small stereoelectronic effect is observed for **5(1)** and **4(1)** (i.e., $K_{\mathbf{5(1)}}/K_{\mathbf{4(1)}}$ = 4) whereas the presence of a second trifluoromethyl group undoubtedly enhances the acidity, and leads to a larger binding constant and a much bigger epimeric ratio (i.e., $K_{\mathbf{5(2)}}/K_{\mathbf{4(2)}}$ = 320). This latter stereoelectronic effect involves the comparison of an equatorial methoxy group and an axial benzyloxy substituent, but the steric difference presumably is of minor importance. This assumption is based on the orientation of the benzyl group being away from the hydroxyl substituents, and the observation that the binding constants for the methyl ether **4(1)** and its benzyl ether analog are essentially the same (i.e., 210 and 170 M^{-1}, respectively).[34] A plausible explanation for this large stereoelectronic effect is that the C−OMe bond dipole is in a favorable orientation in the bound complex when the ether is in the equatorial position.[41] An attractive bifurcated C–

H interaction with the two hydroxyl groups is also present in the computed structure of the bound complex. More specifically, the axial methine hydrogen on the carbon bearing the equatorial methoxy group of **5(2)** is predicted on average to move 0.103 to 0.109 Å closer to the oxygen atoms of the hydroxyl groups upon binding chloride anion. Since these C–H•••OH distances decrease from 2.530 and 2.539 Å to 2.421 and 2.436 Å, the association of Cl^- can be viewed as inducing a weak C–H•••OH hydrogen bond. This suggestion is supported by the large observed down field shift of the axial hydrogen upon addition of 1 equivalent of TBACl ($\Delta\delta$ = 0.30 ppm). Taken together, the favorable bond dipole orientation and the C–H•••OH interaction are energetically more important than the OH•••OH hydrogen bond in the chloride anion complex of triol **3(2)** since $K_{\mathbf{3(2)}}$ = 12,000 M^{-1} but $K_{\mathbf{5(2)}}$ = 29,000 M^{-1}.

4.3. Experimental Section

4.3.1. General

All reactants, reagents and solvents were purchased from Sigma-Aldrich unless otherwise noted. Dess-Martin periodinane (DMP) was prepared according to previously reported procedures,[42,43] while trimethyl(trifluoromethyl)silane ($TMSCF_3$), 2,3-dichloro-5,6-dicyano-1,4-benzoquinone (DDQ), anhydrous dichloromethane (CH_2Cl_2) and acetonitrile-d_3 (CD_3CN) were purchased from Matrix Scientific, Combi-Blocks, EMD Chemicals and Cambridge Isotope Laboratories, respectively. Tetrahydrofuran (THF) was dried over sodium metal at reflux under an argon atmosphere using benzophenone as an indicator and subsequently was distilled. Glassware (e.g., vials, NMR tubes and flasks) was dried in ovens and allowed to cool under a stream of argon or nitrogen. Hydrogenation

reactions were carried out in a 600 mL Parr stainless steel reactor. TLC analyses were performed on precoated (250 mm) silica gel 60 F-254 plates (Merck) and were visualized by staining with $KMnO_4$ or a hand-held UV lamp. Medium pressure liquid chromatography (MPLC) was carried out with a Biotage Isolera 1 in which the samples were dissolved in a minimal amount of CH_2Cl_2 and syringed on to a silica gel column (Premium R_f Silica Gel, 60A, 40-75 μm). Melting points (m.p.) were measured with a Uni-Melt apparatus (Thomas Hoover) and are uncorrected. NMR spectra were recorded with Varian VI 300 and 500 MHz and Bruker AV 500 MHz spectrometers, and the chemical shifts are reported in ppm. The ^{1}H, ^{13}C and ^{19}F signals were referenced as follows: 7.27 δ (^{1}H, $CHCl_3$), 1.94 δ (^{1}H, CHD_2CN), 77.0 δ (^{13}C, $CDCl_3$), 1.39 δ (^{13}C, CD_3CN) and -78.5 δ (^{19}F, CF_3CO_2H, external calibrant). IR spectra of synthetic samples were recorded on a Nicolet iS5 FT-IR spectrometer with an ATR source while mass spectra of methanolic solutions were obtained with a Bruker ESI-BioTOF; PEG was employed as an internal standard for high resolution data.

4.3.2. Synthetic Procedures for Compounds 5(1) and 5(2)

1-Benzyloxy-3-p-methoxybenzyloxy-5-methoxy myo-inositol monoorthoformate (**7**): 3-Benzyl-oxy-5-*p*-methoxybenzyloxy *myo*-inositol monoorthoformate (**6**)[35] (1.50 g, 3.70 mmol) was dissolved in 10 mL of dry THF in a 50 mL round bottomed flask under argon. After cooling to 0 ˚C, 0.300 g (7.4 mmol) of a 60% dispersion of NaH in mineral oil was added in several portions and the reaction mixture was stirred for 30 min. Methyl iodide (1.40 mL, 3.15 g, 22.2 mmol) was slowly syringed into the flask, and the resulting solution was allowed to warm up to room temperature overnight. A saturated aqueous solution of NH_4Cl (5.0 mL) was carefully added to the reaction mixture, and the resulting organic layer

was separated. Diethyl ether (10 mL) was used to extract the aqueous solution and the combined organic material was washed with 5.0 mL of brine, dried over Na_2SO_4 and concentrated under reduced pressure. Purification of the oily residue by MPLC (5/95 to 50/50 EtOAc/hexanes) afforded 1.30 g (87%) of **7** as a white solid (R_f = 0.21 in 25/75 EtOAc/hexanes, m.p. = 77 – 82 ˚C). ^{1}H NMR (300 MHz, $CDCl_3$) δ 7.33 (br s, 5H), 7.23 (d, *J* = 8.4 Hz, 2H), 6.85 (d, *J* = 8.4 Hz, 2H), 5.51 (s, 1H), 4.72 (d, *J* = 11.7 Hz, 1H), 4.65 (d, *J* = 11.4 Hz, 1H), 4.58 (d, *J* = 11.4 Hz, 1H), 4.52 (d, *J* = 11.7 Hz, 1H), 4.45 (br s, 1H), 4.42 – 4.29 (m, 4H), 3.82 (s, 4H), 3.46 (s, 3H). ^{13}C NMR (125 MHz, $CDCl_3$) δ 159.4, 137.6, 129.6, 129.4, 128.5, 128.0, 127.8, 113.9, 103.2, 74.0, 73.6, 71.8, 71.6, 69.9, 69.8, 69.4, 68.0, 56.7, 55.3. IR (ATR source) 3060, 3034, 2975, 2965, 2933, 2906, 2885, 2836, 2826 cm^{-1}. HRMS-ESI: calc for $C_{23}H_{26}NaO_7^+$ $(M + Na)^+$ 437.1571, found 437.1579.

3-Benzyloxy-5-methoxy myo-inositol monoorthoformate (**8**): 1-Benzyloxy-3-*p*-methoxybenzyl-oxy-5-methoxy *myo*-inositol monoorthoformate **7** (1.20 g, 2.90 mmol) and 1.00 g (4.40 mmol) of DDQ were dissolved in 30 mL of CH_2Cl_2 in a 100 mL round bottomed flask under an argon atmosphere. Water (1.5 mL) was added to the flask and the resulting dark orange solution was stirred overnight. It was then decanted and the orange precipitate was rinsed twice with 30 mL portions of diethyl ether. The combined solutions were successively washed with 30 mL of water and 30 mL of a saturated aqueous solution of $NaHCO_3$ before being transferred to a 250 mL round bottomed flask where it was stirred with 50 mL of a saturated aqueous solution of $NaHSO_3$ until the organic material turned light yellow. Both layers were separated and the aqueous solution was extracted with 20 mL of diethyl ether. The combined organic material was washed with 20 mL of brine, dried over Na_2SO_4 and concentrated under reduced pressure. Purification of the residue by

MPLC (5/95 to 65/35 EtOAc/hexanes) afforded 0.500 g (59%) of **8** as a colorless oil (R_f = 0.35 in 33/67 EtOAc/hexanes). ^{1}H NMR (500 MHz, $CDCl_3$) δ 7.45 – 7.29 (m, 5H), 5.48 (d, *J* = 1.4 Hz, 1H), 4.71 (d, *J* = 11.7 Hz, 1H), 4.65 (d, *J* = 11.7 Hz, 1H), 4.53 – 4.40 (m, 2H), 4.39 – 4.27 (m, 3H), 3.71 (br s, 1H), 3.67 (dd, *J* = 1.5, 2.9 Hz, 1H), 3.50 (s, 3H). ^{13}C NMR (125 MHz, $CDCl_3$) δ 136.0, 128.9, 128.8, 128.1, 102.6, 74.6, 73.3, 71.3, 69.3, 68.6, 67.9, 67.6, 56.8. IR (ATR source) 3488, 3088, 3063, 3030, 3006, 2958, 2932, 2825 cm^{-1}. HRMS-ESI: calc for $C_{15}H_{18}NaO_6^+$ $(M + Na)^+$ 317.0996, found 317.0982.

1-Trifluoromethyl-5-methoxy myo-inositol monoorthoformate (**5(1)**): 3-Benzyloxy-5-methoxy *myo*-inositol monoorthoformate **8** (0.500 g, 1.70 mmol) was dissolved in 20 mL of dry CH_2Cl_2 in a 100 mL round bottomed flask under argon. Dess-Martin periodinane (0.870 g, 2.00 mmol) was added all at once and the resulting cloudy solution was stirred overnight. Diethyl ether (40 mL) and a solution consisting of 20 mL of 10% $Na_2S_2O_3$ and 20 mL of 10% $NaHCO_3$ were added to the flask and the resulting mixture was stirred until the organic layer became clear (~ 15 min). The aqueous phase was saturated with NaCl, separated and extracted with 20 mL of diethyl ether. The combined organic material was dried over Na_2SO_4, concentrated under reduced pressure and purified by MPLC (10/90 EtOAc/hexanes to neat EtOAc) to afford 0.30 g (60%) of the intermediate ketone as a white solid. Its IR spectrum showed a band at 1763 cm^{-1} for the carbonyl stretch.

The intermediate ketone (0.270 g, 0.924 mmol) and 0.270 mL (0.260 g, 1.80 mmol) of $TMSCF_3$ were dissolved in 10 mL of dry THF in a 25 mL round bottomed flask under argon. After cooling to 0 ˚C, 20 μL of 1.0 M TBAF in THF was added all at once and the reaction mixture stirred for 12 h while it was allowed to warm up to room temperature. More TBAF (3.0 mL) was added via syringe at this point and after 45 min the solvent was

removed under reduced pressure. The residual material was diluted with 20 mL of diethyl ether and passed through a plug of silica gel which was subsequently rinsed with 30 mL of diethyl ether. Concentration of the combined ethereal material under reduced pressure afforded an oily residue that was purified by MPLC (5/95 EtOAc/hexanes to 50/50 EtOAc/hexanes) to give 0.290 g (88%) of 1-trifluoromethyl-3-benzyloxy-5-methoxy *myo*-inositol monoorthoformate **9** as a white solid (R_f = 0.35 in 25/75 EtOAc/hexanes). Its ^{19}F NMR spectrum showed a large signal at -81.2 and a 2% impurity at -75.7, but it was used in the next step without further purification.

In a 10 mL round bottomed flask, 0.290 g (0.800 mmol) of the intermediate alcohol **9** was dissolved in 5.0 mL of THF and 0.0970 g of Pearlman's catalyst (20% $Pd(OH)_2/C$) was added. This flask was placed in a Parr hydrogenation apparatus and the system was evacuated and then filled up with hydrogen to 500 psi three times in succession. After magnetically stirring the reaction mixture for 24 h, the pressure was released and 10 mL of diethyl ether was added. Filtration of this material through a small plug of silica gel and a subsequent rinse of the silica with 20 mL of diethyl ether afforded a combined solution that was concentrated under reduced pressure. The solid residue was partially dissolved in hot chloroform and upon cooling to room temperature white crystals were produced and 0.210 g (95%) of **5(1)** with m.p. = 163 – 167 ˚C was isolated. ^1H NMR (500 MHz, CD_3CN) δ 5.49 (br s, 1H), 5.45 (d, *J* = 1.1 Hz, 1H), 4.82 (br s, 1H), 4.59 (dd, *J* = 2.4 and 3.3 Hz, 1H), 4.42 (dd, *J* = 1.8 and 3.7 Hz, 1H), 4.36 (m, 1H), 4.30 (m, 1H), 3.78 (dd, *J* = 1.4 and 3.5 Hz, 1H), 3.47 (s, 3H). ^{13}C NMR (125 MHz, CD_3CN) δ 125.5 (q, *J* = 283 Hz), 103.0, 71.7 (q, *J* = 27.1 Hz), 71.6, 70.4, 70.0, 68.2, 67.8, 57.2. ^{19}F NMR (282 MHz, CD_3CN) δ -80.2. IR

(ATR source) 3244, 3023, 2988, 2963, 2923, 2845 cm^{-1}. HRMS-ESI: calc for $C_9H_{10}F_3O_6^-$ $(M - H)^-$ 271.0435, found 271.0413.

1,3-Trifluoromethyl-1,3-benzyloxy-5-methoxy myo-inositol monoorthoformate (**11**): In a 50 mL round bottomed flask, 0.200 g (0.395 mmol) of 3,5-bis(trifluoromethyl)-3,5-dibenzyloxy *myo*-inositol monoorthoformate **10**[35] was dissolved in 20 mL of dry THF under argon. After cooling to 0 ˚C, 0.0316 g (0.790 mmol) of a 60% dispersion of NaH in mineral oil was added in several portions while the reaction was stirred. The resulting slurry was stirred for an additional 30 min after which 0.250 mL (0.561 g, 3.95 mmol) of CH_3I was slowly syringed into the flask. The reaction mixture was stirred overnight and allowed to warm up to room temperature. A saturated aqueous solution of NH_4Cl (10 mL) was carefully added to the flask and the resulting solution was diluted with 10 mL of diethyl ether. Both layers were separated and the aqueous phase was extracted with 10 mL of diethyl ether. The combined ethereal solution was washed with brine, dried over Na_2SO_4 and concentrated under reduced pressure to afford an oily residue. Purification by MPLC (20/80 EtOAc/hexanes) gave 0.150 (71%) of **11** as a white solid (R_f = 0.59 in 25/75 EtOAc/hexanes, m.p. = 125 - 128 ˚C). ^{1}H NMR (500 MHz, $CDCl_3$) δ 7.24 (m, 2H), 7.19 (m, 4H), 6.96 (m, 4H), 5.67 (d, *J* = 0.90 Hz, 1H), 4.93 (t, *J* = 2.2 Hz, 1H), 4.70 (d, *J* = 10.4 Hz, 2H), 4.67 (dd, *J* = 1.8, 2.2 Hz, 2H), 4.52 (d, *J* = 10.4 Hz, 2H), 3.97 (q, *J* = 1.3 Hz, 1H), 3.57 (s, 3H). ^{13}C NMR (125 MHz, $CDCl_3$) δ 135.9, 128.4, 128.05, 127.7, 124.6 (q, *J* = 293 Hz), 102.6, 74.4 (q, *J* = 25.3 Hz), 69.8, 68.0, 67.4, 67.2, 57.5. ^{19}F NMR (471 MHz, $CDCl_3$) δ -71.3. IR (ATR source) 3093, 3072, 3030, 3012, 2983, 2975, 2942, 2917, 2894, 2841 cm^{-1}. HRMS-ESI: calc for $C_{24}H_{22}F_6NaO_6^+$ $(M + Na)^+$ 543.1213, found 543.1223.

1,3-Trifluoromethyl-5-methoxy myo-inositol monoorthoformate (**5(2)**): In a 10 mL round bottomed flask, 0.090 g (0.17 mmol) of 1,3-trifluoromethyl-1,3-benzyloxy-5-methoxy *myo*-inositol monoorthoformate **11** and 0.045 g of Pearlman's catalyst (20% $Pd(OH)_2/C$) was dissolved in 2.0 mL of THF. The resulting black suspension was placed in a hydrogenation apparatus and the system was evacuated and then filled up with hydrogen to 500 psi three times in succession. After 2 days of stirring with a magnetic stir bar, the pressure was released and the reaction mixture was diluted with 5 mL of diethyl ether. It was then filtered through a plug of silica gel and 20 mL of diethyl ether was used to rinse the silica. The combined ethereal solution was concentrated under reduced pressure to afford a very light brown solid which was partially dissolved in a small amount of hot $CHCl_3$ and allowed to cool to room temperature. White crystals of **5(2)** (0.030 g, 52%) were isolated (m.p. = 232 – 235 ˚C but they turned brown at 209 ˚C). ^{1}H NMR (500 MHz, CD_3CN) δ 5.58 (br s, 2H), 5.55 (d, *J* = 1.3 Hz, 1H), 4.58 (t, *J* = 2.0 Hz, 1H), 4.52 (dd, *J* = 1.8 and 2.2 Hz, 2H), 3.87 (dt, *J* = 1.6 and 1.8 Hz, 1H), 3.52 (s, 3H). ^{13}C NMR (125 MHz, CD_3CN) δ 125.2 (q, *J* = 284 Hz), 118.4, 102.9, 71.5 (q, *J* = 28.0 Hz), 69.9, 66.9, 57.7. ^{19}F NMR (471 MHz, CD_3CN) δ -79.2. IR (ATR source) 3334, 3233, 3025, 2986, 2966, 2918, 2861 cm^{-1}. HRMS-ESI: calc for $C_{10}H_9F_6O_6^-$ $(M - H)^-$ 339.0309, found 339.0307.

4.3.3. Binding Measurements

Acetonitrile-d_3 was dried over 3 Å molecular sieves for several days that had been activated at 320 ˚C for 12 h. Tetrabutylammonium chloride (TBACl) was dried by heating it at 50 ˚C under vacuum for 6 hours, and then was kept in a desiccator over P_2O_5 until it was used. NMR titrations of dilute solutions of the receptor (i.e., < 0.50 mM) maintained at constant concentrations were carried out by syringing in various amounts of TBACl to

septa-capped NMR tubes. Binding isotherms were obtained by monitoring the changes in the C–H chemical shifts. Non-linear 1:1 fits of the data were carried out using the Solver add-on for Excel to obtain the resulting binding constants (*K*, M^{-1}).

4.3.4. IR Studies

IR spectra of receptor solutions and their 1:1 TBACl complexes were obtained in a NaCl solution cell with a fixed path length of 0.10 mm using a Nicolet iS5 FT-IR spectrometer, and the spectra of the solvent and TBACl were subtracted to obtain the final results (i.e., background corrected spectra are reported). Alcohols **5(1)** and **5(2)** were dissolved in dry 1:9 CD_3CN/CCl_4 solutions (the former co-solvent was employed for solubility reasons) and the resulting absorptions were fit using B3LYP/6-31+G(d,p) computed gas-phase vibrational frequencies and intensities for the most stable structures located. Lorentzian functions were employed and the intensities at each wavelength ν in the spectral window are given by $I(\nu) = aI_o/(1 + \{(\nu - b\nu_o)^2/2S^2\})$, where a, b, ν_0, I_0 and S are the intensity correction parameter, frequency scaling factor, computed frequency and intensity, and peak width at half height, respectively. In this work as before, a frequency scaling factor of 0.945 (b) and peak widths at half-height (S) of 10 cm^{-1} and 60 cm^{-1} for the C−H and O−H stretching frequencies, respectively, were used.

4.3.5. Computations

B3LYP/6-31+G(d,p) geometry optimizations and vibrational frequency calculations were carried out using Gaussian 09.[44-46] Zero-point energies (ZPEs) and thermal corrections (TCs) were computed using unscaled vibrational frequencies. In some cases, structures were also calculated in acetonitrile using the conductor-like polarizable

continuum (CPCM) model;[47-50] the most stable gas-phase structures were used as the starting points in these cases.

4.4. Conclusions

The stereo configurations of non-interacting methoxy groups in small molecule receptors were found to have a large effect on these compounds anion recognition abilities and the structures of the resulting anion–receptor complexes. Conversion of an axial ether (**4(2)**) to an equatorial one (**5(2)**) was found to increase the TBACl binding constant by a factor of 320 and the latter compound is a better receptor than the analogous triol with three axial OH groups (i.e., **3(2)**) despite the loss of a hydrogen bond in the anion-bound complex. This appears to be due to a favorable bond dipole in the equatorial ether and a weak C−H•••OH hydrogen bond. These results have implications in designing useful catalysts and molecular receptors.

Chapter 5: Charge–Enhanced Acidity and Catalyst Activation*

Acid-base reactions are among the most common and fundamental transformations in all of chemistry. As a result, the development of new Brønsted acids and bases are of general interest, and have been the subject of extensive research efforts.[1-5] The strengths of these reagents are most commonly measured in water and/or dimethyl sulfoxide (DMSO), both of which are very polar solvents with high dielectric constants.[6] Substituent effects are also routinely studied in polar media whereas most organic transformations are carried out in less polar solvents.[7,8] Structure–reactivity insights from pK_a and substituent effect data, consequently can be misleading. In this work, IR spectroscopy is used to obtain relative acidities of a series of *m*- and *p*-substituted phenols in a nonpolar solvent, and these results are better fit by gas-phase acidities than the corresponding DMSO pK_a values. This observation led us to examine charged substituents in nonpolar solvents, and enhanced acidity and catalytic performance is reported.

In a clever study, Reed, et al. showed that IR spectroscopy can be used to provide relative acidities of the strongest Brønsted acids known to date.[9] This was accomplished by comparing the N–H stretching frequencies of a series of trioctylammonium salts of deprotonated carboranes. It was found that the weaker the interaction of the base, the higher the frequency for this band. Inspired by this work and related studies,[10,11] we obtained the IR spectra of 20 *m*- and *p*-substituted phenols in carbon tetrachloride in the presence and absence of acetonitrile-d_3 (Table 1).[12-17]

* Samet, M.; Buhle, J.; Zhou, Y.; Kass, S. R., Charge–Enhanced Acidity and Catalyst Activation. *J. Am. Chem. Soc.*, **2015**, *137*, 4678–4680. Copyright ACS. Reproduced with permission.

Table 1. Hydroxyl stretching frequencies for substituted phenols in CCl_4 along with their DMSO pK_a and gas-phase acidity values.

Cmpd	ν (cm^{-1})		Δν	pK_a	ΔG°_{acid}[a]
(XC_6H_4OH)	CCl_4	1% ACN[b]	(cm^{-1})	(DMSO)	(kcal mol^{-1})
X =					
m–$(CH_3)_2N$	3616	3464	152	19.1	343.5 ± 2.0
m–H	3611	3454	157	18.0	341.5 ± 1.0[c]
m-CH_3	3611	3448	163	18.2	341.3 ± 1.4[c]
m-CH_3O	3611	3446	165	18.2	341.5 ± 2.0
m–F	3608	3423	185	15.8	337.2 ± 2.0
m–CF_3	3605	3415	190	15.6	332.4 ± 2.0
m–Cl	3606	3415	191	15.8	335.3 ± 2.0
m–NO_2	3599	3387	212	14.4	327.6 ± 2.0
m–CN	3606	3388	218	14.8	329.0 ± 2.0
p–$(CH_3)_2N$	3616	3468	148	19.8	344.4 ± 2.0
p-CH_3O	3616	3463	153	19.1	343.9 ± 2.0
p-CH_3	3613	3453	160	18.9	343.8 ± 2.0
p–F	3608	3442	166	18.0	340.4 ± 2.0
p–Cl	3607	3435	172	16.7	336.5 ± 2.0
p–Br	3607	3415	192	16.4	
p-CH_3CO	3599	3407	192	14.0	328.6 ± 2.0
p–CF_3	3602	3406	196	15.3	330.1 ± 2.0
p-CH_3SO_2	3600	3390	210	13.6	324.2 ± 2.0
p–CN	3597	3380	217	13.2	325.5 ± 2.0
p–NO_2	3594	3373	221	10.8	320.9 ± 2.0
1[d]	3041	3043	–2	12.5 ± 1.0[e]	261.4[f]
2[g]	3576	3247	329	12.5 ± 1.0[e]	261.4[f]
3[h]	3566	3196	370	12.4 ± 1.1[e]	231.1[i]

[a]Equilibrium determinations from ref. 16 unless otherwise noted; some values are the average of two similar results. [b]1% ACN = 1% CD_3CN/99% CCl_4. [c]Measured by threshold collision-induced dissociation (ref. 17). [d]**1** = *p*-$HOC_6H_4N(n\text{-}C_8H_{17})_2CH_3^+ I^-$. [e]Measured by bracketing using two colored indicators. [f]B3LYP/6-31+G(d,p) computations on *p*-$HOC_6H_4N(n\text{-}C_8H_{17})_2CH_3^+$. [g]**2** = *p*-$HOC_6H_4N(n\text{-}C_8H_{17})_2CH_3^+$ $BAr^F{}_4^-$ where Ar^F stands for tetrakis(3,5-bis-(trifluoromethyl)phenyl)borate. [h]**3** = 3-Hydroxy-*N*-octylpyridinium $BAr^F{}_4^-$. [i]This calculated value is for 3-methylpyridinium phenol.

Dilute solutions (5 mM) of the phenols in the latter case gave rise to a sharp band for the "free" O–H stretch around 3600 cm^{-1} (Fig. 1, solid line). Addition of a small amount of

CD_3CN (1% v/v) led to a large 150 – 220 cm^{-1} frequency reduction (i.e., a red shift) and a broadening of the band due to the formation of an ArOH•••$NCCD_3$ hydrogen bond (Fig. 1, dotted line).[18,19]

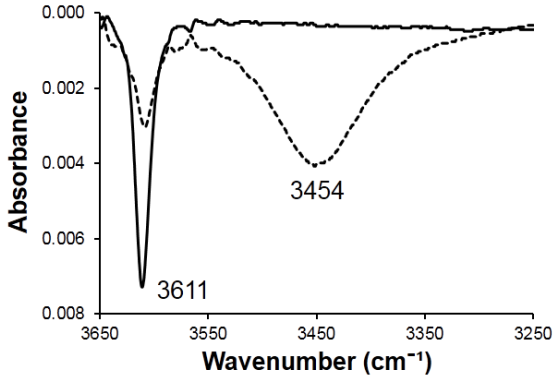

Figure 1. Representative IR spectrum of phenol in CCl_4 (solid line) and in 1% CD_3CN/CCl_4 (dotted line).

A plot of the experimental pK_a values in DMSO versus the observed frequency shifts for both the meta and para isomers is reasonably well fit by a single line in which the *p*-nitro and *p*-acetyl derivatives are omitted from the least squares analysis to improve the correlation coefficient from 0.89 to 0.94 (Fig. 2).[20] A similar correlation between the gas-phase acidities (ΔG°_{acid}) of the phenols and the change in their O–H frequency shifts is obtained for all of the compounds including the *p*-NO_2 and *p*-$COCH_3$ derivatives, but in this case the data are best fit by separate lines for the meta and para isomers (Fig. 3). These results suggest that resonance delocalization is not as effective in carbon tetrachloride as it is in dimethyl sulfoxide because this is a completely stabilizing mechanism for solvent-separated ion pairs (DMSO) but not for tight ion pairs (CCl_4).

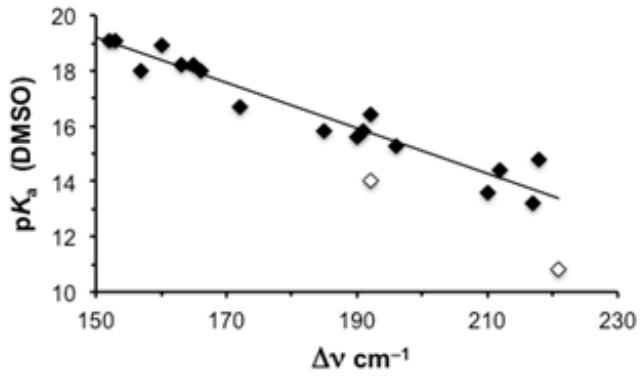

Figure 2. DMSO pK_a values vs *m*- and *p*-substituted phenol O–H frequency shifts in CCl_4 upon addition of CD_3CN. A linear least squares fit of the data affords y (pK_a) = -0.0822(Δν) + 31.6, r^2 = 0.936, where the open diamonds are for the *p*-NO_2 and *p*-$COCH_3$ derivatives which were excluded from the analysis.

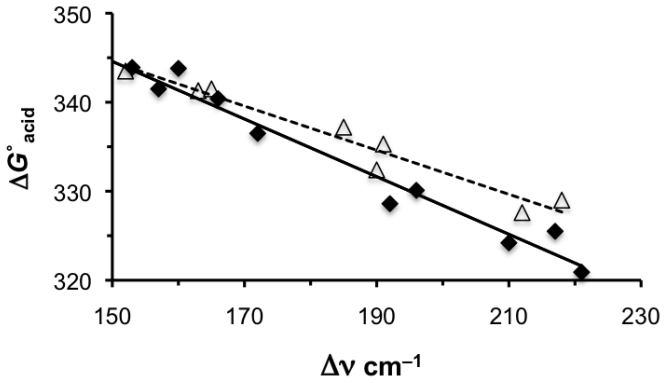

Figure 3. Gas phase acidities (kcal mol^{-1}) vs. O–H frequency shifts for *m*- (triangles) and *p*-substituted (diamonds) phenols. Linear least squares analyses give y (pK_a) = -0.241(Δν) + 380.3, r^2 = 0.950 (meta) [dotted line] and y (pK_a) = -0.324(Δν) + 393.2, r^2 = 0.970 (para) [solid line].

That is, in the latter case charge dispersal diminishes the electrostatic stabilizing interaction between oppositely charged ions and this results in a delicate balance between charge delocalization and Coulombic attraction. In the gas phase, counterions are absent and charge delocalization is of paramount importance, so it is not surprising that the behavior of the para derivatives diverge from the meta isomers. It was unexpected, however, that the gas-phase acidities correlate with those in nonpolar media better than the

DMSO pK_a values. Consequently, they may be more useful in structure/reactivity relationships.

Gas-phase substituents with the largest impact are charged groups whereas in polar media they are much less effective.[21,22] For example, *p*-$COCH_3$, *p*-CN and *p*-NO_2 substituted phenols are all more acidic than the *p*-$N(CH_3)_3^+$ derivative in DMSO[13] but the trimethylammonium ion is predicted to be at least 45 pK_a units (i.e., 62.7 kcal mol^{-1}) more acidic than the other species in the gas phase. This suggests that there should be an acidity reversal for these compounds in nonpolar solvents and a new strategy of enhancing Brønsted acidities and catalytic efficiencies in organic transformations.[23-26] To test this hypothesis, *p*-dioctylaminophenol was synthesized and subsequently methylated with methyl iodide; octyl groups were used to enhance the salt's solubility in carbon tetrachloride. The resulting methyl(dioctyl)ammonium ion (i.e., *p*-$HOC_6H_4N(n\text{-}C_8H_{17})_2CH_3^+$ I^-, **1**) has a broad OH band at 3041 cm^{-1} which indicates that there is a OH•••I^- hydrogen bond even though iodide is a weakly basic anion. Not surprisingly then, the IR spectrum of this salt is essentially unchanged upon addition of 1% CD_3CN. These results imply that **1** is not particularly acidic in CCl_4, and so tetrakis(3,5-bis(trifluoromethyl)phenyl)borate ($BAr^F{}_4^-$)) was used to replace the iodide counterion. The resulting phenol (*p*-$HOC_6H_4N(n\text{-}C_8H_{17})_2CH_3^+$ $BAr^F{}_4^-$, **2**) has an OH stretch at 3576 cm^{-1} which is red-shifted down to 3247 cm^{-1} in the presence of acetonitrile-d_3. This decrease of 329 cm^{-1} is 50% larger than for *p*-nitrophenol, the compound with the biggest shift that we previously observed, and indicates that **2** is more acidic in CCl_4 than the other phenols that were examined.

To assess this result further, the Friedel-Crafts reaction between β-nitrostyrene and *N*-methylindole was studied in chloroform (eq 1).

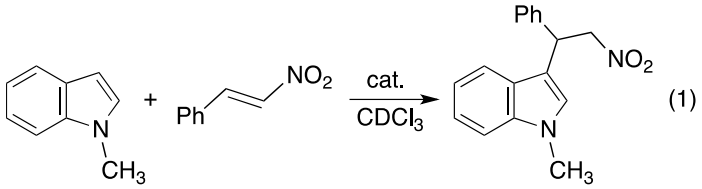

(1)

This transformation was chosen because it is an acid-catalyzed process and its rate should serve as an indicator of the phenol acidity.[24,27] As expected, **1** is a very poor catalyst, *p*-nitrophenol is about 7 times better, and **2** is 200–fold more reactive (Table 2, entries 1–3). These results are in accord with the acidity reversal of *p*-nitrophenol and **2** in going from DMSO to CCl_4. The relative rates of this transformation, however, are expected to be concentration dependent since the reactants are polar compounds and the relative acidity of *p*-nitrophenol and **2** is sensitive to the polarity of the medium. This hypothesis was borne out in that when the concentrations of the two reactants were tripled (entries 5 and 6), $k_2/k_{p\text{-}HOC_6H_4NO_2}$ decreased from 29 to 17. Likewise, when the original concentrations were reduced by a factor of three (entries 7 and 8) the ratio increased from 29 to 64. This latter difference is even larger (i.e., 180) when the reaction is run in toluene-d_8.

Additional gas-phase computations revealed that 3-hydroxy-*N*-methylpyridinium ion is 22 pK_a units (30 kcal mol^{-1}) more acidic than *p*-methyl(dipentyl)ammonium phenol, so the octylammonium $BAr^F{}_4^-$ salt of 3-hydroxypyridine (i.e., **3**) was synthesized. Its IR spectra in CCl_4 and 1% CD_3CN/CCl_4 have bands at 3566 and 3196 cm^{-1}, respectively. This red shift of 370 cm^{-1} indicates that **3** is more acidic than **2** in carbon tetrachloride as predicted by the B3LYP/6-31+G(d,p) calculations. The pyridinium ion **3** was also found to be a more

active catalyst than *p*-nitrophenol and **2** by factors of up to 2,000 and 30, respectively (entries 7-9).

Protonated catalysts have been successfully employed in organic transformations[24,28-31] but provide an additional hydrogen bond donor site that can be actively involved in the reaction. Non-protonated ions eliminate this concern and can enhance acidities of ionizable groups in nonpolar environments. This effect undoubtedly can be reversed to increase the basicity of basic sites, and the exploitation of electrostatics is an exciting avenue for further exploration.[21] Studies along these lines are in progress and even more dramatic effects may be obtained by incorporating the counterion into the reagent at a remote non-interacting location.

Table 2. Kinetic results for a Friedel-Crafts reaction (eq 1).[a]

entry	catalyst	[nitrostyrene], mM	$t_{1/2}$ (h)	$t_{1/2}$ (rel)
1	*p*-$HOC_6H_4NO_2$	83	1,200	1
2	**1**	83	8,400	0.14
3	**2**	83	42	29
4	**3**	83	1.6	750
5	*p*-$HOC_6H_4NO_2$	235	640	1
6	**2**	235	37	17
7	*p*-$HOC_6H_4NO_2$	29	4,100	1
8	**2**	29	64	64
9	**3**	29	2.1	2,000

[a]Three equivalents of *N*-methylindole and a fixed amount of catalyst (8.3 mM) were used in each case.

5.1. Experimental

5.1.1. General

All solvents and reagents were purchased from Sigma-Aldrich except for anhydrous dimethylformamide (DMF), sodium tetrakis(3,5-bis(trifluoromethyl)phenyl)borate ($NaBAr^F_4$), and acetonitrile-d_3 which came from EMD Chemicals, Matrix Scientific, and Cambridge Isotope Laboratories, respectively. Glassware including flasks, vials and NMR tubes were oven dried while septa, microsyringes and IR solution cells were stored in a desiccator containing phosphorous pentoxide. Activated molecular sieves (3 Å) were used to dry CD_3CN and degassed dimethyl sulfoxide (DMSO), and in the latter case this solvent was stored in a glove box under nitrogen before use. Anhydrous CCl_4 was stored under argon without further treatment. TLC analyses were performed on precoated (250 mm) silica gel 60 F-254 plates (Merck) and were visualized by staining with $KMnO_4$ or a hand-held UV lamp. Medium pressure liquid chromatography (MPLC) was carried out with a Biotage Isolera 1 with silica gel columns (Premium R_f Silica Gel, 60A, 40-75µm). Uncorrected melting points (m.p.) were determined with a Thomas Hoover Uni-Melt apparatus in unsealed tubes. Proton, ^{13}C, and ^{19}F NMR spectra were obtained with Varian VI 300 and 500 MHz and Bruker AV 500 instruments and chemical shifts are given in ppm and were referenced as follows: 7.27 δ (^1H, $CHCl_3$), 1.94 δ (^1H, CHD_2CN), 77.0 δ (^{13}C, $CDCl_3$), 1.39 δ (^{13}C, CD_3CN) and -78.5 δ (^{19}F, CF_3CO_2H, external calibrant). IR spectra of synthetic samples were recorded with an ATR source on a Nicolet iS5 FT-IR spectrometer whereas 0.1 and 1.0 mm fixed path length liquid cells with NaCl windows were used for the solution measurements. In the latter case, background corrected spectra of ~5.0 mM phenol solutions were obtained in dry CCl_4 and in 1% CD_3CN/CCl_4 (v:v). Mass spectra

were obtained with a Bruker ESI-BioTOF instrument using methanolic solutions and PEG as an internal standard for high resolution data.

5.1.2. Synthetic Procedures for Compounds 1-4

p-Dioctylaminophenol: *p*-Aminophenol (0.55 g, 5.04 mmol) was dissolved in 10 mL of anhydrous DMF in a 50 mL round bottomed flask under nitrogen. 1-Iodooctane (2.83 g, 11.8 mmol) and potassium carbonate (0.70 g, 5.07 mmol) were slowly added and the resulting solution was stirred for 3 h at 75 ˚C. A second batch of potassium carbonate (0.70 g, 5.07 mmol) was added in several portions, and the resulting mixture was stirred for an additional 6 h. Upon cooling to room temperature it was poured into 40 mL of water and the resulting solution was extracted 3 times with 100 mL portions of hexanes. The combined organic material was dried over $MgSO_4$, concentrated under reduced pressure, and the resulting product was purified by MPLC (hexanes to 10/90 EtOAc/hexanes) to afford 1.20 g (72%) of *p*-dioctylaminophenol as a colorless oil (R_f = 0.24 in 2/98 EtOAc/hexanes). ^{1}H NMR (300 MHz, $CDCl_3$) δ 7.16 (dd, *J* = 1.4, 8.0 Hz, 1H), 7.09 (ddd, *J* = 1.5, 8.1, 8.1 Hz, 1H), 6.95 (dd, *J* = 1.1, 8.1 Hz, 1H), 6.86 (ddd, *J* = 1.5, 7.7, 7.7 Hz, 1H), 2.85 (t, *J* = 7.0 Hz, 4H), 1.44 – 1.16 (m, 24H), 0.89 (t, *J* = 6.6 Hz, 6H). ^{13}C NMR (75 MHz, $CDCl_3$) δ 153.7, 137.4, 126.4, 123.0, 119.7, 113.4, 56.4, 31.8, 29.4, 29.2, 27.7, 27.3, 22.6, 14.1. IR (ATR source) 3318, 3044, 2953, 2923, 2854 cm^{-1}. HRMS-ESI: calc for $C_{22}H_{40}NO^+$ $(M + H)^+$ 334.3104, found 334.3081.

p-Methyldioctylammonium phenol iodide (**1**): *p*-Dioctylaminophenol (0.94 g, 2.82 mmol) was transferred to a 10 mL round bottomed flask under argon and 4.00 g (28.2 mmol) of iodomethane was added in one portion. The reaction flask was covered with aluminum foil and allowed to stand for 72 h at room temperature without stirring. Pentane

(~3 mL) was then slowly added along the edge of the flask so that it was placed on top of the reaction mixture and slowly diffused into the solution. Crystals of **1** formed after 5 h, and they were separated and washed several times with pentane and CCl_4 to afford 0.70 g (50%) of **1** as a light yellow solid. A portion of this material was recrystallized by dissolving it in 3 mL of methanol and slowly adding ~ 3 mL of deionized water with vigorous stirring. A cloudy solution resulted, and it was placed in a refrigerator at –5 ˚C for 24 h during which time light yellow needles of **1** formed (m.p. 119 – 121 ˚C). ^{1}H NMR (500 MHz, $CDCl_3$) δ 9.93 (br s, 1H), 8.00 (d, *J* = 5.5 Hz, 1H), 7.39 (dd, *J* = 7.4, 8.3 Hz, 1H), 7.16 (d, *J* = 8.3 Hz, 1H), 6.97 (dd, *J* = 7.4, 8.3 Hz, 1H), 4.61 (dd, *J* = 10.7, 11.9 Hz, 2H), 3.77 (dd, *J* = 10.7, 11.3 Hz, 2H), 3.54 (s, 3H), 1.55 (m, 2H), 1.44 – 1.13 (m, 22H), 0.85 (dd, *J* = 6.7, 7.0 Hz, 6H). ^{13}C NMR (125 MHz, $CDCl_3$) δ 150.1, 132.2, 126.4, 121.9, 121.9, 121.0, 120.7, 66.1, 49.1, 31.6, 29.1, 28.9, 26.2, 23.7, 22.5, 14.0. IR (ATR source) 3053, 2951, 2921 2870, 2851 cm^{-1}. HRMS-ESI: calc for $C_{23}H_{42}NO^+$ $(M - I)^+$ 348.3261, found 348.3265.

p-Methyldioctylammonium phenol tetrakis(3,5-bis(trifluoromethyl)phenyl)borate (**2**): Sodium tetrakis(3,5-bis(trifluoromethyl)phenyl)borate (100 mg, 0.11 mmol) and 50 mg (0.105 mmol) of **1** were transferred to a vial and 1.5 mL of CH_2Cl_2 was added. This mixture was stirred for 20 h at room temperature and was then filtered through a small pad of silica gel. The dichloromethane was removed under reduced pressure to afford 0.11 g (85%) of **2** as a viscous yellow oil. ^{1}H NMR (500 MHz, $CDCl_3$) δ 7.73 (s, 8H), 7.55 (s, 4H), 7.37 (ddd, *J* = 1.5, 7.4, 7.8 Hz, 1H), 7.14 (dd, *J* = 1.0, 8.3 Hz, 1H), 7.02 (ddd, *J* = 1.5, 7.3, 8.8 Hz, 1H), 6.87 (dd, *J* = 1.0, 7.8 Hz, 1H), 6.00 (br s, 1H), 4.38 (ddd, *J* = 4.4, 12.7, 13.2 Hz, 2H), 3.35 (ddd, *J* = 4.9, 11.8, 12.7 Hz, 2H), 3.29 (s, 3H), 1.52 (m, 2H), 1.34 – 1.10 (m,

22H), 0.83 (dd, J = 6.9, 7.3 Hz, 6H). ^{13}C NMR (125 MHz, $CDCl_3$) δ 161.6 (q, $^1J_{B\text{-}C}$ = 49.6 Hz), 147.4, 134.8, 133.2, 128.9 (qq, $^3J_{B\text{-}C}$ = 2.7 Hz and $^2J_{F\text{-}C}$ = 31.6 Hz), 125.9, 124.5 (q, $^1J_{F\text{-}C}$ = 271 Hz), 123.1, 122.5, 119.4, 117.5 (septet, $^3J_{F\text{-}C}$ = 3.6 Hz), 67.1, 48.9, 31.4, 28.70, 28.69, 25.9, 23.3, 22.4, 13.9. ^{19}F NMR (471 MHz, $CDCl_3$) δ -64.9. IR (ATR source) 3598, 2959, 2933, 2862 cm^{-1}. HRMS-ESI: calc for $C_{32}H_{12}BF_{24}^-$ (M – $C_{23}H_{42}NO)^-$ 863.0654, found 863.0654 and calc for $C_{23}H_{42}NO^+$ (M – $BAr^F{}_4)^+$ 348.3261, found 348.3254.

3-Hydroxy-N-octylpyridinium iodide: In a 100 mL round bottomed flask, 1.00 g (10.5 mmol) of 3-hydroxypyridine was added to 30 mL of dry acetonitrile. 1-Iodooctane (1.99 mL, 2.65 g, 11.0 mmol) was syringed into the reaction mixture in one portion and the resulting solution was stirred and gently refluxed for 20 h under argon. Upon cooling to room temperature, the solvent was removed under vacuum to give an oily brown residue. Column chromatography of this material with a small ~5 cm long plug of silica gel in a pipette was carried out first with dichloromethane and then ethyl acetate. The latter material was concentrated with a rotary evaporator to yield 1.21 g (34%) of the product as a viscous brown oil. ^{1}H NMR (500 MHz, $CDCl_3$) δ 10.31 (br s, 1H), 8.86 (s, 1H), 8.31 (s, 1H), 8.23 (s, 1H), 7.82 (s, 1H), 4.60 (t, J = 6.9 Hz, 2H), 2.03 (m, 2H), 1.45 – 1.18 (m, 10H), 0.86 (t, J = 6.8 Hz, 3H). ^{13}C NMR (125 MHz, $CDCl_3$) δ 158.2, 134.5, 132.6, 132.5, 128.5, 62.5, 31.5, 31.4, 28.9, 28.8, 26.0, 22.5, 14.0. IR (ATR source) 3336, 3047, 3023, 2954, 2926, 2855, 2734, 2616, 2515 cm^{-1}. HRMS-ESI: calc for $C_{13}H_{22}NO^+$ (M - I)$^+$ 208.1696, found 208.1688.

3-Hydroxy-N-octylpyridinium tetrakis(3,5-bis(trifluoromethyl)phenyl)borate (**3**): 3-Hydroxy-*N*-octylpyridinium iodide (35.2 mg, 0.105 mmol) and 100 mg of $NaBAr^F{}_4$ were used to carry out the salt metathesis reaction according to the procedure for the synthesis

of **2**. This afforded 80.0 mg (71%) of **3** as a brown gummy compound. ^{1}H NMR (500 MHz, $CDCl_3$) δ 8.08 – 7.35 (m, 16H), 6.73 (brs, 1H), 4.24 (t, *J* = 7.6 Hz, 2H), 1.91 (m, 2H), 1.39 – 1.16 (m, 10H), 0.86 (t, *J* = 6.6 Hz, 3H). ^{13}C NMR (125 MHz, $CDCl_3$) δ 161.6 (q, $^{1}J_{B\text{-}C}$ = 49.7 Hz), 156.4, 134.9, 134.7, 132.0, 131.7, 129.02 (qq, $^{3}J_{B\text{-}C}$ = 2.7 Hz, $^{2}J_{F\text{-}C}$ = 31.6 Hz), 128.97, 124.4 (q, $^{1}J_{F\text{-}C}$ = 271 Hz), 117.6 (septet, $^{3}J_{F\text{-}C}$ = 3.6 Hz), 63.3, 31.4, 31.2, 28.7, 28.6, 25.9, 22.4, 13.9. ^{19}F NMR (471 MHz, $CDCl_3$) δ -64.9. IR (ATR source) 3588, 3176, 3104, 3086, 2958, 2935, 2863 cm^{-1}. HRMS-ESI: calc for $C_{32}H_{12}BF_{24}^-$ $(M - C_{13}H_{22}NO)^-$ 863.0654, found 863.0636 and calc for $C_{13}H_{22}NO^+$ $(M - BAr^F{}_4)^+$ 208.1696, found 208.1708.

5.1.3. Computations

Geometry optimizations and vibrational frequencies were computed at the Minnesota Supercomputer Institute for Advanced Computational Research with the Gaussian 09 suite of programs using B3LYP and the 6-31+G(d,p) basis set.[32-34] Conformers of *p*-diethyl(methyl)ammonium phenol were explored and the most favorable one located was used as the starting point for the geometry optimization of *p*-methyl(dipentyl)ammonium phenol. The conjugate base of the resulting structure was used as the starting point for its geometry optimization. Energetics are reported at 298 K and unscaled vibrational frequencies were used in this regard.

5.1.4. Kinetics

Reactions were carried out under inert atmosphere in capped NMR tubes and their progress was monitored by ^{1}H NMR using signals at 8.04 and 5.23 ppm corresponding to β-nitrostyrene and the Friedel-Crafts product, respectively. In all cases, a 3:1 ratio of *N*-

methylindole and β-nitrostyrene were used along with a constant catalyst concentration of 8.3 mM. The resulting data were fit using second-order kinetics (i.e., ln([*N*-methylindole][β-nitro-styrene]$_o$/[β-nitrostyrene][*N*-methylindole]$_o$) = k([*N*-methylindole]$_o$ – [β-nitro-styrene]$_o$)t to obtain rate constants and the first half-lifes of the limiting reagent.

5.1.5. Titrations

Coulometric titrations of **1–3** were carried out in dry DMSO using two standard indicators with known pK_a values and colored conjugate bases. Both forward and reverse directions were examined by either adding a phenol (i.e., **1–3**) or the selected indicator to a dilute 1.0 mM dimsyl potassium solution and then adding the other acid. For **1** and **2**, 9-phenylthiofluorene (pK_a = 15.4) and 9-phenylsulfonylfluorene (pK_a = 11.5) were used. Colored solutions were observed in both directions only for the latter indicator and the favored direction indicates that it is more acidic than both **1** and **2**. For **3**, 9-carbo-methoxyfluorene ((pK_a = 10.3) and 9-phenylsulfonylfluorene were employed, but equilibration was only detected with the weaker acid. This suggests that the pK_a of **3** is between 11.3 and 13.5.

Chapter 6: Preorganized Hydrogen Bond Donor Catalysts: Acidities and Reactivities*

6.1. Introduction

Enzymes employ multiple stabilizing interactions such as inductive effects and hydrogen bond networks (HBNs) to control their structures and catalyze a wide variety of biochemical transformations.[1-7] For example, an array of hydrogen bonds has been implicated in playing a key role in the catalytic activity of ketosterioid isomerase by enhancing the acidity of the active site tyrosine residue from a pK_a value of 10.5 to 6.3.[2] Drawing inspiration from observations such as this, considerable effort has been expended mimicking enzyme behavior to develop more reactive and selective metal-free small molecule catalysts.[8-14] Thioureas play a particularly important role in this regard.[15-24]

Preorganization is well known to play a critical role in enzyme catalysis but generally has not been exploited in the design of hydrogen bond catalysts.[1,25,26] Schreiner has proposed that weak C–H···S hydrogen bonds in bis(3-trifluoromethyl-phenyl)thiourea (**1**) and related species with strong electron withdrawing groups (EWG) have enhanced populations of the reactive *Z,Z* conformers compared to dicyclohexylthiourea (**2**) and other derivatives that lack such substituents (Fig. 1).[17] While the thioureas with EWG are found to be more active catalysts, this may be a reflection of their greater acidity rather than

* Samet, M.; Kass, S. R., Preorganized Hydrogen Bond Donor Catalysts: Acidities and Reactivities. *J. Org. Chem.* accepted. DOI: 10.1021/acs.joc.5b01475. Copyright ACS. Reproduced with permission.

entropic effects due to preorganization. Unfortunately, suitable examples probing structural rigidity differences between compounds with the same acidity are lacking.[27,28]

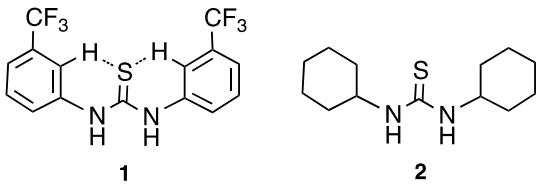

Figure 1. Bis(3-trifluoromethyl-phenyl)thiourea (**1**) and dicyclohexylthiourea (**2**).

In this work the acidities of a series of adamantane-like triols **3(0) – 3(3)** (Fig. 2), where the parenthetical number indicates how many trifluoromethyl groups are present in the compound, were measured in DMSO. These results reveal that **3(3)** has the same acidity as **4** and is 1000-fold less acidic than **5**, but was found to be up to two orders of magnitude more effective as a catalyst than these flexible acyclic analogs. The effects of the CF_3 groups also revealed that highly distant dependent inductive effects can be transmitted over long distances via HBNs, and that gas-phase acidities appear to correlate with catalytic reaction rates in nonpolar media as well or better than DMSO pK_a values.

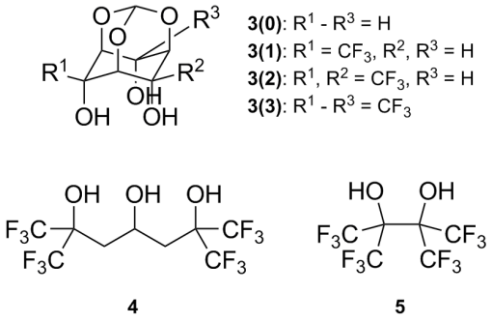

Figure 2. Adamantane-like triols **3(0) – 3(3)** and triol **4** and diol **5**.

6.2. Result and Discussion

Inductive effects are commonly exploited in designing more efficient catalysts and host compounds in molecular recognition.[12,17,29-31] Their impact, however, falls off rapidly with distance. For example, by substituting a trifluoromethyl group for an α-hydrogen in methanol the aqueous and DMSO acidities are enhanced by 3.1 and 5.5 pK_a units, respectively, whereas CF_3 incorporation at the γ-position of 1-propanol lowers the pK_a values by only 0.7 (H_2O) and 1.2 (DMSO).[32,33] In contrast, a long range inductive effect was recently proposed in the gas phase for triols **3(0)** – **3(3)** due to their HBNs.[34] To assess this situation in condensed media, their pK_a's were measured in DMSO.

Equilibrium acidities of **3(0)**, **3(2)**, and **3(3)** were determined as illustrated in eq. 1 by ^{1}H NMR spectroscopy (Table 1).[35]

$$AH + Ind^- \underset{}{\overset{K}{\rightleftharpoons}} A^- + IndH \quad (1)$$

$$pK_a(AH) = pK_a(IndH) - \log K$$

Table 1. Experimental and computed DMSO acidities.[a]

	pK_a		
Cmpd	exptl	B3LYP[b]	M06-2X[c]
3(0)	17.6 ± 0.4	18.3	18.0
3(1)	13.5 ± 0.5	11.5	11.4
3(2)	9.5 ± 0.3	9.1	8.6
3(3)	7.3 ± 0.3	6.2	6.4
4	7.1 ± 0.3	10.4	8.0
5	4.8 ± 0.1	3.5	5.4
$(CF_3)_3COH$	10.7	10.9	12.3
avg. error		1.3	1.1

[a]Relative acidities were computed and the experimental pKa of 1,1,1,3,3,3-hexafluoro-2-propanol (17.9, see ref. 44b) was used to obtain the indicated values. bB3LYP = B3LYP/6-311+G(d,p). cM06-2X = M06-2X/maug-cc-pVT(+d)Z.

Preliminary colorimetric titrations were also carried out for triol **3(1)** and these experiments indicate that it is more acidic than 9-(phenylthio)fluorene (pK_a = 15.4) and less acidic than 9-(phenylsulfonyl)fluorene (pK_a = 11.5).[36,37] These bracketing results suggest that 13.0 < pK_a(**3(1)**) < 14.0, and so pK_a(**3(1)**) = 13.5 ± 0.5 was assigned. These measured acidities span a 10 pK_a unit range from 7.3 to 17.6 which indicates that these triols are up to 10^3 and 10^5-fold more acidic than perfluoro-*tert*-butanol (pK_a = 10.7) and acetic acid (pK_a = 12.6), respectively.[33] Even the least acidic of these four compounds (i.e., **3(0)**) is ~13 orders of magnitude more acidic than an ordinary aliphatic alcohol such as 2-propanol (pK_a = 30.3) due to the HBN and inductive effect of the three oxygen atoms incorporated into the ring skeleton. It is also a stronger acid than 1,3,5-pentanetriol by 2.1 pK_a units and similar in acidity to phenol (pK_a = 18.0).[36]

Substitution of one of the equatorial hydrogens in **3(0)** at a hydroxyl bearing carbon by a trifluoromethyl group increases the acidity of the resulting triol (i.e., **3(1)**) by 4.1 pK_a units. Subsequent additions of a second and third CF_3 substituent result in additional pK_a enhancements of 4.0 and 2.2. The effect of the first CF_3 group is not surprising since it presumably is attached to the carbon bearing the hydroxyl substituent that is ionized upon deprotonation (i.e., the α-carbon) and exerts a strong stabilizing inductive effect. In contrast, the second CF_3 group is separated from the formally charged site by three intervening carbons and is located at the γ carbon, so only a small inductive stabilization of ~1.2 pK_a units would be expected in the absence of the HBN.[33] The large and additive nature of the second trifluoromethyl substituent can be viewed as a long range inductive effect transmitted by the HBN. Equivalently, this effect can be ascribed to an enhanced hydrogen bond due to the presence of the added electron withdrawing group. The effect of

the remote substituent due to the HBN, consequently, is reminiscent of π-conjugation in that the consequence of an electron-withdrawing group is transmitted over a long distance. As for the third CF_3 group, it is less effective than the other two as one would expect for an increasingly stabilized and delocalized anion.

Computations of the DMSO acidities of **3(0) – 3(3)** and related compounds were carried out using a polarized continuum model (Table 1). Both the B3LYP/6-311+G(d,p)[38,39] and M06-2X/maug-cc-pVT(+d)Z[40-43] results are in excellent accord with experiment in that the maximum errors are 3.3 (B3LYP) and 2.1 (M06-2X) pK_a units and the average unsigned errors are 1.3 and 1.1 pK_a units, respectively. If one uses perfluoro-*tert*-butanol instead of 1,1,1,3,3,3-hexafluoro-2-propanol as the reference acid, than there is little change in the results and the average errors are 1.3 (B3LYP) and 1.6 (M06-2X) pK_a units. For some reason when 2,2,2-trifluroethanol is employed as the reference compound, however, the average deviation from experiment increases to 4.1 pK_a units for both computational methods.

Triols **3(0)** – **3(3)** can serve as Brønsted acid and hydrogen bond catalysts. Their rigid structures should provide an entropic advantage over acyclic analogs and may enhance their catalytic abilities in an analogous manner to the preorganization of enzymes in biological systems. To assess this possibility, the Friedel-Crafts reaction between β-nitrostyrene and *N*-methylindole was investigated (eq 2). Triol **4** and diol **5** were selected for comparison purposes because the former alcohol is as acidic as **3(3)** and the latter is even stronger.[29]

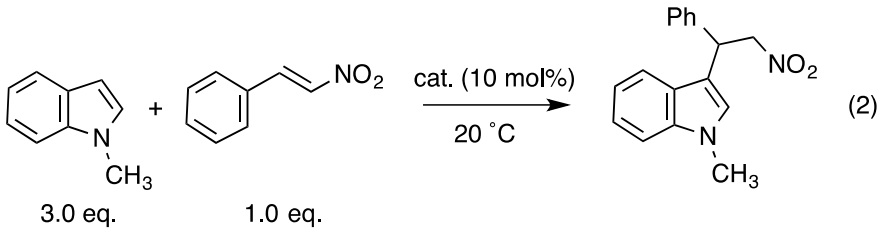

(2)

In the presence of **3(3)** the reaction was almost complete in 16 hours when carried out in toluene-d_8 at room temperature, and the second order half-life is 2.8 hours (Table 2).

Table 2. Kinetic results for the acid-catalyzed Friedel-Crafts reaction of *N*-methylindole and β-nitrostyrene.

entry	cat.	solvent	t (h)	conv.[a]	$t_{1/2}$ (h)
1	no cat.	$C_6D_5CD_3$	360	no rxn	
2	**3(3)**	$C_6D_5CD_3$	16.3	96	2.8
3	**4**	$C_6D_5CD_3$	504	75	232
4	**5**	$C_6D_5CD_3$	96	95	21.8
5	**3(2)**	$C_6D_5CD_3$/ 1% CD_3CN	192	75	88.1
6	**3(3)**	$C_6D_5CD_3$/ 1% CD_3CN	49	94	10.3
7	**6**	$C_6D_5CD_3$/ 1% CD_3CN	168	62	111

[a]conv. = conversion (%)

Both **4** and **5** are much less efficient catalysts and their transformations take place ~100 and 10 times more slowly. No reaction was observed in the absence of a catalyst after 15 days and consequently these results indicate that the DMSO acidities of these catalysts do not correlate with the reaction rates. In many respects this should not be surprising as DMSO is a very polar solvent with a high dielectric constant whereas toluene is nonpolar and has a small dielectric constant (i.e., 47.2 vs 2.4, respectively).[44] Computed B3LYP/6-311+G(d,p) and M06-2X/ maug-cc-pVT(+d)Z gas-phase acidities (Table 3), however, are in keeping with the observed reactivity order. This finding is consistent with our previous

report showing that the acidities of a series of substituted phenols in a non-polar solvent (CCl_4) are better correlated with their gas-phase acidities than their DMSO pK_a values.[45]

Solubility is an issue for **3(0)** – **3(2)** as these compounds have fewer trifluoromethyl groups than **3(3)** and do not dissolve in toluene-d_8. To explore these species, a small amount of acetonitrile-d_3 (1% v/v) was added as a cosolvent. This enabled **3(2)** and Schreiner's thiourea ($(3,5\text{-}(CF_3)_2C_6H_3NH)_2CS$, **6**)[15] to be examined, but since CD_3CN is a hydrogen bond acceptor its presence was expected to slow down the reaction.

Table 3. Computed B3LYP/6-311+G(d,p) and M06-2X/ maug-cc-pVT(+d)Z gas-phase acidities.

cmpd	ΔG°_{acid}	
	B3LYP	M06-2X
3(0)	327.6	326.9
3(1)	314.9	313.7
3(2)	307.8	306.4
3(3)	301.5	300.3
4	309.6	310.8
5	302.8	307.6

This was observed for **3(3)** in that the presence of CD_3CN was found to retard the transformation by a factor of ~4 (entries 2 and 6, Table 2). Nevertheless, both **3(2)** and **3(3)** were found to be more effective catalysts than **6** despite the thiourea being more acidic than **3(2)** in DMSO (i.e., pK_a = 8.5 (**6**) and 9.5 (**3(2)**)).[30]

All four triols **3(0)** – **3(3)** catalyze the aminolysis of styrene oxide with aniline at 60 ˚C under solvent-free conditions (eq 3 and Table 4). Interestingly, the reactivity and selectivity orders follow the DMSO and not the gas-phase acidities. That is, the lower the pK_a value of the catalyst, the faster the reaction and, in general, the greater the selectivity for the

addition product at the more hindered position (i.e., **7**). This presumably is due to the polar nature of the reactants and the corresponding medium that results.

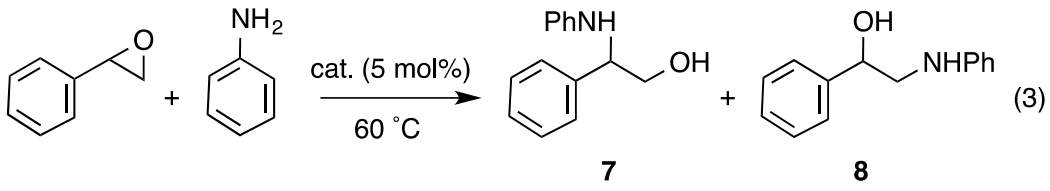

Table 4. Acid-catalyzed aminolysis of styrene oxide with aniline.

entry	cat.	time (h)	conv.[a]	k_{rel}	pdt ratio (%)	
					7	**8**
1	no cat.	3.5	4.0	1.0	35	65
2	**3(0)**	3.5	11	3.0	54	46
3	**3(1)**	3.5	58	33	75	25
4	**3(2)**	3.5	90	220	84	16
5	**3(3)**	1.0	96	580	91	9
6	**4**	0.5	69	370	81	19
7	**5**	0.25	68	710	88	12

[a]conv. = conversion (%)

Alcohols **3(0)**, **3(1)** and binol were examined as catalysts for the room temperature Morita-Baylis-Hillman reaction between hydrocinnamaldehyde and cyclohexanone in the presence of two equivalents of tributylphosphine (eq 4).

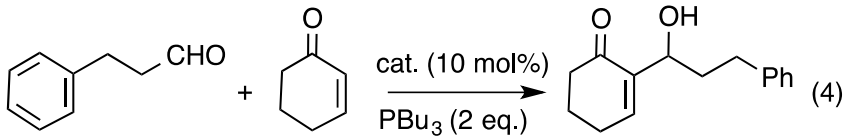

Table 5. Acid-catalyzed Morita-Baylis-Hillman results.

entry	cat.	t (h)	conversion (%)
1	no cat.	7	14
2	**3(0)**	3.5	98
3	**3(1)**	7	56
4	binol	7	98

This transformation was essentially complete within 3.5 hours when **3(0)** was employed whereas only 14% conversion was observed in double the time without the triol (Table 5). More acidic catalysts such as **3(1)** and binol, which is estimated to be ~3.9 pK_a units more acidic than **3(0)**,[46,47] were found to be less effective. This can be explained by deactivation of the catalysts by the presence of basic tributylphosphine. As a result, **3(2)** and **3(3)** were not examined in this transformation.

6.3. Conclusion

Acidity measurements of the pK_a's of **3(0)** – **3(3)** were carried out in DMSO and reveal that a HBN is analogous to π-electron delocalization in that both can transmit charge-stabilizing effects over long distances. More specifically, incorporation of a CF_3 group at a hydroxyl bearing carbon in **3(0)** (i.e., the α-carbon) enhances the acidity by 4.1 pK_a units and the addition of a remote second CF_3 substituent at one of the γ-carbons leads to the same increase in acidity (i.e., 4.0 pK_a units). These rigid triols also serve as Brønsted acid and hydrogen bond catalysts in organic transformations. Their reactivity was compared to flexible analogs of similar or greater acidity, and in a nonpolar environment the entropic advantage of the locked-in triols was found to lead to rate differences as large as 100-fold. The relative reactivity order was also found to correlate with the catalysts gas-phase

acidities (ΔG°_{acid}) and not their DMSO pK_a values. This finding taken together with a previous report showing that the acidities of substituted phenols in CCl_4 are better fit by ΔG°_{acid} than their DMSO pK_a's[47] suggests that this is a general observation. In a polar medium the observed benefit of a rigid versus a flexible catalyst was greatly diminished, and DMSO pK_a values are a better guide to reactivity than gas-phase acidities.

6.4. Experimental

6.4.1. General

Compounds **3(0)** – **3(3)** and **4** were synthesized as previously described.[29,30,48] Molecular sieves (3 Å) were activated at 320 ˚C overnight and then used to dry solvents over the course of a few days. DMSO and DMSO-d_6 were degassed by carrying out 3 freeze-pump-thaw cycles and stored over freshly activated molecular sieves in a dry box under a nitrogen atmosphere for up to several days before use. NMR tubes, vials and flasks were oven dried and kept in a dry box along with needles, syringes and NMR caps. Pentane was dried over P_2O_5 at reflux for 1 hour and subsequently distilled. Dimsyl potassium (i.e., KCH_2SOCH_3) was prepared daily under argon by reacting DMSO for 45 min with a 30% suspension of potassium hydride in mineral oil that had been washed 3 times with dry pentane. A 500 MHz spectrometer was used at 295 K to record ^{1}H NMR spectra.

6.4.2. Acidity Determinations

The acidities of triols **3(0)**, **3(2)** and **3(3)** were measured in dry DMSO at 23 ˚C by ^{1}H NMR as previously described.[32] Multiple measurements were performed for each compound using one of the following indicators: 1,2,2-triphenylethanone (pK_a = 18.8), 9-

carbomethoxy-fluorene (pK_a = 10.3), or (9-fluorenyl)triphenylphosphonium bromide (pK_a = 6.6).[33] Alcohol **3(1)** was examined by carrying out colorimetric titrations with 9-(phenylthio)fluorene (pK_a = 15.4) and 9-(phenylsulfonyl)fluorene (pK_a = 11.5) in both the forward and reverse directions.[33] Since the conjugate bases of these two indicators give colored solutions, it was possible to determine the favored direction and the magnitude of the equilibrium constant in both instances (i.e., ≤ 1 or ≥ 1). DMSO acidity values for additional compounds are provided in the appendix for chapter 6.

6.4.3. Friedel-Crafts Reactions

In a capped NMR tube, 0.0075 g (0.050 mmol) of β-nitrostyrene and 10 mol% of the catalyst (0.0050 mmol) were dissolved in 0.58 mL of the solvent under argon. *N*-Methylindole (19 μL, 0.020 g, 0.15 mmol) was syringed into the NMR tube at room temperature and the reaction progress was monitored using the ^{1}H NMR signals at 8.04 and 5.23 ppm for the limiting reactant and the Friedel-Crafts product, respectively. A second-order kinetic expression (i.e., $\ln([N\text{-methylindole}][\beta\text{-nitrostyrene}]_o/[\beta\text{-nitrostyrene}][N\text{-meth-ylindole}]_o) = k([N\text{-methylindole}]_o - [\beta\text{-nitrostyrene}]_o)t$) was used to fit the data and obtain both the rate constants and the first half-lifes for the disappearance of β-nitrostyrene.

6.4.4. Aminolysis of Styrene Oxide

In a 0.5 dram vial, 23 μL (0.024 g, 0.20 mmol) of styrene oxide, 18 μL (0.018 g, 0.20 mmol) of aniline and 5 mol% (0.010 mmol) of the catalyst were mixed together at 60 ˚C. Reaction progress was qualitatively monitored by TLC (20/80 EtOAc/hexanes) on 250 mm

60 F-254 silica gel plates. At select times aliquots were withdrawn and dissolved in 0.60 mL of $CDCl_3$, and their ^1H NMR spectra were obtained.

6.4.5. Morita-Baylis-Hillman Transformations

Cyclohexenone (48 μL, 0.048 g, 0.50 mmol), hydrocinnamaldehyde (33 μL, 0.034 g, 0.25 mmol) and 10 mol% (0.025 mmol) of the catalyst were dissolved in 0.25 mL of THF-d_8 under argon in a capped NMR tube. Tributylphosphine (130 μL, 0.11 g, 0.52 mmol) was added via syringe at room temperature and the reaction progress was monitored as a function of time by monitoring the disappearance of the aldehyde signal at 9.72 ppm in the ^1H NMR spectra.

6.4.6. Computations

All of the calculations carried out in this work were performed at the Minnesota Supercomputer Institute for Advanced Computational Research using Gaussian 09.[34] Full geometry optimizations and vibrational frequencies were carried out on triols **3(0)** – **3(3)** and their conjugate bases with the B3LYP density functional and the 6-31+G(d,p) basis set.[35,36] The most stable conformers located were reoptimized with the larger 6-311+G(d,p) basis set as well as with the M06-2X functional and the aug-cc-pVDZ basis set.[37-40] Vibrational frequencies were recomputed with the latter method and in this case single-point energies were subsequently carried out with the maug-cc-pVT(+d)Z basis set.[41] Conductor-like polarized continuum model (CPCM)[42,43] B3LYP/6-311+G(d,p) and M06-2X/aug-cc-pVDZ single point energies were also computed to obtain relative DMSO pK_a values. These results were converted to absolute values by using 1,1,1,3,3,3-hexafluoro-2-

propanol as a reference compound and employing its experimentally measured pK_a of 17.9.[4]

Bibliography

References for Chapter 1

(1) Arunan, E.; Desiraju, G. R.; Klein, R. A.; Sadlej, J.; Scheiner, S.; Alkorta, I.; Clary, D. C.; Crabtree, R. H.; Dannenberg, J. J.; Hobza, P.; Kjaergaard, H. G.; Legon, A. C.; Mennucci, B.; Nesbitt, a. D. J., Definition of the Hydrogen Bond. *Pure Appl. Chem.* **2011**, *83*, 1637–1641.

(2) Perrin, C. L.; Nielson, J. B., Strong Hydrogen Bonds in Chemistry and Biology. *Annu. Rev. Phys. Chem.* **1997**, *48*, 511-544.

(3) MacMillan, D. W. C., The Advent and Development of Organocatalysis. *Nature* **2008**, *2008*, 304-308.

(4) Sinnott, M., *Comprehensive Biological Catalysis*. Academic Press: London, 1998.

(5) Miller, C., ClC Chloride Channels Viewed Through a Transporter Lens. *Nature* **2006,** *440*, 484-489.

(6) Frey, P. A., Strong Hydrogen Bonding in Molecules and Enzymatic Complexes. *Magn. Reson. Chem.* **2001,** *39*, 5190-5198.

(7) Frey, P. A.; Whitt, S. A.; Tobin, J. B., A Low-Barrier Hydrogen Bond in the Catalytic Triad of Serine Proteases. *Science* **1994,** *264*, 1927-1930.

(8) Badger, R. M., The Relation between the Energy of a Hydrogen Bond and the Frequencies of the OH Bands. *J. Chem. Phys.* **1940,** *8*, 288-289.

(9) Kuhn, L. P.; Wires, R. A., The Hydrogen Bond. VI. Equilibrium between Hydrogen Bonded and Nonbonded Conformation of α,ω-Diol Monomethyl Ethers. *J. Am. Chem. Soc.* **1964,** *86*, 2161-2165.

(10) Wood, P. A.; Allen, F. H.; Pidcock, E., Hydrogen-bond Directionality at the Donor H Atom-Analysis of Interaction Energies and Database Statistics. *Cryst. Eng. Comm.* **2009,** *11*, 1563–1571.

(11) (a) Mock, W. L.; Morsch, L. A., Low Barrier Hydrogen Bonds within Salicylate Mono-anions. *Tetrahedron* **2001,** *57*, 2957-2964; (b) Childs, W.; Boxer, S. G., Proton Affinity of the Oxyanion Hole in the Active Site of Ketosteroid Isomerase. *Biochemistry* **2010,** *49*, 2725-2731.

(12) Zeegers-Huyskens, T., Hydrogen Bonding Equilibria in Solution and Gas-Phase Protonic Acidities or Basicities. *J. Mol. Liq.* **1986,** *32*, 191-207.

(13) (a) Magonski, J.; Pawlak, Z.; Jasinski, T., Dissociation Constants of Substituted Phenols and Homoconjugation Constants of the Corresponding Phenol-Phenolate Systems in Acetonitrile. *J. Chem. Soc., Faraday Trans.* **1993,** *89*, 119-122; (b) Peter Guthrie, J., Short Strong Hydrogen Bonds: Can They Explain Enzymic Catalysis? *Chem. Biol.* **1996,** *3*, 163-170; (c) Shan, S.-O.; Herschlag, D., The Change in Hydrogen Bond Strength Accompanying Charge Rearrangement: Implications for Enzymatic Catalysis. *Proc. Natl. Acad. Sci.* **1996,** *93*, 14474-14479.

(14) (a) Pašalić, H.; Aquino, A. J. A.; Tunega, D.; Haberhauer, G.; Gerzabek, M. H.; Georg, H. C.; Moraes, T. F.; Coutinho, K.; Canuto, S.; Lischka, H., Thermodynamic Stability of Hydrogen-Bonded Systems in Polar and Nonpolar Environments. *J. Comput. Chem.* **2010,** *31*, 2046-2055; (b) Pasalic, H.; Tunega, D.; Aquino, A. J. A.; Haberhauer, G.; Gerzabek, M. H.; Lischka, H., The Stability of the Acetic Acid Dimer in Microhydrated Environments and in Aqueous Solution. *Phys. Chem. Chem. Phys.* **2012,** *14*, 4162-4170; (c) Sigala, P. A.; Ruben, E. A.; Liu, C. W.; Piccoli, P. M. B.; Hohenstein, E. G.; Martínez, T. J.; Schultz, A.

J.; Herschlag, D., Determination of Hydrogen Bond Structure in Water versus Aprotic Environments To Test the Relationship Between Length and Stability. *J. Am. Chem. Soc.* **2015,** *137*, 5730–5740.

(15) Rospenk, M.; Zeegers-Huyskens, T., Solvent Effect on the Intramolecular Hydrogen Bond Strength and on the Isotopic Ratio ν_{NH^+}/ν_{ND^+} in a Trisubstituted Mannich Base. *J. Phys. Chem.* **1987,** *91*, 3974-3977.

(16) Wohlfarth, C., Dielectric Constant of Acetonitrile. In *Springer Materials - The Landolt-Börnstein Database (http://www.springermaterials.com)* [Online] Lechner, M. D., Ed. Springer-Verlag: Berlin Heidelberg, 2008.

(17) Wohlfarth, C., Dielectric Constant of Dimethylsulfoxide. In *Springer Materials - The Landolt-Börnstein Database (http://www.springermaterials.com)* [Online] Lechner, M. D., Ed. Springer-Verlag: Berlin Heidelberg, 2008.

(18) Kolthoff, I. M.; Chantooni, M. K., Intramolecular Hydrogen Bonding Involving Hydroxyl Groups in Mono- and Dianions of Diprotic Acids in Acetonitrile and Dimethyl Sulfoxide. *J. Am. Chem. Soc.* **1976,** *98*, 5063-5068.

(19) (a) McCoy, L. L., The Geometry of Intramolecular Hydrogen Bonding in 1,2-Dicarboxylic Acids. *J. Am. Chem. Soc.* **1967,** *89*, 1673-1677; (b) McDaniel, D. H.; Brown, H. C., Hydrogen Bonding as a Factor in the Ionization of Dicarboxylic Acids. *Science* **1953,** *118*, 370-372; (c) Crowder, C. A.; Bartmess, J. E., Gas-Phase Acidities of Diols. *J. Am. Soc. Mass. Spectrom.* **1993,** *4*, 723-726; (d) Shan, S.-O.; Herschlag, D., Energetic Effects of Multiple Hydrogen Bonds. Implications for Enzymatic Catalysis. *J. Am. Chem. Soc.* **1996,** *118*, 5515-5518; (e) Tian, Z.; Fattahi, A.; Lis, L.; Kass, S. R., Single-Centered Hydrogen-Bonded Enhanced Acidity (SHEA) Acids: A New Class of Brønsted Acids. *J.*

Am. Chem. Soc. **2009,** *131*, 16984-16988; (f) Shokri, A.; Abedin, A.; Fattahi, A.; Kass, S. R., Effect of Hydrogen Bonds on pK_a Values: Importance of Networking. *J. Am. Chem. Soc.* **2012,** *134*, 10646-10650; (g) Shokri, A.; Wang, Y.; O'Doherty, G. A.; Wang, X.-B.; Kass, S. R., Hydrogen-Bond Networks: Strengths of Different Types of Hydrogen Bonds and an Alternative to the Low Barrier Hydrogen-Bond Proposal. *J. Am. Chem. Soc.* **2013,** *135*, 17919-17924.

(20) (a) Ramond, T. M.; Davico, G. E.; Schwartz, R. L.; Lineberger, W. C., Vibronic Structure of Alkoxy Radicals via Photoelectron Spectroscopy. *J. Chem. Phys.* **2000,** *112*, 1158-1169; (b) Higgins, P. R.; Bartmess, J. E., The Gas Phase Acidities of Long Chain Alcohols. *Int. J. Mass Spectrom.* **1998,** *175*, 71-79; (c) Ellison, G. B.; Engleking, P. C.; Lineberger, W. C., Photoelectron Spectroscopy of Alkoxide and Enolate Negative Ions. *J. Phys. Chem.* **1982,** *86*, 4873-4878.

(21) (a) Shokri, A.; Schmit, J.; Wang, X.-B.; Kass, S. R., Hydrogen Bonded Arrays: the Power of Multiple Hydrogen Bonds. *J. Am. Chem. Soc.* **2012,** *134*, 2094-2099.

(22) (a) Dieter, S., *Selectivities in Lewis Acid Promoted Reactions.* Kluwer Academic Publishers: Dordrecht, 1989; Vol. 289; (b) Yamamoto, H., *Lewis Acids in Organic Synthesis*. Wiley-VCH: Weinheim, 2000; (c) Yamamoto, H.; Ishihara, K., *Acid Catalysis in Modern Organic Synthesis*. Wiley-VCH: Weinheim, 2008; Vol. 1.

(23) (a) Kobayashi, S.; Manabe, K., Green Lewis Acid Catalysis in Organic Synthesis. *Pure Appl. Chem.* **2000,** *72*, 1373-1380; (b) Kobayashi, S.; Manabe, K., Development of Novel Lewis Acid Catalysts for Selective Organic Reactions in Aqueous Media. *Acc. Chem. Res.* **2002,** *35*, 209-217.

(24) (a) Hunt, I. R.; Rauk, A.; Keay, B. A., Why Do Catalytic Quantities of Lewis Acid Generally Yield More Product than 1.1 Equiv in the Intramolecular Diels-Alder Reaction with a Furan Diene? 2. AM1 Calculations and Mathematical Simulation of the Equilibria. *J. Org. Chem.* **1996,** *61*, 751-757; (b) Funatomi, T.; Nakazawa, S.; Matsumoto, K.; Nagase, R.; Tanabe, Y., Ti-mediated Direct and Highly Stereoselective Mannich Reactions between Esters and Oxime Ethers. *Chem. Commun.* **2008**, 771-773; (c) Ohkata, K.; Miyamoto, K.; Matsumura, S.; Akiba, K.-Y., Highly Asymmetric Induction in the Diels-Alder Reaction of 3-Alkoxycarbonyl-Substituted Coumarin. *Tetrahedron Lett.* **1993,** *34*, 6575-6578; (d) Singleton, D. A.; Merrigan, S. R.; Beno, B. R.; Houk, K. N., Isotope Effects for Lewis Acid Catalyzed Diels-Alder Reactions. The Experimental Transition State. *Tetrahedron Lett.* **1999,** *40*, 5817-5821; (e) Schreiner, P. R., Metal-free Organocatalysis through Explicit Hydrogen Bonding Interactions. *Chem. Soc. Rev.* **2003,** *32*, 289-296.

(25) Oppolzer, W.; Rodriguez, I.; Blagg, J.; Bernardinelli, G., Asymmetric Diles-Alder Reactions: X-Ray Crystal-Structure Analysis of [N-((E)-But-2-enoyl)bornane-10,2-sultam]tetrachlorotitanium). *Helv. Chim. Acta* **1989,** *72*, 123-130.

(26) (a) Akiyama, T., Stronger Brønsted Acids. *Chem. Rev.* **2007,** *107*, 5744-5758; (b) Doyle, A. G.; Jacobsen, E. N., Small-Molecule H-Bond Donors in Asymmetric Catalysis. *Chem. Rev.* **2007,** *107*, 5713-5743; (c) Shokri, A.; Wang, X.-B.; Kass, S. R., Electron-Withdrawing Trifluoromethyl Groups in Combination with Hydrogen Bonds in Polyols: Brønsted Acids, Hydrogen-Bond Catalysts, and Anion Receptors. *J. Am. Chem. Soc.* **2013,** *135*, 9525−9530. (d) Parmar, D.; Sugiono, E.; Raja, S.; Rueping, M., Complete Field Guide to Asymmetric BINOL-Phosphate Derived Brønsted Acid and Metal Catalysis: History

and Classification by Mode of Activation; Brønsted Acidity, Hydrogen Bonding, Ion Pairing, and Metal Phosphates. *Chem. Rev.* **2014,** *114*, 9047-9153.

(27) (a) Hine, J.; Linden, S.-M.; Kanagasabapathy, V. M., 1,8-Biphenylenediol Is a Double-Hydrogen-Bonding Catalyst for Reaction of an Epoxide with a Nucleophile. *J. Am. Chem. Soc.* **1985,** *107*, 1082-1083; (b) Kelly, T. R.; Meghani, B.; Ekkundi, V. S., Diels-Alder Reactions: Rate Acceleration Promoted by a Biphenylenediol. *Tetrahedron Lett.* **1990,** *31*, 3381-3384.

(28) (a) Thadani, A. N.; Stankovic, A. R.; Rawal, V. H., Enantioselective Diels–Alder Reactions Catalyzed by Hydrogen Bonding. *Proc. Natl. Acad. Sci.* **2004,** *101*, 5846-5850; (b) Zhang, X.; Du, H.; Wang, Z.; Wu, Y.-D.; Ding, K., Experimental and Theoretical Studies on the Hydrogen-Bond-Promoted Enantioselective Hetero-Diels-Alder Reaction of Danishefsky's Diene with Benzaldehyde. *J. Org. Chem.* **2006,** *71*, 2862-2869.

(29) Yamada, Y. M. A.; Ikegami, S., Efficient Baylis–Hillman Reactions Promoted by Mild Cooperative Catalysts and Their Application to Catalytic Asymmetric Synthesis. *Tetrahedron Lett.* **2000,** *41*, 2165–2169.

(30) Yamamoto, H.; Futatsugi, K., Designer Acids: Combined Acid Catalysis for Asymmetric Synthesis. *Angew. Chem. Int. Ed.* **2005,** *44*, 1924-1942.

(31) Sigman, M. S.; Jacobsen, E. N., Schiff Base Catalysts for the Asymmetric Strecker Reaction Identified and Optimized from Parallel Synthetic Libraries. *J. Am. Chem. Soc.* **1998,** *120*, 4901-4902.

(32) (a) Schreiner, P. R.; Wittkopp, A., H-Bonding Additives Act Like Lewis Acid Catalysts. *Org. Lett.* **2002,** *4*, 217-220; (b) Okino, T.; Nakamura, S.; Furukawa, T.;

Takemoto, Y., Enantioselective Aza-Henry Reaction Catalyzed by a Bifunctional Organocatalyst. *Org. Lett.* **2004,** *6*, 625-627.

(33) Reisman, S. E.; Doyle, A. G.; Jacobsen, E. N., Enantioselective Thiourea-Catalyzed Additions to Oxocarbenium Ions. *J. Am. Chem. Soc.* **2008,** *130*, 7198-7199.

(34) Wittkopp, A.; Schreiner, P. R., Metal-Free, Noncovalent Catalysis of Diels-Alder Reactions by Neutral Hydrogen Bond Donors in Organic Solvents and in Water. *Chem. Eur. J.* **2003,** *9*, 407-414.

(35) Jones, C. R.; Pantos, G. D.; Morrison, A. J.; Smith, M. D., Plagiarizing Proteins: Enhancing Efficiency in Asymmetric Hydrogen-Bonding Catalysis through Positive Cooperativity. *Angew. Chem. Int. Ed.* **2009,** *48*, 7391-7394.

(36) Ganesh, M.; Seidel, D., Catalytic Enantioselective Additions of Indoles to Nitroalkenes. *J. Am. Chem. Soc.* **2008,** *130*, 16464–16465.

(37) (a) Malerich, J. P.; Hagihara, K.; Rawal, V. H., Chiral Squaramide Derivatives are Excellent Hydrogen Bond Donor Catalysts. *J. Am. Chem. Soc.* **2008,** *130*, 14416–14417; (b) Ni, X.; Li, X.; Wang, Z.; Cheng, J.-P., Squaramide Equilibrium Acidities in DMSO. *Org. Lett.* **2014,** *16*, 1786−1789.

(38) Broughman, J. R.; Shank, L. P.; Takeguchi, W.; Schultz, B. D.; Iwamoto, T.; Mitchel, K. E.; Tomich, J. M., Distinct Structural Elements That Direct Solution Aggregation and Membrane Assembly in the Channel-Forming Peptide M2GlyR. *Biochemistry* **2002,** *41*, 7350–7358.

(39) (a) Alfonso, I.; Quesada, R., Biological Activity of Synthetic Ionophores: Ion Transporters as Prospective Drugs? *Chem. Sci.* **2013,** *4*, 3009–3019; (b) Busschaert, N.; Gale, P. A., Small-Molecule Lipid-Bilayer Anion Transporters for Biological Applications.

Angew. Chem. Int. Ed. **2013,** *52*, 1374–1382; (c) Rambo, B. M.; Sessler, J. L., Oligopyrrole Macrocycles: Receptors and Chemosensors for Potentially Hazardous Materials. *Chem. Eur. J.* **2011,** *17*, 4946–4959; (d) Gale, P. A., Anion Receptor Chemistry. *Chem. Commun.* **2011,** *47*, 82-86.

(40) (a) He, J.; Quiocho, F., A Nonconservative Serine to Cysteine Mutation in the Sulfate-binding Protein, a Transport Receptor. *Science* **1991,** *251*, 1479-1481; (b) Luecke, H.; Quiocho, F. A., High Specificity of a Phosphate Transport Protein Determined by Hydrogen Bonds. *Nature* **1990,** *347*, 402-406; (c) M. G. Antonisse, M.; N. Reinhoudt, D., Neutral Anion Receptors: Design and Application. *Chem. Commun.* **1998,** 443-448.

(41) (a) Bondy, C. R.; Loeb, S. J., Amide Based Receptors for Anions. *Coord. Chem. Rev.* **2003,** *240*, 77-99; (b) Choi, K.; Hamilton, A. D., Macrocyclic Anion Receptors Based on Directed Hydrogen Bonding Interactions. *Coord. Chem. Rev.* **2003,** *240*, 101-110; (c) Kang, S. O.; Hossain, M. A.; Bowman-James, K., Influence of Dimensionality and Charge on Anion Binding in Amide-Based Macrocyclic Receptors. *Coord. Chem. Rev.* **2006,** *250*, 3038-3052; (d) Caltagironea, C.; Gale, P. A., Anion Receptor Chemistry: Highlights From 2007. *Chem. Soc. Rev.* **2009,** *38*, 520-563.

(42) Sessler, J. L.; Gale, P. A.; Cho, W. S., *Anion Receptor Chemistry*. RSC publishing: Cambridge, 2006.

(43) Andersson, C. E.; Mowbray, S. L., Activation of Ribokinase by Monovalent Cations. *J. Mol. Biol.* **2002,** *315*, 409–419.

(44) Davis, A. P.; Perry, J. J.; Wareham, R. S., Anion Recognition by Alkyl Cholates: Neutral Anionophores Closely Related to a Natural Product. *Tetrahedron Lett.* **1998,** *39*, 4569-4572.

(45) Winstanley, K. J.; Sayer, A. M.; Smith, D. K., Anion Binding by Catechols—an NMR, Optical and Electrochemical Study. *Org. Biomol. Chem.* **2006,** *4*, 1760–1767.

References for Chapter 2

(1) Guo, H.; Salahub, D. R. Cooperative Hydrogen Bonding and Enzyme Catalysis. *Angew. Chem. Int. Ed.* **1998**, *37*, 2985-2990.

(2) Wlodek, S. T.; Antosiewicz, J.; Briggs, J. M. On the Mechanism of Acetylcholinesterase Action: The Electrostatically Induced Acceleration of the Catalytic Acylation Step. *J. Am. Chem. Soc.* **1997**, *119*, 8159-8165.

(3) Warshel, A. Energetics of Enzyme Catalysis. *Proc. Nati. Acad. Sci. USA* **1978**, *75*, 5250-5254.

(4) Hanoian, P.; Sigala, P. A.; Herschlag, D.; Hammes-Schiffer, S. Hydrogen Bonding in the Active Site of Ketosteroid Isomerase: Electronic Inductive Effects and Hydrogen Bond Coupling. *Biochemistry* **2010**, *49*, 10339-10348.

(5) Demetrius, L. Role of Enzyme-Substrate Flexibility in Catalytic Activity: an Evolutionary Perspective. *J. Theor. Biol.* **1998**, *194*, 175-194.

(6) Sigala, P. A.; Kraut, D. A.; Caaveiro, J. M. M.; Pybus, B.; Ruben, E. A.; Ringe, D.; Petsko, G. A.; Herschlag, D. Testing Geometrical Discrimination within an Enzyme Active Site: Constrained Hydrogen Bonding in the Ketosteroid Isomerase Oxyanion Hole. *J. Am. Chem. Soc.* **2008**, *130*, 13696-13708.

(7) Akiyama, T.; Kotke, M.; Berkessel, A.; Payette, J. N.; Etzenbach – Effers, K.; Hayashi, Y.; Rapakko, S.; Schreiner, P. R.; Wierenga R. K.; Shoji, M., *et al*. *Hydrogen Bonding in Organic Synthesis*. Pihko, P. M., Ed.; Wiley-VCH: Weinheim, 2009.

(8) Beletskiy, E. V.; Schmidt, J.; Wang, X.-B.; Kass, S. R. Three Hydrogen Bond Donor Catalysts: Oxyanion Hole Mimics and Transition State Analogues. *J. Am. Chem. Soc.* **2012**, *134*, 18534−18537.

(9) Tian, Z.; Fattahi, A.; Lis, L.; Kass, S. R. Neutral Intramolecular Hydrogen-Bonded Bases. *Croat. Chem. Acta* **2009**, 82, 41-45.

(10) Tian, Z.; Fattahi, A.; Lis, L.; Kass, S. R. Single-Centered Hydrogen-Bonded Enhanced Acidity (SHEA) Acids: A New Class of Brønsted Acids. *J. Am. Chem. Soc.* **2009**, *131*, 16984-16988.

(11) Shokri, A.; Schmidt, J.; Wang, X. B.; Kass, S. R. Hydrogen Bonded Arrays: The Power of Multiple Hydrogen Bonds. *J. Am. Chem. Soc.* **2012**, *134*, 2094-2099.

(12) Shokri, A.; Abedin, A.; Fattahi, A.; Kass, S. R. Effect of Hydrogen Bonds on pK_a Values: Importance of Networking. *J. Am. Chem. Soc*. **2012**, *134*, 10646-10650.

(13) Shokri, A.; Wang, X. B.; Kass, S. R. Electron-Withdrawing Trifluoromethyl Groups in Combination with Hydrogen Bonds in Polyols: Bronsted Acids, Hydrogen-Bond Catalysts, and Anion Receptors. *J. Am. Chem. Soc*. **2013**, *135*, 9525-9530.

(14) Shokri, A.; Wang, Y.; O'Doherty, G. A.; Wang, X.-B.; Kass, S. R. Hydrogen Bond Networks: Strengths of Different Types of Hydrogen Bonds and An Alternative to the Low Barrier Hydrogen Bond Proposal. *J. Am. Chem*. **2013**, *135*, 17919-17924.

(15) Warshel, A. Electrostatic Origin of the Catalytic Power of Enzymes and the Role of Preorganized Active Sites. *J. Biol. Chem.* **1998**, *273*, 27035-27038.

(16) Angyal, S. J. *myo*-Inositol 4,6-Carbonate: An Easily Prepared Small Molecule with Three syn-Axial Hydroxyl Groups. *Carbohydr. Res.* **2000**, *325*, 313-320.

(17) Lee, H. W.; Kishi, Y. Synthesis of Mono and Unsymmetrical Bis Ortho Esters of *scyllo*-Inositol. *J. Org. Chem.* **1985**, *50*, 4402-4404.

(18) Sarmah, M. P.; Shashidhar, M. S. Sulfonate Protecting Groups. Improved Synthesis of *scyllo*-Inositol and Its Orthoformate from *myo*-Inositol. *Carbohydr. Res.* **2003**, *338*, 999-1001.

(19) Becke, A. D. Density-Functional Thermochemistry. III. The Role of Exact Exchange *J. Chem. Phys.* **1993**, *98*, 5648-5652.

(20) Lee, C.; Yang, W.; Parr, R. G. Development of the Colle-Salvetti Correlation-Energy Formula into a Functional of the Electron Density. *Phys. Rev. B* **1988**, *37*, 785–789.

(21) Zhao, Y.; Truhlar, D. G. How Well Can New-Generation Density Functionals Describe the Energetics of Bond-Dissociation Reactions Producing Radicals? *J. Phys. Chem. A* **2008**, *112*, 1095–1099.

(22) Zhao, Y.; Truhlar, D. G. The M06 Suite of Density Functionals for Main Group Thermochemistry, Thermochemical Kinetics, Noncovalent Interactions, Excited states, and Transition Elements: Two New Functionals and Systematic Testing of Four M06-class Functionals and 12 Other Functional. *Theor. Chem. Acc.* **2008**, *120*, 215-241.

(23) Zhao, Y.; Truhlar, D. G. Density Functionals with Broad Applicability in Chemistry. *Acc. Chem. Res.* **2008**, *41*, 157–167.

(24) Dunning, Jr., T. H. Gaussian Basis Sets for Use in Correlated Molecular Calculations. I. The Atoms Boron Through Neon and Hydrogen. *J. Chem. Phys*. **1989**, *90*, 1007-1023.

(25) Frisch, M. J.; Trucks, G. W.; Schlegel, H. B.; Scuseria, G. E.; Robb, M. A.; Cheeseman, J. R.; Scalmani, G.; Barone, V.; Mennucci, B.; Petersson, G. A., *et al*. Gaussian 09. Gaussian, Inc., Wallingford CT, 2009.

(26) Papajak, E.; Truhlar, D. G. Efficient Diffuse Basis Sets for Density Functional Theory. *J. Chem. Theory Comput.* **2010**, *6*, 597-601.

(27) Wang, X. B.; Wang, L. S. Development of a Low-Temperature Photoelectron Spectroscopy Instrument Using an Electrospray Ion Source and a Cryogenically Controlled Ion Trap. *Rev. Sci. Instrum*. **2008**, *79*, 073108.

(28) Ramond, T. M.; Davico, G. E.; Schwartz, R. L.; Lineberger, W. C. Vibronic Structure of Alkoxy Radicals via Photoelectron Spectroscopy. *J. Chem. Phys.* **2000**, *112*, 1158-1169.

(29) Mihalick, J. E.; Gatev, G. G.; Brauman, J. I. *Electron Photodetachment Spectroscopy of Solvated Anions: $RO^{-}HF^{-}$ or $ROH^{-}F^{-}$?* ***J. Am. Chem. Soc*.** **1996**, *118*, 12424-12431.

(30) Wang, X. B.; Woo, H. K.; Wang, L. S.; Minofar, B.; Jungwirth, P. *Determination of the Electron Affinity of the Acetyloxyl Radical (CH_3COO) by Low-Temperature Anion Photoelectron Spectroscopy and Ab Initio Calculations. J. Phys. Chem. A* **2006**, *110*, 5047-5050.

(31) Weaver, A.; Arnold, D. W.; Bradforth, S. E.; Neumark, D. M. Examination of the $^2A'_2$ and $^2E'$ States of NO_3 by Ultraviolet Photoelectron Spectroscopy of NO_3^-. *J. Chem. Phys.* **1991**, *94*, 1740-1751.

(32) Wang, X. B.; Wang, L. S. The Electronic Structure and Electron Affinities of Higher Chlorine Oxide Radicals ClO_x (x = 2–4) from Photoelectron Spectroscopy of ClO_X^- Anions. *J. Chem. Phys.* **2000**, *113*, 10928-10933.

(33) Wang, X. B.; Vorpagel, E. R.; Yang, X.; Wang, L. S. Experimental and Theoretical Investigations of the Stability, Energetics, and Structures of $H_2PO_4^-$, $H_2P_2O_7^{2-}$, and $H_3P_3O_{10}^{2-}$ in the Gas Phase. *J. Phys. Chem. A* **2001**, *105*, 10468-10474.

(34) Berzinsh, U.; Gustafsson, M.; Hanstorp, D.; Klinkmuller, A.; Ljungblad, U.; Martensson-Pendrill, A. M. Isotope Shift in the Electron Affinity of Chlorine. *Phys. Rev. A* **1995**, *51*, 231-238.

(35) Boeckman, Jr., R. K.; Shao, P.; Mullins, J. J. The Dess-Martin Periodinane: 1,1,1-Triacetoxy-1,1-Dihydro-1,2-Benziodoxol-3(1H)-one. *Org. Synth.* **2000**, *77*, 141-152.

(36) Frigerio, M.; Santagostino, M.; Sputore, S. A User-Friendly Entry to 2-Iodoxybenzoic Acid (IBX). *J. Org. Chem.* **1999**, *64*, 4537-4538.

References for Chapter 3

(1) Dutzler, R.; Campbell, E. B.; Cadene, M.; Chait, B. T.; MacKinnon, R. *Nature* **2002**, *415*, 287-294.

(2) Koropatkin, N. M.; Pakrasi, H. B.; Smith, T. J. *J. Proc. Natl. Acad. Sci. U.S.A.* **2006**, *103*, 9820-9825.

(3) Luecke, H.; Quiocho, F. A. *Nature 347* **1990**, *347*, 402-406.

(4) Miller, C. *Nature* **2006**, *440*, 484-489.

(5) Omata, T. *Plant Cell Physiol.* **1995**, *36*, 207-213.

(6) Pflugrath, J. W.; Quiocho, F. A. *Nature* **1985**, *314*, 257-260.

(7) Ayling, A. J.; Pérez-Payán, M. N.; Davis, A. P. *J. Am. Chem. Soc.* **2001**, *123*, 12716-12717.

(8) Winstanley, K. J.; Sayer, A. M.; Smith, D. K. *Org. Biomol. Chem.* **2006**, *4*, 1760-1767.

(9) Shokri, A.; Schmidt, J.; Wang, X.-B.; Kass, S. R. *J. Am. Chem. Soc.* **2012**, *134*, 16944-16947.

(10) Beletskiy, E. V.; Schmidt, J.; Wang, X.-B.; Kass, S. R. *J. Am. Chem. Soc.* **2012**, *134*, 18534-18537.

(11) Shokri, A.; Deng, S. H. M.; Wang, X.-B.; Kass, S. R. *Org. Chem. Front.* **2014**, *1*, 54-61.

(12) Santacroce, P. V.; Davis, J. T.; Light, M. E.; Gale, P. A.; Iglesias-Sánchez, J. C.; Prados, P.; Quesada, R. *J. Am. Chem. Soc.* **2007**, *129*, 1886-1887.

(13) Shokri, A.; Wang, X.-B.; Kass, S. R. *J. Am. Chem. Soc.* **2013**, *135*, 9525-9530.

(14) (a) Wüthrich, K. *J. Biol. Chem.* **1990**, *265*, 22059-22062. (b) Opella, S. J.; Marassi, F. M. *Chem. Rev.* **2004**, *104*, 3587−3606.

(15) Buhlmann, P.; Pretsch, E.; Bakker, E. *Chem. Rev.* **1998**, *98*, 1593-1687.

(16) Smith, D. K. *Org. Biomol. Chem.* **2003**, *1*, 3874-3877.

(17) Chial, K.; Stelzig, S. H.; Gropeanu, R.; Weil, T.; Klapper, M.; Müllen, K. *Macromolecules* **2009**, *42*, 7545-7552.

(18) Hay, B. P.; Firman, T. K.; Moyer, B. A. *J. Am. Chem. Soc.* **2005**, *127*, 1810-1819.

(19) Merenbloom, S. I.; Flick, T. G.; Daly, M. P.; Williams, E. R. *J. Am. Soc. Mass Spectrom.* **2011**, *22*, 1978-1990.

(20) Bartmess, J. E. *NIST Chemistry WebBook, NIST Standard Reference Database Number 6;* Mallard, W. G., Lustrum, P. J., Eds.; National Institute of Standards and Technology: Gaithersburg, MD 20899 (http://webbook.nist.gov).

(21) Shokri, A.; Schmidt, J.; Wang, X. -B.; Kass, S. R. *J. Am. Chem. Soc.* **2011**, *134*, 2094-2099.

(22) For previous studies using IR spectroscopy to probe anion binding in solution, see: (a) Allerhand, A.; Schleyer, P. v. R. *J. Am. Chem. Soc.* **1963**, *85*, 1233-1237. (b) Kavallieratos, K.; Bertao, C. M.; Crabtree, R. H. *J. Org. Chem.* **1999**, *64*, 1675-1683.

(23) For a review on gas phase IR studies that addresses anion bound complexes, see: Eyler, J. R. *Mass Spectrom. Rev.* **2009**, *28*, 448-467.

(24) Kuhn, L. P. *J. Am. Chem. Soc.* **1952**, *74*, 2492-2499.

(25) Vedernikova, E. V.; Gafurov, M. M.; Ataev, M. B. *Russ. Phys. J.* **2011**, *53*, 843-848.

(26) Leberknight, C. E.; Ord, J. A. *Phys. Rev.* **1937**, *51*, 430-433.

(27) The predicted spectra for conformers ***a*** and ***b*** in Fig. 1 are similar, and while the computed spectrum shown in Fig. 3 is for ***a***, that for ***b*** (see Fig. S6) also provides a good fit to the data and there is no basis to prefer one structure over the other at this time.

(28) Samet, M.; Wang, X.-B.; Kass, S. R. *J. Phys. Chem. A* **2014, *118,*** 5989–5993.

(29) The alternate 1 HB structure of **1Me(1)** • Cl^- is 3.8 kcal mol^{-1} less stable. This is due to the hydroxyl group on the carbon bearing the trifluoromethyl substitutent being a hydrogen bond acceptor and lone pair–lone pair electron repulsion between the chloride anion and one of the fluorines on the CF_3 group.

(30) (a) Boeckman, Jr., R. K.; Shao, P.; Mullins, J. J. *Org. Synth.* **2000**, *77*, 141-152. (b) Frigerio, M.; Santagostino, M.; Sputore, S. *J. Org. Chem.* **1999**, *64*, 4537-4538.

(31) Krief, A.; Dumont, W.; Billen, D.; Letesson, J.-J.; Lestrate, P.; Murphyc, P. J.; Lacroix, D. *Tetrahedron Lett.* **2004**, *45*, 1461-1463.

(32) Connors, K. A. Binding Constants: The Measurement of Molecular Complex Stability, Wiley-Interscience: New York, 1987; pp 432.

(33) Frisch, M. J.; Trucks, G. W.; Schlegel, H. B.; Scuseria, G. E.; Robb, M. A., et al. *Gaussian 09*, Gaussian, Inc., Wallingford CT, 2009.

(34) Becke, A. D. *J. Chem. Phys*. **1993**, *98*, 5648-5652.

(35) Lee, C.; Yang, W.; Parr, R. G. *Phys. Rev. B* **1988**, *37*, 785-789.

References for Chapter 4

(1) L. Simón, F. M. Muñiz, S. Sáez, C. Raposo and J. R. Morán, *Eur. J. Org. Chem.* 2007, 4821-4830.

(2) L. Simón and J. M. Goodman, *J. Org. Chem.* 2010, **75**, 1831-1840.

(3) R. Dutzler, E. B. Campbell, M. Cadene, B. T. Chait and R. MacKinnon, *Nature* 2002, **415**, 287-294.

(4) N. M. Koropatkin, D. W. Koppenaal, H. B. Pakrasi and T. J. Smith, *J. Biol. Chem.* 2007, **282**, 2606-2614.

(5) N. M. Koropatkin, H. B. Pakrasi and T. J. Smith, *J. Proc. Natl. Acad. Sci. U.S.A.* 2006, **103**, 9820-9825.

(6) H. Luecke and F. A. Quiocho, *Nature* 1990, **347**, 402-406.

(7) C. Miller, *Nature* 2006, **440**, 484-489.

(8) Z. Zhang and P. R. Schreiner, *Chem. Soc. Rev.* 2009, **38**, 1187-1198.

(9) S. E. Reisman, A. G. Doyle and E. N. Jacobsen, *J. Am. Chem. Soc.* 2008, **130**, 7198-7199.

(10) Y. Zhao, C. Beuchat, Y. Domoto, J. Gajewy, A. Wilson, J. Mareda, N. Sakai and S. Matile, *J. Am. Chem. Soc.* 2014, **136**, 2101-2111.

(11) I. T. Raheem, P. S. Thiara, E. A. Peterson and E. N.Jacobsen, *J. Am. Chem. Soc.* 2007, **129**, 13404-13405.

(12) C. J. E. Haynes, N. Busschaert, I. L. Kirby, J. Herniman, M. E. Light, N. J. Wells, I. Marques, V. Félix and P. A. Gale, *Org. Biomol. Chem.* 2014, **12**, 62-72.

(13) A. P. Davis, D. N. Sheppard and B. D. Smith, *Chem. Soc. Rev.* 2007, **36**, 348-357.

(14) O. A. Okunola, J. L. Seganish, K. J. Salimian, P. Y. Zavalij and J. T. Davis, *Tetrahedron* 2007, **63**, 10743-10750.

(15) P. V. Santacroce, J. T. Davis, M. E. Light, P. A. Gale, J. C. Iglesias-Sánchez, P. Prados and R. Quesada, *J. Am. Chem. Soc.* 2007, **129**, 1886-1887.

(16) R. M. Duke, E. B. Veale, F. M. Pfeffer, P. E. Krugerc and T. Gunnlaugsson, *Chem. Soc. Rev.* 2010, **39**, 3936-3953.

(17) C. Suksai and T. Tuntulani, *Chem. Soc. Rev.* 2003, **32**, 192-202.

(18) A. Shokri, S. H. M. Deng, X.-B. Wang and S. R. Kass, *Org. Chem. Front.* 2014, **1**, 54-61.

(19) A. Shokri, J. Schmidt, X.-B. Wang and S. R. Kass, *J. Am. Chem. Soc.* 2012, **134**, 16944−16947.

(20) E. V. Beletskiy, J. Schmidt, X.-B. Wang and S. R. Kass, *J. Am. Chem. Soc.* 2012, **134**, 18534−18537.

(21) A. L. Sisson, J. P. Clare and A. P. Davis, *Chem. Commun.* 2005, 5263-5265.

(22) A. Shokri, X.-B. Wang and S. R. Kass, *J. Am. Chem. Soc.* 2013, 135, 9525-9530.

(23) K. J. Winstanley, A. M. Sayer and D. K. Smith, *Org. Biomol. Chem.* 2006, **4**, 1760-1767.

(24) A. J. Ayling, M. N. Perez-Payan and A. P. Davis, *J. Am. Chem. Soc.* **2001**, *123*, 12716-12717.

(25) D. K. Smith, *Org. Biomol. Chem.* 2003, **1**, 3874-3877.

(26) N. Busschaert, J. Jaramillo-Garcia, M. E. Light, J. Herniman, G. J. Langley and P. A. Gale, *RSC Adv.* 2014, **4**, 5389-5393.

(27) J. M. Coteron, F. Hacket and H.-J. Schneider, *J. Org. Chem.* **1996**, *61*, 1429-1435.

(28) S.-I. Kondo, Y. Kobayashi and M. Unno, *Tetrahedron Lett.* 2010, **51**, 2512-2514.

(29) J. B. Huff, B. Askew, R. J. Duff and J. Rebek, Jr., *J. Am. Chem. Soc.* 1988, **110**, 5909-5911.

(30) C. B. Post, M. Karplus, *J. Am. Chem. Soc.* 1986, **108**, 1317-1319.

(31) M. Bruschi, M. Tiberti, A. Guerra and L. D. Gioia, *J. Am. Chem. Soc.* 2014, **136**, 1803-1814.

(32) A. J. Kirby, *CRC Crit. Rev. Biochem.* 1987, 22, 283-315.

(33) K.-C. Chang, T. Minami, P. Koutnik, P. Y. Savechenkov, Y. Liu and P. Anzenbacher, Jr., *J. Am. Chem. Soc.* 2014, **136**, 1520-1525.

(34) M. Samet, M. Danesh-Yazdi, A. Fattahi and S. R. Kass, *J. Org. Chem.* 2015, ***80***, 1130-1135

(35) M. Samet, X.-B. Wang and S. R. Kass, *J. Phys. Chem. A* 2014, **118**, 5989-5993.

(36) L. P. Kuhn, *J. Am. Chem. Soc.* 1952, **74**, 2492-2499.

(37) E. V. Vedernikova, M. M. Gafurov and M. B. Ataev, *Russ. Phys. J.* 2011, **53**, 843-848.

(38) Alcohol O–H stretches red shift upon addition of acetonitrile to their carbon tetrachloride solutions. For example, CF_3CH_2OH has an OH band at 3618 cm^{-1} in CCl_4 and it decreases to 3485 cm^{-1} in a 1% CD_3CN/CCl_4 mixture.

(39) The analogous 1HB structure where the chloride ion interacts with the other hydroxyl group is 0.9 kcal mol^{-1} less stable but provides a good fit to the data and can not be ruled out. The structure for this species is provided in the supporting information.

(40) This energy difference decreases to 0.9 kcal mol^{-1} in acetonitrile based upon B3LYP/6-31+G(d,p)/CPCM computations.

(41) The importance of local dipoles in proteins has been reported, see: J. J. He and F. A. Quiocho, *Prot. Sci.* 1993, **2**, 1643-1647.

(42) R. K. Boeckman, P. Shao and J. J. Mullins, *Org. Syn.* 2004, **10**, 696-698.

(43) M. Frigerio, M. Santagostino and S. Sputore, *J. Org. Chem.* 1999, **64**, 4537-4538.

(44) M. J. Frisch, G. W. Trucks, H. B. Schlegel, G. E. Scuseria, M. A. Robb, J. R. Cheeseman, G. Scalmani, V. Barone, B. Mennucci, G. A. Petersson, H. Nakatsuji, M. Caricato, X. Li, H. P. Hratchian, A. F. Izmaylov, J. Bloino, G. Zheng, J. L. Sonnenberg, M. Hada, M. Ehara, K. Toyota, R. Fukuda, J. Hasegawa, M. Ishida, T. Nakajima, Y. Honda, O. Kitao, H. Nakai, T. Vreven, J. A. Montgomery, Jr., J. E. Peralta, F. Ogliaro, M. Bearpark, J. J. Heyd, E. Brothers, K. N. Kudin, V. N. Staroverov, R. Kobayashi, J. Normand, K. Raghavachari, A. Rendell, J. C. Burant, S.S. Iyengar, J. Tomasi, M. Cossi, N. Rega, J. M. Millam, M. Klene, J. E. Knox, J. B. Cross, V. Bakken, C. Adamo, J. Jaramillo, R. Gomperts, R. E. Stratmann, O. Yazyev, A. J. Austin, R. Cammi, C. Pomelli, J. W. Ochterski, R. L. Martin, K. Morokuma, V. G. Zakrzewski, G. A. Voth, P. Salvador,

J. J. Dannenberg, S. Dapprich, A. D. Daniels, O. Farkas, J. B. Foresman, J. V. Ortiz, J. Cioslowski and D. J. Fox, *Gaussian 09*, Gaussian, Inc., Wallingford, CT, 2009.

(45) A. D. Becke, *J. Chem. Phys.* 1993, **98**, 5648-5652.

(46) C. Lee, W. Yang and R. G. Parr, *Phys. Rev. B* 1988, **37**, 785-789.

(47) V. Barone, M. Cossi and J. Tomasi, *J. Chem. Phys.* 1997, **107**, 3210-3221.

(48) R. Cammi, B. Mennucci and J. Tomasi, *J. Phys. Chem. A* 1998, **102**, 870-875.

(49) R. Cammi, B. Mennucci and J. Tomasi, *J. Phys. Chem. A* 2000, **104**, 4690-4698.

(50) M. Cossi, N. Rega, G. Scalmani and V. Barone, *J. Comput. Chem.* 2003, **24**, 669-681.

References for Chapter 5

(1) Reed, C. A. *Acc. Chem. Res.* **1998**, *31*, 133-139.

(2) Akiyama, T. *Chem. Rev.* **2007**, *107*, 5744-5758.

(3) Yamamoto, H.; Boxer, M. B. *Chimia* **2007**, *61*, 279-281.

(4) Tian, Z.; Fattahi, A.; Lis, L.; Kass, S. R. *J. Am. Chem. Soc.* **2009**, *131*, 16984-16988

(5) Parmar, D.; Sugiono, E.; Raja, S.; Rueping, M. *Chem. Rev.* **2014**, *114*, 9047-9153.

(6) Bordwell, F. G. *Acc. Chem. Res.* **1988**, *21*, 456-463.

(7) Charton, M. In *Progress in Physical Organic Chemistry*; Taft, R. W., Ed.; Interscience: New York, 1981; Vol. 13, p 119-251.

(8) Hansch, C.; Leo, A.; Taft, R. W. *Chem. Rev.* **1991**, *91*, 165-195.

(9) Juhasz, M.; Hoffmann, S.; Stoyanov, E.; Kim, K. C.; Reed, C. A. *Angew. Chem. Int. Ed.* **2004**, *43*, 5352-5355.

(10) Abkowicz-Bienko, A. J.; Latajka, Z. *J. Phys. Chem. A* **2000**, *104*, 1004-1008.

(11) Hussein, M. A.; Millen, D. J.; Mines, G. W. *J. Chem. Soc., Faraday Trans. 2* **1976**, *72*, 686-692.

(12) All acidities come from refs. 6 and 13 – 17.

(13) Bordwell, F. G. et. al. University of Wisconsin Madison's Bordwell pK_a table (http://www.chem.wisc.edu/areas/reich/ pkatable).

(14) Bordwell, F. G.; McCallum, R. J.; Olmstead, W. N. *J. Org. Chem.* **1984**, *49*, 1424-1427.

(15) Bordwell, F. G.; Cheng, J. P. *J. Am. Chem. Soc*. **1991**, *113*, 1736-1743.

(16) Bartmess, J. E. *NIST Chemistry WebBook, NIST Standard Reference Database Number 6*; W. G. Mallard, P. J. Lustrum, Eds.; National Institute of Standards and Technology: Gaithersburg, MD 20899 (http://webbook.nist.gov).

(17) Angel, L. A.; Ervin, K. M. *J. Phys. Chem. A* **2006**, *110*, 10392-10403.

(18) One hydrogen bond criterion typically observed is a red shift in the IR. Arunan, E., et al., *Pure Appl. Chem.* **2011**, *83*, 1637-1641.

(19) Similar results are observed in $CDCl_3$ and 1% CD_3CN/99% $CDCl_3$ (i.e., *p*-XC_6H_4OH, X = H (3598 and 184 cm^{-1}), Br (3596 and 188 cm^{-1}), CN (3582 and 227 cm^{-1}), NO_2 (3580 and 240 cm^{-1}), and **2** (3555 and 320 cm^{-1}) where the values in parentheses are ν and $\Delta\nu$, respectively.

(20) Separate plots for the meta and para derivatives do not lead to improved data fits.

(21) Patrick, J. S.; Yang, S. S.; Cooks, R. G. *J. Am. Chem. Soc.* **1996**, *118*, 231-232.

(22) Strittmatter, E. F.; Wong, R. L.; Williams, E. R. *J. Am. Chem. Soc.* **2000**, *122*, 1247-1248.

(23) For related studies employing protonated catalysts, charged metal-templated hydrogen bond donors and pyridinium cations as anion-binding catalysts, , see: refs. 24-26, respectively.

(24) Ganesh, M.; Seidel, D. *J. Am. Chem. Soc.* **2008**, *130*, 16464-16465.

(25) (a) Scherer, A.; Mukherjee, T.; Hampel, F.; Gladysz, J. A. *Organometallics* **2014**, *33*, 6709-6722. (b) Mukherjee, T.; Ganzmann, C.; Bhuvanesh, N.; Gladysz, J. A. *Organometallics* **2014**, *33*, 6723-6737.

(26) Berkessel, A.; Das, S.; Pekel, D.; Neudörfl, J.-M. *Angew. Chem. Int. Ed.* **2014**, *53*, 11660-11664.

(27) Shokri, A.; Wang, X. B.; Kass, S. R. *J. Am. Chem. Soc*. **2013**, *135*, 9525-9530.

(28) Huang, J.; Corey, E. J. *Org. Lett.* **2004**, *6*, 5027-5029.

(29) Bolm, C.; Rantanen, T.; Schiffers, I.; Zani, L. *Angew. Chem. Int. Ed.* **2005**, *44*, 1758-1763.

(30) Takenaka, N.; Sarangthem, R. S.; Seerla, S. K. *Org. Lett.* **2007**, *9*, 2819-2822.

(31) Auvil, T. J.; Schafer, A. G.; Mattson, A. E. *Eur. J. Org. Chem.* **2014**, 2633-2646.

(32) Frisch, M. J.; Trucks, G. W.; Schlegel, H. B.; Scuseria, G. E.; Robb, M. A.; Cheeseman, J. R.; Scalmani, G.; Barone, V.; Mennucci, B.; Petersson, G. A., *et al*. Gaussian 09. Gaussian, Inc., Wallingford CT, 2009.

(33) Becke, A. D. *J. Chem. Phys.* **1993**, *98*, 5648-5652.

(34) Lee, C.; Yang, W.; Parr, R. G. *Phys. Rev. B* **1988**, *37*, 785-789.

References for Chapter 6

(1) Hammes-Schiffer, S. *Biochemistry* **2013**, *52*, 2012−2020.

(2) Schwans, J. P.; Sunden, F.; Gonzalez, A.; Tsai, Y.; Herschlag, D. *Biochemistry* **2013**, *52*, 7840−7855.

(3) Kraut, S.; Bebenroth, D.; Nierth, A.; Kobitski, A. Y.; Nienhaus, G. U.; Jaschke, A. *Nucleic Acids Research* **2012**, *40*, 1318−1330.

(4) Hanoian, P.; Hammes-Schiffer, S. *Biochemistry* **2011**, *50*, 6689−6700.

(5) Kamerlin, S. C. L.; Sharma, P. K.; Chu, Z. T.; Warshel, A. *Proc. Natl. Acad. Sci. U. S. A.* **2010**, *107*, 4075−4080.

(6) Hanoian, P.; Sigala, P. A.; Herschlag, D.; Hammes-Schiffer, S. *Biochemistry* **2010**, *49*, 10339−10348.

(7) Guo, H.; Salahub, D. R. *Angew. Chem. Int. Ed.* **1998**, *37*, 2985-2990.

(8) Rueping, M.; Koenigs, R. M.; Atodiresei, I. *Chem. Eur. J.* **2010**, *16*, 9350-9365.

(9) *Hydrogen Bonding in Organic Synthesis*. Pihko, P. M., Ed.; Wiley-VCH: Weinheim, 2009.

(10) MacMillan, D. W. C. *Nature* **2008**, *455*, 304−308.

(11) List, B. *Chem. Rev.* **2007**, *107*, 5413−5415.

(12) Akiyama, T. *Chem. Rev.* **2007**, *107*, 5744−5758.

(13) Akiyama, T.; Itoh, J.; Fuchibe, K. *Adv. Synth. Catal.* **2006**, *348*, 999−1010.

(14) *Hydrogen Bonding in Organic Synthesis*; Pihko, P. M., Ed.; Wiley-VCH: Weinheim, Germany, 2009; pp 1−395.

(15) Schreiner, P. R.; Wittkopp, A. *Org. Lett.* **2002**, *4*, 217−220.

(16) Schreiner, P. R. *Chem. Soc. Rev.* **2003**, *32*, 289−296.

(17) Wittkopp, A.; Schreiner, P. R. *Chem. Eur. J.* **2003**, *9*, 407−414.

(18) Takemoto, Y. *Org. Biomol. Chem.* **2005**, *3*, 4299-4306.

(19) Taylor, M. S.; Jacobsen, E. N. *Angew. Chem., Int. Ed*. **2006**, *45*, 1520-1543.

(20) Stephen, J. C. *Chem. Eur. J*. **2006**, *12*, 5418-5427.

(21) Kotke, M.; Schreiner, P. R. *Synthesis* **2007**, 779-790.

(22) Doyle, A. G.; Jacobsen, E. N. *Chem. Rev*. **2007**, *107*, 5713-5743.

(23) Zhang, Z.; Schreiner, P. R. *Chem. Soc. Rev*. **2009**, *38*, 1187-1198.

(24) Knowles, R. R.; Jacobsen, E. N. *Proc. Natl. Acad. Sci. U.S.A.* **2010**, *107*, 20678-20685.

(25) Warshel, A. *J. Biol. Chem.* **1998**, *273*, 27035−27038.

(26) Kamerlin, S. C. L.; Sharma, P. K.; Chu, Z. T.; Warshel, A. *Proc. Natl. Acad. Sci. U.S.A.* **2010**, *107*, 4075−4080.

(27) So, S. S.; Burkett, J. A.; Mattson, A. E. *Org. Lett.* **2011**, *13*, 716−719.

(28) Nickerson, D. M.; Angeles, V. V.; Auvil, T. J.; So, S. S.; Mattson, A. E. *Chem. Commun.* **2013**, *49*, 4289−4291.

(29) Shokri, A.; Wang, X.-B.; Kass, S. R. *J. Am. Chem. Soc.* **2013**, *135*, 9525−9530.

(30) Jakab, G.; Tancon, C.; Zhang, Z.; Lippert, K. M.; Schreiner, P. R. *Org. Lett.* **2012**, *14*, 1724−1727.

(31) Lippert, K. M.; Hof, K.; Gerbig, D.; Ley, D.; Hausmann, H.; Guenther, S.; Schreiner, P. R. *Eur. J. Org. Chem.* **2012**, 5919−5927.

(32) (a) Bordwell, F. G. *Acc. Chem. Res.* **1988**, *21*, 456-463. (b) Bordwell, F. G. et. al. University of Wisconsin Madison's Bordwell pK_a table (http://www.chem.wisc.edu-/areas/reich/pkatable).

(33) The pK_a of 1-propanol and 4,4,4-trifluorobutanol do not appear to have been measured in DMSO so a linear correlation between aqueous and DMSO acidities was used to provide

estimates of 29.0 and 27.8, respectively. For additional details, see the supporting information.

(34) Samet, M.; Wang, X.-B.; Kass, S. R. *J. Phys. Chem. A* **2014**, *118*, 5989−5993.

(35) Chu, Y.; Deng, H.; Cheng, J. P. *J. Org. Chem.* **2007**, *72*, 7790-7793.

(36) Tian, Z.; Fattahi, A.; Lis, L.; Kass, S. R. *J. Am. Chem. Soc.* **2009**, *131*, 16984−16988.

(37) Matthews, W. S.; Bares, J. E.; Bartmess, J. E.; Bordwell, F. G.; Cornforth, F. J.; Drucker, G. E.; Margolin, Z.; McCallum, R. J.; McCollum, G. J.; Vanier, N. R. *J. Am. Chem. Soc.* **1975**, *92*, 7006−7014.

(38) Becke, A. D. *J. Chem. Phys.* **1993**, *98*, 5648-5652.

(39) Lee, C.; Yang, W.; Parr, R. G. *Phys. Rev. B* **1988**, *37*, 785−789.

(40) Zhao, Y.; Truhlar, D. G. *J. Phys. Chem. A* **2008**, *112*, 1095−1099.

(41) Zhao, Y.; Truhlar, D. G. *Theor Chem Account* **2008**, *120*, 215−241.

(42) Zhao, Y.; Truhlar, D. G. *Acc. Chem. Res.* **2008**, *41*, 157−167.

(43) Papajak, E.; Truhlar, D. G. *J. Chem. Theory Comput.* **2010**, *6*, 597-601.

(44) *CRC Handbook of Chemistry and Physics*, 95th ed.; Boca Raton, FL 2014.

(45) Samet, M.; Buhle, J.; Zhou, Y.; Kass, S. R. *J. Am. Chem. Soc.* **2015**, *137*, 4678−4680.

(46) An estimate of 14.2 was obtained for binol from a correlation of aqueous and DMSO pK_a's (see supporting information) and a computed prediction of 13.2 was recently reported (ref. 47); an average value of 13.7 was adopted in this work.

(47) Yang, C.; Xue, X.-S.; Li, X.; Cheng, J.-P. *J. Org. Chem.* **2014**, *79*, 4340-4351.

(48) Loeb, S. J.; Martin, J. W. L.; Willis, C. J. *J. Can. J. Chem.* **1978**, *56*, 2369−2373.

(49) Frisch, M. J.; et al., Gaussian, Inc., Wallingford CT, 2009.

(50) Dunning, T. H., Jr. *J. Chem. Phys.* **1989**, *90*, 1007-1023.

(51) Barone, V.; Cossi, M.; Tomasi, J. *J. Chem. Phys.* **1997**, *107*, 3210−3221.

(52) Cammi, R.; Mennucci, B.; Tomasi, J. *J. Phys. Chem. A* **1998**, *102*, 870−875.

Appendices

Appendix for Chapter 2

For XYZ coordinates and electronic energies see:

http://pubs.acs.org/doi/abs/10.1021/jp505308v

NMR Spectra

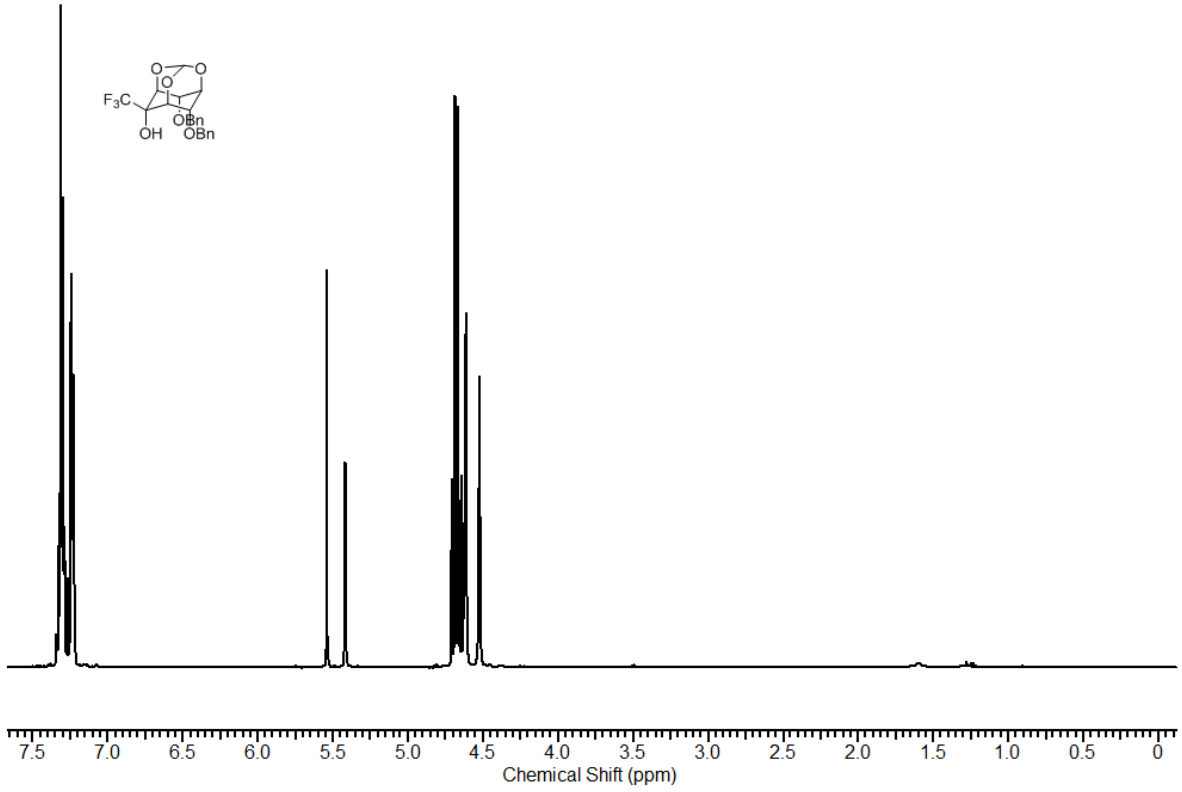

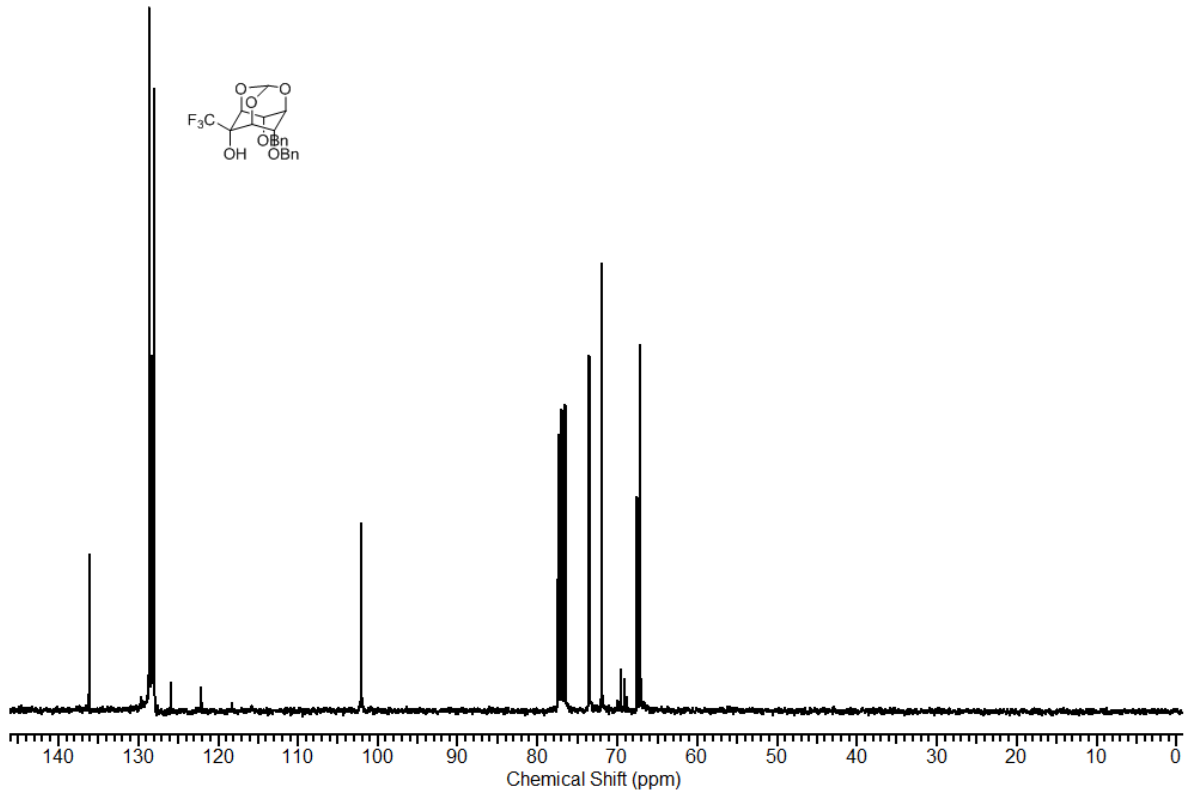
F3C
OBn
OH
OBn
140
130
120
110
100
90
80
70
60
50
40
30
20
10
0
Chemical Shift (ppm)

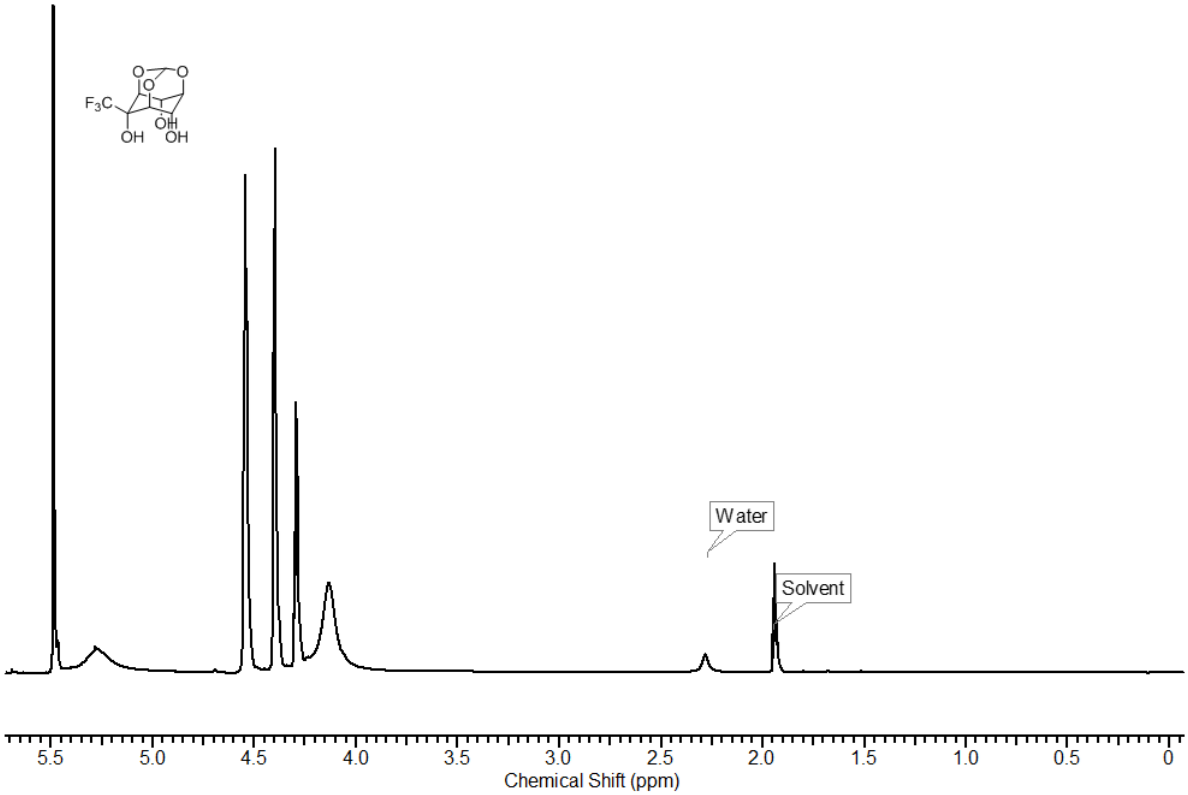
F3C
OH
OH
OH
Water
Solvent
5.5
5.0
4.5
4.0
3.5
3.0
2.5
2.0
1.5
1.0
0.5
0
Chemical Shift (ppm)

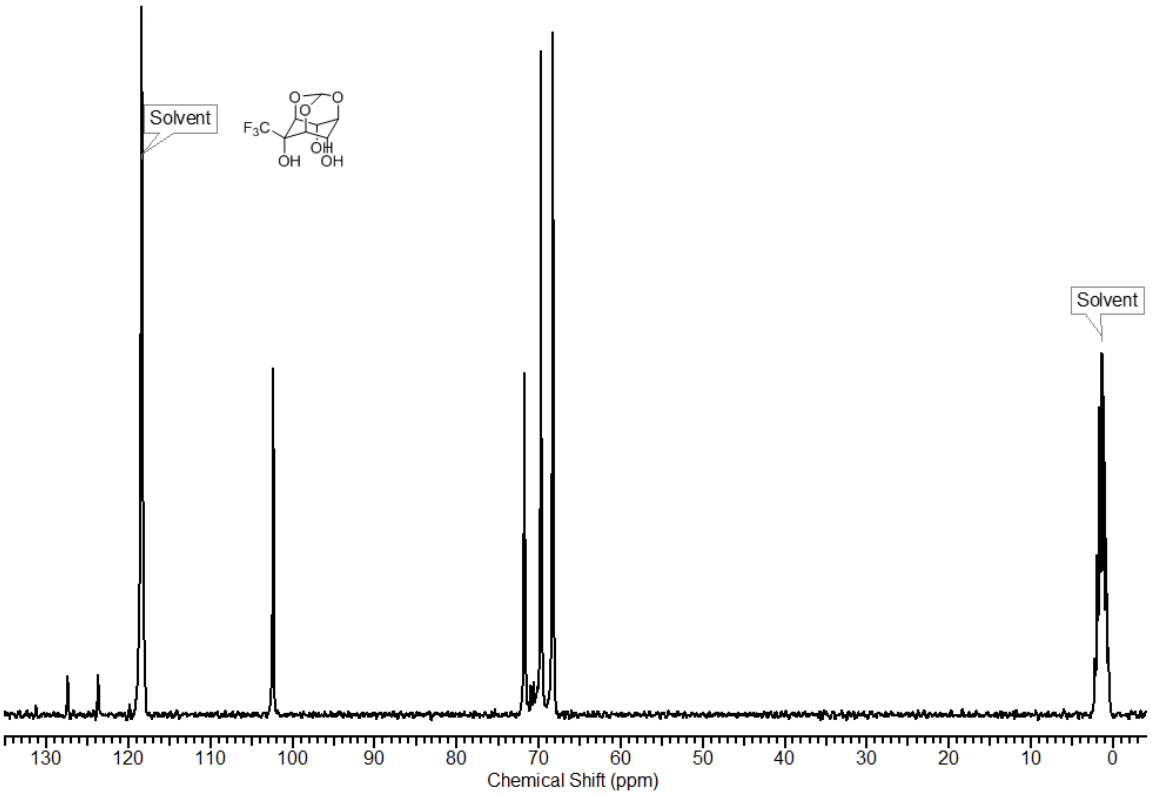
Solvent
Solvent
130
120
110
100
90
80
70
60
50
40
30
20
10
0
Chemical Shift (ppm)

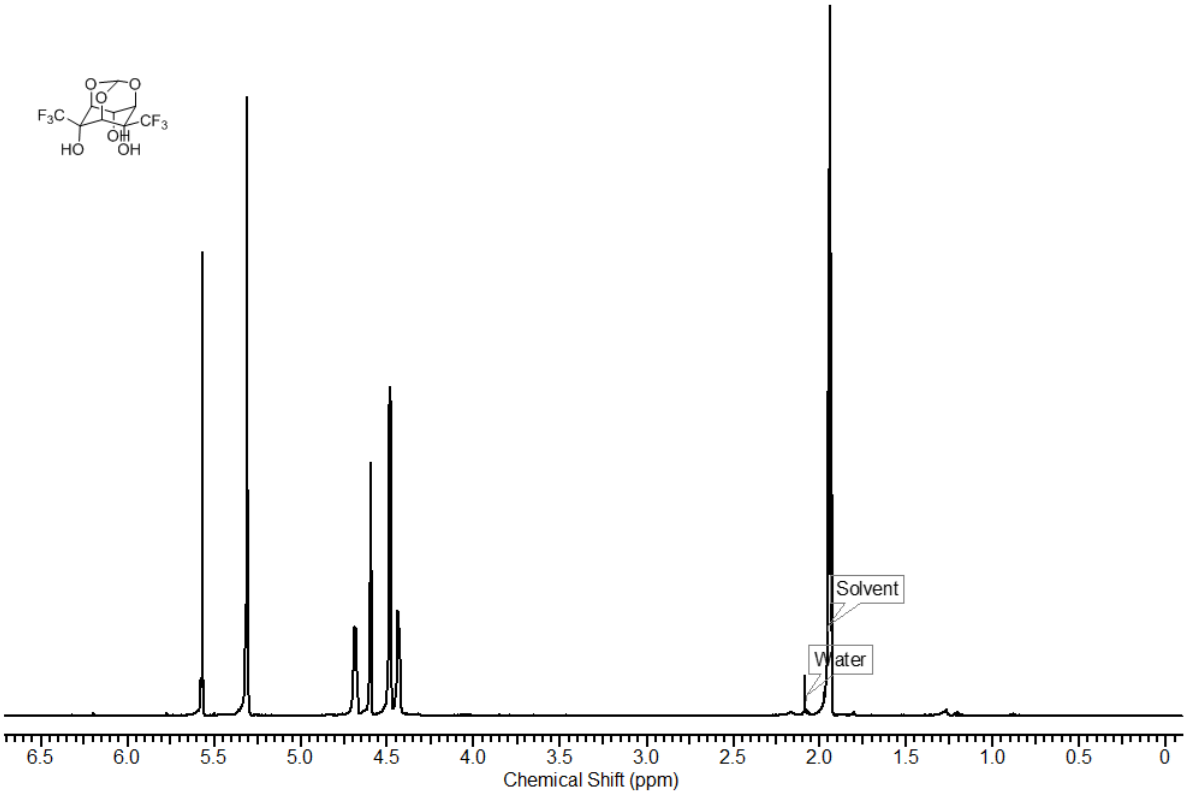
Solvent
Water
6.5
6.0
5.5
5.0
4.5
4.0
3.5
3.0
2.5
2.0
1.5
1.0
0.5
0
Chemical Shift (ppm)

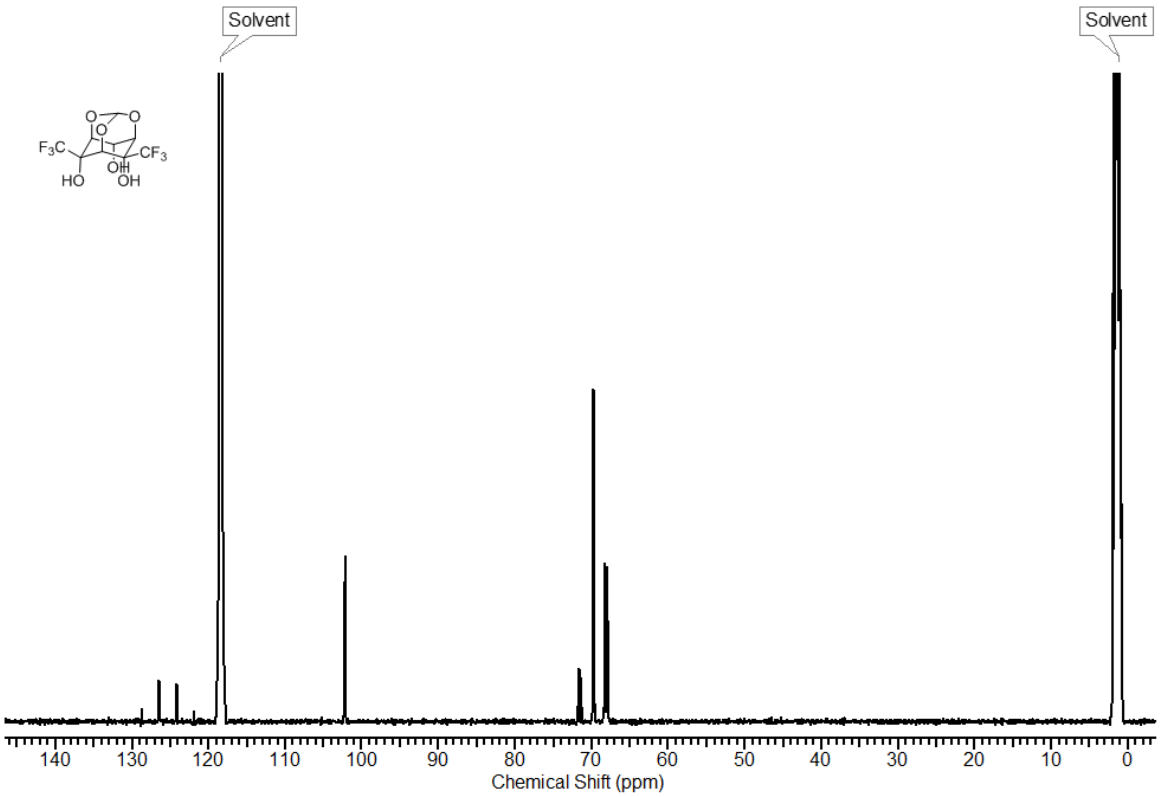
Solvent
Solvent
F3C
CF3
HO
OH
OH
140
130
120
110
100
90
80
70
60
50
40
30
20
10
0
Chemical Shift (ppm)

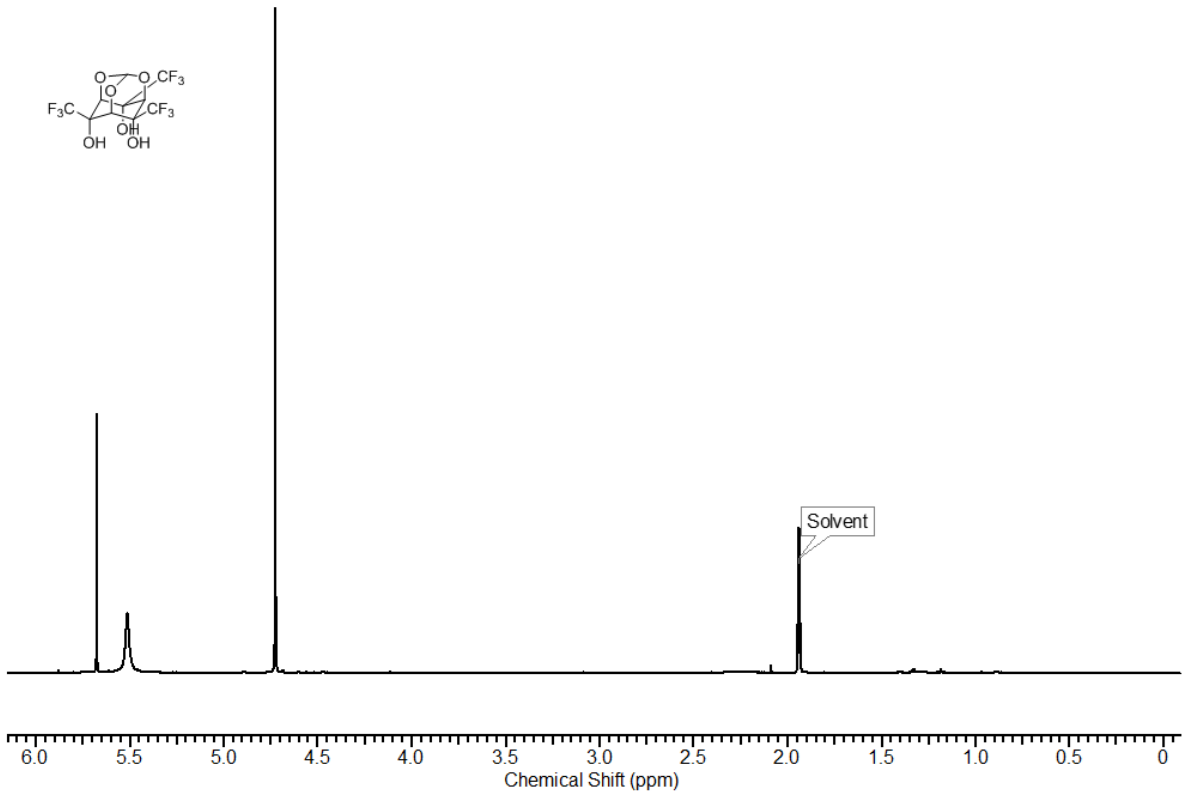
CF3
F3C
CF3
OH
OH
OH
Solvent
6.0
5.5
5.0
4.5
4.0
3.5
3.0
2.5
2.0
1.5
1.0
0.5
0
Chemical Shift (ppm)

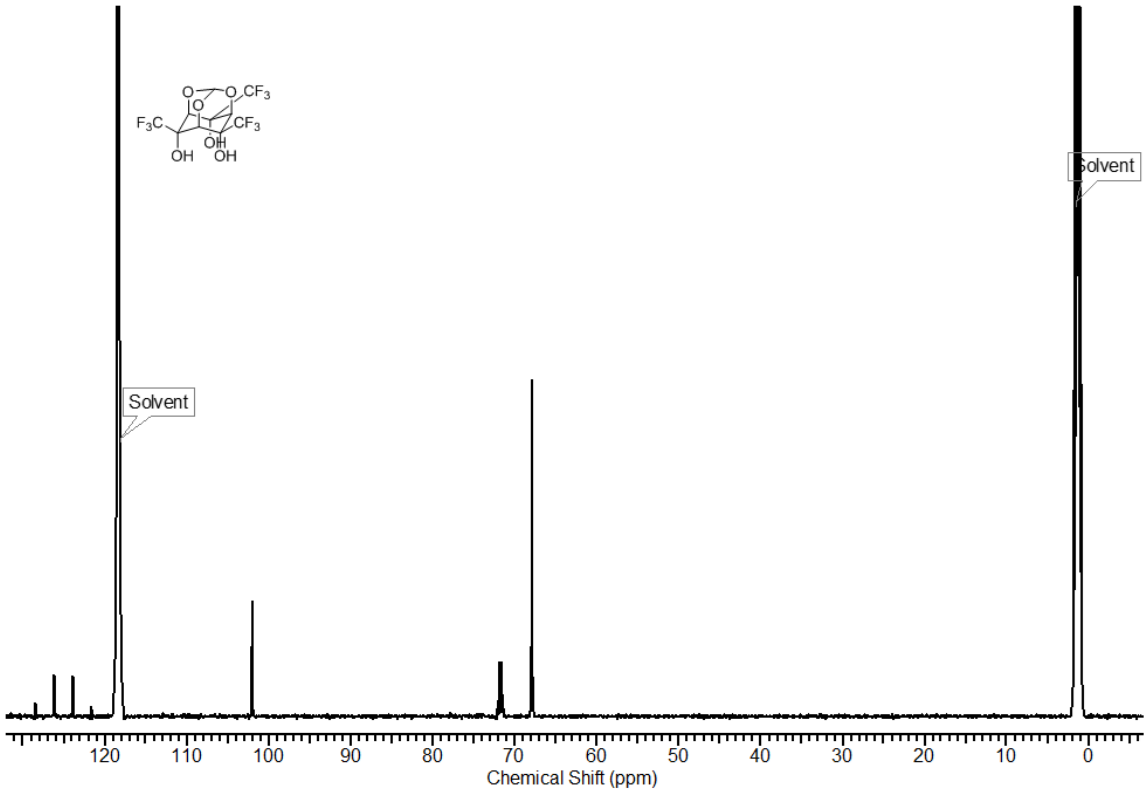

Complete Reference 7.

Akiyama, T.; Kotke, M.; Berkessel, A.; Payette, J. N.; Etzenbach – Effers, K.; Hayashi, Y.; Rapakko, S.; Schreiner, P. R.; Wierenga R. K.; Shoji, M.; Yamamoto, H. *Hydrogen Bonding in Organic Synthesis*. Pihko, P. M., Ed.; Wiley-VCH: Weinheim, 2009.

Complete Reference 25.

Frisch, M. J.; Trucks, G. W.; Schlegel, H. B.; Scuseria, G. E.; Robb, M. A.; Cheeseman, J. R.; Scalmani, G.; Barone, V.; Mennucci, B.; Petersson, G. A.; Nakatsuji, H.; Caricato, M.; Li, X.; Hratchian, H. P.; Izmaylov, A. F.; Bloino, J.; Zheng, G.; Sonnenberg, J. L.; Hada,

M.; Ehara, M.; Toyota, K.; Fukuda, R.; Hasegawa, J.; Ishida, M.; Nakajima, T.; Honda, Y.; Kitao, O.; Nakai, H.; Vreven, T.; Montgomery, Jr., J. A.; Peralta, J. E.; Ogliaro, F.; Bearpark, M.; Heyd, J. J.; Brothers, E.; Kudin, K. N.; Staroverov, V. N.; Kobayashi, R.; Normand, J.; Raghavachari, K.; Rendell, A.; Burant, J. C.; Iyengar, S. S.; Tomasi, J.; Cossi, M.; Rega, N.; Millam, J. M.; Klene, M.; Knox, J. E.; Cross, J. B.; Bakken, V.; Adamo, C.; Jaramillo, J.; Gomperts, R.; Stratmann, R. E.; Yazyev, O.; Austin, A. J.; Cammi, R.; Pomelli, C.; Ochterski, J. W.; Martin, R. L.; Morokuma, K.; Zakrzewski, V. G.; Voth, G. A.; Salvador, P.; Dannenberg, J. J.; Dapprich, S.; Daniels, A. D.; Farkas, O.; Foresman, J. B.; Ortiz, J. V.; Cioslowski, J.; Fox, D. J. *Gaussian 09*, Gaussian, Inc., Wallingford, CT, 2009.

Appendix for Chapter 3

For XYZ coordinates and electronic energies see:

http://pubs.acs.org/doi/abs/10.1021/jo502652z

Table S1. Titration data for chloride binding to **1(0)** in CD_3CN.

V (μL of Cl^- added)	[Cl^-] mM[a]	[**1(0)**] mM	δ (C−H) in ppm[b]	Δδ (ppm)	%bound[c]
0.0	0.00	0.32[d]	4.2444	0.0000	0.0
2.0	0.277	0.32	4.2601	0.0157	9.5
4.0	0.552	0.32	4.2786	0.0342	20.8
10	1.37	0.32	4.3079	0.0635	38.6
20	2.69	0.32	4.3363	0.0919	55.9
30	3.97	0.32	4.3568	0.1124	68.4
50	6.41	0.32	4.3773	0.1329	80.8
80	9.81	0.32	4.3851	0.1407	85.6
130	14.8	0.32	4.3900	0.1456	88.6
230	23.1	0.32	4.3939	0.1495	90.9
350	30.7	0.32	4.3988	0.1544	93.9
500	37.9	0.32	4.3988	0.1544	93.9

[a]A 83.4 mM TBACl and 0.32 mM **1(0)** stock solution was used. [b]NMR spectra were recorded with a 500 MHz spectrometer and the chemical shifts are referenced to the residual solvent signal at 1.94 δ. [c]Bound (%) = 100 × $\Delta\delta/\Delta\delta_{max}$, where $\Delta\delta_{max}$ = 0.1644 ppm. [d]The initial volume was 600 μL.

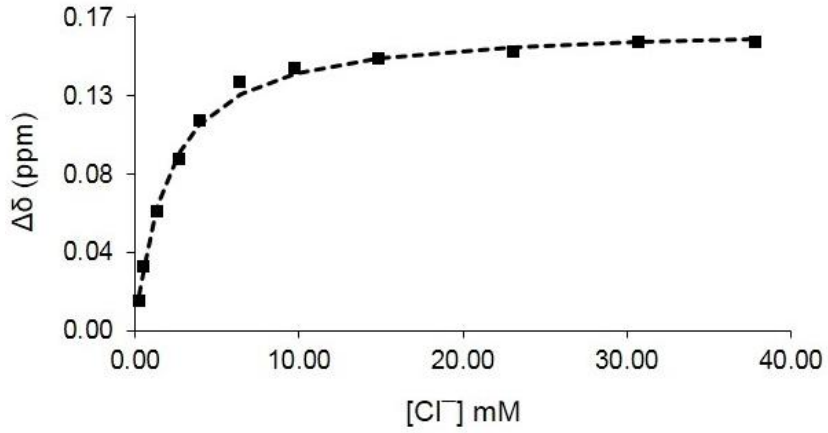

Figure S1. Non-linear 1:1 chloride binding isotherm for **1(0)** in CD_3CN. The square points are for the experimental results and the dashed line represents the non-linear fit of the data.

Table S2. Titration data for chloride binding to **1(1)** in CD_3CN.

V (μL of Cl^- added)	[Cl^-] mM[a]	[**1(1)**] mM	δ (C−H) in ppm[b]	Δδ (ppm)	%bound[c]
0.0	0.00	0.32[d]	4.4027	0.0000	0.0
2.0	0.179	0.32	4.4730	0.0703	27.3
4.0	0.357	0.32	4.5170	0.1143	44.4
6.0	0.534	0.32	4.5307	0.1280	49.7
10	0.884	0.32	4.5658	0.1631	63.3
16	1.40	0.32	4.5942	0.1915	74.3
24	2.07	0.32	4.6147	0.2120	82.3
34	2.89	0.32	4.6284	0.2257	87.6
50	4.14	0.32	4.6401	0.2374	92.1
80	6.34	0.32	4.6489	0.2462	95.5
130	9.58	0.32	4.6537	0.2510	97.4
230	14.9	0.32	4.6557	0.2530	98.2
330	19.0	0.32	4.6557	0.2530	98.2

[a]A 53.1 mM TBACl and 0.32 mM **1(1)** stock solution was used. [b]NMR spectra were recorded with a 500 MHz spectrometer and the chemical shifts are referenced to the residual solvent signal at 1.94 δ. [c]Bound (%) = 100 × $\Delta\delta/\Delta\delta_{max}$, where $\Delta\delta_{max}$ = 0.2577 ppm. [d]The initial volume was 590 μL.

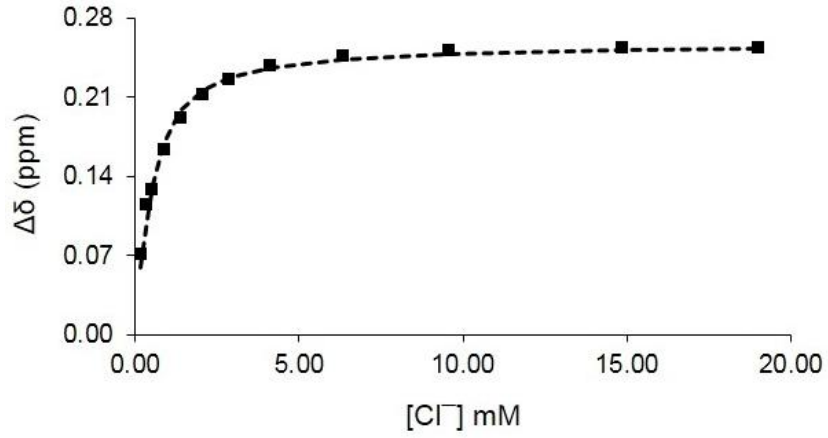

Figure S2. Non-linear 1:1 chloride binding isotherm for **1(1)** in CD_3CN. The square points are for the experimental results and the dashed line represents the non-linear fit of the data.

Table S3. Titration data for chloride binding to **1(2)** in CD_3CN.

V (μL of Cl^- added)	[Cl^-] mM[a]	[**1(2)**] mM	δ (C−H) in ppm[b]	Δδ (ppm)	%bound[c]
0.0	0.00	0.29[d]	4.5971	0.0000	0.0
2.0	0.016	0.29	4.6088	0.0117	3.0
10	0.079	0.29	4.6625	0.0654	16.7
16	0.12	0.29	4.7026	0.1055	27.0
24	0.18	0.29	4.7583	0.1612	41.2
34	0.26	0.29	4.8130	0.2159	55.2
44	0.33	0.29	4.8481	0.2510	64.2
56	0.41	0.29	4.8775	0.2804	71.7
70	0.50	0.29	4.9029	0.3058	78.2
90	0.63	0.29	4.9214	0.3243	82.9
140	0.90	0.29	4.9439	0.3468	88.7
240	1.36	0.29	4.9576	0.3605	92.2
440	2.01	0.29	4.9683	0.3712	94.9

[a]A 4.65 mM TBACl and 0.29 mM **1(2)** stock solution was used. [b]NMR spectra were recorded with a 500 MHz spectrometer and the chemical shifts are referenced to the residual solvent signal at 1.94 δ. [c]Bound (%) = 100 × $\Delta\delta/\Delta\delta_{max}$, where $\Delta\delta_{max}$ = 0.3911 ppm. [d]The initial volume was 580 μL.

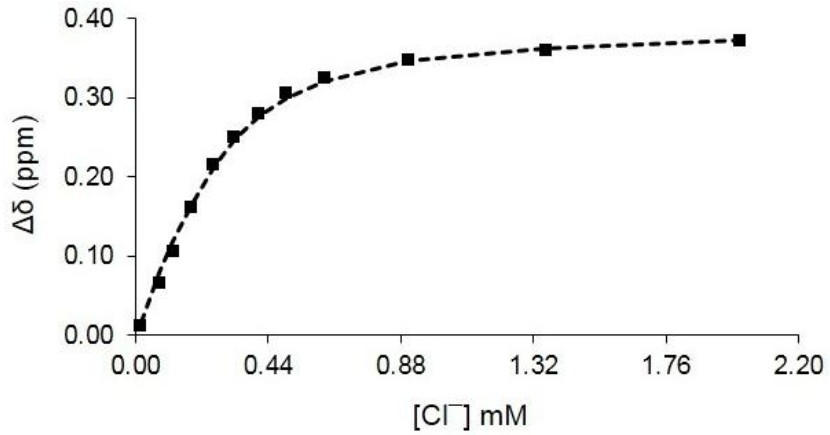

Figure S3. Non-linear 1:1 chloride binding isotherm for **1(2)** in CD_3CN. The square points are for the experimental results and the dashed line represents the non-linear fit of the data.

Table S4. Titration data for chloride binding to **1(3)** in CD_3CN.

V (μL of Cl^- added)	[Cl^-] mM[a]	[**1(3)**] mM	δ (C−H) in ppm[b]	Δδ (ppm)	%bound[c]
0	0.00	0.43[d]	4.7280	0.0000	0.0
2.0	0.015	0.43	4.7309	0.0029	2.1
6.0	0.044	0.43	4.7397	0.0117	8.3
10	0.072	0.43	4.7475	0.0195	13.8
20	0.142	0.43	4.7700	0.0420	29.8
30	0.209	0.43	4.7905	0.0625	44.4
40	0.274	0.43	4.8100	0.0820	58.2
50	0.337	0.43	4.8286	0.1006	71.4
60	0.399	0.43	4.8462	0.1182	83.9
80	0.516	0.43	4.8608	0.1328	94.3
100	0.626	0.43	4.8648	0.1368	97.2
140	0.828	0.43	4.8687	0.1407	99.9

[a]A 4.32 mM TBACl and 0.43 mM **1(3)** stock solution was used. [b]NMR spectra were recorded with a 500 MHz spectrometer and the chemical shifts are referenced to the residual solvent signal at 1.94 δ. [c]Bound (%) = 100 × $\Delta\delta/\Delta\delta_{max}$, where $\Delta\delta_{max}$ = 0.1408 ppm. [d]The initial volume was 590 μL.

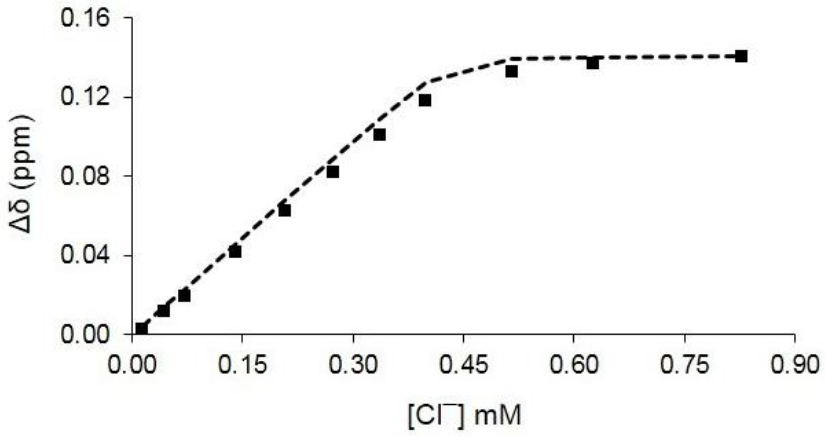

Figure S4. Non-linear 1:1 chloride binding isotherm for **1(3)** in CD_3CN. The square points are for the experimental results and the dashed line represents the non-linear fit of the data.

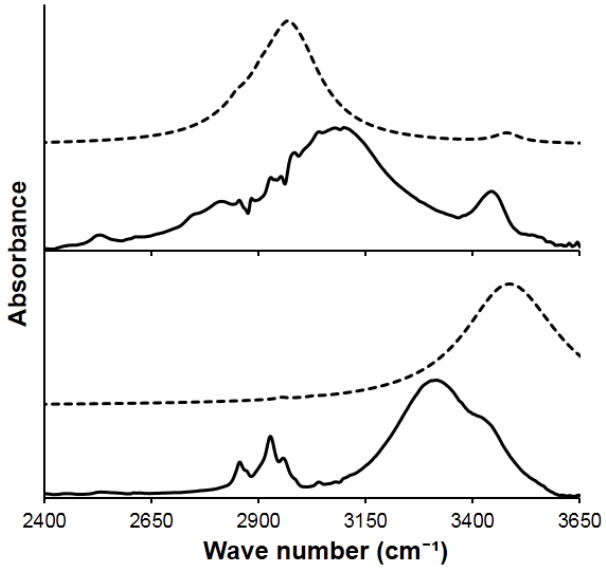

Figure S5. Experimental (solid lines) and B3LYP/6-31+G(d,p) computed (dashed lines) IR spectra of **1(3)** (bottom) and **1(3)** • Cl^- (top).

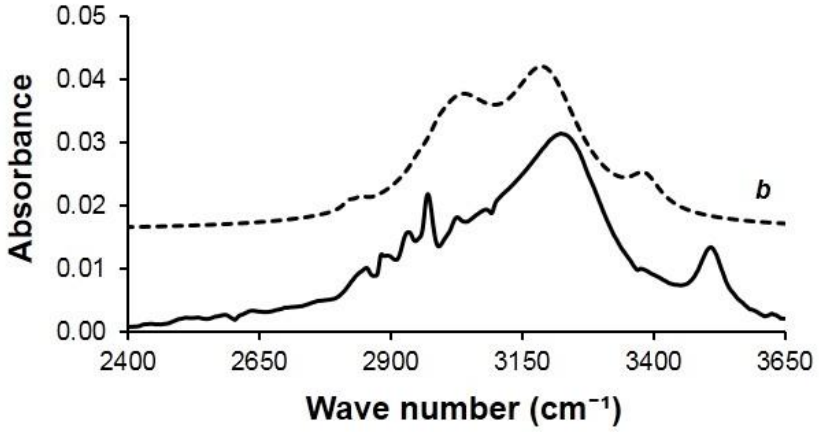

Figure S6. Experimental IR spectrum of **1(1)** • Cl^- (solid line) and the B3LYP/6-31+G(d,p) prediction (dotted line) for conformer ***b*** as illustrated in Fig. 1 of the manuscript.

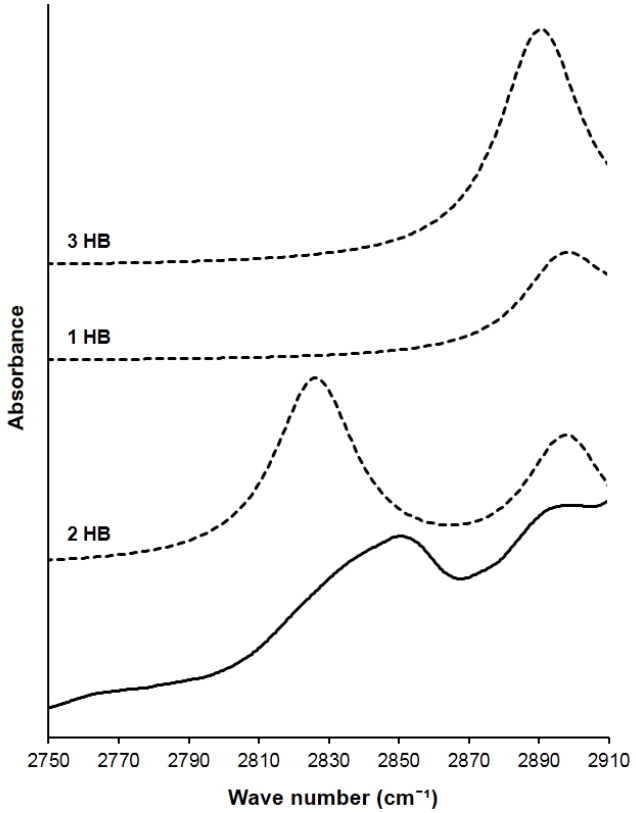

Figure S7. Experimental (solid line) and B3LYP/6 31+G(d,p) computed (dashed lines) IR spectra of the low frequency C–H stretching region of **1(1)** • Cl^- conformers recorded in 30% CD_3CN/70% CCl_4 with Ph_4PCl.

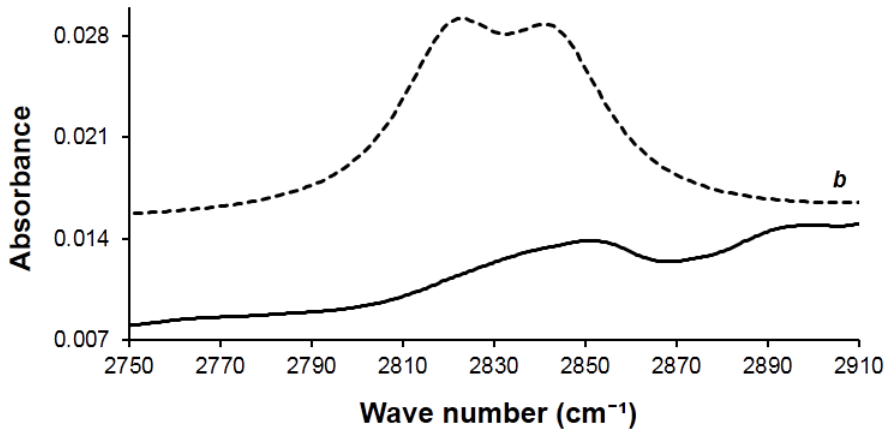

Figure S8. Experimental (solid line) and B3LYP/6-31+G(d,p) computed (dashed line) IR spectra of the low frequency C–H stretching region of **1(1)** • Cl^- in 30% CD_3CN/70% CCl_4 with Ph_4PCl. The calculated conformer is for ***b*** as illustrated in Fig. 1 of the manuscript.

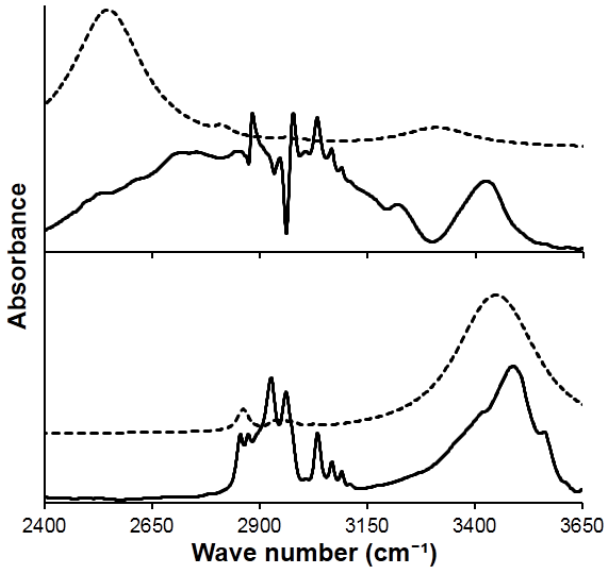

Figure S9. Experimental (solid lines) and B3LYP/6-31+G(d,p) computed (dashed lines) IR spectra of **1Bn(2)** (bottom) and **1Bn(2)** • Cl^- (top).

Table S5. Experimental and computed IR frequencies.

cmpd (X)	frequencies (cm^{-1})		cmpd X•Cl^-	frequencies (cm^{-1})				
	Expt	calc[1]		expt	calc[1]			
					a	***b***	***c***	***d***
1(1)	*3436*	*3492*	**1(1) • Cl^-**	*3509*	*3515*	*3388*	*3495*	*3266*
	3029	3024		*3224*	*3115*	*3189*	*3300*	2990
	2970	2945		3026	2993	*3040*	*2446*	2949
	2930	**2915**		2970	2960	2992	2997	**2892**
	2856			**2933**	**2900**	2953	2951	
				2882	**2828**	**2843**	**2900**	
				2853		**2825**		
1(3)	*3443*	*3492*	**1(3) • Cl^-**	*3443*	*3480*			
	3315	*3467*		*3095*	*2972*			
					1 HB	2 HB		
1Bn(1)	*3565*	*3534*	**1Bn(1) • Cl^-**	*3425*	*3315*	*3140*		
	3475	*3434*		*3010*	*2865*			
1Bn(2)	*3568*	*3478*	**1Bn(2) • Cl^-**	*3430*	*3320*	*3140*		
	3500	*3422*		*2860*	*2553*			

[1]Italized frequencies correspond to O–H stretches and bold values are for the equatorial C–H stretching modes.

^{1}H and ^{13}C NMR spectra of 1αMe(1), 1Bn(1) and 1Me(1)

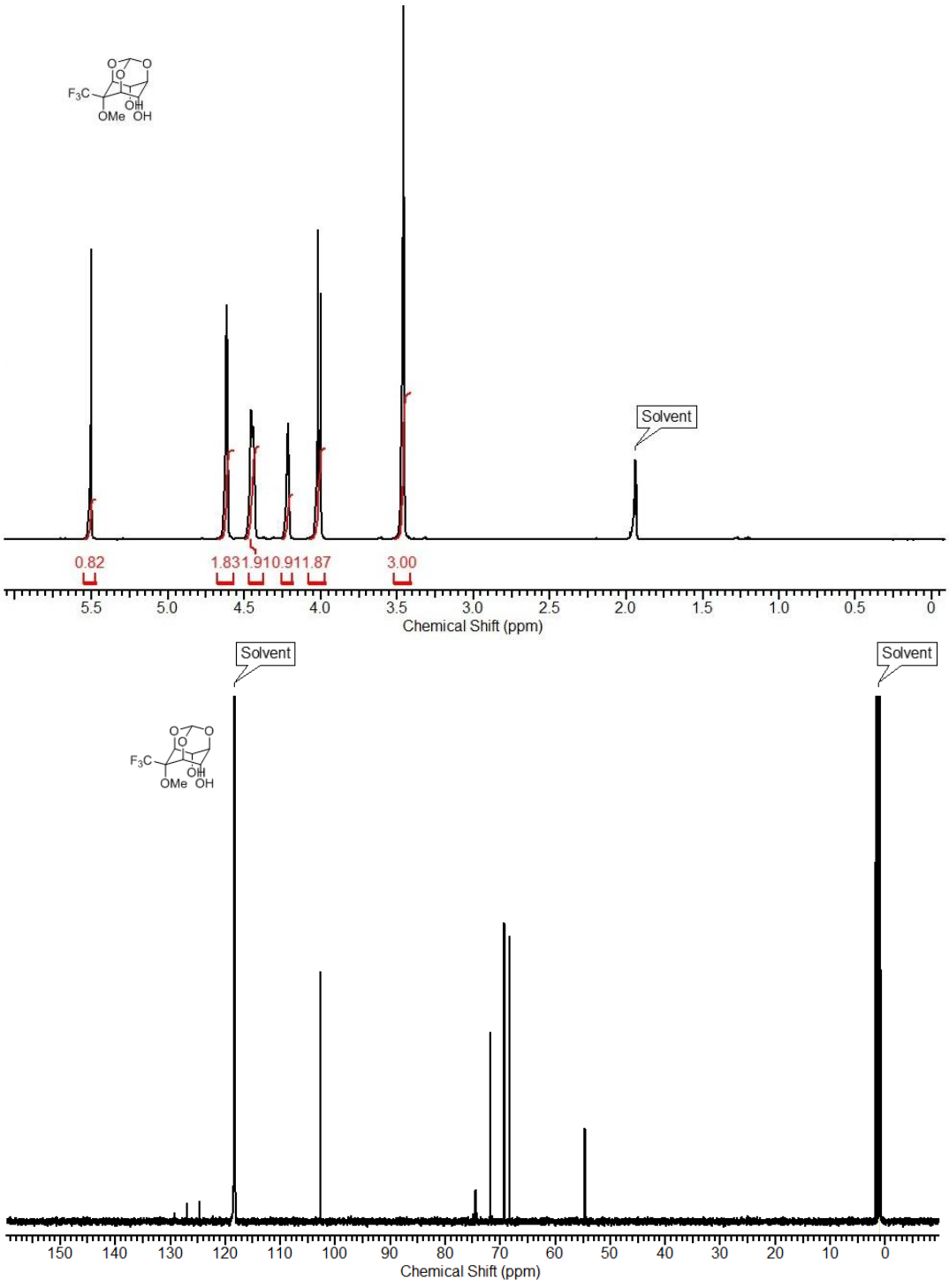

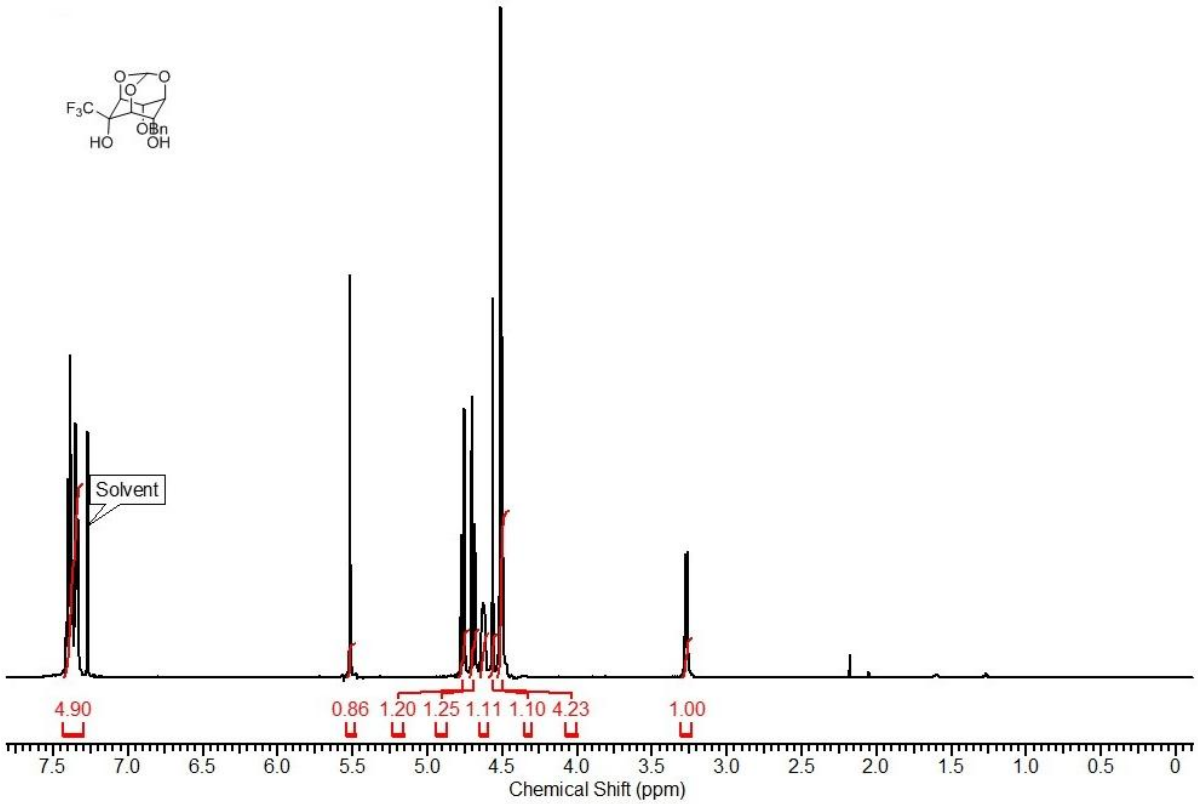
Solvent
4.90
0.86
1.20
1.25
1.11
1.10
4.23
1.00
7.5
7.0
6.5
6.0
5.5
5.0
4.5
4.0
3.5
3.0
2.5
2.0
1.5
1.0
0.5
0
Chemical Shift (ppm)

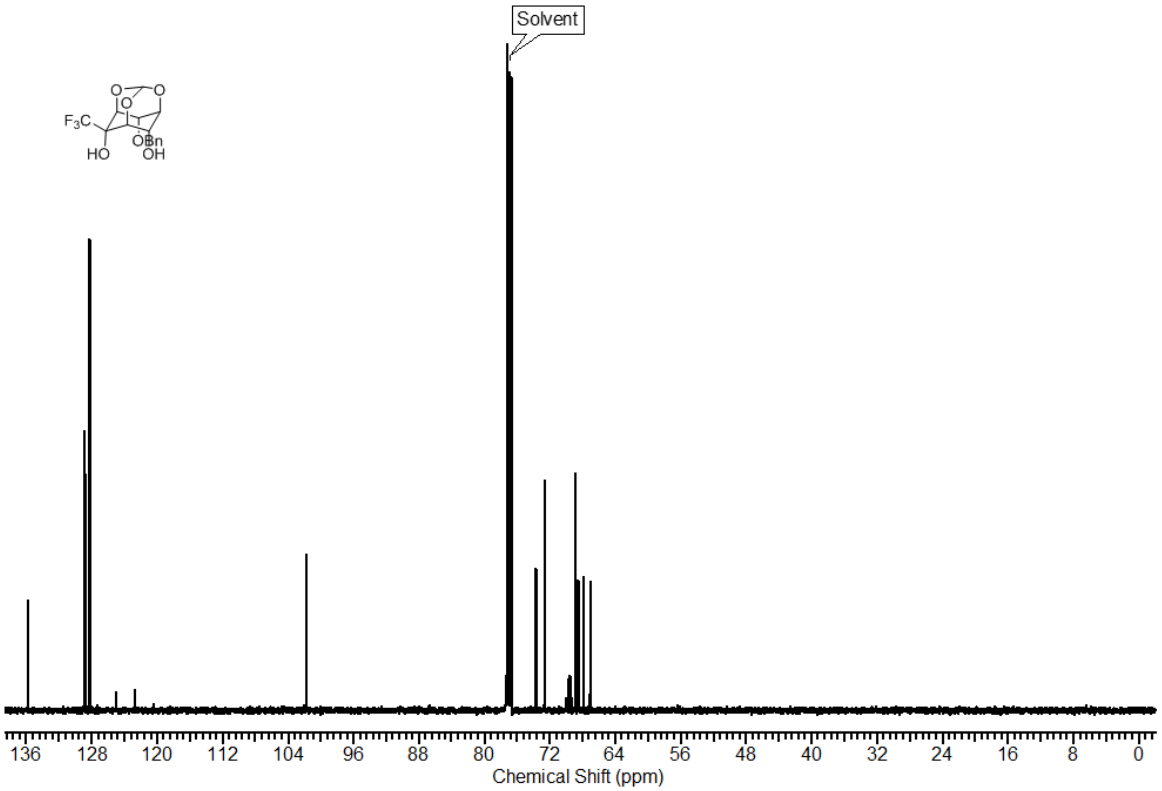
Solvent
136
128
120
112
104
96
88
80
72
64
56
48
40
32
24
16
8
0
Chemical Shift (ppm)

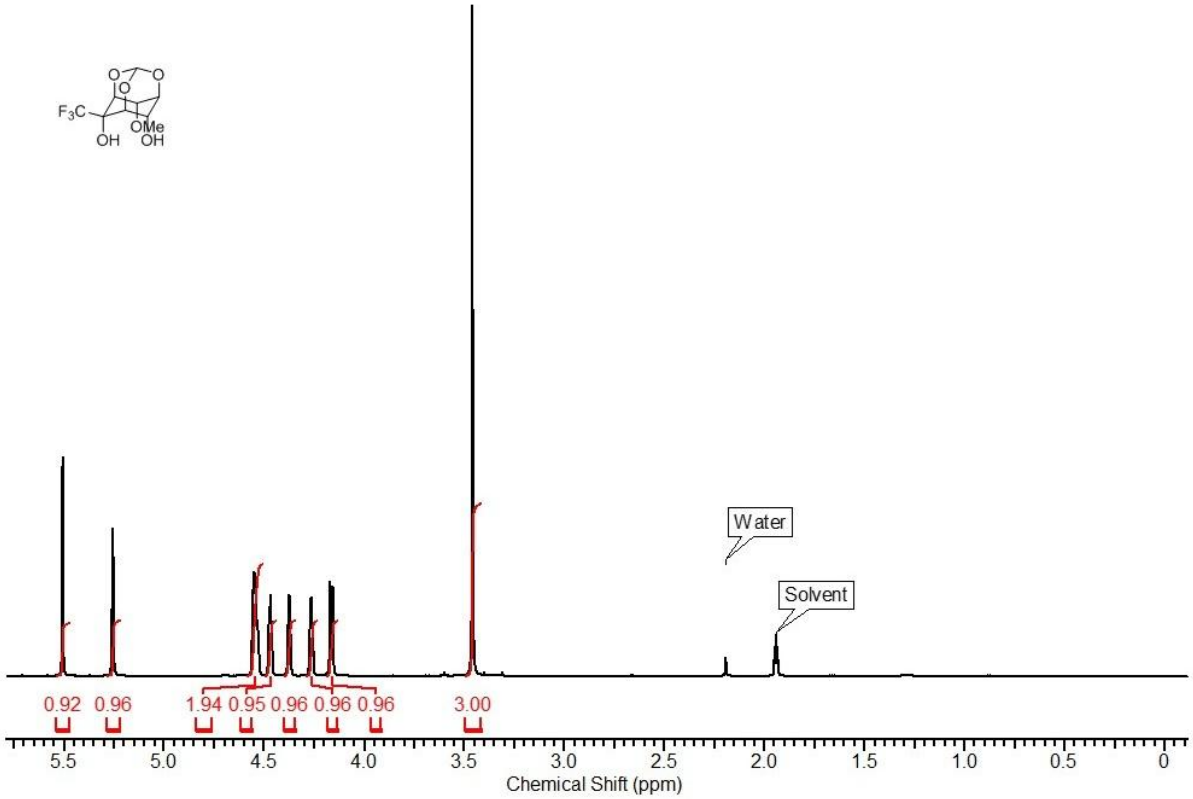
F3C
OMe
OH
OH
Water
Solvent
0.92
0.96
1.94
0.95
0.96
0.96
0.96
3.00
5.5
5.0
4.5
4.0
3.5
3.0
2.5
2.0
1.5
1.0
0.5
0
Chemical Shift (ppm)

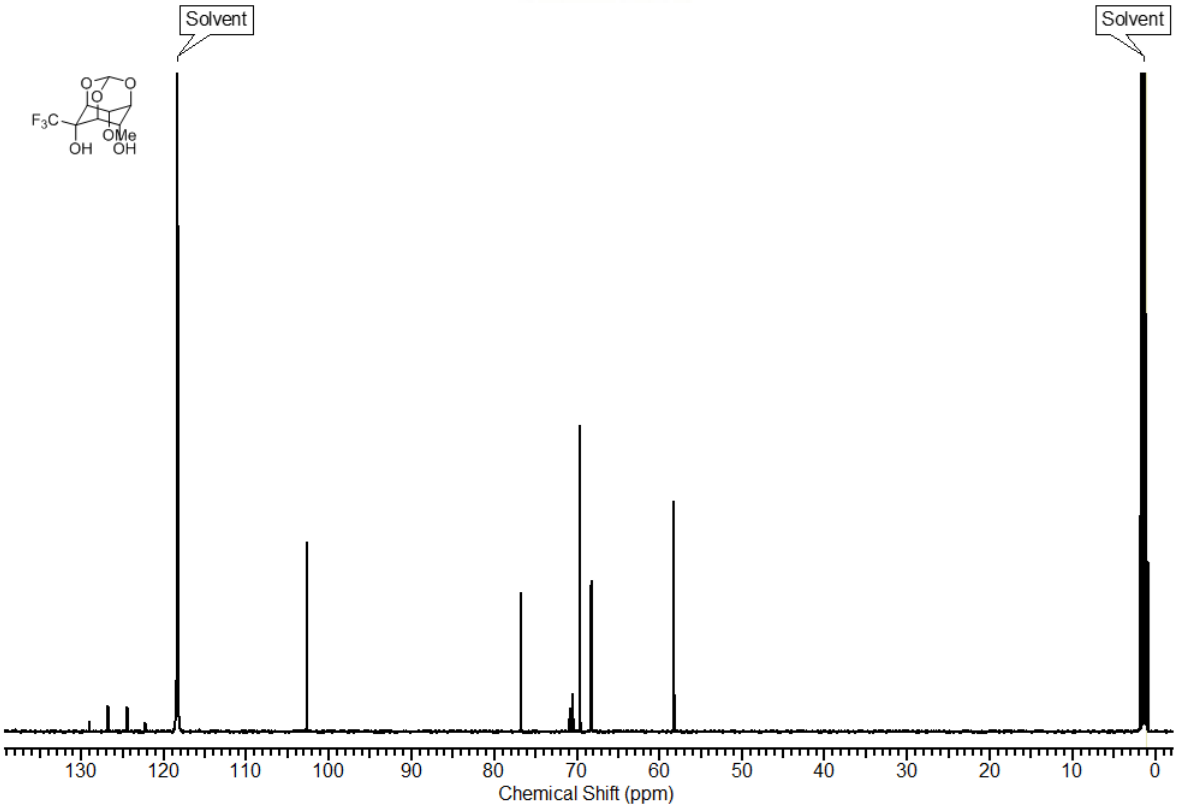
Solvent
Solvent
F3C
OMe
OH
OH
130
120
110
100
90
80
70
60
50
40
30
20
10
0
Chemical Shift (ppm)

Complete reference 33:

Frisch, M. J.; Trucks, G. W.; Schlegel, H. B.; Scuseria, G. E.; Robb, M. A.; Cheeseman, J. R.; Scalmani, G.; Barone, V.; Mennucci, B.; Petersson, G. A.; Nakatsuji, H.; Caricato, M.; Li, X.; Hratchian, H. P.; Izmaylov, A. F.; Bloino, J.; Zheng, G.; Sonnenberg, J. L.; Hada, M.; Ehara, M.; Toyota, K.; Fukuda, R.; Hasegawa, J.; Ishida, M.; Nakajima, T.; Honda, Y.; Kitao, O.; Nakai, H.; Vreven, T.; Montgomery, Jr., J. A.; Peralta, J. E.; Ogliaro, F.; Bearpark, M.; Heyd, J. J.; Brothers, E.; Kudin, K. N.; Staroverov, V. N.; Kobayashi, R.; Normand, J.; Raghavachari, K.; Rendell, A.; Burant, J. C.; Iyengar, S. S.; Tomasi, J.; Cossi, M.; Rega, N.; Millam, J. M.; Klene, M.; Knox, J. E.; Cross, J. B.; Bakken, V.; Adamo, C.; Jaramillo, J.; Gomperts, R.; Stratmann, R. E.; Yazyev, O.; Austin, A. J.; Cammi, R.; Pomelli, C.; Ochterski, J. W.; Martin, R. L.; Morokuma, K.; Zakrzewski, V. G.; Voth, G. A.; Salvador, P.; Dannenberg, J. J.; Dapprich, S.; Daniels, A. D.; Farkas, O.; Foresman, J. B.; Ortiz, J. V.; Cioslowski, J.; Fox, D. J. *Gaussian 09*, Gaussian, Inc., Wallingford, CT, 2009.

Appendix for Chapter 4

For XYZ coordinates and electronic energies see:

http://pubs.rsc.org/en/content/articlelanding/2015/ob/c4ob02470b#!divAbstract

NMR Spectra

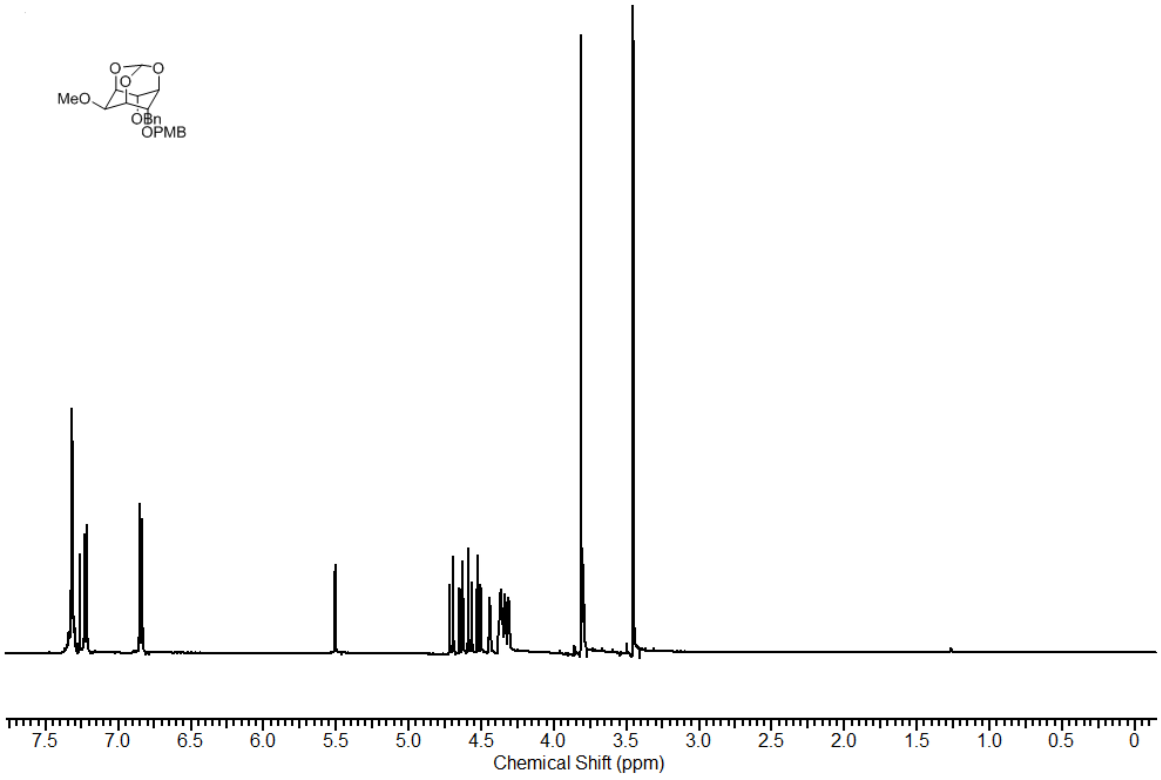

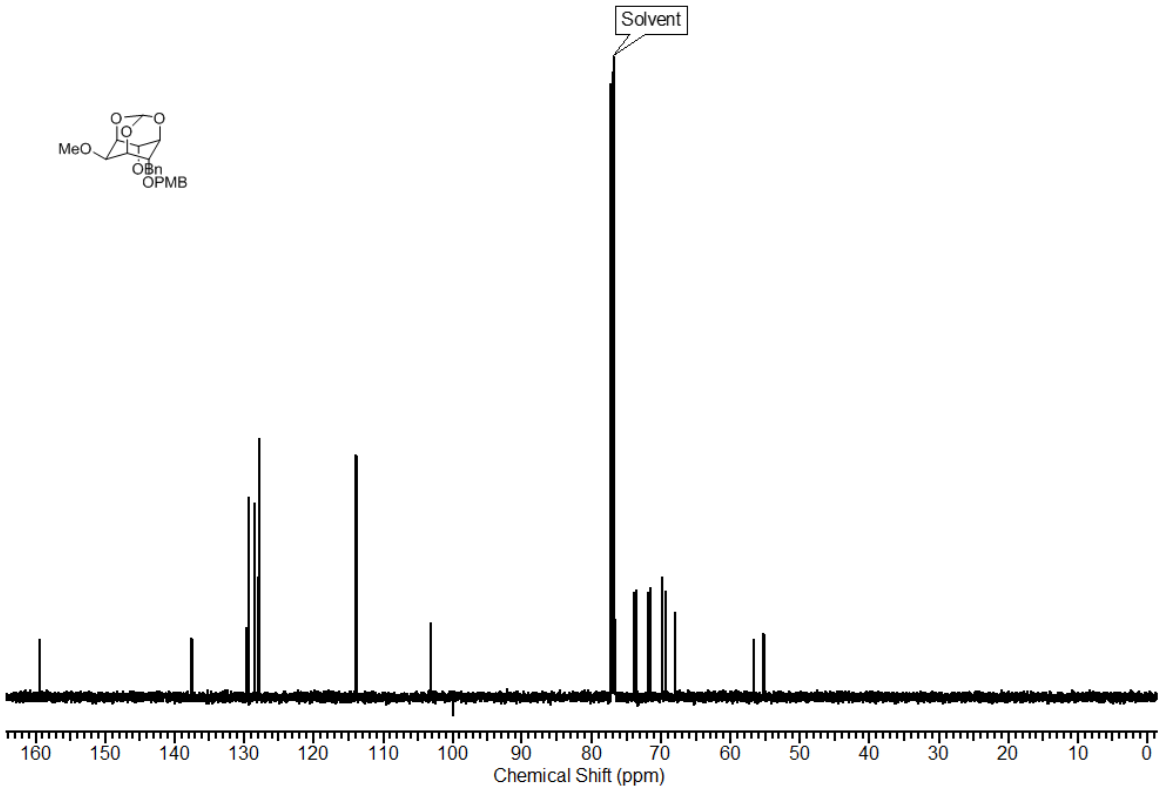
Solvent
MeO
OBn
OPMB
160
150
140
130
120
110
100
90
80
70
60
50
40
30
20
10
0
Chemical Shift (ppm)

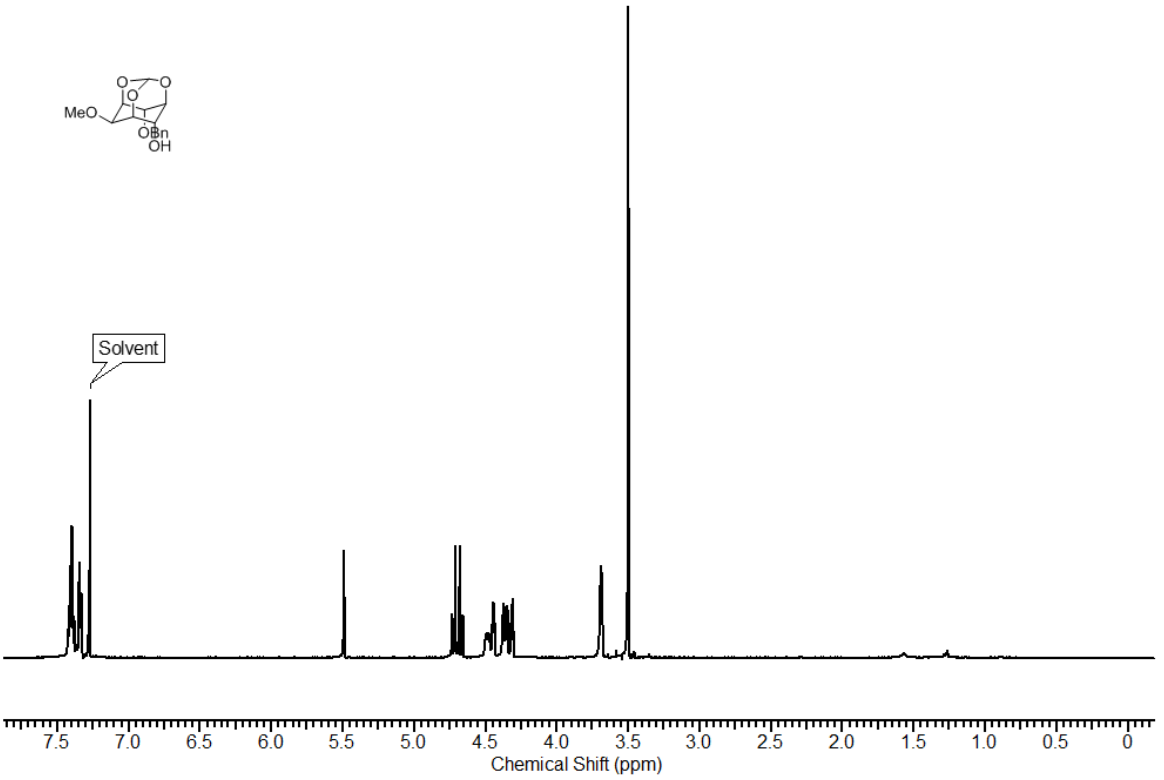
MeO
OBn
OH
Solvent
7.5
7.0
6.5
6.0
5.5
5.0
4.5
4.0
3.5
3.0
2.5
2.0
1.5
1.0
0.5
0
Chemical Shift (ppm)

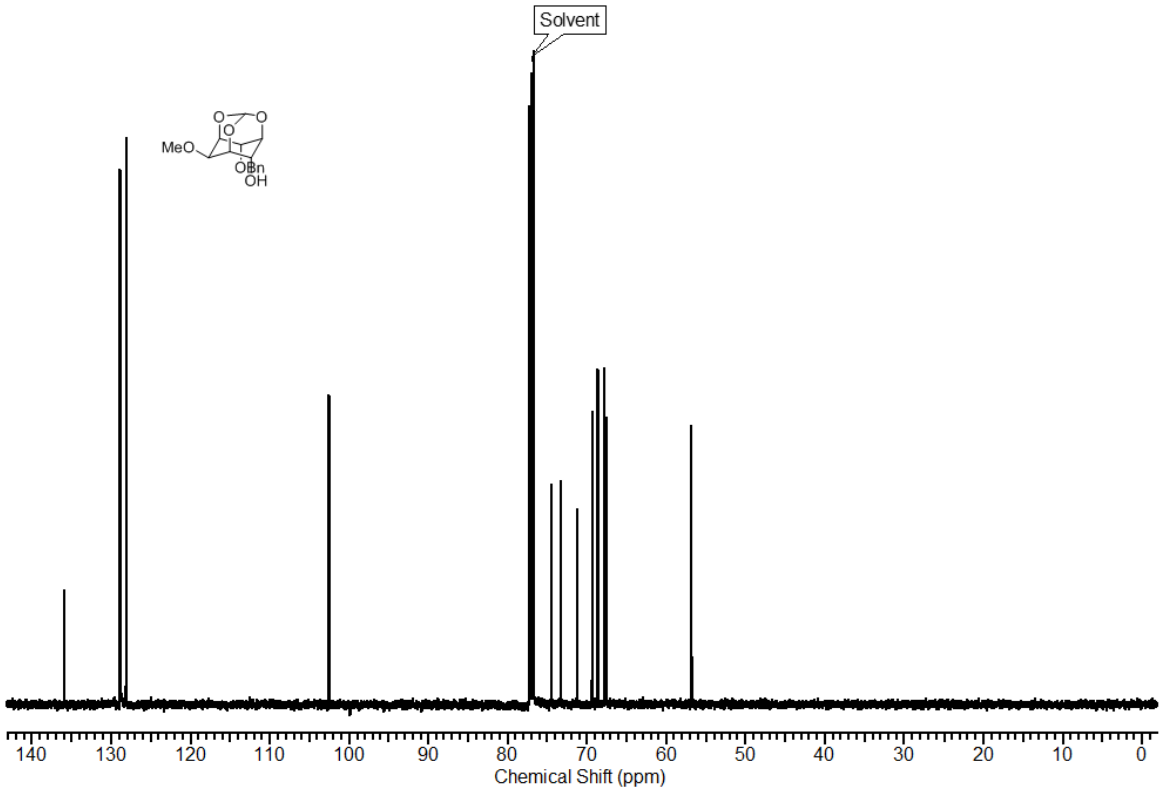
Solvent
MeO
OBn
OH
140
130
120
110
100
90
80
70
60
50
40
30
20
10
0
Chemical Shift (ppm)

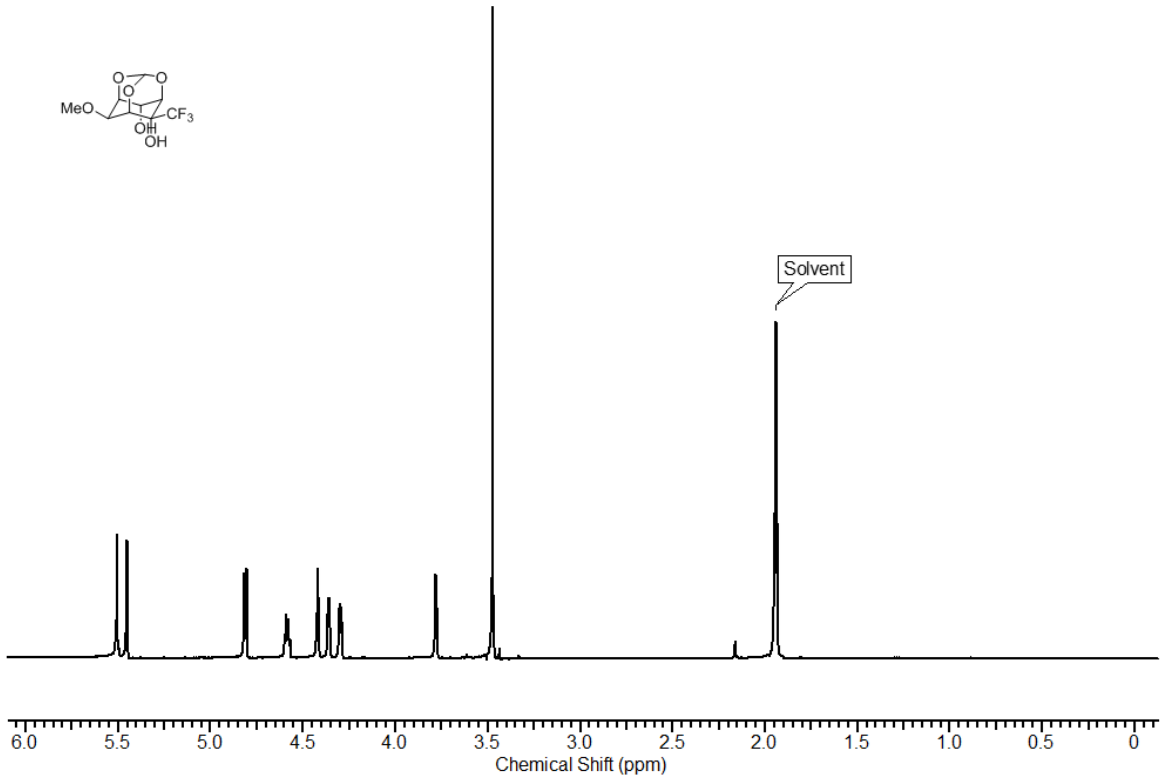
MeO
CF3
OH
OH
Solvent
6.0
5.5
5.0
4.5
4.0
3.5
3.0
2.5
2.0
1.5
1.0
0.5
0
Chemical Shift (ppm)

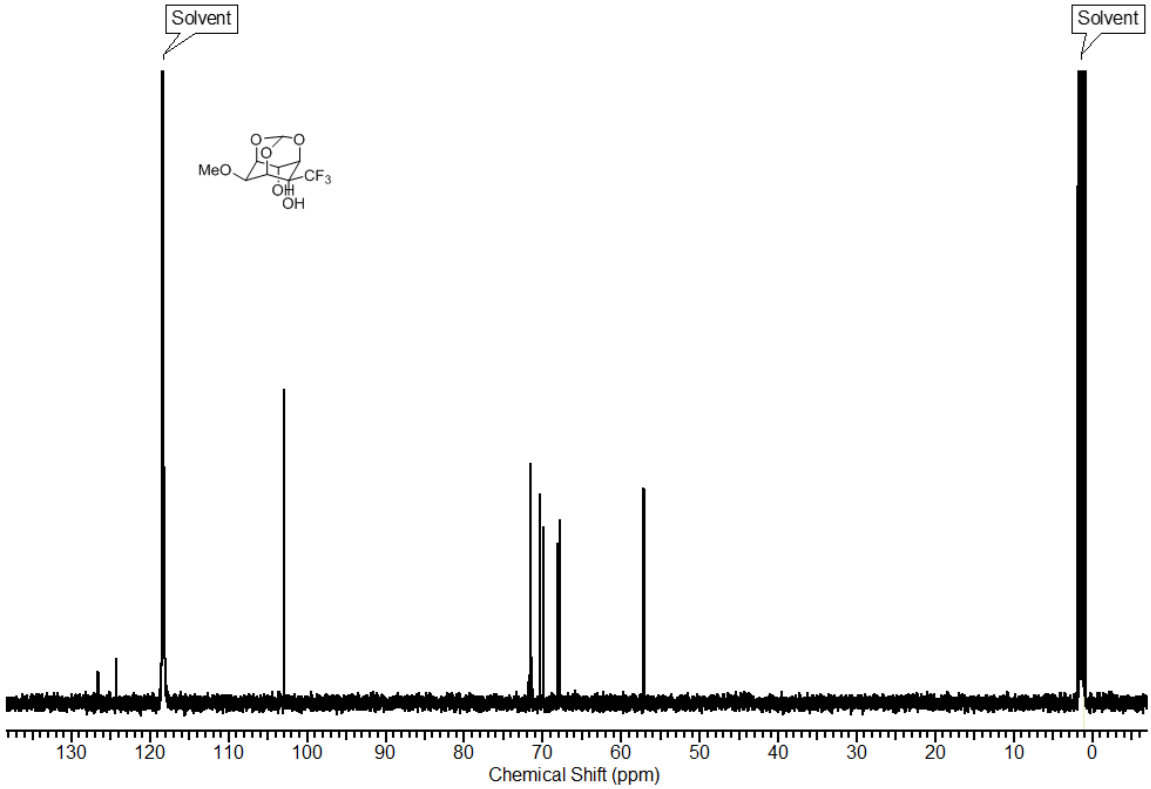
Solvent
Solvent
MeO
CF3
OH
OH
130
120
110
100
90
80
70
60
50
40
30
20
10
0
Chemical Shift (ppm)

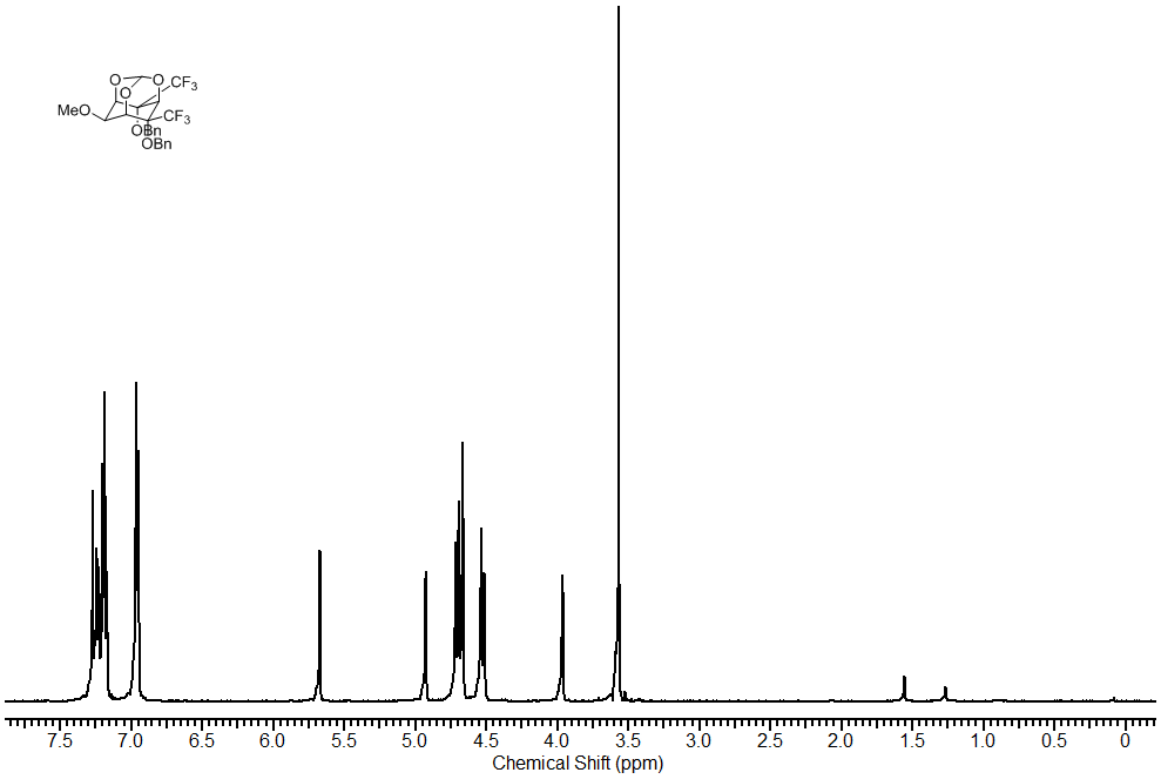
CF3
MeO
CF3
OBn
OBn
7.5
7.0
6.5
6.0
5.5
5.0
4.5
4.0
3.5
3.0
2.5
2.0
1.5
1.0
0.5
0
Chemical Shift (ppm)

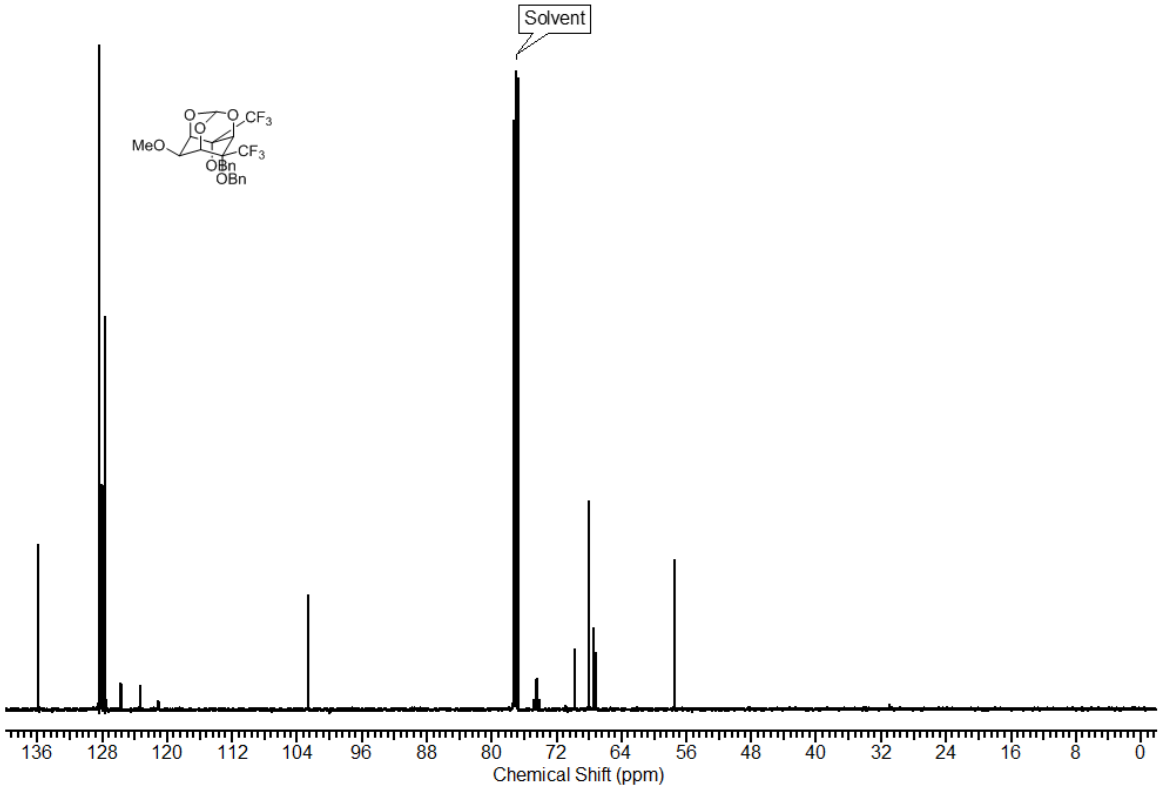
Solvent
MeO
CF3
CF3
OBn
OBn
136
128
120
112
104
96
88
80
72
64
56
48
40
32
24
16
8
0
Chemical Shift (ppm)

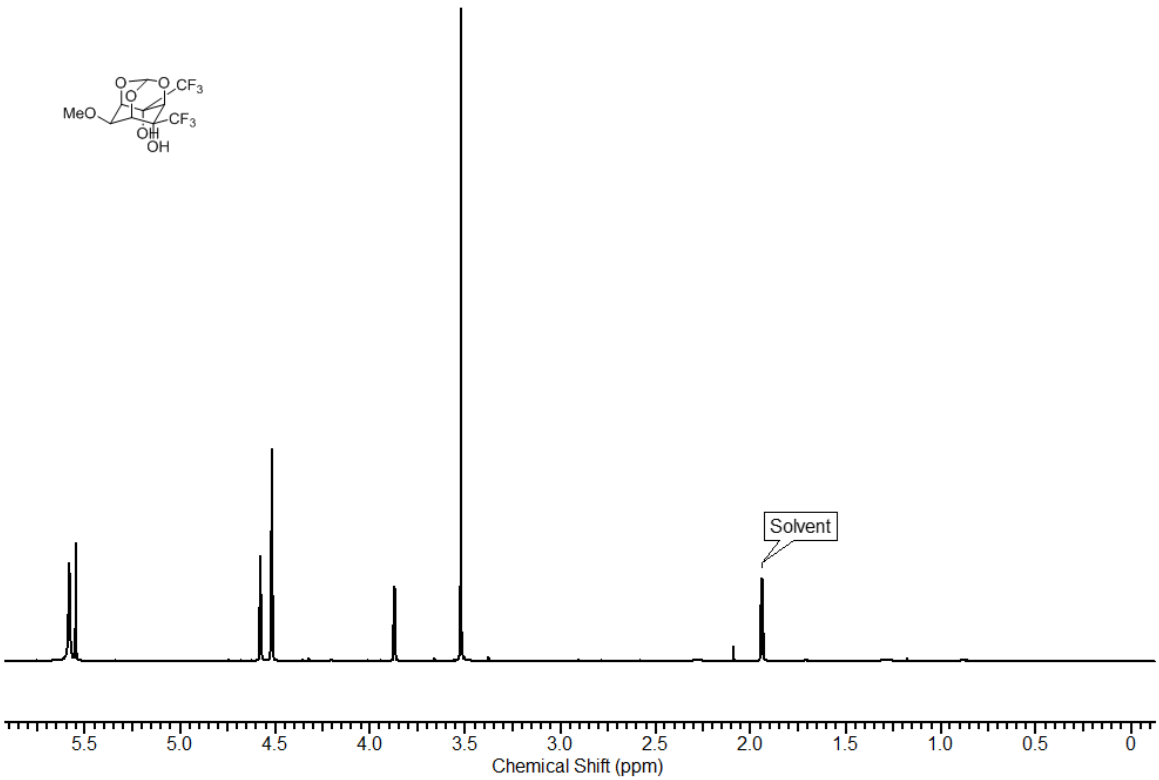
MeO
CF3
CF3
OH
OH
Solvent
5.5
5.0
4.5
4.0
3.5
3.0
2.5
2.0
1.5
1.0
0.5
0
Chemical Shift (ppm)

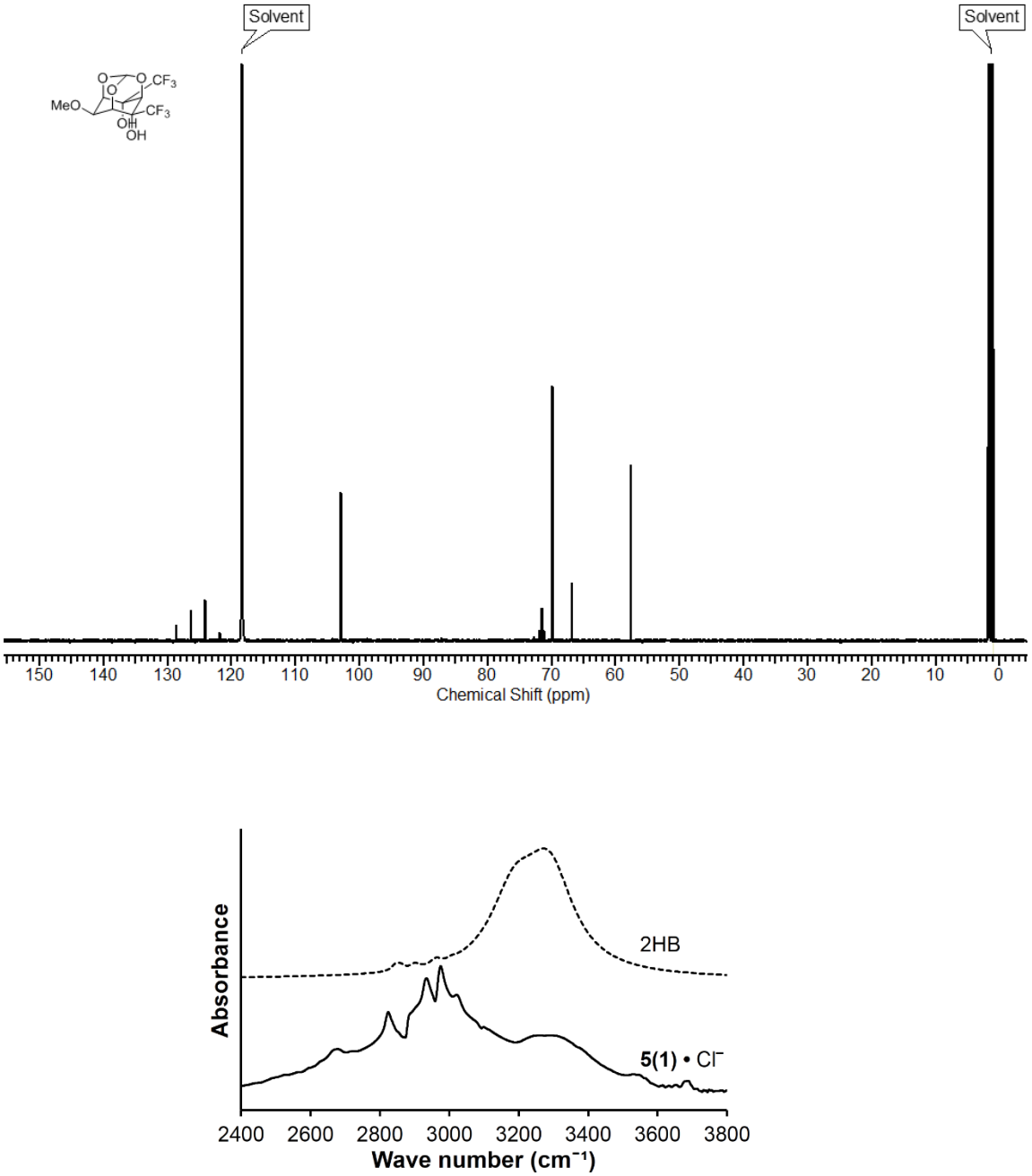

Figure S1. Experimental IR spectrum of **5(1)** • Cl^- (solid line) and the B3LYP/6-31+G(d,p) prediction (dotted line) for the less stable conformer with 2 primary hydrogen bonds to chloride ion.

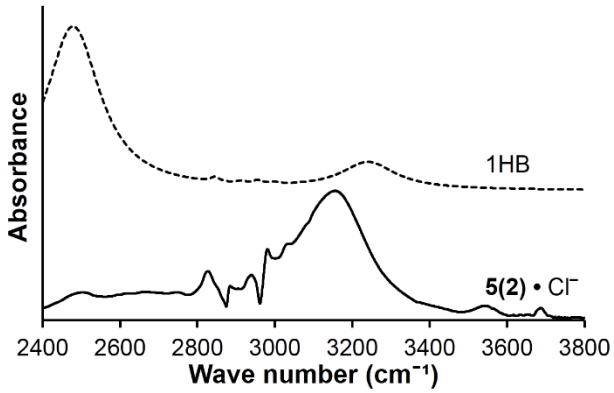

Figure S2. Experimental IR spectrum of **5(2)** • Cl^- (solid line) and the B3LYP/6-31+G(d,p) computed (dotted line) for the less stable conformer with 1 primary and 1 secondary hydrogen bonds to chloride ion.

Table S1. Titration data for chloride binding to **5(1)** in CD_3CN.

V (μL of Cl^- added)	[Cl^-] mM[a]	[**5(1)**] mM	δ (C–H) in ppm[b]	Δδ (ppm)	%bound[c]
0	0.00	0.45[d]	4.3587	0.0000	0.0
1.00	0.13	0.45	4.3705	0.0118	7.2
3.00	0.38	0.45	4.3959	0.0372	22.8
6.00	0.77	0.45	4.4125	0.0538	32.9
10.0	1.28	0.45	4.4349	0.0762	46.6
15.0	1.92	0.45	4.4535	0.0948	58.0
22.0	2.82	0.45	4.4691	0.1104	67.5
32.0	4.10	0.45	4.4828	0.1241	75.9
50.0	6.41	0.45	4.4945	0.1358	83.1
90.0	11.5	0.45	4.5053	0.1466	89.7
170	21.8	0.45	4.5101	0.1514	92.6

[a]A 75.62 mM TBACl and 0.45 mM **5(1)** stock solution was used. [b]NMR spectra were recorded with a Varian VI–500 spectrometer and the chemical shifts are referenced to the residual solvent signal at 1.94 δ. [c]Bound (%) = 100 × $\Delta\delta/\Delta\delta_{max}$, where $\Delta\delta_{max}$ = 0.1635 ppm. [d]The initial volume was 590 μL.

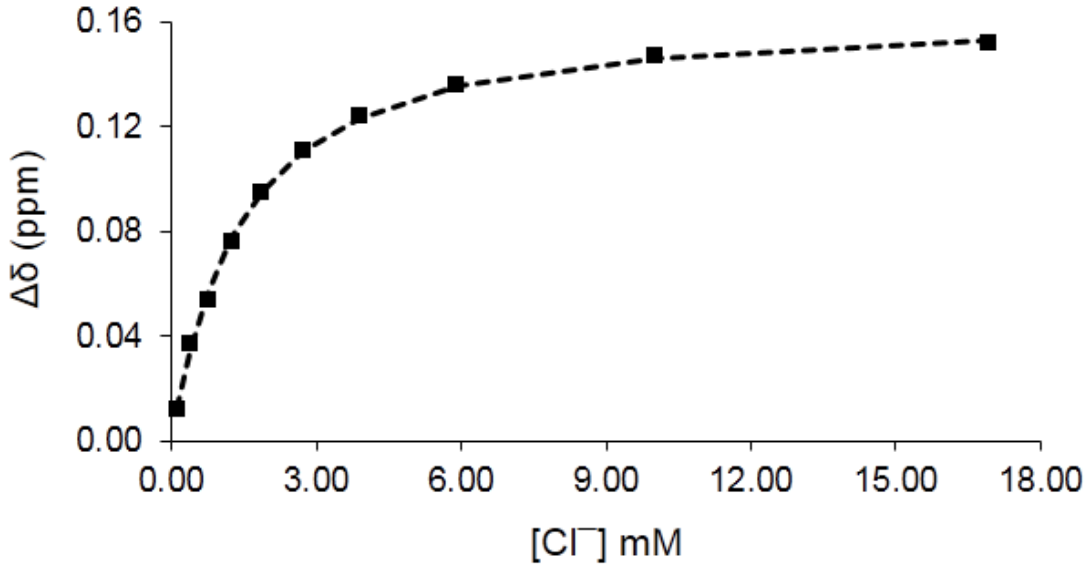

Figure S3. Non-linear 1:1 chloride binding isotherm for **5(1)** in CD_3CN, where the dashed line represents the fit to the experimental data (i.e., the squares).

Table S2. Titration data for chloride binding to **5(2)** in CD_3CN.

V (μL of Cl^- added)	[Cl^-] mM[a]	[**5(2)**] mM	δ (C−H) in ppm[b]	Δδ (ppm)	%bound[c]
0	0.00	0.47[d]	4.5990	0.0000	0.0
2.00	0.027	0.47	4.6166	0.0176	4.5
6.00	0.082	0.47	4.6616	0.0626	16.2
12.0	0.16	0.47	4.7212	0.1222	31.5
22.0	0.30	0.47	4.8130	0.2140	55.2
32.0	0.43	0.47	4.8745	0.2755	71.1
42.0	0.57	0.47	4.9136	0.3146	81.2
54.0	0.73	0.47	4.9409	0.3419	88.3
66.0	0.90	0.47	4.9536	0.3546	91.5
80.0	1.09	0.47	4.9634	0.3644	94.1
100	1.36	0.47	4.9712	0.3722	96.1

[a]A 8.01 mM TBACl and 0.47 mM **5(2)** stock solution was used. [b]NMR spectra were recorded with a Varian VI–500 spectrometer and the chemical shifts are referenced to the residual solvent signal at 1.94 δ. [c]Bound (%) = 100 × $\Delta\delta/\Delta\delta_{max}$, where $\Delta\delta_{max}$ = 0.3873 ppm. [d]The initial volume was 590 μL.

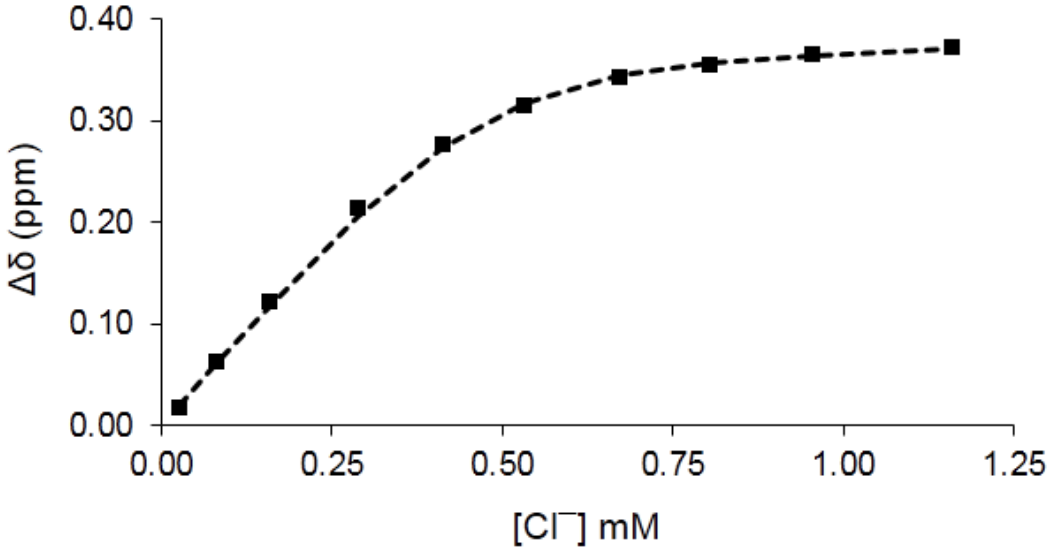

Figure S4. Non-linear 1:1 chloride binding isotherm for **5(2)** in CD_3CN, where the dashed line represents the fit to the experimental data (i.e., the squares).

Appendix for Chapter 5

For XYZ coordinates and electronic energies see:

http://pubs.acs.org/doi/abs/10.1021/jacs.5b01805

NMR Spectra

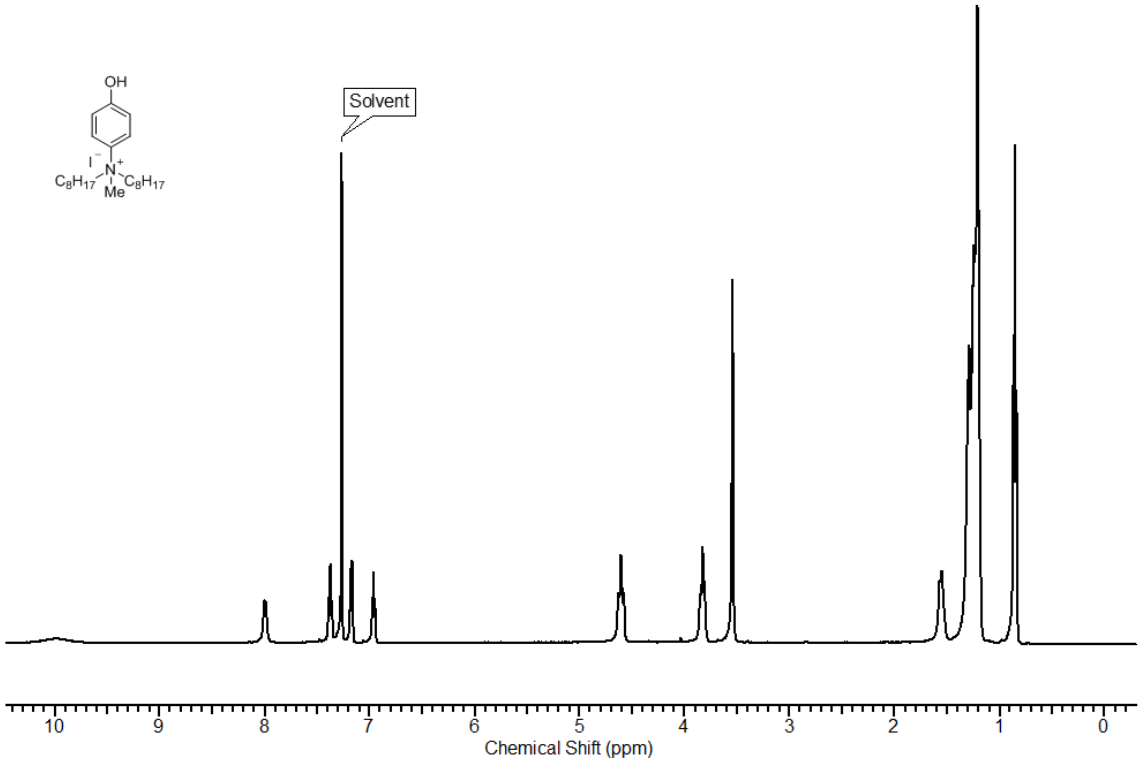

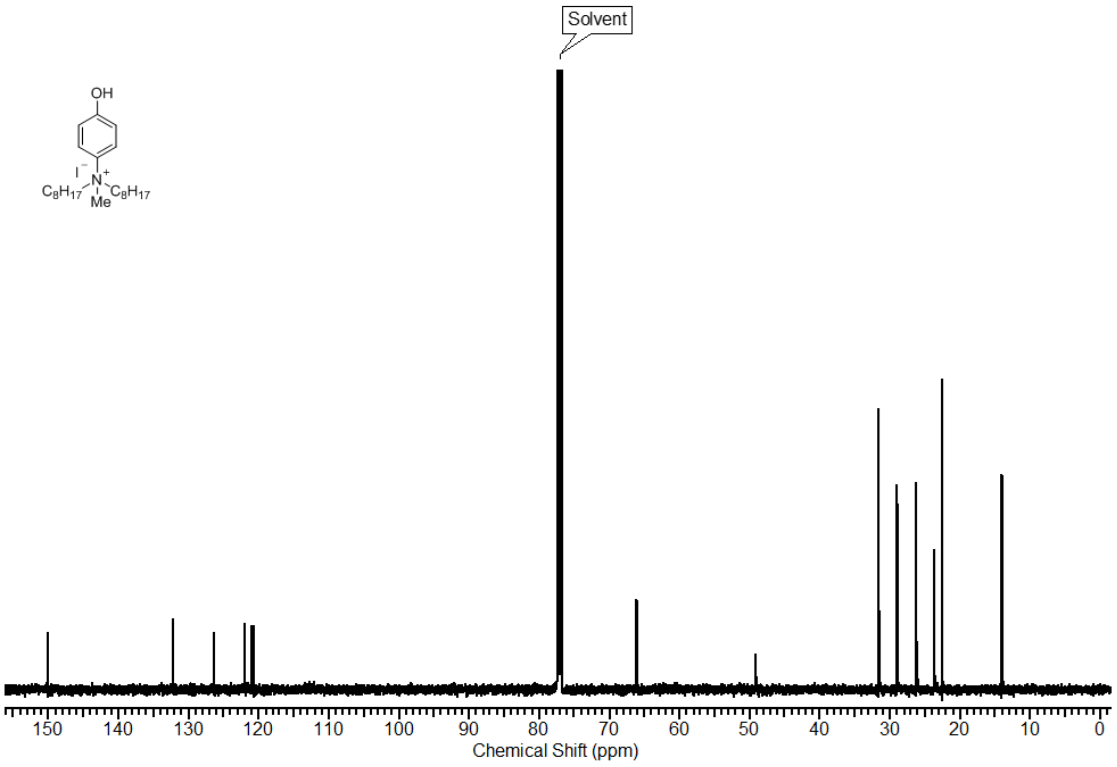
Solvent
OH
I⁻
N⁺
C8H17
C8H17
Me
150 140 130 120 110 100 90 80 70 60 50 40 30 20 10 0
Chemical Shift (ppm)

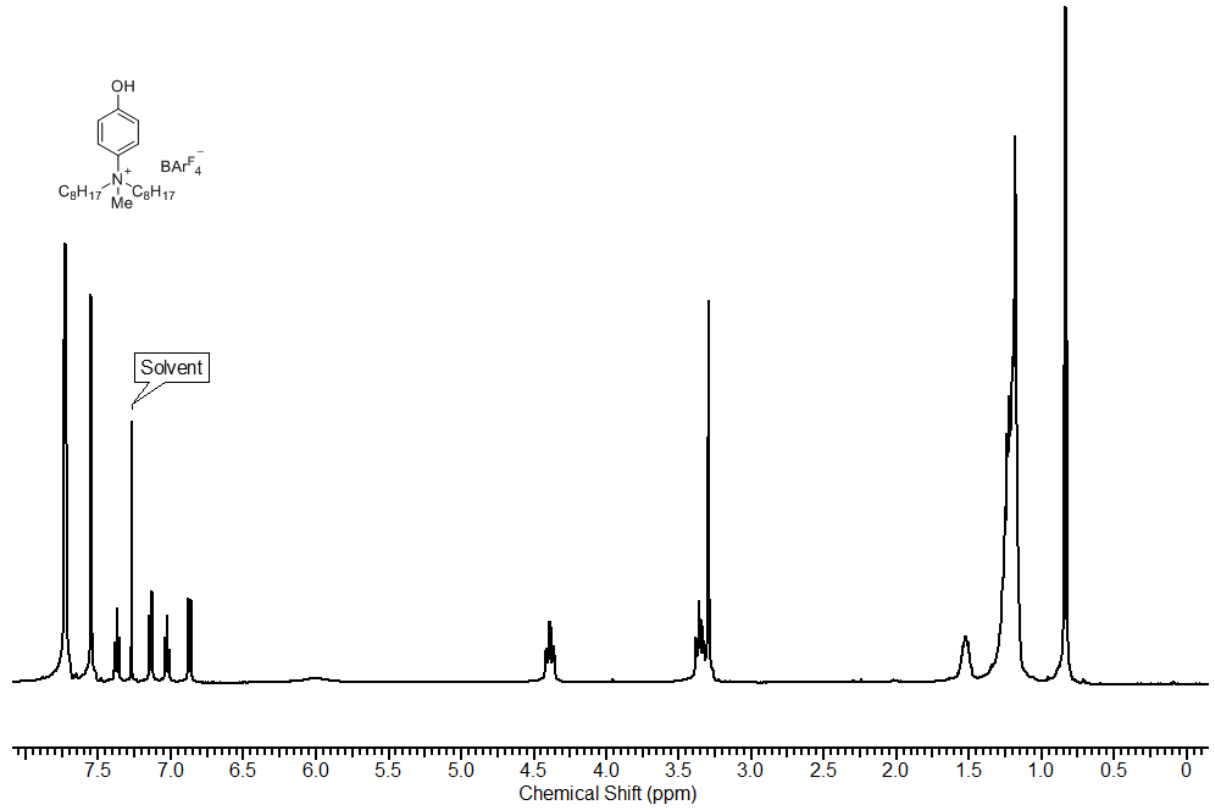
OH
BArF4⁻
N⁺
C8H17
C8H17
Me
Solvent
7.5 7.0 6.5 6.0 5.5 5.0 4.5 4.0 3.5 3.0 2.5 2.0 1.5 1.0 0.5 0
Chemical Shift (ppm)

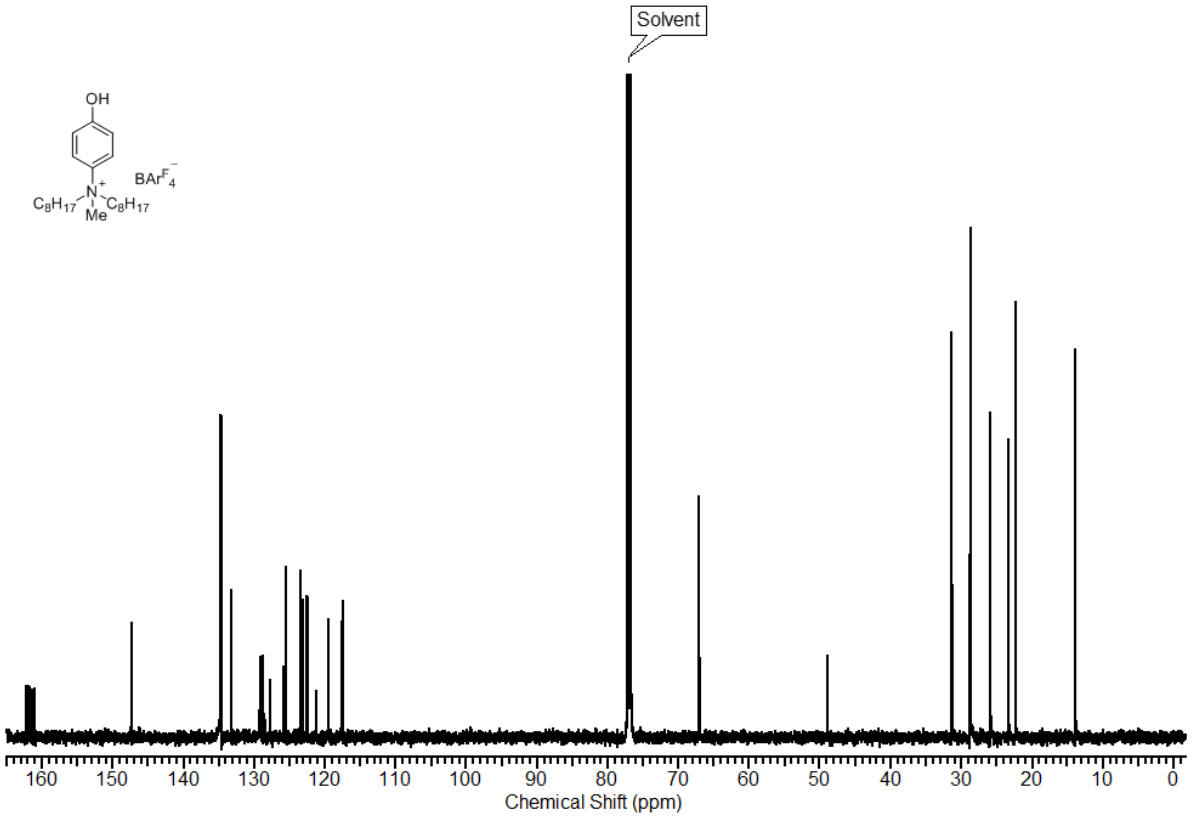
Solvent
OH
BArF4−
C8H17
N+
Me
C8H17
160 150 140 130 120 110 100 90 80 70 60 50 40 30 20 10 0
Chemical Shift (ppm)

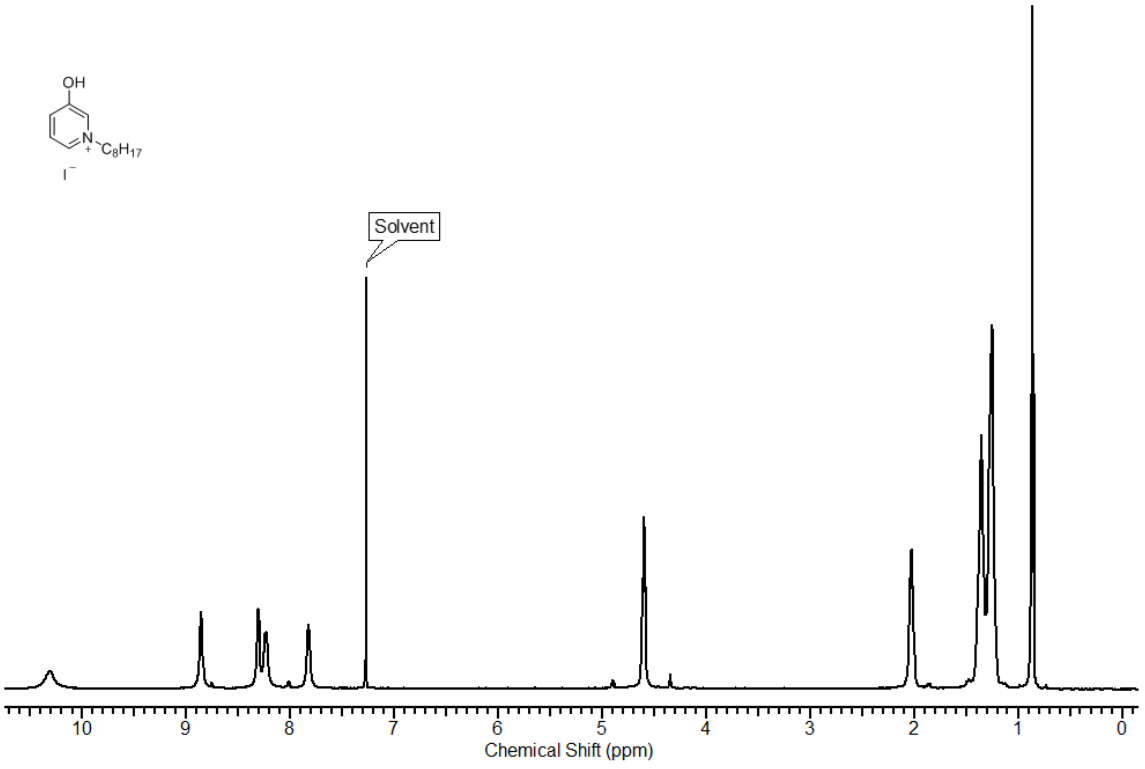
OH
N+
C8H17
I−
Solvent
10 9 8 7 6 5 4 3 2 1 0
Chemical Shift (ppm)

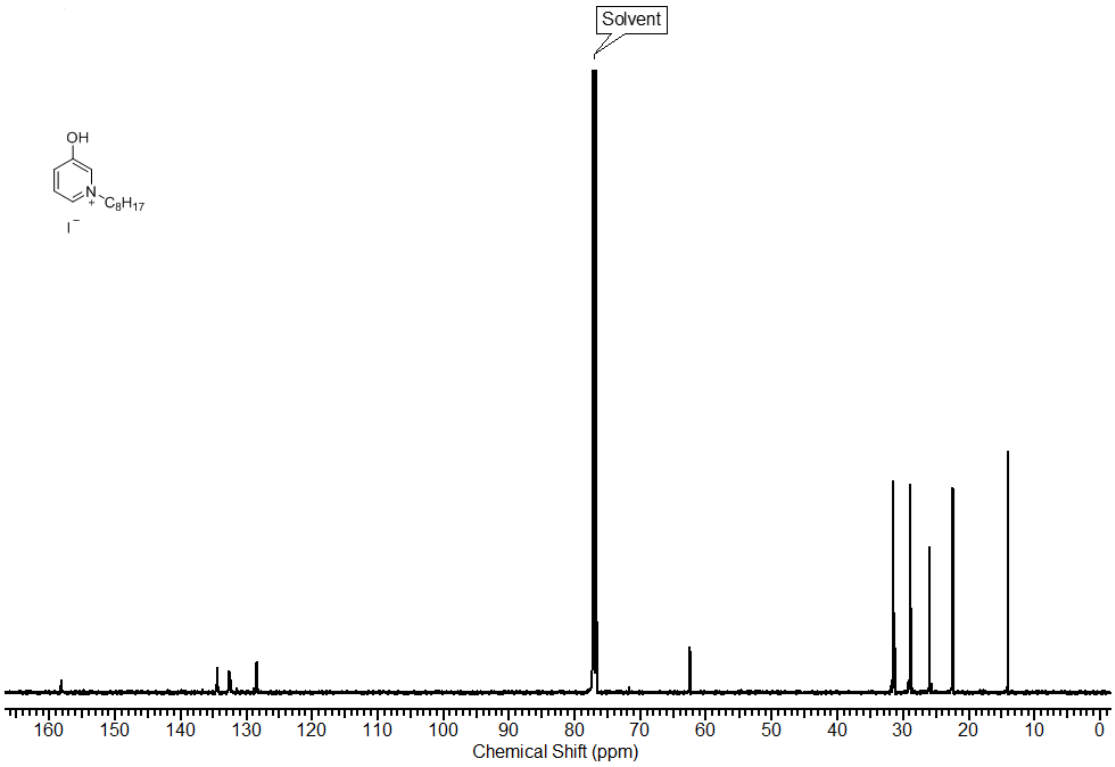
Solvent
OH
N
+
C8H17
I−
160
150
140
130
120
110
100
90
80
70
60
50
40
30
20
10
0
Chemical Shift (ppm)

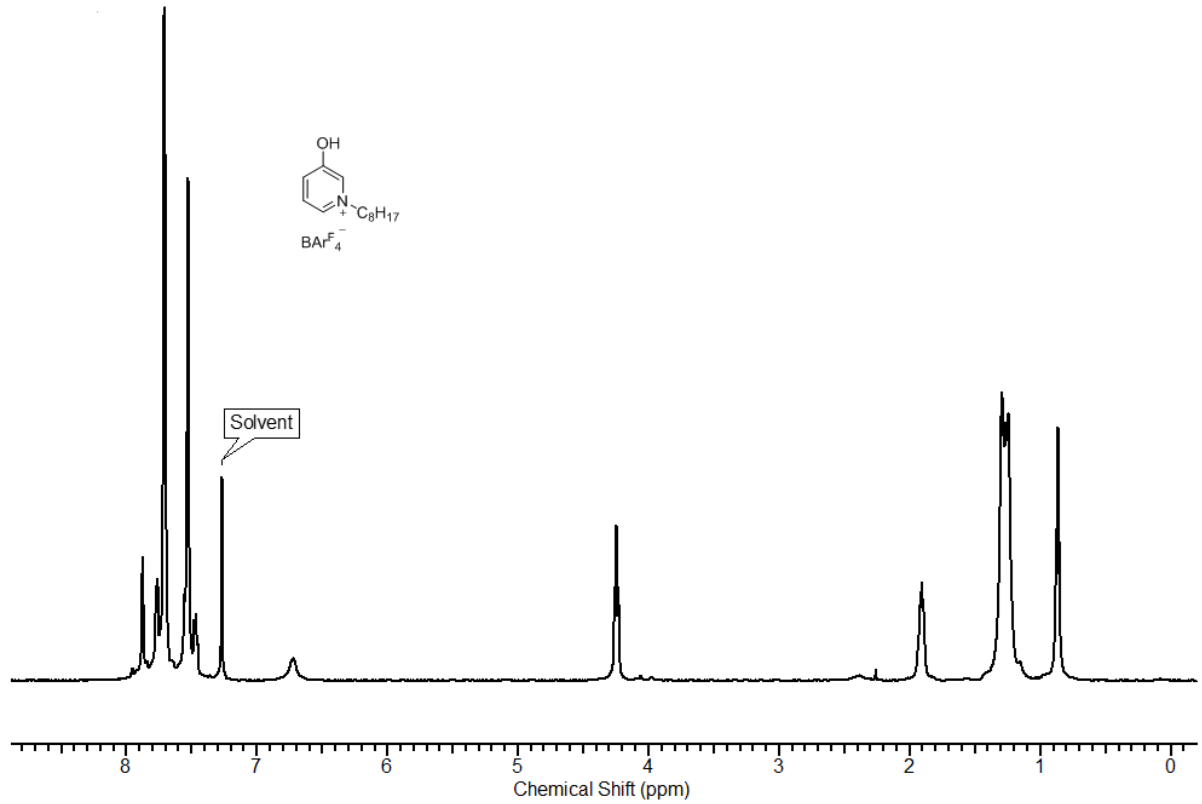
OH
N
+
C8H17
BArF4−
Solvent
8
7
6
5
4
3
2
1
0
Chemical Shift (ppm)

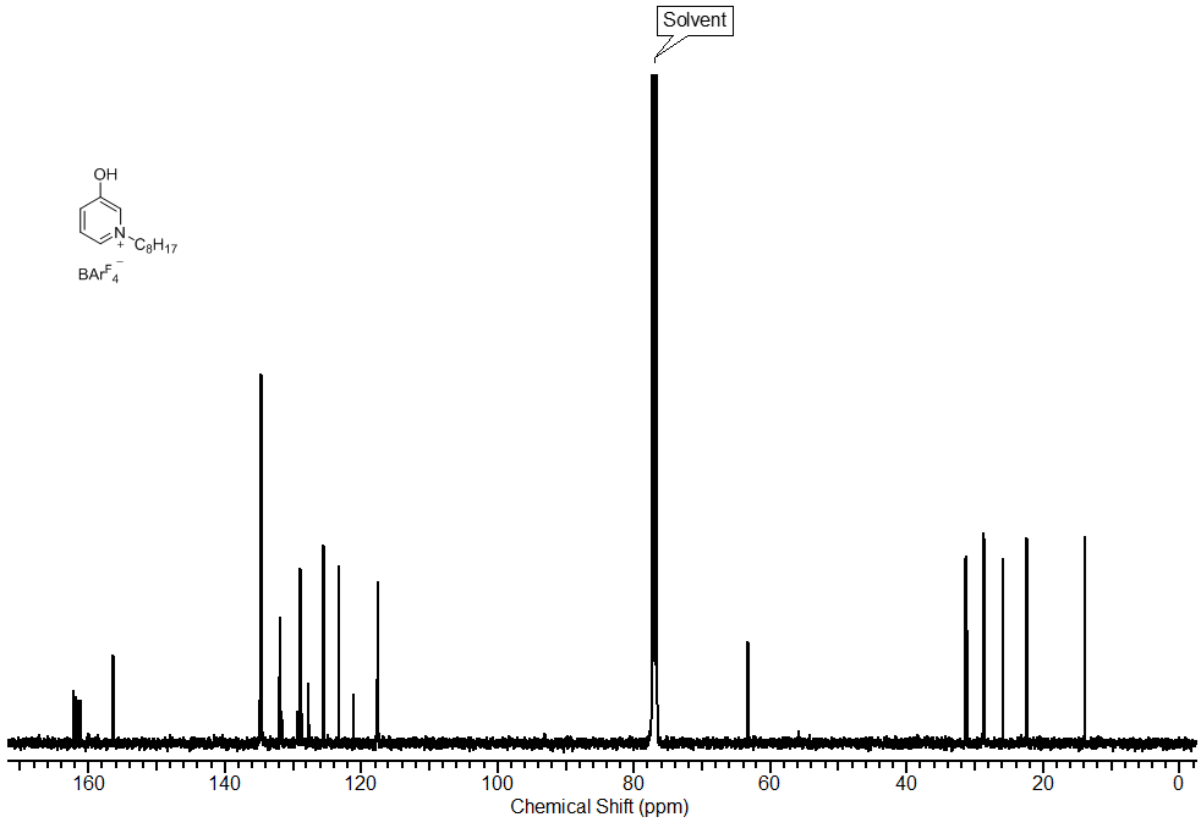
Solvent
OH
N
+
C8H17
BArF4
160
140
120
100
80
60
40
20
0
Chemical Shift (ppm)

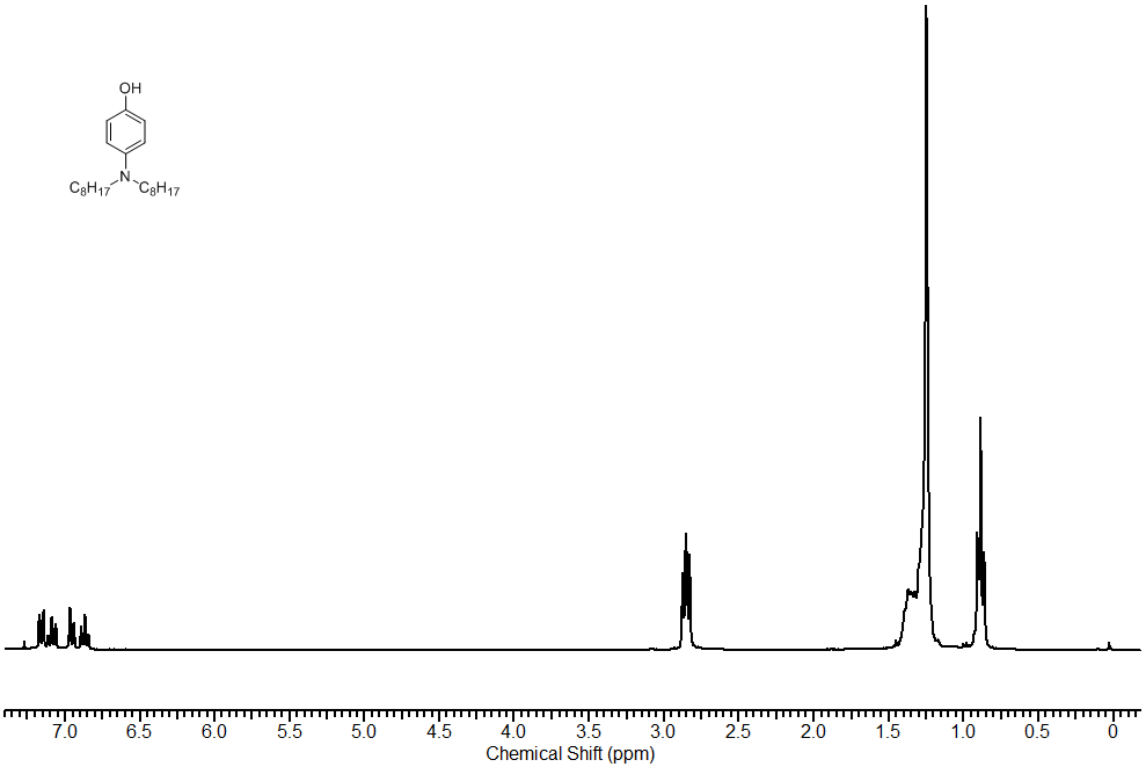
OH
N
C8H17
C8H17
7.0
6.5
6.0
5.5
5.0
4.5
4.0
3.5
3.0
2.5
2.0
1.5
1.0
0.5
0
Chemical Shift (ppm)

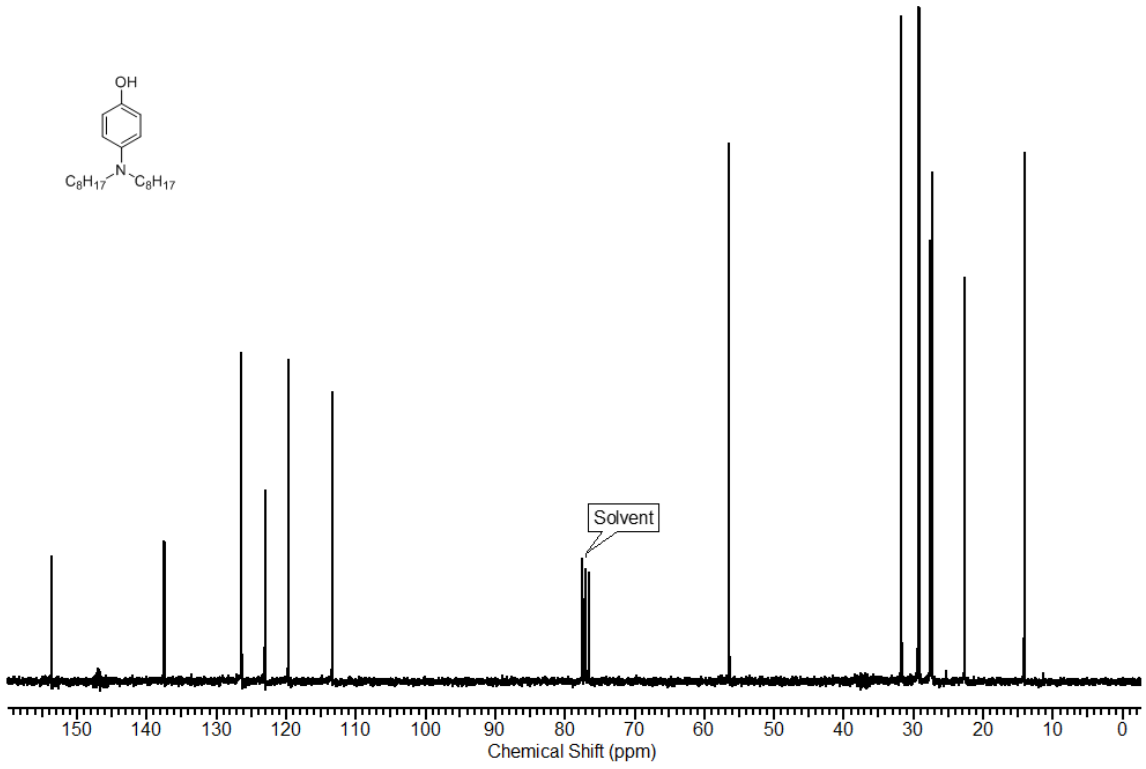

Table S1. Kinetic data for *p*-substituted phenols **1–2** and two pyridinium salts (**3** and its corresponding iodide).

time (h)	conversion (%)
[*p*-nitrophenol] = 8.3 mM, [β-nitrostyrene]$_o$ = 83 mM, [*N*-methylindole]$_o$ = 250 mM, solvent = $CDCl_3$	
12.1	0.72
24.0	1.44
60.1	3.84
96.1	6.38
[*p*-nitrophenol] = 8.3 mM, [β-nitrostyrene]$_o$ = 29 mM, [*N*-methylindole]$_o$ = 85 mM, solvent = $CDCl_3$	
96.2	1.46
191.1	3.93
264.1	5.22
409.2	8.94
[*p*-nitrophenol] = 8.3 mM, [β-nitrostyrene]$_o$ = 235 mM, [*N*-methylindole]$_o$ = 706 mM, solvent = $CDCl_3$	
9.2	1.03
16.2	1.84
24.2	2.74

36.2	4.11
48.2	5.68
96.3	11.1
[*p*-nitrophenol] = 8.3 mM, [β-nitrostyrene]$_o$ = 29 mM, [*N*-methylindole]$_o$ = 85 mM, solvent = $C_6D_5CD_3$	
343.0	0.93
[**1**] = 8.3 mM, [β-nitrostyrene]$_o$ = 83 mM, [*N*-methylindole]$_o$ = 250 mM, solvent = $CDCl_3$	
168.2	1.46
241.2	1.89
368.3	4.92
[**2**] = 8.3 mM, [β-nitrostyrene]$_o$ = 83 mM, [*N*-methylindole]$_o$ = 250 mM, solvent = $CDCl_3$	
3.23	3.85
24.1	27.5
32.1	37.9
40.1	45.9
48.1	52.4
72.1	65.8
96.1	75.7
132.1	85.7
[**2**] = 8.3 mM, [β-nitrostyrene]$_o$ = 29 mM, [*N*-methylindole]$_o$ = 85 mM, solvent = $CDCl_3$	
24.1	17.7
54.3	37.9
96.1	59.0
171.6	79.9
[**2**] = 8.3 mM, [β-nitrostyrene]$_o$ = 235 mM, [*N*-methylindole]$_o$ = 706 mM, solvent = $CDCl_3$	
9.1	15.3
16.1	25.4
24.1	35.4
36.0	47.2
48.1	58.0
96.1	80.5
[**2**] = 8.3 mM, [β-nitrostyrene]$_o$ = 29 mM, [*N*-methylindole]$_o$ = 85 mM, solvent = $C_6D_5CD_3$	
24.3	10.5
72.0	29.4
120.4	40.9
159.0	57.3
343.0	75.7

[3-hydroxy-*N*-octylpyridinium iodide] = 8.3 mM, [β-nitrostyrene]$_o$ = 83 mM, [*N*-methylindole]$_o$ = 250 mM, solvent = $CDCl_3$	
48.0	4.3
[**3**] = 8.3 mM, [β-nitrostyrene]$_o$ = 83 mM, [*N*-methylindole]$_o$ = 250 mM, solvent = $CDCl_3$	
0.5	16.5
1.0	32.3
1.6	45.1
2.5	63.4
4.1	79.6
[**3**] = 8.3 mM, [β-nitrostyrene]$_o$ = 29 mM, [*N*-methylindole]$_o$ = 85 mM, solvent = $CDCl_3$	
0.9	24.0
1.1	30.1
3.4	64.0
4.1	70.5
5.1	78.0
6.7	85.4
8.1	90.2

Complete citation to reference 18 and 32:

(18) Arunan, E.; Desiraju, G. R.; Klein, R. A.; Sadlej, J.; Scheiner, S.; Alkorta, I.; Clary, D. C.; Crabtree, R. H.; Dannenberg, J. J.; Hobza, P.; Kjaergaard, H. G.; Legon, A. C.; Mennucci, B.; Nesbitt, D. J. *Pure Appl. Chem.* **2011**, *83*, 1637-1641.

(32) Frisch, M. J.; Trucks, G. W.; Schlegel, H. B.; Scuseria, G. E.; Robb, M. A.; Cheeseman, J. R.; Scalmani, G.; Barone, V.; Mennucci, B.; Petersson, G. A.; Nakatsuji, H.; Caricato, M.; Li, X.; Hratchian, H. P.; Izmaylov, A. F.; Bloino, J.; Zheng, G.; Sonnenberg, J. L.; Hada, M.; Ehara, M.; Toyota, K.; Fukuda, R.; Hasegawa, J.; Ishida, M.; Nakajima, T.; Honda, Y.; Kitao, O.; Nakai, H.; Vreven, T.; Montgomery, Jr., J. A.; Peralta, J. E.; Ogliaro, F.; Bearpark, M.; Heyd, J. J.; Brothers, E.; Kudin, K. N.; Staroverov, V. N.; Kobayashi, R.; Normand, J.; Raghavachari, K.; Rendell, A.; Burant, J. C.; Iyengar, S. S.; Tomasi, J.; Cossi, M.; Rega, N.; Millam, J. M.; Klene, M.; Knox, J. E.; Cross, J. B.; Bakken, V.; Adamo, C.; Jaramillo, J.; Gomperts, R.; Stratmann, R. E.; Yazyev, O.; Austin, A. J.; Cammi, R.; Pomelli, C.; Ochterski, J. W.; Martin, R. L.; Morokuma, K.; Zakrzewski, V. G.; Voth, G. A.; Salvador, P.; Dannenberg, J. J.; Dapprich, S.; Daniels, A. D.; Farkas, O.; Foresman, J. B.; Ortiz, J. V.; Cioslowski, J.; Fox, D. J. *Gaussian 09*, Gaussian, Inc., Wallingford, CT, 2009.

Appendix for Chapter 6

For XYZ coordinates and electronic energies see:

http://pubs.acs.org/doi/full/10.1021/acs.joc.5b01475

Table S1. Kinetic data for **3(2)**, **3(3)**, **4**, **5**, and Schreiner's thiourea (**6**).

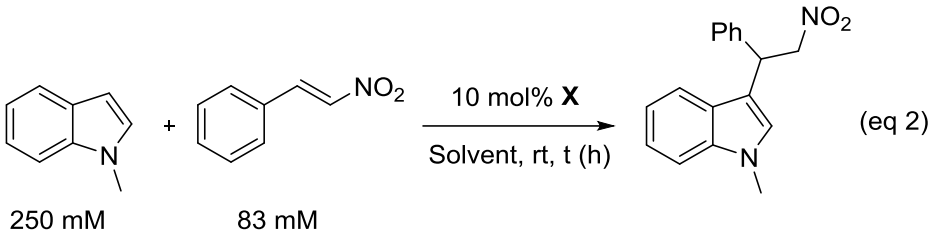

(eq 2)

time (h)	conversion (%)
[**X**] = [**3(3)**] = 8.3 mM in $C_6D_5CD_3$	
0.5	9.2
1.1	21.6
2.6	44.8
6.1	78.7
16.3	96.2
[**X**] = [**3(3)**] = 8.3 mM in $C_6D_5CD_3$ / 1%CD_3CN	
3.1	12.5
7.1	30.9
13.1	50.8
19.1	64.5
25.1	74.6
49.1	93.5
[**X**] = [**3(2)**] = 8.3 mM in $C_6D_5CD_3$ / 1%CD_3CN	
5.1	2.6
23.8	17.0
48.1	24.3
72.1	37.6
126.1	58.5
192.1	74.6

[**X**] = [**4**] = 8.3 mM in $C_6D_5CD_3$	
6.1	1.9
24.1	7.6
72.1	20.2
168.1	39.5
240	49.8
504	75.2
[**X**] = [**5**] = 8.3 mM in $C_6D_5CD_3$	
3.3	8.8
6.1	19.6
21.1	47.8
29.4	58.1
48.1	75.8
72.1	90.9
96.1	95.2
[**X**] = [**6**] = 8.3 mM in $C_6D_5CD_3$ / 1%CD_3CN	
12.1	4.9
24.1	8.2
48.1	22.3
96.1	41.7
168.1	62.1

Table S2. Water and DMSO acidities of aliphatic alcohols.[44,49]

cmpd	pK_a (water)	pK_a (DMSO)
MeOH	15.5	29.0
EtOH	15.9	29.8
PrOH	16.1	29.0[a],30.1[b]
i-PrOH	17.1	30.3
t-BuOH	19.2	32.2
CF_3CH_2OH	12.4	23.5
$(CF_3)_2CHOH$	9.3	17.9
$(CF_3)_3COH$	5.1	10.7
$CF_3CH_2CH_2OH$	14.6[c]	26.6[a]
$CF_3(CH_2)_2CH_2OH$	15.4[c]	27.8[a]

[a]Estimated using the linear least squares line in Fig. S1. [b]The average of the values for EtOH and *i*-PrOH. [c]Ouellette, R. J., Rawn J. D. *Organic Chemistry: Structure, Mechanism, and Synthesis*, Elsevier: San Diego, 2014.

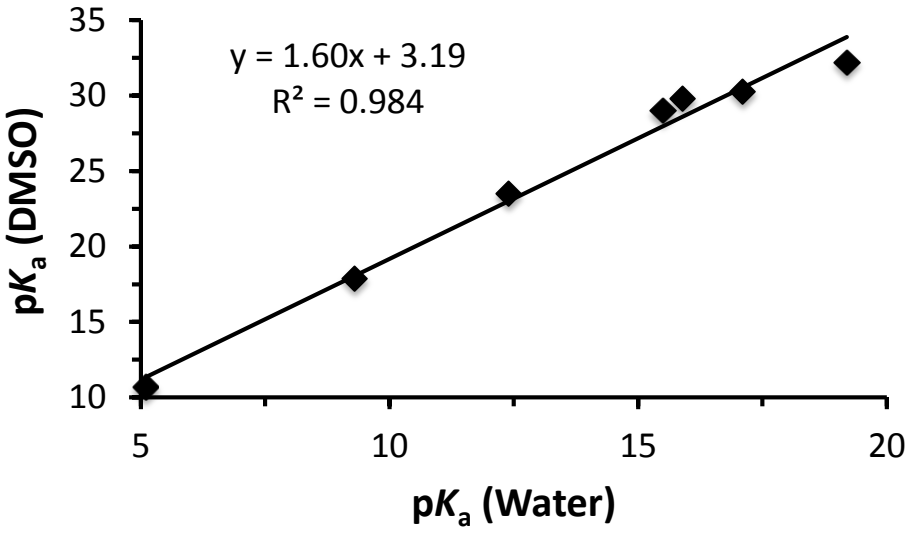

Figure S1. Linear relationship between water and DMSO acidities of aliphatic alcohols.

Table S3. Water and DMSO acidities of aromatic alcohols.[44,49]

cmpd	pK_a (water)	pK_a (DMSO)
2,4,6-$(NO_2)_3C_6H_2OH$	0.4	0.0
2,4-$(NO_2)_2C_6H_3OH$	4.1	5.1
4-$HOC_6N_4NO_2$	7.1	10.8
4-HOC_6N_4CN	8.0	13.2
3-$HOC_6N_4NO_2$	8.4	14.4
3-HOC_6N_4CN	8.6	14.8
3-$HOC_6N_4CF_3$	8.7	15.6
1,2-$C_6H_4(OH)_2$	9.5	15.7[a]
2-naphthol	9.6	17.1
phenol	10.0	18.0
p-Me	10.3	18.9
binol	8.3	14.2[b],13.2[c]

[a]Bordwell 1/9/80 unpublished pK_a table; a computed value of 14.6 has been reported, see: Zhu, X.-Q.; Wang, C.-H.; Liang, H. *J. Org. Chem.* **2010**, *75*, 7240-7257. [b]Estimated using the linear least squares line in Fig. S2. [c]Predicted value from ref. 52.

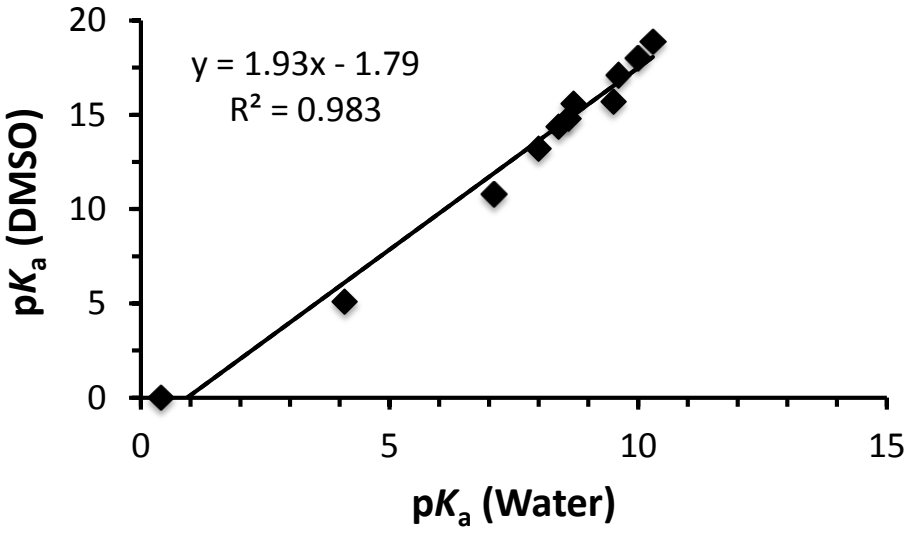

Figure S2. Linear relationship between water and DMSO acidities of phenol derivatives.

Complete citation to reference 49:

Frisch, M. J.; Trucks, G. W.; Schlegel, H. B.; Scuseria, G. E.; Robb, M. A.; Cheeseman, J. R.; Scalmani, G.; Barone, V.; Mennucci, B.; Petersson, G. A.; Nakatsuji, H.; Caricato, M.; Li, X.; Hratchian, H. P.; Izmaylov, A. F.; Bloino, J.; Zheng, G.; Sonnenberg, J. L.; Hada, M.; Ehara, M.; Toyota, K.; Fukuda, R.; Hasegawa, J.; Ishida, M.; Nakajima, T.; Honda, Y.; Kitao, O.; Nakai, H.; Vreven, T.; Montgomery, Jr., J. A.; Peralta, J. E.; Ogliaro, F.; Bearpark, M.; Heyd, J. J.; Brothers, E.; Kudin, K. N.; Staroverov, V. N.; Kobayashi, R.; Normand, J.; Raghavachari, K.; Rendell, A.; Burant, J. C.; Iyengar, S. S.; Tomasi, J.; Cossi, M.; Rega, N.; Millam, J. M.; Klene, M.; Knox, J. E.; Cross, J. B.; Bakken, V.; Adamo, C.; Jaramillo, J.; Gomperts, R.; Stratmann, R. E.; Yazyev, O.; Austin, A. J.; Cammi, R.; Pomelli, C.; Ochterski, J. W.; Martin, R. L.; Morokuma, K.; Zakrzewski, V. G.; Voth, G. A.; Salvador, P.; Dannenberg, J. J.; Dapprich, S.; Daniels, A. D.; Farkas, O.; Foresman, J. B.; Ortiz, J. V.; Cioslowski, J.; Fox, D. J. *Gaussian 09*, Gaussian, Inc., Wallingford, CT, 2009.